A Thesis Submitted for the Degree of PhD at the University of Warwick

Permanent WRAP URL:

http://wrap.warwick.ac.uk/103803

Copyright and reuse:

This thesis is made available online and is protected by original copyright.

Please scroll down to view the document itself.

Please refer to the repository record for this item for information to help you to cite it.

Our policy information is available from the repository home page.

For more information, please contact the WRAP Team at: wrap@warwick.ac.uk

warwick.ac.uk/lib-publications
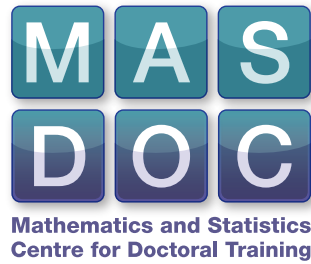
Mean traffic behaviour in Poissonian cities

by

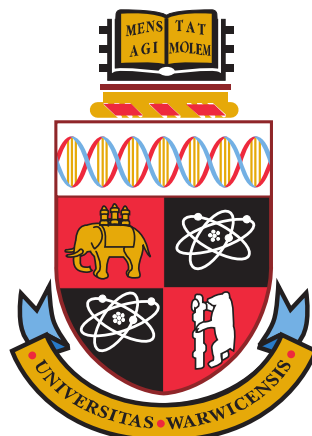## Rodolfo Miguel Gameros Leal

Thesis

Submitted for the degree of

Doctor of Philosophy

Mathematics Institute

The University of Warwick

March 2018

Contents

List of Figures

Acknowledgments

Declarations

I, Rodolfo Miguel Gameros Leal, declare that, to the best of my knowledge, the material contained in this thesis is original and my own work except where otherwise indicated, cited or commonly known.

The material in this thesis is submitted to the University of Warwick for the degree of Doctor of Philosophy, and has not been submitted to any other university or for any other degree.

Abstract

The Poissonian city is a model where a Poisson line process of unit intensity Π is being used as a transportation network inside a disk of radius n. In order to achieve a better understanding of this framework we first compile in chapter 1 the main results from Stochastic Geometry and a brief summary of similar research in the topic of transportation networks and also other possible applications for line processes. In chapter 2 we study the asymptotic mean traffic flow at any point $\boldsymbol{q} = (tn, un)$ inside the Poissonian city conditioning on the presence of an horizontal line $\ell_q : y = un$ that passes through $\boldsymbol{q}$, that is $\ell_q \in \Pi$. Later, in chapter 3 we use Palm Theory to compute the asymptotic mean traffic flow inside a subregion of the Poissonian city. Then, chapter 4 compares the asymptotic mean traffic density inside the Poissonian city with the study done by Beeching for the British railway system. The differences between the British railway system and the theoretical model provided by the Poissonian city motivates us to modify some of the assumptions in our model. In chapter 5, we adapt previous results to the Poissonian city taken place inside a variety of ellipses $\boldsymbol{E}_c$, where the parameter c is used to change the eccentricity of the ellipse. Finally, chapter 6 presents a new possible generalization for the Poissonian city and open problems related with this new approach. Also other possible approaches are mentioned for future research.

Chapter 1

Introduction and literature review

The history of random lines goes back to Buffon's needle problem [19] in the 18th century. In recent times it has found applications in the designing of effective/optimal spatial networks where geographical location of vertices/nodes plays an important role. By a network we understand a set of points/nodes, interpreted as *cities*, joined together in pairs by lines/edges, interpreted as *roads*, the union of all the streets taken to go from one city (point) to another will be call a *route*. Notice that the lines can intersect each other on other points beyond the nodes that they connect.

The initial interest arose from considerations concerning what might be a good statistical measure for the performance of spatial transportation networks. When designing a network, as explained by Gastner and Newman [18], it is natural to regard its total length as a *cost*, especially in the case of a transportation network. This cost can be related to the materials needed to construct the roads or rails, for example; as well as the maintenance required to keep the network working. On the other hand, the *efficiency* or *benefit* of a transportation network consists in the existence of short-length routes between cities, permitting short times of transportation from one point to another. One way to measure this benefit is to compare the shortest route length between cities $\boldsymbol{x_i}$, $\boldsymbol{x_j}$ in a given network $G(\boldsymbol{x^n})$, denoted by $\ell(\boldsymbol{x_i}, \boldsymbol{x_j})$, against the Euclidean distance, $d(\boldsymbol{x_i}, \boldsymbol{x_j}) = \|\boldsymbol{x_i} - \boldsymbol{x_j}\|_2$, between them. Another approach, taken by Gastner and Newman [18], measures the efficiency of a network as the excess length between the routes from all points $\boldsymbol{x_i}$ to a root node $\boldsymbol{x_0}$, and their corresponding Euclidean distances, that is they used $\sum_i \ell(\boldsymbol{x_i}, \boldsymbol{x_0}) - d(\boldsymbol{x_i}, \boldsymbol{x_0})$ as an statistic for the network efficiency, where lower values corresponds to better networks. An interesting problem regarding the design of networks is to be able to control this trade-off between its total length, which one will like to minimize, but yet have all the cities connected in such a way that the network still possess short-length routes between all cities or most of them.

In 2008, Aldous and Kendall [3] constructed a network $G(\boldsymbol{x^n})$, to link n points, $\boldsymbol{x^n} = \{\boldsymbol{x_1}, \ldots, \boldsymbol{x_n}\}$ in general position, inside a square of area n, bearing in mind

the above mentioned problem on the design of networks, which can be expressed as follows:

(a) The excess length regarding this network and the shortest network connecting all points (*Steiner Tree* [38], $ST(\boldsymbol{x^n})$) is $\mathcal{O}(n)$, that is

$$\lim_{n\to\infty} \frac{\text{excess length}(G(\boldsymbol{x^n}))}{n} = 0 \,, \qquad (1.1)$$

where excess length$(G(\boldsymbol{x^n})) = $ length$(G(\boldsymbol{x^n})) - $ length$(ST(\boldsymbol{x^n}))$.

(b) The excess distance considering the average of the difference between the shortest route length in $G(\boldsymbol{x^n})$ and their straight-line distance is $\mathcal{O}(\log n)$, i.e.

$$\limsup_{n\to\infty} \frac{\text{excess distance}(G(\boldsymbol{x^n}))}{\log n} < \infty \,, \qquad (1.2)$$

where excess distance$(G(\boldsymbol{x^n})) = \frac{1}{n(n-1)} \sum_{i\neq j} (\ell(\boldsymbol{x_i}, \boldsymbol{x_j}) - d(\boldsymbol{x_i}, \boldsymbol{x_j}))$ is the average excess of the shortest routes in $G(\boldsymbol{x^n})$ against the corresponding Euclidean distances.

In order to achieve this, the main idea is to superimpose a sparse stationary and isotropic Poisson line process over the minimum-length connected network, the Steiner Tree. The mentioned analysis uses the notion of *near-geodesics* routes between start and end points. These are paths built between pairs of points using the perimeter of the cell containing these two points, which is constructed using only the Poisson lines that does not separate them. These ideas will be explained in more depth in chapter 2.

An alternative statistic for measuring the short-length routes property is also mentioned by Aldous and Kendall [3], called the *ratio-statistic*, defined as

$$\text{ratio}(G(\boldsymbol{x^n})) = \frac{1}{n(n-1)} \sum_{i\neq j} r(\boldsymbol{x_i}, \boldsymbol{x_j}) \,, \quad \text{where} \quad r(\boldsymbol{x_i}, \boldsymbol{x_j}) = \frac{\ell(\boldsymbol{x_i}, \boldsymbol{x_j})}{d(\boldsymbol{x_i}, \boldsymbol{x_j})} - 1 \,.$$

Another approach is given by the maximum value of $r(\boldsymbol{x_i}, \boldsymbol{x_j})$, denoted $R_{\max}$. However, it seems too extreme to consider a network as inefficient just because it does not have a direct route between two particular cities, e.g. the UK railway should not necessarily be thought as inefficient just because it does not have a very direct route between Cambridge and Oxford. Some disadvantages of these ratio statistics are described by Aldous and Shun [4], where they proposed a new statistic to approach this problem, denoted by R, which is an intermediate statistic between the above mentioned ratio-statistics (average and maximum), as it combines both ideas. First consider

$$\rho(d) \quad = \quad \text{mean value of } r(\boldsymbol{x_i}, \boldsymbol{x_j}) \text{ over city-pairs with } d(\boldsymbol{x_i}, \boldsymbol{x_j}) = d \,,$$

and then define

$$R \quad = \quad \max_{0 \le d < \infty} \rho(d) \,. \tag{1.3}$$

Therefore, a value $R = 0.10$ means that on every scale of distance d (as we considering the maximum over all the possible distances d) the route lengths are on average at most 10% longer than the straight-line distance.

Later on, Kendall introduced in 2011 the notion of a *Poissonian City* [25], that is a random network of connections over a disk of radius n, where connections are made by random line patterns based on a stationary and isotropic Poisson line process, denoted by Π. Again, pairs of points in the disk are connected by near-geodesics, with initial/final segments of the path formed by traveling on the opposite direction to that of the destination/source until they hit a line that belongs to Π. Now, if we consider that each pair of points in the disk generates an infinitesimal flow, shared equally between these two near-geodesics derived from the line pattern, and we condition on one of the Poisson lines passing through the origin, $\boldsymbol{o}$, it can be shown that the mean flow at the centre is asymptotic to $2n^3$. Moreover, the scaled flow has a distribution which converges to a proper non-trivial distribution limit, i.e. the asymptotic flow at the centre of the Poissonian City is well-behaved. Actually, this distribution is asymptotically equivalent to a 4-volume of an unbounded region in $\mathbb{R}^4$ determined by an improper anisotropic Poisson line process defined on an infinite strip through the change of scale given by $\tilde{x} = x/n$ and $\tilde{y} = y/\sqrt{n}$. One of the main results in this Thesis generalizes the above mentioned result to any given point, $\boldsymbol{q}$ on the Poissonian city conditioning on the presence of a line $\ell_q(\theta)$ in the Poisson line process Π that goes through the point $\boldsymbol{q}$ and makes an angle θ with the x-axis.

In 2014, Kendall [27] established an alternative representation for this 4-volume in terms of a pair of monotonic concave curves denominated *seminal curves*. At the same time, this work proves that a calculation in terms of initial segments of these seminal curves can be used to approximate the 4-volume up to an explicit $\mathcal{L}_1$-error. This can be made as small as desired, an idea that supplies the necessary theory to approximate and effectively simulate the 4-volume. Nevertheless, it does not make explicit the amount of computational effort one requires to achieve stage N approximations to the volume. This is a non-trivial task, since account must be taken of the effort required to approximate each stage $n = 1, 2, \ldots, N$. More on these ideas was developed in [17].

In order to understand the above formulation one needs to be familiar with the idea of a *line process*, which will be explained below together with some of the main line process results in the field of Stochastic Geometry.

1.1 Notation

Throughout we will use $(\Omega, \mathcal{F}, \mathbb{P})$ to denote a probability space. Line processes will be denoted by Π as a random set/pattern, and $\Pi = \{\ell_1, \ell_2, \ldots\}$ will denote the realization of Π, that is $\Pi = \Pi(\omega)$, represents a specific set of lines. Here ℓ_i will stand for a typical line of the process; notice that one should think about Π as a set of lines instead of a list of lines, that means the order given by the list is not relevant at all. The intensity of Π will be denoted by a constant λ (in the case of isotropic homogeneity) or Λ (in more general cases).

A Poisson point process will be denoted by Φ (representing the random pattern). Also in an abuse of notation we will denote the induced random measure by Φ, here the random measure $\Phi(B)$ represents the amount of points from the random pattern Φ that belongs to the deterministic set B. A particular realization will usually by denoted by $\varphi = \{\boldsymbol{x_1}, \boldsymbol{x_2}, \ldots\}$, where $\boldsymbol{x_i}$ represents the specific location for one of the points, in the sequence φ, but their order is not relevant at all. As before, their intensity will be written as λ or Λ, as appropriate.

As well, the Lebesgue measure in $\mathbb{R}^d$, denoted by $\mathrm{Leb}_d(\cdot)$, will be used frequently. Also, we will distinguish a point, $\boldsymbol{x_i}$, from its coordinates, (x_i, y_i). A non-random set of points will usually be written as $\boldsymbol{x^n} = \{\boldsymbol{x_1}, \ldots, \boldsymbol{x_n}\}$, where n refers to the amount of points being considered; and $G(\boldsymbol{x^n})$ will typically denote a given network that connects the configuration of points $\boldsymbol{x^n}$.

Additional notation includes the ball of radius r around the point $\boldsymbol{x_0}$, $\mathcal{B}_r(\boldsymbol{x_0}) = \{\boldsymbol{x} \in \mathbb{R}_d : \|\boldsymbol{x} - \boldsymbol{x_0}\|_d \leq r\}$, where often the centre $\boldsymbol{x_0}$ will be the origin, denoted by $\boldsymbol{o}$. Compact sets will usually be denoted by the letter K and the cardinality of a given set by $\#$.

1.2 Point Process

The mathematical definition for a point process Φ on $\mathbb{R}^d$ is a random variable that takes values in a measurable space $(\mathbb{S}, \mathcal{S})$, where $\mathbb{S}$ is the family of all sets of points φ in $\mathbb{R}^d$ which satisfies two regularity conditions:

- The set φ is *locally finite*, meaning that each bounded subset of $\mathbb{R}^d$ must contain only a finite number of points from φ.

- The set is *simple*, i.e. if $\varphi = \{x_n : n \in \mathbb{N}\}$ then $x_i \neq x_j$ whenever $i \neq j$. In other words, there never will be two points on the same location.

While, the σ-field $\mathcal{S}$ is defined as the smallest σ-field on $\mathbb{S}$ such that all the mappings $\varphi \to \varphi(B)$ are measurable, where B runs through the bounded Borel sets. Recall,

in this notation $\varphi(B)$ denotes the number of points, from the configuration $\varphi \in \mathbb{S}$, in the set B. The σ-field $\mathcal{S}$ contains the so-called *configuration sets*, often denoted as Y or Z. For example $Y_B = \{\varphi \in \mathbb{S} : \varphi(B) = 0\} \subseteq \mathbb{S}$, corresponds to the set of all point sequences that have no point in a given fixed set B.

As already mentioned before, for convenience we will often used the notation $\varphi = \{x_1, x_2, \ldots\} = \{x_n, n \in \mathbb{N}\}$. However, the order of this list is arbitrary. From now on, every time a point process is mentioned, this will satisfies the above regularity conditions (locally finite and simple), unless otherwise stated.

Formally a point process Φ is a measurable mapping from a probability space $(\Omega, \mathcal{F}, \mathbb{P})$ into $(\mathbb{S}, \mathcal{S})$. Intuitively, that means that Φ is a random choice of one of the $\varphi \in \mathbb{S}$. It generates a distribution on $(\mathbb{S}, \mathcal{S})$, described as the distribution $\mathbb{P}$ of Φ. An intuitive idea for the case in $\mathbb{R}^2$ is to consider an abstract dice with infinitely many faces. Each one of those faces will correspond to a realization of Φ, that is an specific sequence or pattern of points on the plane, i.e. $\varphi = \Phi(\omega)$.

1.3   Line Process

In this section, we provide a brief summary of the line process theory described in the book *Stochastic Geometry and its Applications* [13, Chapter 8] that will be required for the remaining of this work. To begin with, we define a line process.

DEFINITION 1.1 (Line Process). *[13, p. 306]*
A line process is a random collection of lines in the plane which is locally finite, that is, only finitely many lines hit each compact planar set, K.

In the following chapters, we will focus on undirected line processes. Nevertheless, it is easier to illustrate the basic ideas with directed line processes and the results can be easily transferred to the undirected case.

A *directed line* is a line together with a preferred direction along the line. The collection of all directed lines in the plane will be denoted by $A^*(2,1)$, and the family of all undirected lines by $A(2,1)$. Clearly, we have a $2 : 1$ correspondence between elements of $A^*(2,1)$ and of $A(2,1)$, obtained by ignoring the direction. Here, $A(d,k)$ denotes the affine linear subspace of dimension k (for $k \in \{1, 2, \ldots, d-1\}$ in $\mathbb{R}^d$, which are also called k-flats or k-planes.

The analysis regarding basic notions of $A^*(2,1)$ can be simplified through the $1 : 1$ correspondence between this set of lines and the set of points on the surface of a cylinder in $\mathbb{R}^3$. To achieve that, one has to parametrize a directed planar line $\ell \in A^*(2,1)$ using a convenient set of coordinates, given by $\{(r, \theta) : r \in \mathbb{R} \text{ and } \theta \in (0, 2\pi]\}$, which corresponds to: (see figure 1.1)

- θ : the angle between ℓ and a reference line, generally the x-axis, measured in anti-clockwise direction.

- r : the perpendicular *signed* distance from ℓ to a reference point, which usually lies on the reference line. In our case we take the origin, $\boldsymbol{o}$, where the sign is positive if $\boldsymbol{o}$ lies to the left of ℓ when looking in its direction.

This supplies a $1:1$ correspondence between the directed lines in $A^*(2,1)$ and the surface of the cylinder

$$\boldsymbol{C^*} \quad = \quad \left\{ (\cos\theta, \sin\theta, r) \in \mathbb{R}^3 : r \in \mathbb{R}, \theta \in (0, 2\pi] \right\} \ .$$
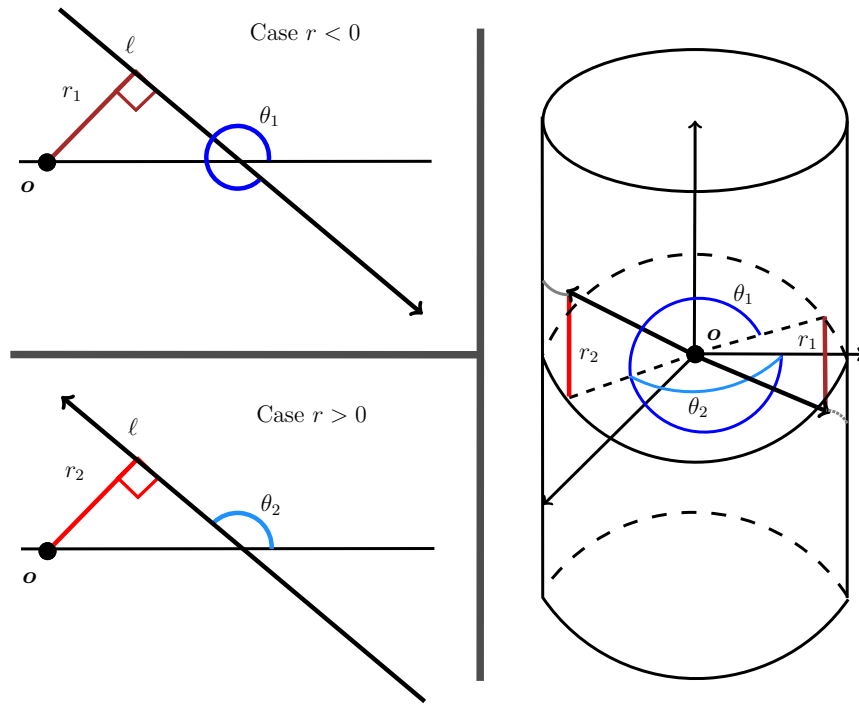
Figure 1.1: Illustration of the parametrization (r, θ) at the left, together with their corresponding points in $\boldsymbol{C^*}$ at the right.

Therefore, since each undirected line in $A(2,1)$ corresponds to a pair of directed lines, it also corresponds to a pair of points in $\boldsymbol{C^*}$. Actually, these two points are reflections of each other through the origin, as shown at the right of figure 1.1. As representative of the undirected line, we will select the point that is in the half-cylinder lying to one side of a fixed plane including the cylinder axis, so $A(2,1)$ has a $1:1$ correspondence with

$$\boldsymbol{C} = \left\{ (\cos\theta, \sin\theta, r) \in \mathbb{R}^3 : r \in \mathbb{R}, \theta \in (0, \pi] \right\} \ .$$

Remark: Notice that there exists a twist as the angle θ approaches to 0, then its representative point jumps from one edge of the half-cylinder to the other (where $\theta = \pi$), while the value of the coordinate r changes sign. In effect, the appropriate

representing space for undirected lines is a *Möbius strip* of infinite width.

Remark: There is an alternative parametrization which can be useful for certain calculations, where now the coordinates are given by $\{(p, \hat{\theta}) : p \in \mathbb{R}$ and $\hat{\theta} \in (0, 2\pi]\}$, which represents:

- $\hat{\theta}$: the angle between ℓ and a reference line, generally the x-axis, measured in anti-clockwise direction.

- p : the *signed* distance from the intersection point, between ℓ and the reference line, and a reference point (on the reference line). In our case we take the origin, o, as the reference point. Hence, p is the x-coordinate of the intersection of the line ℓ with the horizontal $y = 0$.

Notice that this alternative parametrization is defective, since if $\theta = 2\pi$ then there is no intersection with the x-axis, so p is ill-defined. Nevertheless, in the special case of invariant Poisson lines process this situation can be neglected as it is confined to an event of probability zero.

Hence, to analyze a line process one can apply all the theory developed for *point process*, one just needs to adapt it to the representation space. That is, directed line process give rise to measures on the cylinder C^*. Meanwhile, undirected lines give rise to measures on the half-cylinder C. In particular, we will focus on *Poisson line processes*, for directed lines we have that those processes can be defined as Poisson point processes on C^*, so their distributions are defined by their intensity measures. Even more, since our specific case refers to a *stationary* and *isotropic* Poisson line processes, their intensity measure should be invariant under translations and rotations. So we have the following result, which assures us that the measure on C^*, that is invariant under the translation-symmetry group induced by planar translations, is unique up to a multiplicative factor.

THEOREM 1.1 (Invariant Measures). *[13, Chapter 8, Theorem 8.1]*

(a) *Suppose that μ is a locally finite measure on C^* which is invariant under the translation-symmetry group (plane-translation-invariant). Then μ is of the form*

$$\mu(\,\mathrm{d}r\,\mathrm{d}\theta\,) \quad = \quad \mathrm{Leb}_1(\,\mathrm{d}r\,)\kappa(\,\mathrm{d}\theta\,)\,, \qquad\qquad (1.4)$$

for some finite measure κ on $(0, 2\pi]$, where Leb_1 denotes the one-dimensional Lebesgue measure.

(b) *Suppose that μ is a locally finite measure on C^* which is invariant under the motion-symmetry group. Then μ is a constant multiple of Lebesgue measure on C^**

$$\mu(\,\mathrm{d}r\,\mathrm{d}\theta\,) \quad = \quad m\,\mathrm{d}r\,\mathrm{d}\theta\,, \qquad\qquad (1.5)$$

for some constant m with $0 \leq m < \infty$. If $m = 1$ then μ is the surface measure on $\boldsymbol{C^*}$ (regarding $\boldsymbol{C^*}$ as a cylinder in $\mathbb{R}^3$).

The measure μ that corresponds to the multiplicative factor $m = 1$ is called *standard invariant measure*. The analogous invariant measure result holds true for $A(2, 1)$ through the correspondence with $\boldsymbol{C}$, where now $m = 1/2$, thus $\mu(\,\mathrm{d}r\,\mathrm{d}\theta\,) = 1/2\,\mathrm{d}r\,\mathrm{d}\theta$ will be called the standard invariant measure for the undirected lines, due to the $2 : 1$ correspondence between $A^*(2, 1)$ and $A(2, 1)$.

Moreover, one can derive a formula for the invariant measure of hitting sets using geometric arguments. In order to achieve that, we first define what we mean by a hitting set.

DEFINITION 1.2 (Hitting-set of K). *[8, p. 17]*
Let K be a compact subset and Π a line process, then the hitting set of K, denoted by $[K]$, is defined as

$$[K] \quad = \quad \{\ell \in \Pi : \ell \Uparrow K\}\,,$$

where $\ell \Uparrow K$ should be reads as "ℓ hits K", and means that $\ell \cap K \neq \emptyset$ [23].

The hitting event expresses the idea that a random set, ℓ in our case, intersects a non-random set, K, that is why we introduce the notation $\ell \Uparrow K$ instead of just using the notation $\ell \cap K \neq \emptyset$; since one generally relates an intersection with two non-random sets. Hence, $[K]$ consists of the collection of lines, $\ell \in \Pi$, that hits the set K, so $[K] \subseteq \Pi$. Now, we are able to state the result that gives us an explicit formula for the invariant measure of hitting-sets.

THEOREM 1.2 (Hitting Sets Measures). *[13, Chapter 8, Theorem 8.2]*
If μ is a motion-symmetric measure on $\boldsymbol{C^*}$, then for planar compact convex sets K, we have that

$$\mu([K]) \quad = \quad 2mL(K)\,, \tag{1.6}$$

where $L(K)$ denotes the perimeter of K and m is the same multiplicative factor as in equation (1.5).

Remark: This provides an intuitive reason to take $m = 1/2$ as the normalization factor for the invariant Poisson line process, since this will ensure that the number of hits in a unit segment will be in average one.

As we can see, the analysis of line processes can be regarded as a special case of the theory of planar point processes over the surface of the cylinder $\boldsymbol{C^*}$ for directed lines, or the half-cylinder $\boldsymbol{C}$ for undirected lines. This implies, that the definitions of *stationary* (translation-invariant) and *motion invariance* (stationary and isotropic) are similar to the corresponding definitions for point processes; the main difference lies in the replacement of the usual translation and motion groups in $\mathbb{R}^2$ by the

translation-symmetry and motion-symmetry groups in $\boldsymbol{C^*}$ or $\boldsymbol{C}$, accordingly. The general case for a translation-symmetry is given by $T_{(s,\psi)}$, which corresponds to a translation through a distance s in a direction that makes an angle ψ with the x-axis (reference line) in the plane, that will act on $\boldsymbol{C^*}$ in the following way (see figure 1.2)

$$T_{(s,\psi)}(r,\theta) \quad = \quad (r + s\sin(\theta - \psi), \theta) . \tag{1.7}$$

On the other hand, the general case for a motion-symmetry group is given by a rotation of the lines by an angle ψ, denoted by R_ψ, which will act on $\boldsymbol{C^*}$ as follows (see figure 1.2)

$$R_\psi(r,\theta) \quad = \quad (r, \theta + \psi) . \tag{1.8}$$
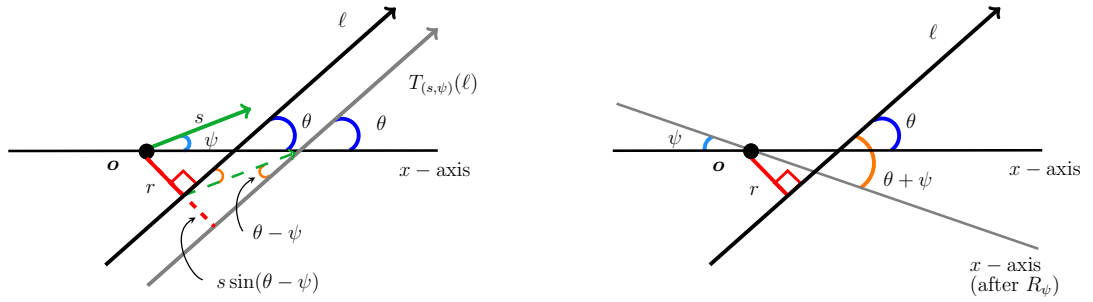
Figure 1.2: Illustration of the transformations $T_{(s,\psi)}$ and R_ψ.

Therefore one has the following definitions.

DEFINITION 1.3 (Stationary Line Process). *[13, p. 307]*
A line process $\Pi = \{\ell_1, \ell_2, \ldots\}$ is stationary if $\Pi_T = \{T(\ell_1), T(\ell_2), \ldots\}$ has the same distribution as a line process for every translation $T_{(s,\psi)}$ of the plane as in (1.7), and this is to say that, in the $\boldsymbol{C^*}$ representation, the point process:

$$\Phi_{TC^*} = \{(r(\ell_1) + s\sin(\theta(\ell_1) - \psi), \theta(\ell_1)), (r(\ell_2) + s\sin(\theta(\ell_2) - \psi), \theta(\ell_2)), \ldots\} ,$$

has the same distribution as

$$\Phi_{C^*} = \{(r(\ell_1), \theta(\ell_1)), (r(\ell_2), \theta(\ell_2)), \ldots\} , \tag{1.9}$$

for each $s \in \mathbb{R}$ and $\psi \in (0, 2\pi]$, where the additions of angles are interpreted modulo 2π.

DEFINITION 1.4 (Motion Invariant Line Process). *[13, p. 307]*
A line process is motion-invariant if it has the stationary property and in addition the line process $\Pi_R = \{R(\ell_1), R(\ell_2), \ldots\}$ has the same distribution for every rotation R_ψ of the plane as in (1.8), that is, in the $\boldsymbol{C^*}$ representation, the point process:

$$\Phi_{RC^*} = \{(r(\ell_1), \theta(\ell_1) + \psi), (r(\ell_2), \theta(\ell_2) + \psi), \ldots\} ,$$

also has the same distribution as Φ_{C^*} given by (1.9) for each $\psi \in (0, 2\pi]$, where again the additions of angles are interpreted modulo 2π.

Now, we analyze the idea of the intensity of a line process. A directed line process Π, when regarded as a point process Φ_{C^*} on $\boldsymbol{C^*}$, yields an intensity measure Λ_{C^*} for all Borel sets B on $\boldsymbol{C^*}$, given by:

$$\Lambda_{C^*}(B) \quad = \quad \mathbb{E}\left[\Phi_{C^*}(B)\right], \tag{1.10}$$

here $\Phi_{C^*}(B) = \#\{(r, \theta) \in \Phi_{C^*} : (r, \theta) \in [B])\}$ represents the amount of points from Φ_{C^*} contained in B. If Π is stationary, then Λ_{C^*} is translation-symmetric, and if Λ_{C^*} is locally finite then Theorem 1.1 can be applied, were equation (1.4) yields to

$$\Lambda_{C^*}(\,\mathrm{d}(r, \theta)) \quad = \quad \lambda \,\mathrm{d}r \mathscr{R}(\,\mathrm{d}\theta),$$

where λ is a constant, whose interpretation will become clear later, and $\mathscr{R}$ is a probability measure on $(0, 2\pi]$, called the *rose of directions* of Π. The rose of directions can be thought as the distribution of the direction of a typical line $\ell \in \Pi$.

If Π is motion-invariant, then again by Theorem 1.1, but now applying formula (1.5), we get

$$\Lambda_{C^*}(\,\mathrm{d}(r, \theta)) \quad = \quad \lambda \,\mathrm{d}r \frac{\mathrm{d}\theta}{2\pi},$$

where the constant $\lambda/(2\pi)$ is then the intensity of the representing point process Φ_{C^*} with respect to the standard invariant measure $\mathrm{d}r \,\mathrm{d}\theta$.

To explain the interpretation of λ in the above formulae, one requires the next definition.

DEFINITION 1.5 (Intensity Measure). *[13, p. 307]*
If the line process Π is stationary, then invariance arguments can be applied to the line length measure for all planar Borel sets B to define the intensity measure of Π as follows

$$\Lambda(B) \quad = \quad \mathbb{E}\left[\sum_{\ell \in \Pi} \mathrm{Leb}_{1,\ell}(\ell \cap B)\right] = \mathbb{E}\left[\sum_{\ell \in [B]} \mathrm{Leb}_{1,\ell}(\ell \cap B)\right], \tag{1.11}$$

where $\mathrm{Leb}_{1,\ell}$ is the Lebesgue measure on the line ℓ. That means that $\Lambda(B)$ represents the mean total length of all line pieces of Π that hits B.

Since Λ is a translation-invariant measure on $\mathbb{R}^2$, there exists a constant L_B such that for all planar Borel sets B the following formula holds

$$\Lambda(B) \quad = \quad L_B \,\mathrm{Leb}_2(B). \tag{1.12}$$

Hence, L_B is the mean line length per unit area. The relationship between λ and L_B can be determined by applying formula (1.10) to a special set B, namely, $B = \mathcal{B}_1(\boldsymbol{o})$.

First, we notice that the length of the chord in $\mathcal{B}_1(\boldsymbol{o})$ of a line ℓ at a distance r from the origin is $2\sqrt{1-r^2}$, see Figure 1.3; then using the *Campbell Theorem* [29, Section 3.2] we get the following relation

$$
\begin{aligned}
\pi L_B &= \Lambda(B(\boldsymbol{o},1)) = \mathbb{E}\left[\sum_{\ell \in [B(\boldsymbol{o},1)]} \mathrm{Leb}_{1,\ell}(\ell \cap B(\boldsymbol{o},1))\right] \\
&= \mathbb{E}\left[\sum_{(r,\theta)\in\Phi_{C^*}:|r|\leq 1} 2\sqrt{1-r^2}\right] = 2\int_0^{2\pi}\int_{-1}^1 \sqrt{1-r^2}\Lambda_{C^*}(\,\mathrm{d}(r,\theta)) \\
&= 2\lambda\int_{-1}^1 \sqrt{1-r^2}\,\mathrm{d}r = \lambda\pi\,.
\end{aligned}
$$

Hence $\lambda = L_B$, that is λ represents the mean line length per unit area.

Undirected line processes satisfy similar relations, but subject to replacement of $\mathrm{d}r\,\mathrm{d}\theta/(2\pi)$ by $\mathrm{d}r\,\mathrm{d}\theta/\pi$ and conversion of the rose of directions $\mathscr{R}$ into a distribution over $(0,\pi]$ as required.
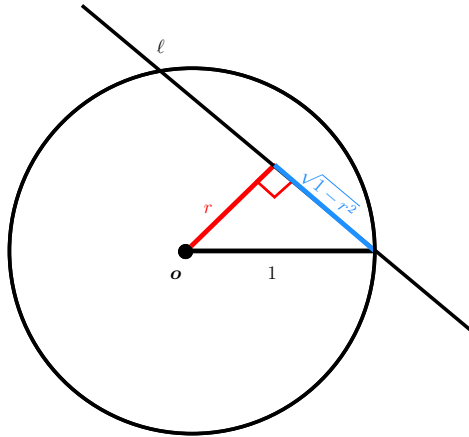
Figure 1.3: Illustration of the length of the chord in $\mathcal{B}_1(\boldsymbol{o})$.

1.4 Generalizations: Flat process and Fibre process

The idea of a *line process* in $\mathbb{R}^2$ generalize naturally to the idea of a *plane process* in $\mathbb{R}^3$ and this can be generalized to random systems of k-dimensional planes in $\mathbb{R}^d$, with $k \in \{1,\ldots d-1\}$, such process are usually known as *flat processes* [42, Section 4.4]. In this context, planar line processes will refer to the particular case, where $k = 1$ and $d = 2$, planes processes will correspond to $k = 2$ and $d = 3$. Of course, we can also think of line processes in space, which will be the case for $k = 1$ and $d = 3$. Furthermore, in $\mathbb{R}^d$ for $k = 1$ we talk of *line processes*, and for $k = d - 1$, of *hyper-*

plane processes. To formalize this idea one can think about a k-flat process in $\mathbb{R}^d$ as a point process in the affine Grassmannian of k-dimensional subspaces, denoted by $A(d,k)$, where $k \in \{1, \ldots, d-1\}$, idea already explored in the previous section where we analyzed the family of directed and undirected lines, $A^*(2,1)$ and $A(2,1)$ respectively.

Another way to generalize the idea of *line processes* is that of a *fibre processes*, which models random collections of curves in $\mathbb{R}^d$. Following, the same analogy as before, fibre processes can lead to *surface processes* in $\mathbb{R}^3$ and this can be generalized to the *manifold processes* of Mecke [32]. These are random systems of manifolds of fixed dimension, k, embedded in $\mathbb{R}^d$, which can be thought of as the solution set of some system of equations $f_1(x) = 0, \ldots, f_k(x) = 0$. To illustrate these ideas, we gave the formal definition of a fibre and how this can lead to the idea of fibre process.

DEFINITION 1.6 (Fibre). *[13, p. 314]*
A fibre γ is a subset of $\mathbb{R}^2$ which is the image of a curve $\gamma(t) = (\gamma_1(t), \gamma_2(t))$ such that

(i) $\gamma : [0,1] \to \mathbb{R}^2$ is once continuously differentiable.

(ii) $|\gamma'(t)|^2 = |\gamma_1'(t)|^2 + |\gamma_2'(t)|^2 > 0$ for all t.

(iii) The mapping γ is one-to-one, so that a fibre does not intersect itself.

Then, a *fibre system*, ϕ, is a closed subset of $\mathbb{R}^2$ which can be represented as a union of countably many fibres $\gamma^{(i)}$, with the property that any compact set, K, is only intersected by a finite amount of fibres, and such that distinct fibres have no points in common, unless these are end-points. This can be expressed as:

$$\gamma^{(i)}((0,1)) \cap \gamma^{(j)}((0,1)) = \emptyset, \qquad \text{whenever } i \neq j \,.$$

The length measure, for Borel sets B, corresponding to the fibre system ϕ is then defined in terms of the measures $\gamma^{(i)}$

$$\phi(B) \quad = \quad \sum_{\gamma^{(i)} \in \phi} \gamma^{(i)}(B) \,,$$

where by the measures $\gamma^{(i)}$ we refer to

$$\gamma^{(i)}(B) \quad = \quad \mathcal{H}_1(\gamma^{(i)} \cap B) = \int_0^1 \mathbb{1}_B(\gamma^{(i)}(t)) \sqrt{\gamma_1^{'(i)}(t)^2 + \gamma_2^{'(i)}(t)^2} \ \mathrm{d}t \,,$$

in which the *Hausdorff measure* $\mathcal{H}_1$ [13, equation 1.84] is used, so that $\mathcal{H}_1(\gamma^{(i)} \cap B)$ stands for the length of the fibre $\gamma^{(i)}$ in the set B.

The family of all planar fibre systems is denoted by $\mathbb{D}$ and is endowed with a σ-algebra $\mathscr{D}$ generated by sets of the form

$$\{\phi \in \mathbb{D} : \phi(B) < x\}$$

for planar Borel sets, B, and positive numbers, x. Therefore, one can think of a planar *fibre process* Φ as a random variable taking values in $(\mathbb{D}, \mathscr{D})$, that is to say, a measurable mapping from an underlying probability space $(\Omega, \mathcal{F}, \mathbb{P})$ to $(\mathbb{D}, \mathscr{D})$. As before, the same symbol, Φ, is also used to denote the corresponding random length measure. Thereby the theory of fibre process can be studied as a special part of the theory of random measures, as well as the theory of random sets [34].

1.5   Examples of Applications

The main application for line processes that will be studied in this work concerns how they can serve as models for traffic in spatial networks. For example:

1. Gastner and Newman [18] study spatial networks that are designed to distribute a commodity. Hence, the efficiency of these networks are measured in terms of the length of their routes to the root node.

2. Aldous and Kendall [3] consider a particular kind of network, given by Steiner Trees with a superimposed sparse Poisson line process (isotropic and stationary of unit intensity). This paper will be discussed in more detail in chapter 2.

3. Aldous et al. [2] study spatial networks as inter-city roads and conjecture the shape of the curve $R_{\max}^*(L)$, that is the minimum possible value of $R_{\max}$ for a given (normalized) network length L, with $R_{\max}^*$ defined as $\max_d r(\boldsymbol{x_i}, \boldsymbol{x_j})$, where the maximum is over all nodes whose Euclidean distance is equal to d. Finally they compare real-world networks against this theoretical curve.

4. Aldous and Shun [4] explains why ratio statistics are not necessarily a good summary statistic to measure the property of short-length routes in spatial networks, especially when one studies their asymptotic behavior as $n \to \infty$. They propose a new statistic to achieve this goal, R.

5. Kendall [25, 26, 27] follow-up work from Aldous and Kendall [3]. Kendall introduced the idea of a *Poissonian City* and analyzed some of its main features. Furthermore, the author introduced the notion of traffic flows in this kind of networks and some of its distribution properties. These notions will be studied in more detail in following chapters.

6. Dujmović et al. [15] analyze the *stretch factor* between two vertices, that is the ratio between the length of the shortest route in the graph $G(\boldsymbol{x^n})$ and the Euclidean distance between them. But, in contrast to Aldous and Kendall

[3], instead of finding a *light* network (small total length), this paper focus on finding a *sparse* network (small amount of edges).

7. Winston and Mannering [46] emphasize the importance of using new technologies to improve efficiency of highway pricing, which would benefit the following aspects: travel speeds, reliability and reduce highway expenditures. The authors try to measure the cost of road congestions and to find out where to set efficient tolls to avoid them.

The range of applications for line processes is much broader than given here, including areas such as Stereology [9] and the reconstruction of images that can be applied to Positron Emission Tomography (PET), where the main idea is to apply Theorem 1.2 to measure the size of organs or tumors. For example:

1. Vardi et al. [44] describe various estimation techniques for the image reconstruction problem of PET, viewed as a statistical estimation from incomplete data: Maximum Likelihood Estimators (using EM algorithm), least squares, and the method of moments.

2. Johnstone and Silverman [21] provide exact *minimax* convergence rates of estimation over suitable smoothness class of functions. Since the main idea of the PET reconstruction problem is to apply the *Radon transform* [31] of the density f, that is the line integral of f along the line ℓ with coordinates (r, θ) in the detector space, where the line ℓ corresponds to chords that connects N equally spaced points on the circumference of a particular disk.

3. O'Sullivan [36] studies asymptotic approximations and numerical simulations to examine the least squares and maximum likelihood approaches for image reconstruction in the PET problem with more details.

The planar Poisson line process and the Poisson plane process also play a relevant role in the construction of random tessellations, see van Lieshout [43] and Chapter 9 of the book *Stochastic Geometry and its Applications* [13]. Finally, Poisson and Cox line processes can be used as simple mathematical models for random systems of long fibres with weak curvature.

1.6 Directory of results

In chapter 2 we generalize the result presented by Kendall [25, Theorem 5], regarding the mean amount of traffic flow through the centre of the Poissonian city, conditioned on the presence of one line passing through the centre $\boldsymbol{o}$. This idea is generalized to any point $\boldsymbol{q} = (tn, un)$ in the Poissonian city conditioning on the presence of an horizontal line $\ell_q : y = un$.

Chapter 3 sets out the framework of *Palm theory*, which will be required in order to compare the traffic behaviour in the Poissonian city with a data set from an actual transportation network, say data regarding the British railway system considered in British Railways Board [12]. Palm theory can be applied so that the result developed in chapter 2 provides an insight regarding the computations required to make this comparison possible. Also, through conditional probability and Palm theory we show that there is a direct relation between the traffic flow generated by random points (source and destination nodes) in the Poisson line process Π and the traffic flow generated by random points in the whole disk of radius n $\mathcal{B}_n(\boldsymbol{o})$. Notice that in the second case, the source and destinations nodes almost surely will not belong to Π, and that corresponds with the approach taken in chapter 2. However, the first approach sets a more realistic framework, as the points of interest (source and destination) do belong to the transportation network (the Poisson line Process Π).

Then, in chapter 4, we compare the asymptotic mean traffic distribution on the Poissonian city with the data provided by British Railways Board [12], specifically figure 1 from its Appendix 1, see figure 1.4. The result developed in chapter 2 together with the Palm theory presented in chapter 3 will allow us to compute the traffic density across the Poissonian city. By traffic density we mean a curve that explains how the proportion for the total traffic changes in terms of the proportion of the network being considered. The approach to make this comparison is explained here and implemented numerically using the R computing environment. At the same time, we develop an analytic formulae to described the traffic density curve in the Poissonian city.

In chapter 5, we attempt to improve the fit developed in chapter 4 by generalizing the model for the Poissonian city. The generalization to be considered will analyse the line process Π taking place over a variety of ellipses, each one of them corresponding to different values for the eccentricity, instead of a disk. However, numerical evidence suggests that there is actually no change at all between the traffic density on the original Poissonian city and any elliptic Poissonian city. The density traffic curve studied here turns out to be related to *Elliptic Integrals*. The last sections of this chapter analyse this relation more thoroughly in order to explain the invariance of this curve in an analytic way.

Chapter 6 discusses possible future research on different approaches to generalize the Poissonian city in order to make it a more realistic framework for transportation networks. The main development here is how the Poissonian city will look like if instead of considering a Poisson line process Π, to construct our routes, one use a Poisson segment process Ξ, where the length of each segment is a fixed quantity, say h. Some connections with similar research on this topic are briefly mentioned. Finally, we summarize the results developed along this research and outline possible

Figure 1.4: Cumulative Distribution of different types of Traffic over Route Miles in the British Railways system, figure taken from the Appendix 1 of British Railways Board [12, Figure 1].

directions for future research on the topic.

Chapter 2

Traffic behaviour across the Poissonian city

Kendall [25] introduced the notion of a Poissonian city, that is a random network of connections based on a Poisson line process of unit intensity, Π, over a disk of radius n, denoted by $\mathcal{B}_n(\boldsymbol{o})$. Any two points $\boldsymbol{p}^-$ and $\boldsymbol{p}^+$ in $\mathcal{B}_n(\boldsymbol{o})$ will almost surely not be hit by any of the lines from the Poisson line process Π and will therefore fail to be connected by Π. Arbitrarily let $\boldsymbol{p}^-$ be the source and $\boldsymbol{p}^+$ the destination. Accordingly, the movement from $\boldsymbol{p}^-$ to $\boldsymbol{p}^+$ will be given by the semi-perimeter routing rule [3]:

1. Consider the Poisson tessellation related to the Poisson line process Π. Then construct the convex cell $\mathcal{C}(\boldsymbol{p}^-, \boldsymbol{p}^+)$ containing $\boldsymbol{p}^-$ and $\boldsymbol{p}^+$ by deleting all Poisson lines from Π that separate $\boldsymbol{p}^-$ from $\boldsymbol{p}^+$.

2. From the source, $\boldsymbol{p}^-$, proceed in exactly the opposite direction to the destination, $\boldsymbol{p}^+$, until one first encounters a Poisson line $\ell \in \Pi$. This line will be part of the cell boundary $\partial\mathcal{C}(\boldsymbol{p}^-, \boldsymbol{p}^+)$, denote this point by $\tilde{\boldsymbol{p}^-}$.

3. Now, continue along in one or the other direction (clockwise or anti-clockwise), proceeding along the boundary of the cell $\mathcal{C}(\boldsymbol{p}^-, \boldsymbol{p}^+)$.

4. Continue along $\partial\mathcal{C}(\boldsymbol{p}^-, \boldsymbol{p}^+)$ until one reaches the set $\{t(\boldsymbol{p}^+ - \boldsymbol{p}^-) + \boldsymbol{p}^- : t \geq 0\}$, which is the ray extending from $\boldsymbol{p}^-$ and through $\boldsymbol{p}^+$, denote this point by $\tilde{\boldsymbol{p}^+}$. From $\tilde{\boldsymbol{p}^+}$ proceed down this ray to the destination $\boldsymbol{p}^+$.

Remark: Notice that if we exchange the roles for $\boldsymbol{p}^-$ and $\boldsymbol{p}^+$, the semi-perimeter routing rule will be exactly the same route. The only difference will be given by the traffic flow, which will be on the opposite direction, but still along the same route.

Depending on the choice of direction at step 3, this yields one of two possible routes. These are defined to be the *near-geodesics* from $\boldsymbol{p}^-$ to $\boldsymbol{p}^+$, see figure 2.1. These routes are to be considered in contrast to the actual *network geodesics*, which will
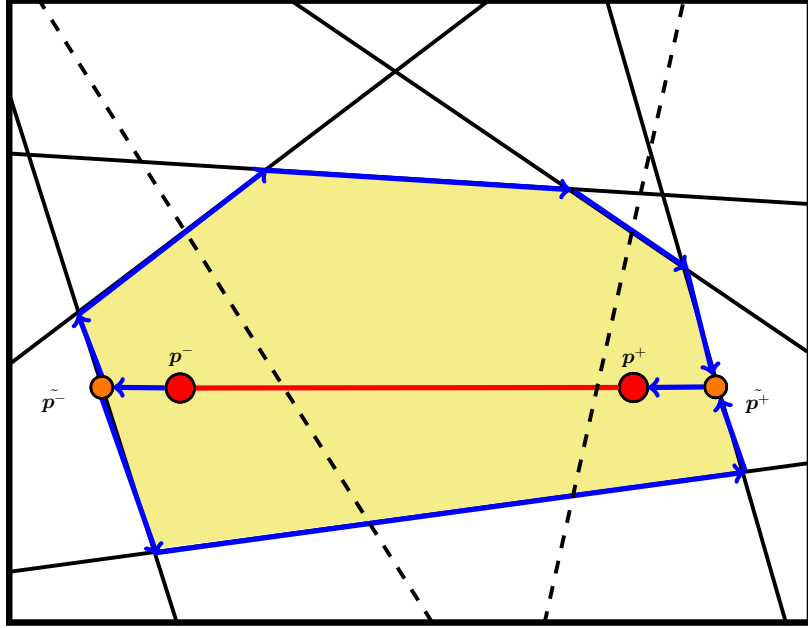
Figure 2.1: Construction of the convex cell $\mathcal{C}(\boldsymbol{p}^-, \boldsymbol{p}^+)$ (yellow tile), whose boundary, $\partial\mathcal{C}(\boldsymbol{p}^-, \boldsymbol{p}^+)$, represents the union of the two near-geodesics from $\boldsymbol{p}^-$ to $\boldsymbol{p}^+$. Figure based on [24, Figure 1]

always use the shortest network path, but can only be found by solving a difficult optimization problem. Nonetheless, Kendall [25, Section 2.3] shows that these near-geodesics are a good approximation to the true network geodesics.

This chapter analyses the asymptotic behaviour for the mean traffic at any point $\boldsymbol{q}$ in the Poissonian city using two different approaches: first, a direct computation regarding this expected value; and second, a coupling argument involving an improper anisotropic Poisson line process, $\tilde{\Pi}$.

Kendall [25, Theorem 5] showed that the mean traffic flow at the centre of the Poissonian city, conditioned on the presence of one line that goes through the centre, behaves asymptotically as $2n^3$. The following section will generalize the previous result to any point $\boldsymbol{q} = (tn, un)$ across the Poissonian city, conditioning on a horizontal line, $\ell_q : y = un$, passing through $\boldsymbol{q}$.

2.1 Mean traffic at any particular point

Set $\boldsymbol{q} = (tn, un)$, with $u \in [-1, 1]$ and $t \in [-\sqrt{1-u^2}, \sqrt{1-u^2}]$, and condition on a horizontal line $\ell_q : y = un$ being part of Π. Considering the (r, θ) coordinate system used to parametrize the line process Π, ℓ_q will be represented by $(u, 0)$. Since the disk has rotational symmetry, these calculations can be applied regardless of the angle θ from the conditioning line $\ell_q(\theta)$ passing through $\boldsymbol{q}$. To achieve this one will only require to apply a rotation to transform the original line $\ell_q(\theta)$ into an horizontal line,

which is an implicit change of coordinates, and then applied the results that we are going to explain below.

Consider that every $\boldsymbol{p}^-$ and $\boldsymbol{p}^+$ from $\mathcal{B}_n(\boldsymbol{o})$ generates an infinitesimal amount of flow: $\mathrm{d}\boldsymbol{p}^- \, \mathrm{d}\boldsymbol{p}^+$. This is divided equally between the two *near-geodesics* given by the semi-perimeter routing rule. Thence, the flow through $\boldsymbol{q}$ is expressed in terms of a 4-volume, which is given by the set

$$\mathcal{D}_n^q \quad = \quad \left\{ (\boldsymbol{p}^-, \boldsymbol{p}^+) \in \mathcal{B}_n(\boldsymbol{o})^2 : p_1^- < p_1^+, \boldsymbol{q} \in \partial\mathcal{C}(\boldsymbol{p}^-, \boldsymbol{p}^+) \right\} , \quad\quad (2.1)$$

where $\mathcal{C}(\boldsymbol{p}^-, \boldsymbol{p}^+)$ stands for the convex cell containing $\boldsymbol{p}^-$ and $\boldsymbol{p}^+$ which arises by deleting all the Poisson lines that separates $\boldsymbol{p}^-$ from $\boldsymbol{p}^+$ as explained before. In consequence, $\partial\mathcal{C}(\boldsymbol{p}^-, \boldsymbol{p}^+)$ is the union of the two possible near-geodesics that can be used to connect $\boldsymbol{p}^-$ and $\boldsymbol{p}^+$ through the semi-perimeter routing rule. Then the distribution of the total traffic through $\boldsymbol{q}$ is given by

$$T_n^q \quad = \quad \frac{1}{2} \iint \mathbb{1}_{\{(\boldsymbol{p}^-, \boldsymbol{p}^+) \in \mathcal{D}_n^q\}} \, \mathrm{d}\boldsymbol{p}^- \, \mathrm{d}\boldsymbol{p}^+ = \frac{1}{2} \iint_{\mathcal{B}_n(\boldsymbol{o})^2} \mathbb{1}_{\{p_1^- < p_1^+, \boldsymbol{q} \in \partial\mathcal{C}(\boldsymbol{p}^-, \boldsymbol{p}^+)\}} \, \mathrm{d}\boldsymbol{p}^- \, \mathrm{d}\boldsymbol{p}^+ \; .$$
$$(2.2)$$

The following two lemmas are required to understand the asymptotic behaviour, as $n \to \infty$, of the mean traffic flow through $\boldsymbol{q}$ under the circumstances described above. They focus on the performance of integrals with the following form:

$$\int_0^\pi \int_0^{R_1 n} \int_0^{R_2 n} g(r, s, \theta) r \, \mathrm{d}r \, s \, \mathrm{d}s \, \theta \, \mathrm{d}\theta , \quad\quad (2.3)$$

here $g(r, s, \theta) = \exp\left(-\frac{1}{2}(r + s - \sqrt{r^2 + s^2 + 2rs\cos\theta})\right)$ is a function in terms of r, s, θ; and $R_1, R_2 > 0$ are arbitrarily fixed values.

LEMMA 2.1. *[Small θ contribution]*
Consider the function $g(r, s, \theta)$ as before and a region of the form

$$\mathcal{A}_n \quad = \quad \{(r, s, \theta) : 0 \leq r \leq R_1 n, 0 \leq s \leq R_2 n, 0 \leq \theta \leq w_n\} ,$$

for some constants $R_1, R_2 > 0$ and $w_n \downarrow 0$ of the form $w_n = 1/n^\beta$, for any $\beta \in (0, 1/2)$. Then

$$\frac{n^\beta}{n^\beta + 1} R_1 R_2 (R_1 + R_2) n^3 \quad \leq \quad \iiint_{\mathcal{A}_n} g(r, s, \theta) r \, \mathrm{d}r \, s \, \mathrm{d}s \, \theta \, \mathrm{d}\theta \quad \leq \quad R_1 R_2 (R_1 + R_2) n^3 ,$$

therefore as $n \to \infty$ one can conclude that

$$\iiint_{\mathcal{A}_n} g(r, s, \theta) r \, \mathrm{d}r \, s \, \mathrm{d}s \, \theta \, \mathrm{d}\theta \quad \sim \quad R_1 R_2 (R_1 + R_2) n^3 .$$

19

Proof. First, consider the rescaled variables $r = \tilde{r}n$ and $s = \tilde{s}n$. Therefore

$$\int_0^{w_n} \int_0^{R_2 n} \int_0^{R_1 n} \exp\left(-\frac{1}{2}(r + s - \sqrt{r^2 + s^2 + 2rs\cos\theta})\right) r\, dr\, s\, ds\, \theta\, d\theta$$

$$= n^4 \int_0^{w_n} \int_0^{R_2} \int_0^{R_1} \exp\left(-\frac{n}{2}(\tilde{r} + \tilde{s} - \sqrt{\tilde{r}^2 + \tilde{s}^2 + 2\tilde{r}\tilde{s}\cos\theta})\right) \tilde{r}\, d\tilde{r}\, \tilde{s}\, d\tilde{s}\, \theta\, d\theta$$

$$= n^4 \left(\int_0^{w_n} \int_0^{R_2} \int_0^{\frac{R_1}{R_2}\tilde{s}} \exp\left(-\frac{n}{2}(\tilde{r} + \tilde{s} - \sqrt{\tilde{r}^2 + \tilde{s}^2 + 2\tilde{r}\tilde{s}\cos\theta})\right) \tilde{r}\, d\tilde{r}\, \tilde{s}\, d\tilde{s}\, \theta\, d\theta \right.$$

$$\left. + \int_0^{w_n} \int_0^{R_2} \int_{\frac{R_1}{R_2}\tilde{s}}^{R_1} \exp\left(-\frac{n}{2}(\tilde{r} + \tilde{s} - \sqrt{\tilde{r}^2 + \tilde{s}^2 + 2\tilde{r}\tilde{s}\cos\theta})\right) \tilde{r}\, d\tilde{r}\, \tilde{s}\, d\tilde{s}\, \theta\, d\theta \right).$$

$$(2.4)$$

Now, rescale the variable $\tilde{r}$ using $\tilde{r} = \hat{r}\tilde{s}$ and then rewrite $\sqrt{\hat{r}^2 + 1 + 2\hat{r}\cos\theta}$ as $\sqrt{(\hat{r} + 1)^2 - 2\hat{r}(1 - \cos\theta)}$. So, after factoring $(\hat{r}+1)$ the first integral in (2.4) satisfies

$$\int_0^{w_n} \int_0^{R_2} \int_0^{\frac{R_1}{R_2}\tilde{s}} \exp\left(-\frac{n}{2}(\tilde{r} + \tilde{s} - \sqrt{\tilde{r}^2 + \tilde{s}^2 + 2\tilde{r}\tilde{s}\cos\theta})\right) \tilde{r}\, d\tilde{r}\, \tilde{s}\, d\tilde{s}\, \theta\, d\theta$$

$$= \int_0^{w_n} \int_0^{R_2} \int_0^{\frac{R_1}{R_2}} \exp\left(-\frac{n\tilde{s}}{2}(\hat{r} + 1 - \sqrt{\hat{r}^2 + 1 + 2\hat{r}\cos\theta})\right) \hat{r}\, d\hat{r}\, \tilde{s}^3\, d\tilde{s}\, \theta\, d\theta$$

$$= \int_0^{w_n} \int_0^{R_2} \int_0^{\frac{R_1}{R_2}} \exp\left(-\frac{n\tilde{s}}{2}(\hat{r} + 1 - \sqrt{(\hat{r} + 1)^2 - 2\hat{r}(1 - \cos\theta)})\right) \hat{r}\, d\hat{r}\, \tilde{s}^3\, d\tilde{s}\, \theta\, d\theta$$

$$= \int_0^{w_n} \int_0^{R_2} \int_0^{\frac{R_1}{R_2}} \exp\left(-\frac{n\tilde{s}(\hat{r} + 1)}{2}\left(1 - \sqrt{1 - \frac{2\hat{r}(1 - \cos\theta)}{(\hat{r} + 1)^2}}\right)\right) \hat{r}\, d\hat{r}\, \tilde{s}^3\, d\tilde{s}\, \theta\, d\theta.$$

Notice that $\sqrt{1 - 2z} \sim 1 - z$ as $z \downarrow 0$, for $z = \hat{r}(1 - \cos\theta)/(\hat{r}+1)^2$ (which tends to zero as $\theta \downarrow 0$). In other words, $\sqrt{1 - 2z} \leq 1 - z$ for $z \in [0, 1/2]$ and $1 - z(1+w_n) \leq \sqrt{1 - 2z}$ for $z \in [0, 2w_n/(1 + w_n)^2]$. In consequence, the first integral in the last expression from (2.4) can be bounded above and below as follows

$$\int_0^{w_n} \int_0^{R_2} \int_0^{\frac{R_1}{R_2}} \exp\left(-\frac{n\tilde{s}\hat{r}}{2(\hat{r} + 1)}(1 - \cos\theta)(1 + w_n)\right) \hat{r}\, d\hat{r}\, \tilde{s}^3\, ds\, \theta\, d\theta \quad \leq$$

$$\int_0^{w_n} \int_0^{R_2} \int_0^{\frac{R_1}{R_2}} \exp\left(-\frac{n\tilde{s}(\hat{r} + 1)}{2}\left(1 - \sqrt{1 - \frac{2\hat{r}(1 - \cos\theta)}{(\hat{r} + 1)^2}}\right)\right) \hat{r}\, d\hat{r}\, \tilde{s}^3\, d\tilde{s}\, \theta\, d\theta$$

$$\leq \int_0^{w_n} \int_0^{R_2} \int_0^{\frac{R_1}{R_2}} \exp\left(-\frac{n\tilde{s}\hat{r}}{2(\hat{r} + 1)}(1 - \cos\theta)\right) \hat{r}\, d\hat{r}\, \tilde{s}^3\, ds\, \theta\, d\theta. \quad (2.5)$$

To analyse the upper bound, consider the change of variable $v = 1 - \cos\theta$, so

$$\int_0^{w_n} \int_0^{R_2} \int_0^{\frac{R_1}{R_2}} \exp\left(-\frac{n\tilde{s}\hat{r}}{2(\hat{r} + 1)}(1 - \cos\theta)\right) \hat{r}\, d\hat{r}\, \tilde{s}^3\, d\tilde{s}\, \theta\, d\theta$$

$$= \int_0^{1-\cos w_n} \int_0^{R_2} \int_0^{\frac{R_1}{R_2}} \exp\left(-\frac{n\tilde{s}\hat{r}}{2(\hat{r} + 1)}v\right) \hat{r}\, d\hat{r}\, \tilde{s}^3\, d\tilde{s}\, \frac{\theta}{\sin\theta}\, dv.$$

Even more, since $\theta \in [0, w_n]$ then we can approximate $\theta/\sin \theta$ by a Taylor series argument, say $\sin \theta = \theta - \theta^3/3! + \psi^5/5!$ for some $\psi \in (0, w_n)$. In consequence, $1 \leq \theta/\sin \theta \leq \theta/(\theta - \theta^3/3!) = 1 + \theta^2/(6 - \theta^2) \leq 1 + w_n^2/5$, for any $\theta \in [0, w_n]$. These inequalities implies that

$$\int_0^{1-\cos w_n} \int_0^{R_2} \int_0^{\frac{R_1}{R_2}} \exp\left(-\frac{n\tilde{s}\hat{r}}{2(\hat{r}+1)} v\right) \hat{r} \, d\hat{r} \, \tilde{s}^3 \, d\tilde{s} \, dv$$

$$\leq \int_0^{1-\cos w_n} \int_0^{R_2} \int_0^{\frac{R_1}{R_2}} \exp\left(-\frac{n\tilde{s}\hat{r}}{2(\hat{r}+1)} v\right) \hat{r} \, d\hat{r} \, \tilde{s}^3 \, d\tilde{s} \, \frac{\theta}{\sin \theta} \, dv \leq$$

$$\left(1 + \frac{w_n^2}{5}\right) \int_0^{1-\cos w_n} \int_0^{R_2} \int_0^{\frac{R_1}{R_2}} \exp\left(-\frac{n\tilde{s}\hat{r}}{2(\hat{r}+1)} v\right) \hat{r} \, d\hat{r} \, \tilde{s}^3 \, d\tilde{s} \, dv \, .$$

Therefore, as $n \to \infty$, so that $w_n \downarrow 0$,

$$\int_0^{1-\cos w_n} \int_0^{R_2} \int_0^{\frac{R_1}{R_2}} \exp\left(-\frac{n\tilde{s}\hat{r}}{2(\hat{r}+1)} v\right) \hat{r} \, d\hat{r} \, \tilde{s}^3 \, d\tilde{s} \, \frac{\theta}{\sin \theta} \, dv$$

$$\sim \int_0^{1-\cos w_n} \int_0^{R_2} \int_0^{\frac{R_1}{R_2}} \exp\left(-\frac{n\tilde{s}\hat{r}}{2(\hat{r}+1)} v\right) \hat{r} \, d\hat{r} \, \tilde{s}^3 \, d\tilde{s} \, dv \, .$$

Notice that the integral for v from 0 to $(1 - \cos w_n)$ will behave asymptotically in the same way as the integral from 0 to ∞, as long as

$$\exp\left(-\frac{n\tilde{s}\hat{r}}{2(\hat{r}+1)}(1 - \cos w_n)\right) \to 0 \qquad \text{as } n \to \infty \, .$$

This happens when $\lim_{n\to\infty} n(1 - \cos w_n) = \infty$, which is the case for any $\beta \in (0, 1/2)$, since by Taylor expansion series argument: $1 - \cos w_n = w_n^2/2! - \psi^4/4!$ for some $\psi \in (0, 2w_n)$, so

$$\frac{w_n^2}{2!}\left(1 - \frac{w_n^2}{3}\right) n \leq (1 - \cos w_n)n \leq \frac{w_n^2}{2!} n \, .$$

Recall, $w_n = 1/n^\beta$. Hence, for $\beta \in (0, 1/2)$

$$\lim_{n\to\infty} \frac{w_n^2}{2!}\left(1 - \frac{w_n^2}{3}\right) n = \lim_{n\to\infty} \frac{n^{1-2\beta}}{2}\left(1 - \frac{1}{3n^{2\beta}}\right) = \infty \, .$$

Therefore, as $n \to \infty$

$$\int_{1-\cos w_n}^\infty \int_0^{R_2} \int_0^{\frac{R_1}{R_2}} \exp\left(-\frac{n\tilde{s}\hat{r}}{2(\hat{r}+1)} v\right) dv \, \hat{r} \, d\hat{r} \, \tilde{s}^3 \, d\tilde{s}$$

$$= \int_0^{R_2} \int_0^{\frac{R_1}{R_2}} \frac{2(\hat{r}+1)}{n\tilde{s}\hat{r}} \exp\left(-\frac{n\tilde{s}\hat{r}}{2(\hat{r}+1)}(1 - \cos w_n)\right) \hat{r} \, d\hat{r} \, \tilde{s}^3 \, d\tilde{s} = o\left(\frac{1}{n}\right) \, .$$

Thus, asymptotically as $n \to \infty$ it follows that:

$$\int_0^{1-\cos w_n} \int_0^{R_2} \int_0^{\frac{R_1}{R_2}} \exp\left(-\frac{n\tilde{s}\hat{r}}{2(\hat{r}+1)}v\right)\hat{r}\,d\hat{r}\,\tilde{s}^3\,d\tilde{s}\,dv$$

$$\sim \quad \int_0^{\frac{R_1}{R_2}} \int_0^{R_2} \int_0^{\infty} \exp\left(-\frac{n\tilde{s}\hat{r}}{2(\hat{r}+1)}v\right)dv\,\tilde{s}^3\,d\tilde{s}\,\hat{r}\,d\hat{r}$$

$$= \quad \int_0^{\frac{R_1}{R_2}} \int_0^{R_2} \frac{2(\hat{r}+1)}{n\tilde{s}\hat{r}}\tilde{s}^3\,d\tilde{s}\,\hat{r}\,d\hat{r} = \frac{1}{n}\int_0^{\frac{R_1}{R_2}} 2(\hat{r}+1)\,d\hat{r}\int_0^{R_2}\tilde{s}^2\,d\tilde{s}$$

$$= \quad \frac{1}{n}\left(\left(\frac{R_1}{R_2}+1\right)^2 - 1\right)\frac{R_2^3}{3} = \frac{1}{n}\frac{R_1^2 + 2R_1R_2 + R_2^2 - R_2^2}{R_2^2}\frac{R_2^3}{3}$$

$$= \quad \frac{1}{3n}R_2(R_1^2 + 2R_1R_2)\,.$$

On the other hand, the asymptotic behaviour for the lower bound in (2.5) can be found by following exactly the same computations as in the upper bound, since $(1+w_n)$ is just another constant for the triple integral (recall $w_n = 1/n^\beta$). That is, first consider the change of variable $v = 1 - \cos\theta$, so

$$\int_0^{w_n} \int_0^{R_2} \int_0^{\frac{R_1}{R_2}} \exp\left(-\frac{n\tilde{s}\hat{r}}{2(\hat{r}+1)}(1-\cos\theta)(1+w_n)\right)\hat{r}\,d\hat{r}\,\tilde{s}^3\,d\tilde{s}\,\theta\,d\theta$$

$$= \quad \int_0^{1-\cos w_n} \int_0^{R_2} \int_0^{\frac{R_1}{R_2}} \exp\left(-\frac{n\tilde{s}\hat{r}}{2(\hat{r}+1)}v(1+w_n)\right)\hat{r}\,d\hat{r}\,\tilde{s}^3\,d\tilde{s}\,\frac{\theta}{\sin\theta}\,dv\,.$$

Then, since $1 \le \theta/\sin\theta \le 1 + w_n^2/5$ for any $\theta \in [0, w_n]$, it follows that

$$\int_0^{1-\cos w_n} \int_0^{R_2} \int_0^{\frac{R_1}{R_2}} \exp\left(-\frac{n\tilde{s}\hat{r}}{2(\hat{r}+1)}v(1+w_n)\right)\hat{r}\,d\hat{r}\,\tilde{s}^3\,d\tilde{s}\,dv$$

$$\le \quad \int_0^{1-\cos w_n} \int_0^{R_2} \int_0^{\frac{R_1}{R_2}} \exp\left(-\frac{n\tilde{s}\hat{r}}{2(\hat{r}+1)}v(1+w_n)\right)\hat{r}\,d\hat{r}\,\tilde{s}^3\,d\tilde{s}\,\frac{\theta}{\sin\theta}\,dv \quad \le$$

$$\left(1+\frac{w_n^2}{5}\right)\int_0^{1-\cos w_n} \int_0^{R_2} \int_0^{\frac{R_1}{R_2}} \exp\left(-\frac{n\tilde{s}\hat{r}}{2(\hat{r}+1)}v(1+w_n)\right)\hat{r}\,d\hat{r}\,\tilde{s}^3\,d\tilde{s}\,dv\,.$$

Moreover, as in the case for the upper bound in (2.5) the above integral for v from 0 to $(1 - \cos w_n)$ behaves asymptotically (as $n \to \infty$) the same way as the integral from 0 to ∞, therefore

$$\int_0^{1-\cos w_n} \int_0^{R_2} \int_0^{\frac{R_1}{R_2}} \exp\left(-\frac{n\tilde{s}\hat{r}}{2(\hat{r}+1)}v(1+w_n)\right)\hat{r}\,\mathrm{d}\hat{r}\,\tilde{s}^3\,\mathrm{d}\tilde{s}\,\mathrm{d}v$$

$$\sim \int_0^{\frac{R_1}{R_2}} \int_0^{R_2} \int_0^{\infty} \exp\left(-\frac{n\tilde{s}\hat{r}}{2(\hat{r}+1)}v(1+w_n)\right)\mathrm{d}v\,\tilde{s}^3\,\mathrm{d}\tilde{s}\,\hat{r}\,\mathrm{d}\hat{r}$$

$$= \int_0^{\frac{R_1}{R_2}} \int_0^{R_2} \frac{2(\hat{r}+1)}{n\tilde{s}\hat{r}(1+w_n)}\tilde{s}^3\,\mathrm{d}\tilde{s}\,\hat{r}\,\mathrm{d}\hat{r}$$

$$= \frac{1}{n(1+w_n)}\int_0^{\frac{R_1}{R_2}} 2(\hat{r}+1)\,\mathrm{d}\hat{r}\int_0^{R_2}\tilde{s}^2\,\mathrm{d}\tilde{s}$$

$$= \frac{1}{n(1+w_n)}\left(\left(\frac{R_1}{R_2}+1\right)^2-1\right)\frac{R_2^3}{3}$$

$$= \frac{1}{n(1+w_n)}\frac{R_1^2+2R_1R_2+R_2^2-R_2^2}{R_2^2}\frac{R_2^3}{3}$$

$$= \frac{n^\beta}{n^\beta+1}\frac{1}{3n}R_2(R_1^2+2R_1R_2)\,.$$

In conclusion

$$\int_0^{w_n}\int_0^{R_2}\int_0^{\frac{R_1}{R_2}}\exp\left(-\frac{n\tilde{s}\hat{r}}{2(\hat{r}+1)}(1-\cos\theta)(1+w_n)\right)\hat{r}\,\mathrm{d}\hat{r}\,\tilde{s}^3\,\mathrm{d}s\,\theta\,\mathrm{d}\theta$$

$$\sim \frac{1}{1+w_n}\frac{1}{3n}R_2(R_1^2+2R_1R_2) \quad = \quad \frac{n^\beta}{n^\beta+1}\frac{1}{3n}R_2(R_1^2+2R_1R_2)\,.$$

In consequence from (2.5) it follows that the first integral in the last expression of (2.4) satisfies the following inequalities

$$\frac{n^\beta}{n^\beta+1}\frac{1}{3n}R_2(R_1^2+2R_1R_2) \quad\le$$

$$\int_0^{w_n}\int_0^{R_2}\int_0^{\frac{R_1}{R_2}}\exp\left(-\frac{n\tilde{s}(\hat{r}+1)}{2}\left(1-\sqrt{1-\frac{2\hat{r}(1-\cos\theta)}{(\hat{r}+1)^2}}\right)\right)\hat{r}\,\mathrm{d}\hat{r}\,\tilde{s}^3\,\mathrm{d}\tilde{s}\,\theta\,\mathrm{d}\theta$$

$$\le \quad \frac{1}{3n}R_2(R_1^2+2R_1R_2)\,.$$

In other words, as $n\to\infty$

$$\int_0^{w_n}\int_0^{R_2}\int_0^{\frac{R_1}{R_2}}\exp\left(-\frac{n\tilde{s}(\hat{r}+1)}{2}\left(1-\sqrt{1-\frac{2\hat{r}(1-\cos\theta)}{(\hat{r}+1)^2}}\right)\right)\hat{r}\,\mathrm{d}\hat{r}\,\tilde{s}^3\,\mathrm{d}\tilde{s}\,\theta\,\mathrm{d}\theta$$

$$\sim \quad \frac{1}{3n}R_2(R_1^2+2R_1R_2)\,.$$

Finally, the second integral in the final expression of (2.4) can be rewritten by ex-

changing the order of integration between $\tilde{r}$ and $\tilde{s}$ as follows

$$\int_0^{w_n} \int_0^{R_2} \int_{\frac{R_1}{R_2}\tilde{s}}^{R_1} \exp\left(-\frac{n}{2}(\tilde{r}+\tilde{s}-\sqrt{\tilde{r}^2+\tilde{s}^2+2\tilde{r}\tilde{s}\cos\theta})\right)\tilde{r}\,\mathrm{d}\tilde{r}\,\tilde{s}\,\mathrm{d}\tilde{s}\,\theta\,\mathrm{d}\theta \quad =$$

$$\int_0^{w_n} \int_0^{R_1} \int_0^{\frac{R_2}{R_1}\tilde{r}} \exp\left(-\frac{n}{2}(\tilde{s}+\tilde{r}-\sqrt{\tilde{s}^2+\tilde{r}^2+2\tilde{r}\tilde{s}\cos\theta})\right)\tilde{s}\,\mathrm{d}\tilde{s}\,\tilde{r}\,\mathrm{d}\tilde{r}\,\theta\,\mathrm{d}\theta\,;$$

which, by the same calculations as the first integral (just interchange the roles of R_1 and R_2), leads to the following expression

$$\int_0^{w_n} \int_0^{R_1} \int_0^{\frac{R_2}{R_1}\tilde{r}} \exp\left(-\frac{n}{2}(\tilde{s}+\tilde{r}-\sqrt{\tilde{s}^2+\tilde{r}^2+2\tilde{r}\tilde{s}\cos\theta})\right)\tilde{s}\,\mathrm{d}\tilde{s}\,\tilde{r}\,\mathrm{d}\tilde{r}\,\theta\,\mathrm{d}\theta$$

$$\sim \quad \frac{1}{3n}R_1(R_2^2+2R_2R_1)\,.$$

In conclusion

$$\int_0^{w_n} \int_0^{R_2 n} \int_0^{R_1 n} \exp\left(-\frac{1}{2}(r+s-\sqrt{r^2+s^2+2rs\cos\theta})\right)r\,\mathrm{d}r\,s\,\mathrm{d}s\,\theta\,\mathrm{d}\theta$$

$$\sim \quad n^4\left(\frac{1}{3n}R_2(R_1^2+2R_1R_2)+\frac{1}{3n}R_1(R_2^2+2R_2R_1)\right)$$

$$= \quad n^3\frac{3R_1^2 R_2+3R_1 R_2^2}{3} \quad = \quad R_1 R_2(R_1+R_2)n^3\,.$$

$\square$

Now, to control the other region of integration on (2.3) one can apply the following result.

LEMMA 2.2. *[Large θ contribution]*
Consider the function $g(r,s,\theta)$ as before and a region of the form

$$\mathcal{E}_n \quad = \quad \{(r,s,\theta) : 0 \le r \le R_3 n,\, 0 \le s \le R_3 n,\, w_n \le \theta \le \pi\}\,,$$

for some constant $R_3 > 0$ and $w_n \downarrow 0$ of the form $w_n = 1/n^\beta$, for any $\beta > 0$. Then, asymptotically as $n \to \infty$

$$\iiint_{\mathcal{E}_n} g(r,s,\theta)r\,\mathrm{d}r\,s\,\mathrm{d}s\,\theta\,\mathrm{d}\theta \quad \le \quad 8\frac{(\pi^2-w_n^2)R_3^2}{(1-\cos w_n)^2}n^2 \quad = \quad \mathcal{O}\!\left(n^{2+4\beta}\right)\,.$$

Proof. As in Lemma 2.1, first use the rescaled variables $r = \tilde{r}n$ and $s = \tilde{s}n$. Notice that for this case R_1 and R_2 have the common value R_3, thus the final two integrals in the expression (2.4) are the same (after exchanging the order of integration of $\tilde{r}$

and $\tilde{s}$ in the second integral). That is

$$\int_0^{w_n} \int_0^{R_3} \int_{\frac{R_3}{R_3}\tilde{s}}^{R_3} \exp\left(-\frac{n}{2}(\tilde{r}+\tilde{s}-\sqrt{\tilde{r}^2+\tilde{s}^2+2\tilde{r}\tilde{s}\cos\theta})\right)\tilde{r}\,\mathrm{d}\tilde{r}\,\tilde{s}\,\mathrm{d}\tilde{s}\,\theta\,\mathrm{d}\theta \quad =$$

$$\int_0^{w_n} \int_0^{R_3} \int_0^{\tilde{r}} \exp\left(-\frac{n}{2}(\tilde{s}+\tilde{r}-\sqrt{\tilde{s}^2+\tilde{r}^2+2\tilde{r}\tilde{s}\cos\theta})\right)\tilde{s}\,\mathrm{d}\tilde{s}\,\tilde{r}\,\mathrm{d}\tilde{r}\,\theta\,\mathrm{d}\theta\,.$$

Therefore, it follows

$$\int_{w_n}^{\pi} \int_0^{R_3 n} \int_0^{R_3 n} \exp\left(-\frac{1}{2}(r+s-\rho)\right)r\,\mathrm{d}r\,s\,\mathrm{d}s\,\theta\,\mathrm{d}\theta$$

$$= \quad n^4 \int_{w_n}^{\pi} \int_0^{R_3} \int_0^{R_3} \exp\left(-\frac{n}{2}(\tilde{r}+\tilde{s}-\sqrt{\tilde{r}^2+\tilde{s}^2+2\tilde{r}\tilde{s}\cos\theta})\right)\tilde{r}\,\mathrm{d}\tilde{r}\,\tilde{s}\,\mathrm{d}\tilde{s}\,\theta\,\mathrm{d}\theta$$

$$= \quad 2n^4 \int_{w_n}^{\pi} \int_0^{R_3} \int_0^{\tilde{s}} \exp\left(-\frac{n}{2}(\tilde{r}+\tilde{s}-\sqrt{\tilde{r}^2+\tilde{s}^2+2\tilde{r}\tilde{s}\cos\theta})\right)\tilde{r}\,\mathrm{d}\tilde{r}\,\tilde{s}\,\mathrm{d}\tilde{s}\,\theta\,\mathrm{d}\theta\,.$$

Then, following similar steps as in Lemma 2.1 rescale the variable $\tilde{r}$ using $\tilde{r} = \hat{r}\tilde{s}$, rewrite $\sqrt{\hat{r}^2+1+2\hat{r}\cos\theta}$ as $\sqrt{(\hat{r}+1)^2-2\hat{r}(1-\cos\theta)}$ and use the fact that $\sqrt{1-2z} \leq 1-z$ for $z \in [0,1/2]$, with the same z as before, i.e. $z = (1-\cos\theta)/(r+1)^2$. Thus an upper bound for the desired integral can be produced as follows:

$$2n^4 \int_{w_n}^{\pi} \int_0^{R_3} \int_0^{s} \exp\left(-\frac{n}{2}(\tilde{r}+\tilde{s}-\sqrt{\tilde{r}^2+\tilde{s}^2+2\tilde{r}\tilde{s}\cos\theta})\right)\tilde{r}\,\mathrm{d}\tilde{r}\,\tilde{s}\,\mathrm{d}\tilde{s}\,\theta\,\mathrm{d}\theta$$

$$= \quad 2n^4 \int_{w_n}^{\pi} \int_0^{R_3} \int_0^1 \exp\left(-\frac{n\tilde{s}(\hat{r}+1)}{2}\left(1-\sqrt{1-2\frac{\hat{r}(1-\cos\theta)}{(\hat{r}+1)^2}}\right)\right)\hat{r}\,\mathrm{d}\hat{r}\,\tilde{s}^3\,\mathrm{d}\tilde{s}\,\theta\,\mathrm{d}\theta$$

$$\leq \quad 2n^4 \int_{w_n}^{\pi} \int_0^{R_3} \int_0^1 \exp\left(-\frac{n\tilde{s}\hat{r}}{2(\hat{r}+1)}(1-\cos\theta)\right)\hat{r}\,\mathrm{d}\hat{r}\,\tilde{s}^3\,\mathrm{d}\tilde{s}\,\theta\,\mathrm{d}\theta$$

$$\leq \quad 2n^4 \frac{\pi^2-w_n^2}{2} \int_0^{R_3} \int_0^1 \exp\left(-\frac{n\tilde{s}\hat{r}}{2(\hat{r}+1)}(1-\cos w_n)\right)\hat{r}\,\mathrm{d}\hat{r}\,\tilde{s}^3\,\mathrm{d}\tilde{s}$$

$$\leq \quad n^4(\pi^2-w_n^2) \int_0^{R_3} \int_0^{\infty} \exp\left(-\frac{n\tilde{s}\hat{r}}{4}(1-\cos w_n)\right)\hat{r}\,\mathrm{d}\hat{r}\,\tilde{s}^3\,\mathrm{d}\tilde{s}$$

$$= \quad (\pi^2-w_n^2)\left(\frac{4}{1-\cos w_n}\right)^2 n^2 \int_0^{R_3} \tilde{s}\,\mathrm{d}\tilde{s} \quad = \quad 8(\pi^2-w_n^2)\left(\frac{R_3}{1-\cos w_n}\right)^2 n^2\,.$$

Finally, by Taylor expansion $1-\cos w_n = w_n^2/2! - \psi^4/4!$ for some $\psi \in (0, 2w_n)$, equivalently $w_n^2/2(1-4w_n^2/3) \leq (1-\cos w_n) \leq w_n^2/2$. Therefore

$$8(\pi^2-w_n^2)\left(\frac{2R_3}{w_n^2}\right)^2 n^2 \quad \leq \quad 8(\pi^2-w_n^2)\left(\frac{R_3}{1-\cos w_n}\right)^2 n^2$$

$$\leq \quad 8(\pi^2-w_n^2)\left(\frac{2R_3}{w_n^2(1-\frac{4w_n^2}{3})}\right)^2 n^2\,.$$

Hence, as $w_n = 1/n^\beta$, for some $\beta > 0$ it follows

$$8 \left(\pi^2 - \frac{1}{n^{2\beta}} \right) 4R_3^2 n^{2+4\beta} \quad \leq \quad 8 \left(\pi^2 - \frac{1}{n^{2\beta}} \right) \left(\frac{R_3}{1 - \cos w_n} \right)^2 n^2$$

$$\leq \quad 8\pi^2 4R_3^2 n^{2+4\beta} \left(\frac{1}{1 - \frac{4}{3n^{2\beta}}} \right)^2 .$$

In conclusion

$$8(\pi^2 - w_n^2) \left(\frac{R_3}{1 - \cos w_n} \right)^2 n^2 \quad \sim \quad 32\pi^2 R_3^2 n^{2+4\beta} \qquad \text{as } n \to \infty .$$

$\square$

Thus, the asymptotic behaviour of the mean traffic through $\boldsymbol{q} = (tn, un)$ is characterized by the next result

THEOREM 2.1. *[Mean traffic flow through the point $\boldsymbol{q} = (tn, un)$ and its asymptotic behaviour]*
The mean flow through the point $\boldsymbol{q} = (tn, un)$, $u \in (-1, 1)$ and $t \in (-\sqrt{1 - u^2}, \sqrt{1 - u^2})$, conditioned on the existence of an horizontal line, that is $\ell_q \in \Pi$ with $\ell_q : y = un$, is given by

$$\mathbb{E}[T_n^q] \quad = \quad \frac{1}{2} \iiiint_{\mathcal{D}_{n,-}^q} g(r, s, \alpha_1, \alpha_2) r \, \mathrm{d}r \, s \, \mathrm{d}s \, \mathrm{d}\alpha_1 \, \mathrm{d}\alpha_2$$

$$+ \quad \frac{1}{2} \iiiint_{\mathcal{D}_{n,+}^q} g(r, s, \alpha_1, \alpha_2) r \, \mathrm{d}r \, s \, \mathrm{d}s \, \mathrm{d}\alpha_1 \, \mathrm{d}\alpha_2 . \quad (2.6)$$

Here $g(r, s, \alpha_1, \alpha_2) = \exp\left(-\frac{1}{2}(r + s - \sqrt{r^2 + s^2 + 2rs\cos(\alpha_1 + \alpha_2)}) \right)$ is the probability that there are no lines from the Poisson line process Π separating the points $\boldsymbol{p}^- = (r, \alpha_1)$ and $\boldsymbol{p}^+ = (s, \alpha_2)$ (in polar coordinates with $\boldsymbol{q}$ as the reference point) simultaneously from $\boldsymbol{q}$, where $\mathcal{D}_{n,\pm}^q$ are the appropriate regions of integration for $(r, s, \alpha_1, \alpha_2)$ which depends on the location of the point $\boldsymbol{q}$. Thus

$$\mathcal{D}_{n,-}^q \quad = \quad \{(r, s, \alpha_1, \alpha_2) : r \in [0, h_1^q(\alpha_1)n], s \in [0, h_2^q(\alpha_2)n], \alpha_1 \in [-\pi, 0], \alpha_2 \in [-\pi, 0]\},$$

$$(2.7)$$

$$\mathcal{D}_{n,+}^q \quad = \quad \{(r, s, \alpha_1, \alpha_2) : r \in [0, h_1^q(\alpha_1)n], s \in [0, h_2^q(\alpha_2)n], \alpha_1 \in [0, \pi], \alpha_2 \in [0, \pi]\}.$$

$$(2.8)$$

Here $h_1^q(\alpha_1)$ (respectively $h_2^q(\alpha_2)$) is a continuous function that expresses how the maximum allowed distance from the point $\boldsymbol{p}^-$ (respectively $\boldsymbol{p}^+$) to $\boldsymbol{q}$ changes depending on the angle α_1 (respectively α_2). Therefore

$$h_1^q(\alpha_1) \quad = \quad (x_1 + t)\sec\alpha_1 \qquad \text{and} \qquad h_2^q(\alpha_2) \quad = \quad (x_2 - t)\sec\alpha_2 ,$$

where x_1 (respectively x_2) is the absolute value of the x-coordinate from the intersection point between the line $y = -(x-t)\tan\alpha_1 + u$ (respectively $y = (x-t)\tan\alpha_2 + u$) and the unit circle $x^2 + y^2 = 1$. This leads to the following expressions

$$
\begin{aligned}
x_1 &= |\sqrt{\sec^2\alpha_1 - (u + t\tan\alpha_1)^2} - \tan\alpha_1(u + t\tan\alpha_1)|\cos^2\alpha_1\,, \\
x_2 &= |\sqrt{\sec^2\alpha_2 - (u - t\tan\alpha_2)^2} - \tan\alpha_2(u - t\tan\alpha_2)|\cos^2\alpha_2\,.
\end{aligned}
$$

Moreover, asymptotically as $n \to \infty$

$$
\mathbb{E}[T_n^q] \quad \sim \quad 2\sqrt{1-u^2}(1 - u^2 - t^2)n^3\,. \tag{2.9}
$$
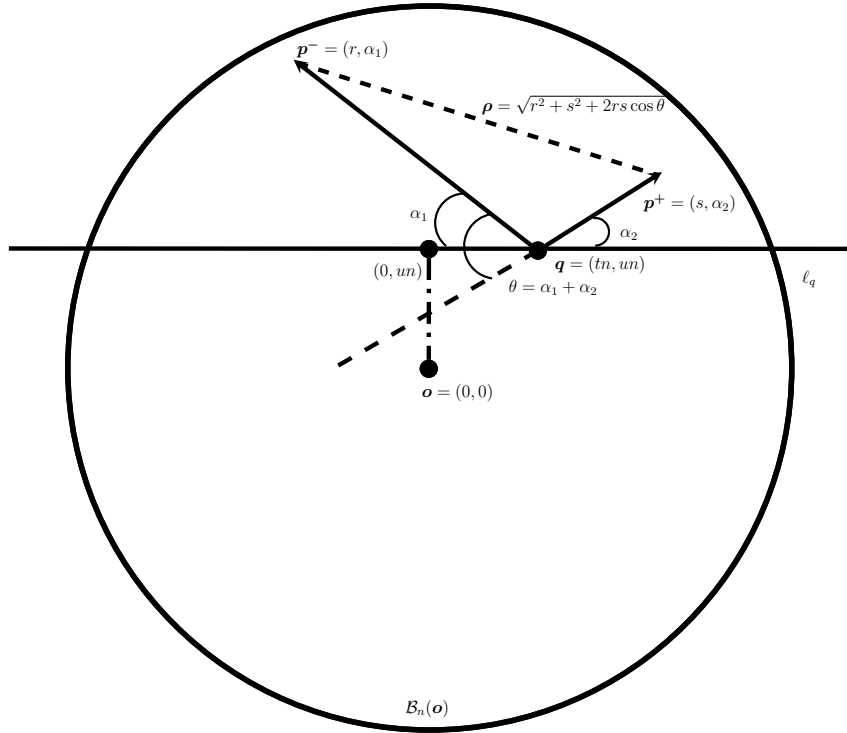
Figure 2.2: Illustration of concepts used in Theorem 2.1.

Proof. First, the expression (2.6) can be derived by stochastic geometry arguments. The traffic flow going from $\boldsymbol{p}^-$ to $\boldsymbol{p}^+$ will contribute to the expected amount of traffic through $\boldsymbol{q}$, as long as $\boldsymbol{q}$ belongs to the semi-perimeter route, as explained above. If $\boldsymbol{p}^-$ and $\boldsymbol{p}^+$ are separated by the line $\ell_q : y = un$, then there will be no contribution from the traffic flow between those points to $\boldsymbol{q}$, because the construction of the semi-perimeter route implies that the line ℓ_q will be censored / deleted for this case. So, both $\boldsymbol{p}^-$ and $\boldsymbol{p}^+$ must lie on the same side of the disk (both above or below the line ℓ_q).

Moreover, to guarantee that $\boldsymbol{q} \in \partial\mathcal{C}(\boldsymbol{p}^-, \boldsymbol{p}^+)$ there should be no lines from the Poisson line process Π that separates simultaneously $\boldsymbol{p}^-, \boldsymbol{p}^+$ from $\boldsymbol{q}$. As we are dealing

with a Poisson process the probability of this event is given by $\exp\left(-\Lambda(A)\right)$: here Λ is the intensity measure of the Poisson line process and A represents the region that should be avoided by the Poisson line process, see figure 2.2.

One has to avoid lines that intersects the segment connecting $\boldsymbol{p}^-$ to $\boldsymbol{q}$ (with length r), or the segment that connects $\boldsymbol{p}^+$ to $\boldsymbol{q}$ (with length s), this can be done by applying Kendall [26, Exercise 1.6]. The invariant measure of this ensemble of lines is bounded above by $r+s$. However, there are some of these lines that should not be considered as they do not separate $\boldsymbol{p}^-,\boldsymbol{p}^+$ simultaneously from $\boldsymbol{q}$. Those lines (that does not belong to A) are exactly the same set of lines that also intersect the segment that connects $\boldsymbol{p}^-$ and $\boldsymbol{p}^+$, whose length is given by $\rho = \sqrt{r^2 + s^2 + 2rs\cos\theta}$, here $\theta = \alpha_1 + \alpha_2$. So the desired expression is

$$\Lambda(A) = \frac{1}{2}\left(r + s - \sqrt{r^2 + s^2 + 2rs\cos\theta}\right).$$

Now, notice that $\alpha_1, \alpha_2 \in [-\pi, \pi]$ and since $p_1^- < p_1^+$ then it follows that $\theta = (\alpha_1 + \alpha_2) \in [-\pi, \pi]$. Therefore

$$
\begin{aligned}
\mathbb{E}[T_n^q] \;=\; & \frac{1}{2}\iint \mathbb{E}[\mathbb{1}_{\{(\boldsymbol{p}^-,\boldsymbol{p}^+)\in\mathcal{D}_n^q\}}]\,\mathrm{d}\boldsymbol{p}^-\;\mathrm{d}\boldsymbol{p}^+ \\
=\; & \frac{1}{2}\iint \mathbb{E}[\mathbb{1}_{\{(\boldsymbol{p}^-,\boldsymbol{p}^+)\in\mathcal{D}_n^q,\,p_2^-,p_2^+\geq un\}}]\,\mathrm{d}\boldsymbol{p}^-\;\mathrm{d}\boldsymbol{p}^+ + \frac{1}{2}\iint \mathbb{E}[\mathbb{1}_{\{(\boldsymbol{p}^-,\boldsymbol{p}^+)\in\mathcal{D}_n^q,\,p_2^-,p_2^+<un\}}]\,\mathrm{d}\boldsymbol{p}^-\;\mathrm{d}\boldsymbol{p}^+ \\
=\; & \frac{1}{2}\int_0^\pi\int_0^\pi\int_0^{h_2^q(\alpha_2)n}\int_0^{h_1^q(\alpha_1)n}\exp\left(-\frac{1}{2}(r+s-\sqrt{r^2+s^2+2rs\cos\theta})\right)r\,\mathrm{d}r\,s\,\mathrm{d}s\,\mathrm{d}\alpha_1\,\mathrm{d}\alpha_2 \\
& + \frac{1}{2}\int_{-\pi}^0\int_{-\pi}^0\int_0^{h_2^q(\alpha_2)n}\int_0^{h_1^q(\alpha_1)n}\exp\left(-\frac{1}{2}(r+s-\sqrt{r^2+s^2+2rs\cos\theta})\right)r\,\mathrm{d}r\,s\,\mathrm{d}s\,\mathrm{d}\alpha_1\,\mathrm{d}\alpha_2\,.
\end{aligned}
$$

Here $h_1^q(\alpha_1)$ is a continuous function that expresses how the maximum allowed distance from the point $\boldsymbol{p}^-$ to $\boldsymbol{q}$ changes depending on the angle it makes. Similarly, $h_2^q(\alpha_2)$ represents the maximum allowed distance from $\boldsymbol{p}^+$ to $\boldsymbol{q}$ in terms of α_2.

All this leads to the first expression:

$$
\begin{aligned}
\mathbb{E}[T_n^q] \;=\; & \frac{1}{2}\iiiint_{\mathcal{D}_{n,-}^q} g(r,s,\alpha_1,\alpha_2)r\,\mathrm{d}r\,s\,\mathrm{d}s\,\mathrm{d}\alpha_1\,\mathrm{d}\alpha_2 \\
& + \frac{1}{2}\iiiint_{\mathcal{D}_{n,+}^q} g(r,s,\alpha_1,\alpha_2)r\,\mathrm{d}r\,s\,\mathrm{d}s\,\mathrm{d}\alpha_1\,\mathrm{d}\alpha_2\,,
\end{aligned}
$$

with

$$
\begin{aligned}
\mathcal{D}_{n,-}^q &= \{(r,s,\alpha_1,\alpha_2) : r \in [0, h_1^q(\alpha_1)n], s \in [0, h_2^q(\alpha_2)n], \alpha_1 \in [-\pi,0], \alpha_2 \in [-\pi,0]\}, \\
\mathcal{D}_{n,+}^q &= \{(r,s,\alpha_1,\alpha_2) : r \in [0, h_1^q(\alpha_1)n], s \in [0, h_2^q(\alpha_2)n], \alpha_1 \in [0,\pi], \alpha_2 \in [0,\pi]\}.
\end{aligned}
$$

Here

$$h_1^q(\alpha_1) = \left(\left(\sqrt{\sec^2\alpha_1 - (u + t\tan\alpha_1)^2} - \tan\alpha_1(u + t\tan\alpha_1)\right)\cos^2\alpha_1 + t\right)\sec\alpha_1,$$

$$h_2^q(\alpha_2) = \left(\left(\sqrt{\sec^2\alpha_2 - (u - t\tan\alpha_2)^2} - \tan\alpha_2(u - t\tan\alpha_2)\right)\cos^2\alpha_2 - t\right)\sec\alpha_2.$$

The asymptotic behaviour of the expected amount of traffic flow through $\boldsymbol{q}$, conditioning on the line $\ell_q : y = un$ being part to the Poisson line process Π will be analysed in three different cases:

- Case 1: $\boldsymbol{q} = (0, 0)$.

- Case 2: $\boldsymbol{q} = (tn, 0)$.

- Case 3: $\boldsymbol{q} = (tn, un)$.

The general idea is to split each region $\mathcal{D}_{n,\pm}^q$ in terms of the angle θ. Consider the region for small angles $\theta \in [0, w_n]$ for $\mathcal{D}_{n,+}^q$ (respectively $\theta \in [-w_n, 0]$ for $\mathcal{D}_{n,-}^q$) and the region for big angles $\theta \in [w_n, \pi]$ (respectively $\theta \in [-\pi, -w_n]$ for $\mathcal{D}_{n,-}^q$). Here w_n is of the form $w_n = 1/n^\beta$ for some $\beta \in (0, 1/4)$. Therefore $w_n \downarrow 0$, as $n \to \infty$, and Lemma 2.1 and Lemma 2.2 can be applied.

- Case $\boldsymbol{q} = (0, 0)$.

First we re-express $\mathcal{D}_{n,-}^q$ and $\mathcal{D}_{n,+}^q$ in terms of $\theta = \alpha_1 + \alpha_2$ and $\gamma = \alpha_1 - \alpha_2$. That is from here until the end of this case we have that

$$\mathcal{D}_{n,-}^q = \{(r, s, \theta, \gamma) : r \in [0, h_1^q(\alpha_1)], s \in [0, h_2^q(\alpha_2)], \theta \in [-\pi, 0], \gamma \in [\theta, -\theta]\},$$

$$\mathcal{D}_{n,+}^q = \{(r, s, \theta, \gamma) : r \in [0, h_1^q(\alpha_1)], s \in [0, h_2^q(\alpha_2)], \theta \in [0, \pi], \gamma \in [-\theta, \theta]\}.$$

Notice that $d\alpha_1\, d\alpha_2 = \frac{1}{2}\, d\theta\, d\gamma$ and that for this particular case since $h_1^q(\alpha_1)$ and $h_2^q(\alpha_2)$ are constant functions, then we can integrate the γ variable over the region $\mathcal{D}_{n,+}^q$, leading to

$$\int_0^\pi \int_0^\pi \int_0^{h_2^q(\alpha_2)n} \int_0^{h_1^q(\alpha_1)n} \exp\left(-\frac{1}{2}(r + s - \sqrt{r^2 + s^2 + 2rs\cos\theta})\right) r\, dr\, s\, ds\, d\alpha_1\, d\alpha_2 =$$

$$\int_0^\pi \int_0^n \int_0^n \int_{-\theta}^\theta \frac{1}{2} \exp\left(-\frac{1}{2}(r + s - \sqrt{r^2 + s^2 + 2rs\cos\theta})\right) d\gamma\, r\, dr\, s\, ds\, d\theta =$$

$$\int_0^\pi \int_0^n \int_0^n \frac{1}{2} \exp\left(-\frac{1}{2}(r + s - \sqrt{r^2 + s^2 + 2rs\cos\theta})\right) 2\theta r\, dr\, s\, ds\, d\theta =$$

$$\int_0^\pi \int_0^n \int_0^n \exp\left(-\frac{1}{2}(r + s - \sqrt{r^2 + s^2 + 2rs\cos\theta})\right) r\, dr\, s\, ds\, \theta\, d\theta. \quad (2.10)$$

Now consider $\hat{\alpha}_1 = -\alpha_1$ and $\hat{\alpha}_2 = -\alpha_2$, since $h_1^q(\alpha_1) = h_2^q(\alpha_2) = 1$ then we can

integrate the γ variable to obtain the following relations

$$\int_{-\pi}^{0}\int_{-\pi}^{0} \mathrm{d}\alpha_1 \, \mathrm{d}\alpha_2 = \int_{\pi}^{0}\int_{\pi}^{0} (-\mathrm{d}\hat{\alpha}_1)\,(-\mathrm{d}\hat{\alpha}_2)$$

$$= \int_{0}^{\pi}\int_{0}^{\pi} \mathrm{d}\hat{\alpha}_1 \, \mathrm{d}\hat{\alpha}_2 = \int_{0}^{\pi}\int_{-\hat{\theta}}^{\hat{\theta}} \frac{1}{2}\,\mathrm{d}\hat{\gamma}\,\mathrm{d}\hat{\theta} = \int_{0}^{\pi} \hat{\theta}\,\mathrm{d}\hat{\theta}, \quad (2.11)$$

here $\hat{\theta} = \hat{\alpha}_1 + \hat{\alpha}_2 = -\alpha_1 - \alpha_2 = -\theta$ (and $\hat{\gamma} = \hat{\alpha}_1 - \hat{\alpha}_2$). Therefore, as in this case the functions h_1^q and h_2^q are equal to the constant 1, and $g(r,s,-\hat{\theta}) = \exp\left(-\frac{1}{2}(r+s-\sqrt{r^2+s^2+2rs\cos(-\hat{\theta})})\right) = g(r,s,\hat{\theta})$ (since $\cos\hat{\theta}$ is an even function) then one obtains

$$\frac{1}{2}\iiint_{\mathcal{D}_{n,-}^q} g(r,s,\theta) r\,\mathrm{d}r\,s\,\mathrm{d}s\,\theta\,\mathrm{d}\theta \quad = \quad \frac{1}{2}\iiint_{\hat{\mathcal{D}}_{n,+}^q} g(r,s,-\hat{\theta}) r\,\mathrm{d}r\,s\,\mathrm{d}s\,\hat{\theta}\,\mathrm{d}\hat{\theta}$$

$$= \quad \frac{1}{2}\iiint_{\hat{\mathcal{D}}_{n,+}^q} g(r,s,\hat{\theta}) r\,\mathrm{d}r\,s\,\mathrm{d}s\,\hat{\theta}\,\mathrm{d}\hat{\theta}, \quad (2.12)$$

with

$$\hat{\mathcal{D}}_{n,+}^q \quad = \quad \{(r,s,\hat{\theta}) : 0 \le r \le n,\, 0 \le s \le n,\, 0 \le \hat{\theta} \le \pi\} \quad = \quad \mathcal{D}_{n,+}^q\,.$$

Thus, it suffices to consider the region $\mathcal{D}_{n,+}^q$, which can be split into two regions in terms of the angle θ. Take $w_n = 1/n^\beta$, then by Lemma 2.1 and Lemma 2.2 the result follows:

$$\mathbb{E}[T_n^q] \quad = \quad \frac{1}{2}\iiint_{\mathcal{D}_{n,-}^q} g(r,s,\theta) r\,\mathrm{d}r\,s\,\mathrm{d}s\,\theta\,\mathrm{d}\theta \quad + \quad \frac{1}{2}\iiint_{\mathcal{D}_{n,+}^q} g(r,s,\theta) r\,\mathrm{d}r\,s\,\mathrm{d}s\,\theta\,\mathrm{d}\theta$$

$$= \quad 2\left(\frac{1}{2}\iiint_{\mathcal{D}_{n,+}^q} g(r,s,\theta) r\,\mathrm{d}r\,s\,\mathrm{d}s\,\theta\,\mathrm{d}\theta\right)$$

$$= \quad \iiint_{\mathcal{A}_n^q} g(r,s,\theta) r\,\mathrm{d}r\,s\,\mathrm{d}s\,\theta\,\mathrm{d}\theta \quad + \quad \iiint_{\mathcal{E}_n^q} g(r,s,\theta) r\,\mathrm{d}r\,s\,\mathrm{d}s\,\theta\,\mathrm{d}\theta$$

$$\sim \quad 2n^3\,.$$

Here

$$\mathcal{A}_n^q \quad = \quad \{(r,s,\theta) : 0 \le r \le n,\, 0 \le s \le n,\, 0 \le \theta \le w_n\},$$
$$\mathcal{E}_n^q \quad = \quad \{(r,s,\theta) : 0 \le r \le n,\, 0 \le s \le n,\, w_n \le \theta \le \pi\},$$

are as in Lemma 2.1 ($R_1 = R_2 = 1$) and Lemma 2.2 ($R_3 = 1$) respectively.

- Case $\boldsymbol{q} = (tn, 0)$.

As in the previous case consider the change of variable given by $\hat{\alpha}_1 = -\alpha_1$ and

$\hat{\alpha}_2 = -\alpha_2$ and notice that h_1^q and h_2^q are even functions, i.e.

$$h_1^q(-\hat{\alpha}_1) = \left(\left(\sqrt{\sec^2(-\hat{\alpha}_1) - (t\tan(-\hat{\alpha}_1))^2} - \tan(-\hat{\alpha}_1)(t\tan(-\hat{\alpha}_1))\right)\cos^2(-\hat{\alpha}_1) + t\right)\sec(-\hat{\alpha}_1)$$

$$= \left(\left(\sqrt{\sec^2\hat{\alpha}_1 - (t\tan\hat{\alpha}_1)^2} - \tan\hat{\alpha}_1(t\tan\hat{\alpha}_1)\right)\cos^2\hat{\alpha}_1 + t\right)\sec\hat{\alpha}_1 \quad = \quad h_1^q(\hat{\alpha}_1),$$

$$h_2^q(-\hat{\alpha}_2) = \left(\left(\sqrt{\sec^2(-\hat{\alpha}_2) - (t\tan(-\hat{\alpha}_2))^2} + \tan(-\hat{\alpha}_2)(t\tan(-\hat{\alpha}_2))\right)\cos^2(-\hat{\alpha}_2) - t\right)\sec(-\hat{\alpha}_2)$$

$$= \left(\left(\sqrt{\sec^2\hat{\alpha}_2 - (t\tan\hat{\alpha}_2)^2} + \tan\hat{\alpha}_2(t\tan\hat{\alpha}_2)\right)\cos^2\hat{\alpha}_2 - t\right)\sec\hat{\alpha}_2 \quad = \quad h_2^q(\hat{\alpha}_2).$$

Therefore,

$$\frac{1}{2}\iiiint_{\mathcal{D}_{n,-}^q} g(r,s,\alpha_1,\alpha_2)r\,\mathrm{d}r\,s\,\mathrm{d}s\,\mathrm{d}\alpha_1\,\mathrm{d}\alpha_2$$

$$= \frac{1}{2}\iiiint_{\hat{\mathcal{D}}_{n,+}^q} g(r,s,-\hat{\alpha}_1,-\hat{\alpha}_2)r\,\mathrm{d}r\,s\,\mathrm{d}s\,(-\mathrm{d}\hat{\alpha}_1)\,(-\mathrm{d}\hat{\alpha}_2)$$

$$= \frac{1}{2}\iiiint_{\hat{\mathcal{D}}_{n,+}^q} g(r,s,\hat{\alpha}_1,\hat{\alpha}_2)r\,\mathrm{d}r\,s\,\mathrm{d}s\,\mathrm{d}\hat{\alpha}_1\,\mathrm{d}\hat{\alpha}_2\,,$$

with

$$\hat{\mathcal{D}}_{n,+}^q = \{(r,s,\hat{\alpha}_1,\hat{\alpha}_2)\,:\,r\in[0,h_1^q(-\hat{\alpha}_1)n],\ s\in[0,h_2^q(-\hat{\alpha}_2)n],\ \hat{\alpha}_1\in[0,\pi],\ \hat{\alpha}_2\in[0,\pi]\}$$

$$= \{(r,s,\hat{\alpha}_1,\hat{\alpha}_2)\,:\,r\in[0,h_1^q(\hat{\alpha}_1)n],\ s\in[0,h_2^q(\hat{\alpha}_2)n],\ \hat{\alpha}_1\in[0,\pi],\ \hat{\alpha}_2\in[0,\pi]\} = \mathcal{D}_{n,+}^q\,.$$

Hence, it is sufficient to analyse the integral over the region $\mathcal{D}_{n,+}^q$. For this case $\mathcal{D}_{n,+}^q$ does not have constant upper bounds for the values of r and s. However, the upper bounds for r and s in the region $\mathcal{D}_{n,+}^q$ are given by continuous functions $h_1^q(\alpha_1)$ and $h_2^q(\alpha_2)$ respectively. Even more, if we re-express the region in terms of θ and γ it can be divided into the following subregions

$$\mathcal{D}_{n,1}^q = \{(r,s,\theta,\gamma)\,:\,0\le r\le h_1^q(\alpha_1)n,\ 0\le s\le h_2^q(\alpha_2)n,\ 0\le\theta\le w_n,\ -\theta\le\gamma\le\theta\}\,,$$

$$\mathcal{D}_{n,2}^q = \{(r,s,\theta,\gamma)\,:\,0\le r\le h_1^q(\alpha_1)n,\ 0\le s\le h_2^q(\alpha_2)n,\ w_n\le\theta\le\pi,\ -\theta\le\gamma\le\theta\}\,.$$

So clearly, $\mathcal{D}_{n,+}^q = \mathcal{D}_{n,1}^q\cup\mathcal{D}_{n,2}^q$. Then, the region $\mathcal{D}_{n,2}^q$ can be bounded by

$$\mathcal{E}_n^q \quad = \quad \{(r,s,\theta,\gamma)\,:\,0\le r\le(1+t)n,\ 0\le s\le(1+t)n,\ w_n\le\theta\le\pi,\ -\theta\le\gamma\le\theta\}\,,$$

i.e. $\mathcal{D}_{n,2}^q\subseteq\mathcal{E}_n^q$. Therefore after integrating the γ variable as in (2.10), we can apply Lemma 2.2 with $R_3 = 1+t$ (as the function to be integrated is positive) to the new regions $\mathcal{D}_{n,2}^q$ and $\mathcal{E}_n^q$ without the γ variable to deduce

$$\iiint_{\mathcal{D}_{n,2}} g(r,s,\theta)r\,\mathrm{d}r\,s\,\mathrm{d}s\,\theta\,\mathrm{d}\theta \quad\le\quad \iiint_{\mathcal{E}_n^q} g(r,s,\theta)r\,\mathrm{d}r\,s\,\mathrm{d}s\,\theta\,\mathrm{d}\theta \quad = \quad \mathcal{O}\left(n^{2+4\beta}\right)\,.$$

On the other hand, one can show that the functions $h_1^q(\alpha_1)$, $h_2^q(\alpha_2)$ are decreasing and increasing on α_1 and α_2 respectively. Therefore, the region $\mathcal{D}_{n,1}^q$ can be bounded

above and below by the following two regions with constant upper bounds for r and s, see figure 2.3

$$\mathcal{A}_{n,-}^q = \left\{ (r,s,\theta,\gamma) : 0 \le r \le h_1^q(w_n)n, \ 0 \le s \le h_2^q(0)n, \ 0 \le \theta \le w_n, \ -\theta \le \gamma \le \theta \right\},$$

$$\mathcal{A}_{n,+}^q = \left\{ (r,s,\theta,\gamma) : 0 \le r \le h_1^q(0)n, \ 0 \le s \le h_2^q(w_n)n, \ 0 \le \theta \le w_n, \ -\theta \le \gamma \le \theta \right\}.$$
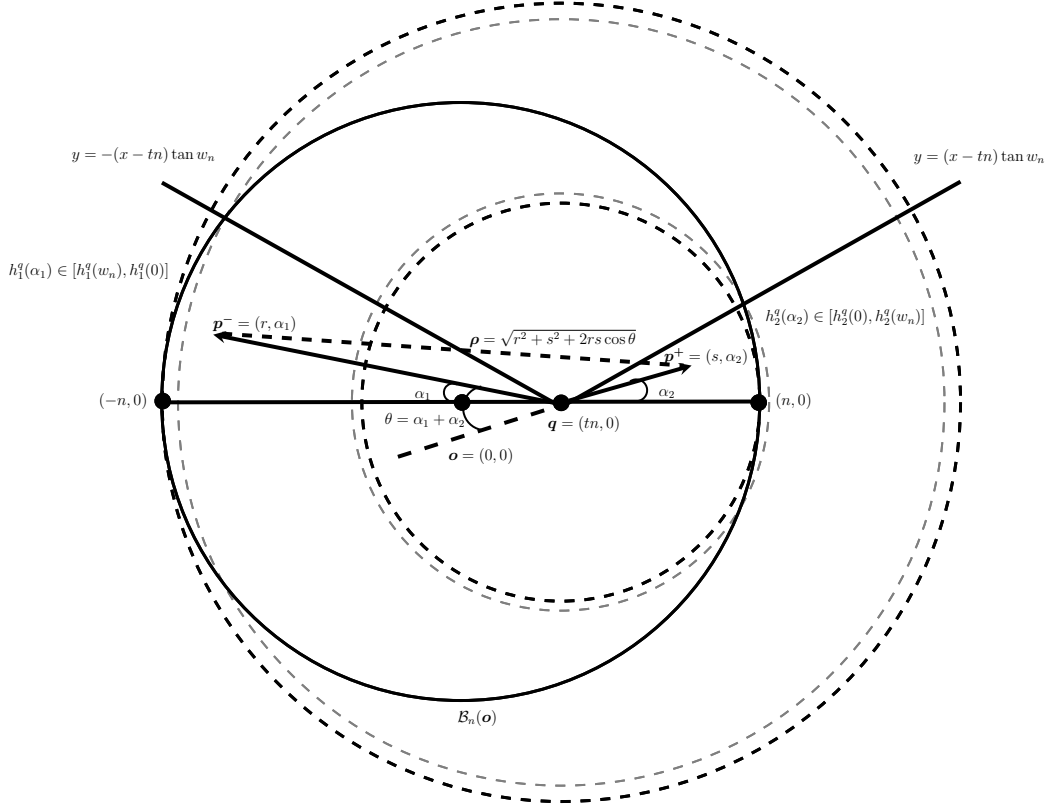
Figure 2.3: How to control the integral over $\mathcal{D}_{n,1}^q$.

Then integrate the γ variable as in (2.10). After that since $\mathcal{A}_{n,-}^q \subseteq \mathcal{D}_{n,1}^q \subseteq \mathcal{A}_{n,+}^q$, (without the γ variable now) Lemma 2.1 over the regions $\mathcal{A}_{n,-}^q$ and $\mathcal{A}_{n,+}^q$ yields to

$$h_1^q(w_n)h_2^q(0)(h_1^q(w_n) + h_2^q(0))n^3 \le \iiint\limits_{\mathcal{D}_{n,1}^q} g(r,s,\theta)r \, \mathrm{d}r \, s \, \mathrm{d}s \, \theta \, \mathrm{d}\theta$$

$$\le h_1^q(0)h_2^q(w_n)(h_1^q(0) + h_2^q(w_n))n^3. \quad (2.13)$$

Finally, by a Taylor expansion series argument it is known that

$$h_1^q(w_n) = h_1^q(0) + \frac{(h_1^q)'(0)}{1!}(w_n - 0) + \frac{(h_1^q)''(0)}{2!}(\psi_1)^2 \quad \text{for some } \psi_1 \in (0, 2w_n),$$

$$h_2^q(w_n) = h_2^q(0) + \frac{(h_2^q)'(0)}{1!}(w_n - 0) + \frac{(h_2^q)''(0)}{2!}(\psi_2)^2 \quad \text{for some } \psi_2 \in (0, 2w_n).$$

Notice, that for this case $(h_1^q)'(0) = (h_2^q)'(0) = 0$, $(h_1^q)''(0) = -t^2$ and $(h_2^q)''(0) = t^2$.

This leads to the following inequalities

$$h_1^q(w_n) \geq h_1^q(0) - \frac{t^2}{2}4w_n^2 = h_1^q(0) - 2t^2 w_n^2 \geq h_1^q(0) - 2w_n^2, \qquad (2.14)$$

$$h_2^q(w_n) \leq h_2^q(0) + \frac{t^2}{2}4w_n^2 = h_2^q(0) + 2t^2 w_n^2 \leq h_2^q(0) + 2w_n^2, \qquad (2.15)$$

since $t \in (-1, 1)$ for this case. Therefore from (2.13), (2.14) and (2.15) it follows that

$$(h_1^q(0) - 2w_n^2)h_2^q(0)(h_1^q(0) - 2w_n^2 + h_2^q(0))n^3 = 2(1-t^2)n^3 - 2(1-t)(3+t)w_n^2 n^3 + 4(1-t)w_n^4 n^3$$

$$\leq \iiint_{\mathcal{D}_{n,1}^q} g(r, s, \theta)r \, \mathrm{d}r \, s \, \mathrm{d}s \, \theta \, \mathrm{d}\theta \leq$$

$$2(1-t^2)n^3 - 2(1+t)(3-t)w_n^2 n^3 + 4(1+t)w_n^4 n^3 = h_1^q(0)(h_2^q(0) + 2w_n^2)(h_1^q(0) + h_2^q(0) + 2w_n^2)n^3.$$

Then as $n \to \infty$ (so $w_n \downarrow 0$). Thus

$$\iiint_{\mathcal{D}_{n,1}^q} g(r, s, \theta)r \, \mathrm{d}r \, s \, \mathrm{d}s \, \theta \, \mathrm{d}\theta = 2(1 - t^2)n^3 + \mathcal{O}\left(n^{3-2\beta}\right),$$

which establishes the result for this case for any $\beta \in (0, 1/4)$.

- Case $\boldsymbol{q} = (tn, un)$.

For the last case, one has to analyse separately the regions $\mathcal{D}_{n,-}^q$ and $\mathcal{D}_{n,+}^q$ as the symmetry argument from the previous cases does not hold anymore. Although, each region, after being re-expressed in terms of θ and γ, can still be separated into two subregions in terms of θ, say

$$\mathcal{D}_{n,+,1}^q = \{(r, s, \theta, \gamma) : r \in [0, h_1^q(\alpha_1)n], \ s \in [0, h_2^q(\alpha_2)n], \ \theta \in [0, w_n], \ \gamma \in [-\theta, \theta]\},$$

$$\mathcal{D}_{n,+,2}^q = \{(r, s, \theta, \gamma) : r \in [0, h_1^q(\alpha_1)n], \ s \in [0, h_2^q(\alpha_2)n], \ \theta \in [w_n, \pi], \ \gamma \in [-\theta, \theta]\}.$$

Thus $\mathcal{D}_{n,+}^q = \mathcal{D}_{n,+,1}^q \cup \mathcal{D}_{n,+,2}^q$. Then, as in the previous cases, the region with large values for θ, $\mathcal{D}_{n,+,2}^q$, can be bounded by a region with constant bounds for r and s, say

$$\mathcal{E}_{n,+}^q = \left\{(r, s, \theta, \gamma) : r \in [0, (1 + \sqrt{t^2 + u^2})n], \ s \in [0, (1 + \sqrt{t^2 + u^2})n], \right.$$

$$\left. \theta \in [w_n, \pi], \ \gamma \in [-\theta, \theta]\right\}. \qquad (2.16)$$

Hence $\mathcal{D}_{n,+,2}^q \subseteq \mathcal{E}_{n,+}^q$. Therefore after integrating the γ variable as in (2.10) (as the function to be integrated is positive) Lemma 2.2 with $R_3 = 1 + \sqrt{t^2 + u^2}$ over the region $\mathcal{E}_{n,+}^q$ (without the γ variable))yields to the following inequality

$$\iiint_{\mathcal{D}_{n,+,2}^q} g(r, s, \theta)r \, \mathrm{d}r \, s \, \mathrm{d}s \, \theta \, \mathrm{d}\theta \leq \iiint_{\mathcal{E}_{n,+}^q} g(r, s, \theta)r \, \mathrm{d}r \, s \, \mathrm{d}s \, \theta \, \mathrm{d}\theta = \mathcal{O}\left(n^{2+4\beta}\right).$$

On the other hand, the functions $h_1^q(\alpha_1)$, $h_2^q(\alpha_2)$ are decreasing on α_1 and α_2 respectively (for a neighbourhood close to 0). Therefore, the region $\mathcal{D}_{n,+,1}^q$ can be bounded above and below by the following two regions with constant upper bounds for r and s, see figure 2.4

$$\mathcal{A}_{n,+,-}^q = \{(r,s,\theta,\gamma) : 0 \leq r \leq h_1^q(w_n)n, \, 0 \leq s \leq h_2^q(w_n)n, \, 0 \leq \theta \leq w_n, \, -\theta \leq \gamma \leq \theta\},$$
$$\mathcal{A}_{n,+,+}^q = \{(r,s,\theta,\gamma) : 0 \leq r \leq h_1^q(0)n, \, 0 \leq s \leq h_2^q(0)n, \, 0 \leq \theta \leq w_n, \, -\theta \leq \gamma \leq \theta\}.$$
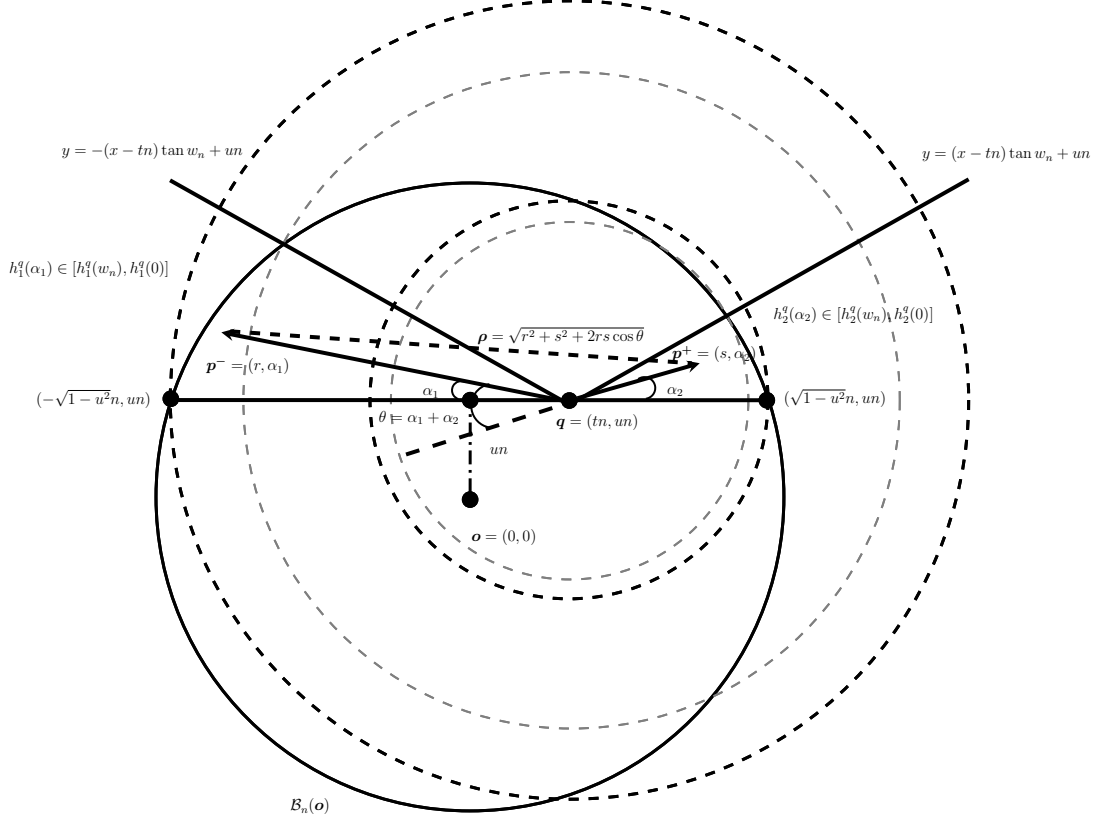
Figure 2.4: How to control the integral over $\mathcal{D}_{n,+,1}^q$.

Then integrating the γ variable as in (2.10), since $\mathcal{A}_{n,+,-}^q \subseteq \mathcal{D}_{n,+,1}^q \subseteq \mathcal{A}_{n,+,+}^q$, Lemma 2.1 over the regions $\mathcal{A}_{n,+,-}^q$ and $\mathcal{A}_{n,+,+}^q$ yields to

$$h_1^q(w_n)h_2^q(w_n)(h_1^q(w_n)+h_2^q(w_n))n^3 \quad \leq \quad \iiint\limits_{\mathcal{D}_{n,+,1}^q} g(r,s,\theta)r\,\mathrm{d}r\,s\,\mathrm{d}s\,\theta\,\mathrm{d}\theta$$

$$\leq \quad h_1^q(0)h_2^q(0)(h_1^q(0)+h_2^q(0))n^3. \quad (2.17)$$

Again, by a Taylor expansion argument, recall that

$$h_1^q(w_n) \quad = \quad h_1^q(0) + \frac{(h_1^q)'(0)}{1!}(\psi_1) \quad \text{for some } \psi_1 \in (0,2w_n),$$

$$h_2^q(w_n) \quad = \quad h_2^q(0) + \frac{(h_2^q)'(0)}{1!}(\psi_2) \quad \text{for some } \psi_2 \in (0,2w_n).$$

34

Now, in this case:

$$(h_1^q)'(0) = -u\left(1 + \frac{t}{\sqrt{1-u^2}}\right) \qquad \text{and} \qquad (h_2^q)'(0) = -u\left(1 - \frac{t}{\sqrt{1-u^2}}\right).$$

So, it is possible to bound $h_1^q(w_n)$ and $h_2^q(w_n)$ from below as follows

$$\begin{aligned}
h_1^q(w_n) &\geq h_1^q(0) - u\left(1 + \frac{t}{\sqrt{1-u^2}}\right) 2w_n \\
&\geq h_1^q(0) - 4uw_n \geq h_1^q(0) - 4w_n, \quad (2.18) \\
h_2^q(w_n) &\geq h_2^q(0) - u\left(1 - \frac{t}{\sqrt{1-u^2}}\right) 2w_n \\
&\geq h_2^q(0) - 4uw_n \geq h_2^q(0) - 4w_n. \quad (2.19)
\end{aligned}$$

Since $u \in (-1, 1)$ and $t \in (-\sqrt{1-u^2}, \sqrt{1-u^2})$ implies that $t/\sqrt{1-u^2} \in (-1, 1)$. Therefore (2.17), (2.18) and (2.19) leads to the following inequalities:

$$\begin{aligned}
&(h_1^q(0) - 4w_n)(h_2^q(0) - 4w_n)(h_1^q(0) + h_2^q(0) - 8w_n)n^3 \\
&= 2\sqrt{1-u^2}(1-u^2-t^2)n^3 - 4(2\sqrt{1-u^2}(\sqrt{1-u^2}-t) + 2\sqrt{1-u^2}(\sqrt{1-u^2}+t) \\
&\quad + 2(1-u^2-t^2))w_n n^3 + 96\sqrt{1-u^2}w_n^2 n^3 - 128w_n^3 n^3 \\
&\leq \iiint_{\mathcal{D}_{n,+,1}^q} g(r,s,\theta)r\,dr\,s\,ds\,\theta\,d\theta \leq 2\sqrt{1-u^2}(1-u^2-t^2)n^3.
\end{aligned}$$

Thus, as $n \to \infty$, then $w_n \downarrow 0$, so

$$\iiint_{\mathcal{D}_{n,+,1}^q} g(r,s,\theta)r\,dr\,s\,ds\,\theta\,d\theta = 2\sqrt{1-u^2}(1-u^2-t^2)n^3 + \mathcal{O}\left(n^{3-\beta}\right).$$

For the region $\mathcal{D}_{n,-}^q$ we will apply a similar argument. First we re-express the region in terms of θ and γ, then separate the whole region into two subregions in terms of the angle θ, say

$$\begin{aligned}
\mathcal{D}_{n,-,1}^q &= \{(r,s,\theta,\gamma) : r \in [0, h_1^q(\alpha_1)n], \ s \in [0, h_2^q(\alpha_2)n], \ \theta \in [-w_n, 0], \ \gamma \in [\theta, -\theta]\}, \\
\hat{\mathcal{D}}_{n,-,2}^q &= \{(r,s,\theta,\gamma) : r \in [0, h_1^q(\alpha_1)n], \ s \in [0, h_2^q(\alpha_2)n], \ \theta \in [-\pi, -w_n], \ \gamma \in [\theta, -\theta]\}
\end{aligned}$$

Hence $\mathcal{D}_{n,-}^q = \mathcal{D}_{n,-,1}^q \cup \mathcal{D}_{n,-,2}^q$. Then, notice that if one considers $\hat{\alpha}_1 = -\alpha_1$, $\hat{\alpha}_2 = -\alpha_2$, $\hat{\theta} = \hat{\alpha}_1 + \hat{\alpha}_2 = -\alpha_1 - \alpha_2 = -\theta$ and $\hat{\gamma} = \hat{\alpha}_1 - \hat{\alpha}_2$ the regions $\mathcal{D}_{n,-,1}^q$ and $\mathcal{D}_{n,-,2}^q$ can be rewritten in terms of these new variables as follows

$$\begin{aligned}
\hat{\mathcal{D}}_{n,-,1}^q &= \{(r,s,\hat{\theta},\hat{\gamma}) : r \in [0, h_1^q(-\hat{\alpha}_1)n], \ s \in [0, h_2^q(-\hat{\alpha}_2)n], \ \hat{\theta} \in [0, w_n], \ \hat{\gamma} \in [-\hat{\theta}, \hat{\theta}]\}, \\
\hat{\mathcal{D}}_{n,-,2}^q &= \{(r,s,\hat{\theta},\hat{\gamma}) : r \in [0, h_1^q(-\hat{\alpha}_1)n], \ s \in [0, h_2^q(-\hat{\alpha}_2)n], \ \hat{\theta} \in [w_n, \pi], \ \hat{\gamma} \in [-\hat{\theta}, \hat{\theta}]\}.
\end{aligned}$$

Also, it is important to notice that $g(r,s,\theta) = g(r,s,-\theta)$. Therefore after integrating

the γ variable as in (2.10) by Lemma 2.2 ($R_3 = 1 + \sqrt{t^2 + u^2}$) it follows

$$\iiint\limits_{\hat{\mathcal{D}}^q_{n,-,2}} g(r,s,\hat{\theta}) r \, \mathrm{d}r \, s \, \mathrm{d}s \, \hat{\theta} \, \mathrm{d}\hat{\theta} \quad \le \quad \iiint\limits_{\mathcal{E}^q_{n,+}} g(r,s,\hat{\theta}) r \, \mathrm{d}r \, s \, \mathrm{d}s \, \hat{\theta} \, \mathrm{d}\hat{\theta} \quad = \quad \mathcal{O}\left(n^{2+4\beta}\right),$$

with $\mathcal{E}^q_{n,+}$ as in (2.16).

For this case the functions $h^q_1(-\hat{\alpha}_1)$, $h^q_2(-\hat{\alpha}_2)$ are decreasing on $-\hat{\alpha}_1$ and $-\hat{\alpha}_2$ respectively (for a neighbourhood close to 0). But still, the region $\hat{\mathcal{D}}^q_{n,-,1}$ can be bounded above and below by two regions with constant upper bounds for r and s, say

$$\hat{\mathcal{A}}^q_{n,-,-} = \{(r,s,\hat{\theta},\hat{\gamma}) : 0 \le r \le h^q_1(0)n, \ 0 \le s \le h^q_2(0)n, \ 0 \le \hat{\theta} \le w_n, \ -\hat{\theta} \le \hat{\gamma} \le \hat{\theta}\},$$
$$\hat{\mathcal{A}}^q_{n,-,+} = \{(r,s,\hat{\theta},\hat{\gamma}) : 0 \le r \le h^q_1(-w_n)n, \ 0 \le s \le h^q_2(-w_n)n, \ 0 \le \hat{\theta} \le w_n, \ -\hat{\theta} \le \hat{\gamma} \le \hat{\theta}\}.$$

Again, integrating the γ variable as in (2.10), since $\hat{\mathcal{A}}^q_{n,-,-} \subseteq \hat{\mathcal{D}}^q_{n,-,1} \subseteq \hat{\mathcal{A}}^q_{n,-,+}$, Lemma 2.1 over the regions $\hat{\mathcal{A}}^q_{n,-,-}$ and $\hat{\mathcal{A}}^q_{n,-,+}$ (without the γ variable) yields to

$$h^q_1(0)h^q_2(0)(h^q_1(0) + h^q_2(0))n^3 \quad \le \quad \iiint\limits_{\hat{\mathcal{D}}^q_{n,-,1}} g(r,s,\hat{\theta}) r \, \mathrm{d}r \, s \, \mathrm{d}s \, \hat{\theta} \, \mathrm{d}\hat{\theta}$$
$$\le \quad h^q_1(-w_n)h^q_2(-w_n)(h^q_1(-w_n) + h^q_2(-w_n))n^3. \quad (2.20)$$

Again, by a Taylor expansion argument, recall that

$$h^q_1(-w_n) \quad = \quad h^q_1(0) + \frac{h^{q'}_1(0)}{1!}(\psi_1) \quad \text{for some } \psi_1 \in (-2w_n, 0),$$
$$h^q_2(-w_n) \quad = \quad h^q_2(0) + \frac{h^{q'}_2(0)}{1!}(\psi_2) \quad \text{for some } \psi_2 \in (-2w_n, 0).$$

So, it is possible to bound $h^q_1(-w_n)$ and $h^q_2(-w_n)$ from above as follows

$$h^q_1(-w_n) \quad \le \quad h^q_1(0) + u\left(1 + \frac{t}{\sqrt{1-u^2}}\right)2w_n$$
$$\le \quad h^q_1(0) + 4uw_n \quad \le \quad h^q_1(0) + 4w_n, \quad (2.21)$$
$$h^q_2(-w_n) \quad \le \quad h^q_2(0) + u\left(1 - \frac{t}{\sqrt{1-u^2}}\right)2w_n$$
$$\le \quad h^q_2(0) + 4uw_n \quad \le \quad h^q_2(0) + 4w_n. \quad (2.22)$$

Since $u \in (-1,1)$ and $t \in (-\sqrt{1-u^2}, \sqrt{1-u^2})$ implies that $t/\sqrt{1-u^2} \in (-1,1)$. In

consequence, putting (2.20) together with (2.21) and (2.22)

$$2\sqrt{1-u^2}(1-u^2-t^2)n^3 \quad \leq \quad \iiint\limits_{\hat{\mathcal{D}}^q_{n,-,1}} g(r,s,\hat{\theta})r\,\mathrm{d}r\,s\,\mathrm{d}s\,\hat{\theta}\,\mathrm{d}\hat{\theta}$$

$$\leq \quad 2\sqrt{1-u^2}(1-u^2-t^2)n^3 + 4(2\sqrt{1-u^2}(\sqrt{1-u^2}-t)+$$

$$2\sqrt{1-u^2}(\sqrt{1-u^2}+t) + 2(1-u^2-t^2))w_n n^3 + 96\sqrt{1-u^2}w_n^2 n^3 + 128w_n^3 n^3$$

$$= (h_1^q(0)+4w_n)(h_2^q(0)+4w_n)(h_1^q(0)+h_2^q(0)+8w_n)n^3\,.$$

Thus, as $n \to \infty$, $w_n \downarrow 0$, so

$$\iiint\limits_{\mathcal{D}^q_{n,-,1}} g(r,s,\theta)r\,\mathrm{d}r\,s\,\mathrm{d}s\,\theta\,\mathrm{d}\theta \quad = \quad 2\sqrt{1-u^2}(1-u^2-t^2)n^3 + \mathcal{O}\left(n^{3-\beta}\right)\,.$$

Therefore, putting all together we obtain the desired result

$$\mathbb{E}[T_n^q] \quad = \quad \frac{1}{2}\iiint\limits_{\mathcal{D}^q_{n,-}} g(r,s,\theta)r\,\mathrm{d}r\,s\,\mathrm{d}s\,\theta\,\mathrm{d}\theta \quad + \quad \frac{1}{2}\iiint\limits_{\mathcal{D}^q_{n,+}} g(r,s,\theta)r\,\mathrm{d}r\,s\,\mathrm{d}s\,\theta\,\mathrm{d}\theta$$

$$= \quad 2\sqrt{1-u^2}(1-u^2-t^2)n^3 \quad + \quad \mathcal{O}\left(n^{3-\beta}\right) \quad + \quad \mathcal{O}\left(n^{2+4\beta}\right)\,,$$

which establishes the theorem for any $\beta \in (0,1/4)$. $\qquad\qquad\qquad\qquad\square$

2.2 Improper Anisotropic Poisson line process

Another way to verify the above calculations is given in this section. This approach provides a shorter exposition, as it depends more on conceptual ideas that arises from the previous section. However, the results developed in this section will not provide any information regarding the second leading term on the asymptotic behaviour for the mean traffic at the point $q = (tn, un)$.

The scaling limit for the distribution of traffic flow through any point, q, in the Poissonian city can be represented by using an improper stationary anisotropic Poisson line process, $\dot{\Pi}$. This section follows the ideas developed by Kendall [25, Section 3.3] with the appropriate modifications. Again, one has to condition on the existence of an horizontal line $\ell_q : y = un$ that passes through $q = (tn, un)$, i.e. $\ell_q \in \Pi$.

Recall that a line process can be parametrized in different ways. Here instead of using the standard coordinates (r, θ), where r represents the distance of the line ℓ to the origin and θ the angle it makes regarding an horizontal line (x-axis). We will use $(p, \hat{\theta})$, with p being the signed distance from q to the intersection between the given horizontal line ℓ_q and the line ℓ that is being parametrised, and $\hat{\theta}$ represents the angle between these two lines (ℓ_q and ℓ), see figure 2.5.
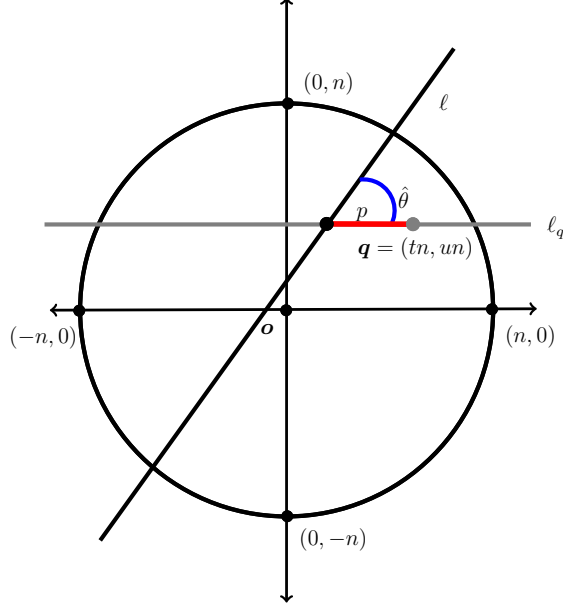
Figure 2.5: Illustration for the alternative coordinates $(p, \hat{\theta})$ used to parametrise a line process Π. For this particular case, p will be a negative number.

In the latter case the intersection points with the line ℓ_q will form a stationary Poisson point process and the angle density is given by $\frac{1}{2}\sin\hat{\theta}$ [26, Lemma 1.1] for $\hat{\theta} \in [0, \pi]$. However, there is a setback with the parametrization $(p, \hat{\theta})$ as all parallel lines to ℓ_q will not be represented, since they do not intersect with ℓ_q. Nonetheless, these specific lines are contained in an event of probability zero, say the set of lines such that $\theta = 2\pi$, using the first coordinates system (r, θ).

Guided by the asymptotics obtained on Theorem 2.1 one desires to rescale the Cartesian coordinates (x, y) in the following way. Shrink the x-axis by a factor of $1/n$ and contract the y-axis by $1/\sqrt{n}$. Therefore, the new set of coordinates is given by $(\tilde{x}, \tilde{y}) = (x/n, y/\sqrt{n})$, see figure 2.6. Accordingly, the new parameters $(\tilde{p}, \tilde{\theta})$ for the line process $\tilde{\Pi}$ can be related with $(p, \hat{\theta})$ by the relations: $\tilde{p} = p/n$ and

$$\tan\tilde{\theta} \quad = \quad \frac{\tilde{y}}{\tilde{x}} = \frac{ny}{\sqrt{n}x} = \sqrt{n}\frac{y}{x} \quad = \quad \sqrt{n}\tan\hat{\theta}\,.$$

One can think as if the line process Π is being transformed into another line process $\tilde{\Pi}$. The intensity of $\tilde{\Pi}$ can be expressed in terms of $(\tilde{p}, \tilde{\theta})$. The Jacobian for the above change of coordinates, i.e. $p = n\tilde{p}$ and $\hat{\theta} = \arctan\left(\frac{1}{\sqrt{n}}\tan\tilde{\theta}\right)$, is given by

$$\left|\frac{\partial(p, \hat{\theta})}{\partial(\tilde{p}, \tilde{\theta})}\right| \quad = \quad \left|\begin{pmatrix} n & 0 \\ 0 & \frac{\sec^2\tilde{\theta}}{1+\frac{1}{n}\tan^2\tilde{\theta}}\frac{1}{\sqrt{n}} \end{pmatrix}\right| \quad = \quad \sqrt{n}\frac{\sec^2\tilde{\theta}}{1+\frac{1}{n}\tan^2\tilde{\theta}}\,.$$

38
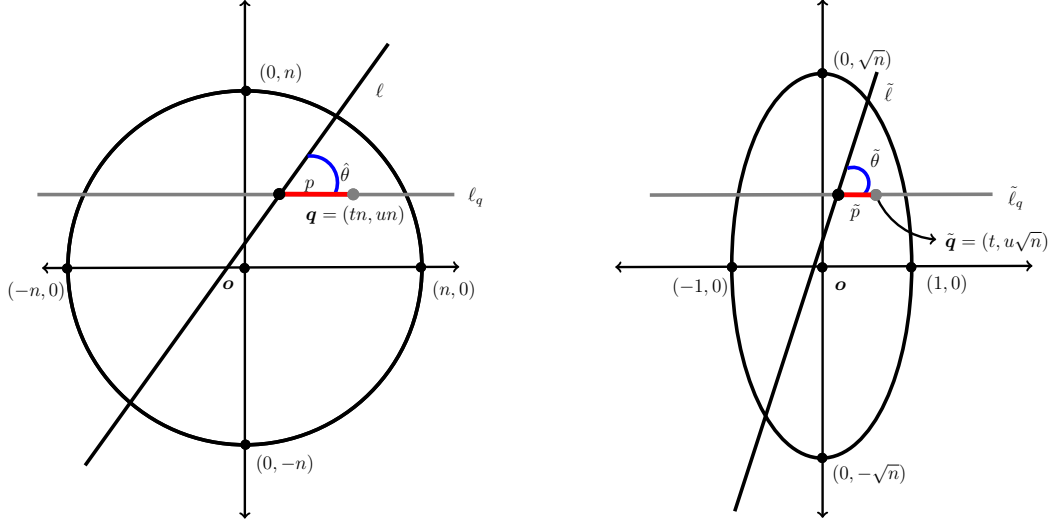
Figure 2.6: Change of coordinates from $(p, \hat{\theta})$ to $(\tilde{p}, \tilde{\theta})$.

Also, observe that

$$
\sin \hat{\theta} \quad = \quad \sin \left(\arctan \left(\frac{1}{\sqrt{n}} \tan \tilde{\theta} \right) \right) \quad = \quad \frac{\tan \tilde{\theta}}{\left(n \left(1 + \frac{1}{n} \tan^2 \tilde{\theta} \right) \right)^{1/2}} \, .
$$

Therefore, the line process $\tilde{\Pi}$ can be parametrized as a Poisson point process on the $(\tilde{p}, \tilde{\theta})$ space with intensity

$$
\Lambda(\, \mathrm{d}(\tilde{p}, \tilde{\theta}) \,) \quad = \quad \frac{1}{2} \frac{\tan \tilde{\theta} \sec^2 \tilde{\theta}}{\left(1 + \frac{1}{n} \tan^2 \tilde{\theta} \right)^{3/2}} \, \mathrm{d}\tilde{p} \, \mathrm{d}\tilde{\theta} \, .
$$

The $\tilde{x}$-axis can be translated to the horizontal line $\tilde{\ell}_q : y = u\sqrt{n}$. Denote the new coordinates after this translation by $(\dot{x}, \dot{y})$, notice that the intensity of the line process $\dot{\Pi}$ is the same as the intensity of the line process $\tilde{\Pi}$; in particular we now have that $\dot{\ell}_q : y = 0$. Taking the limit as $n \to \infty$ one obtains an improper stationary anisotropic Poisson line process with intensity $\Lambda(\, \mathrm{d}(\dot{p}, \dot{\theta})) = \frac{1}{2} \tan \dot{\theta} \sec^2 \dot{\theta} \, \mathrm{d}\dot{p} \, \mathrm{d}\dot{\theta}$. Based on the line process $\dot{\Pi}$ one can achieve a proper stationary isotropic Poisson line process $\tilde{\Pi}_n$ at scale n by randomly thinning the lines with a retention probability that depends monotonically on the line slope, details can be found at Kendall [25, page 31], in such a way that after the thinning of the improper stationary anisotropic Poisson line process we will end up with a $\tilde{\Pi}_n$ with intensity

$$
\begin{aligned}
\Lambda_n(\, \mathrm{d}(\tilde{p}, \tilde{\theta})) \quad &= \quad \frac{1}{2} \frac{\tan \tilde{\theta} \sec^2 \tilde{\theta}}{\left(1 + \frac{1}{n} \tan^2 \tilde{\theta} \right)^{3/2}} \, \mathrm{d}\tilde{p} \, \mathrm{d}\tilde{\theta} \\
&\leq \quad \frac{1}{2} \tan \dot{\theta} \sec^2 \dot{\theta} \, \mathrm{d}\dot{p} \, \mathrm{d}\dot{\theta} \quad = \quad \Lambda(\, \mathrm{d}(\dot{p}, \dot{\theta})) \, .
\end{aligned}
$$

Even more, the limiting improper stationary anisotropic Poisson line process may

be represented in a simple way by a different set of coordinates. That is, we will represent each line in the line process by its intercepts y_- and y_+ on the vertical axis $\tilde{x} = -\sqrt{1-u^2}$ and $\tilde{x} = \sqrt{1-u^2}$, respectively, see figure 2.7. Therefore for a line represented by $(\dot{p}, \dot{\theta})$ one have the following relations:

$$y_- = -\tan\dot{\theta}(\sqrt{1-u^2}+\dot{p}) \qquad \text{and} \qquad y_+ = \tan\dot{\theta}(\sqrt{1-u^2}-\dot{p}).$$
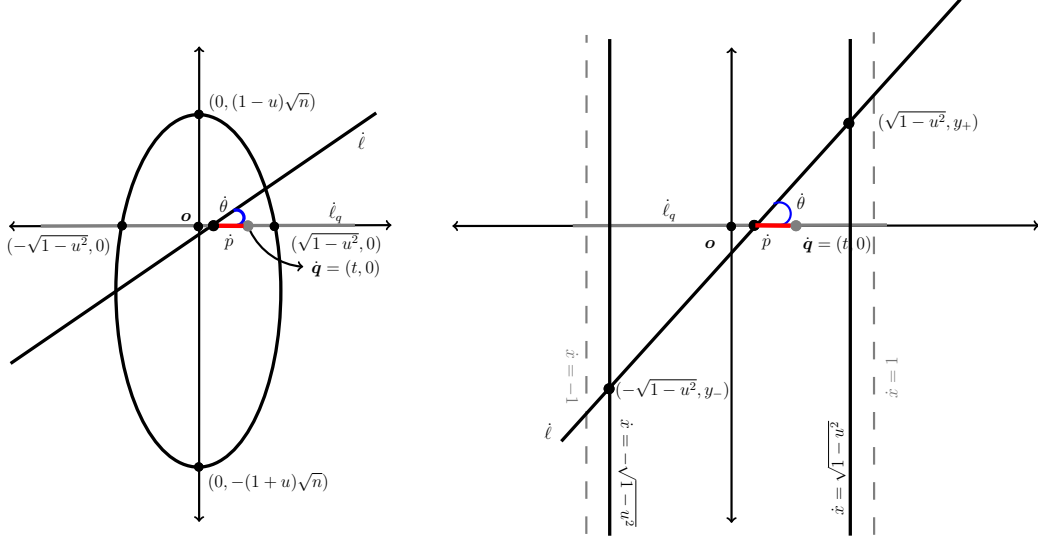
Figure 2.7: Change of coordinates from $(\dot{p}, \dot{\theta})$ to (y_-, y_+).

The Jacobian for this change of coordinates is given by

$$
\begin{aligned}
\left| \frac{\partial(\dot{p}, \dot{\theta})}{\partial(y_-, y_+)} \right| &= \left| \frac{\partial(y_-, y_+)}{\partial(\dot{p}, \dot{\theta})} \right|^{-1} \\
&= \left| \begin{pmatrix} -\tan\dot{\theta} & -(\sqrt{1-u^2}+\dot{p})\sec^2\dot{\theta} \\ -\tan\dot{\theta} & (\sqrt{1-u^2}-\dot{p})\sec^2\dot{\theta} \end{pmatrix} \right|^{-1} = \frac{1}{2\sqrt{1-u^2}\tan\dot{\theta}\sec^2\dot{\theta}}.
\end{aligned}
$$

Thus the intensity becomes

$$
\begin{aligned}
\Lambda(\,\mathrm{d}(y_-, y_+)\,) &= \frac{1}{2}\tan\dot{\theta}\sec^2\dot{\theta}\frac{1}{2\sqrt{1-u^2}\tan\dot{\theta}\sec^2\dot{\theta}}\,\mathrm{d}y_-\,\mathrm{d}y_+ \\
&= \frac{1}{4\sqrt{1-u^2}}\,\mathrm{d}y_-\,\mathrm{d}y_+.
\end{aligned}
$$

The above construction enable us to identify the limiting behaviour for the total traffic flow through the point $\boldsymbol{q} = (tn, un)$ conditioned on the existence of an horizontal line $\ell_q \in \Pi$ that passes through it. To show that this limit is in agreement with the asymptotics proven in Theorem 2.1, we first required the following result

LEMMA 2.3. *[Mean traffic flow at any point via an Improper Stationary Anisotropic Poisson line Process $\tilde{\Pi}$]*
Consider the original Poissonian city, that is the disk of radius n intersected with an

unit intensity Poisson line process Π. *The asymptotic mean traffic flow at any specific point* $\boldsymbol{q} = (tn, un)$ *(with* $u \in (-1, 1)$ *and* $t \in -\sqrt{1-u^2}, \sqrt{1-u^2})$ *conditioning on the presence of an horizontal line* $\ell_q : y = un$, *that is* $\ell_q \in \Pi$, *can be determined via an improper stationary Anisotropic Poisson line process* $\dot{\Pi}$ *over the infinite band* $[-1, 1] \times (-\infty, \infty))$ *with intensity given by* $\Lambda(\,\mathrm{d}(y_-, y_+)) = \frac{1}{4\sqrt{1-u^2}}$. *Even more, the computations through this anisotropic Poisson line process are in agreement with the asymptotics developed in Theorem 2.1, that is, in the improper anisotropic case we have that*

$$\mathbb{E}[T^q] \quad = \quad 2\sqrt{1-u^2}(1-u^2-t^2). \tag{2.23}$$

Proof. The traffic flow in the original Poissonian city through $\boldsymbol{q} = (tn, un)$ over the network generated by Π will correspond with the traffic at $\tilde{\boldsymbol{q}} = (t, u\sqrt{n})$ over the network generated by $\tilde{\Pi}$ after shrinking the x-axis by a factor of $1/n$ and the y-axis by $1/\sqrt{n}$, as shown in figure 2.6. This is due to the fact that the line process Π with intensity $\Lambda(\,\mathrm{d}(r, \theta)) = 1/2\,\mathrm{d}r\,\mathrm{d}\theta$ can be also expressed through the set of coordinates p and $\hat{\theta}$ as explained above; thus the intensity becomes $\Lambda(\,\mathrm{d}(p, \hat{\theta})) = \frac{1}{2}\sin\hat{\theta}\,\mathrm{d}p\,\mathrm{d}\hat{\theta}$. Therefore the line process $\tilde{\Pi}$ has intensity given by

$$\Lambda(\,\mathrm{d}(\tilde{p}, \tilde{\theta})) \quad = \quad \frac{1}{2} \frac{\tan\tilde{\theta}\sec^2\tilde{\theta}}{\left(1 + \frac{1}{n}\tan^2\tilde{\theta}\right)^{3/2}} \,\mathrm{d}\tilde{p}\,\mathrm{d}\tilde{\theta}\,.$$

In the coordinate system given by $(\tilde{x}, \tilde{y})$ we can translate the $\tilde{x}$-axis in such a way that it coincides with the horizontal line $\ell : \tilde{y} = u\sqrt{n}$, denote this new set of coordinates (after the aforementioned translation) by $(\dot{x}, \dot{y})$, i.e. $\dot{x} = \tilde{x}$ and $\dot{y} = \tilde{y} - u\sqrt{n}$. Notice the intensity $\Lambda(\,\mathrm{d}(\tilde{p}, \tilde{\theta}))$ remains unchanged.

Now, with this new set of coordinates, take the limit as $n \to \infty$ and consider the line parametrization given by y_- and y_+ as explained before. Due to the analysis developed in the proof for Theorem 2.1 we know that the asymptotic traffic flow at $\tilde{\boldsymbol{q}}$ will be determined by pair of points with small angles (α_1 and α_2) as their corresponding polar coordinates (taking $\tilde{\boldsymbol{q}}$ as the origin). So, we will focus only in pair of points $(-a+t, b)$ and $(v+t, w)$ such that $-\sqrt{1-u^2} \leq -a+t \leq t \leq v+t \leq \sqrt{1-u^2}$.

First, let us compute the probability that the line segment from $(-a+t, z)$ to $(v+t, z)$ is not separated from the point $\dot{\boldsymbol{q}}$ by the improper line process $\dot{\Pi}$, here $a \in (0, \sqrt{1-u^2}+t)$, $v \in (0, \sqrt{1-u^2}-t)$ and $z > 0$. The mean measure of the lines that implements such kind of separation can be separated into three disjoint sets:

- A contains the separating lines hitting the upper-left gray triangle in figure 2.8.

- C arises from the separating lines hitting the upper-right gray triangles in figure 2.8.

- B is derived from the contribution of the remaining separating lines.
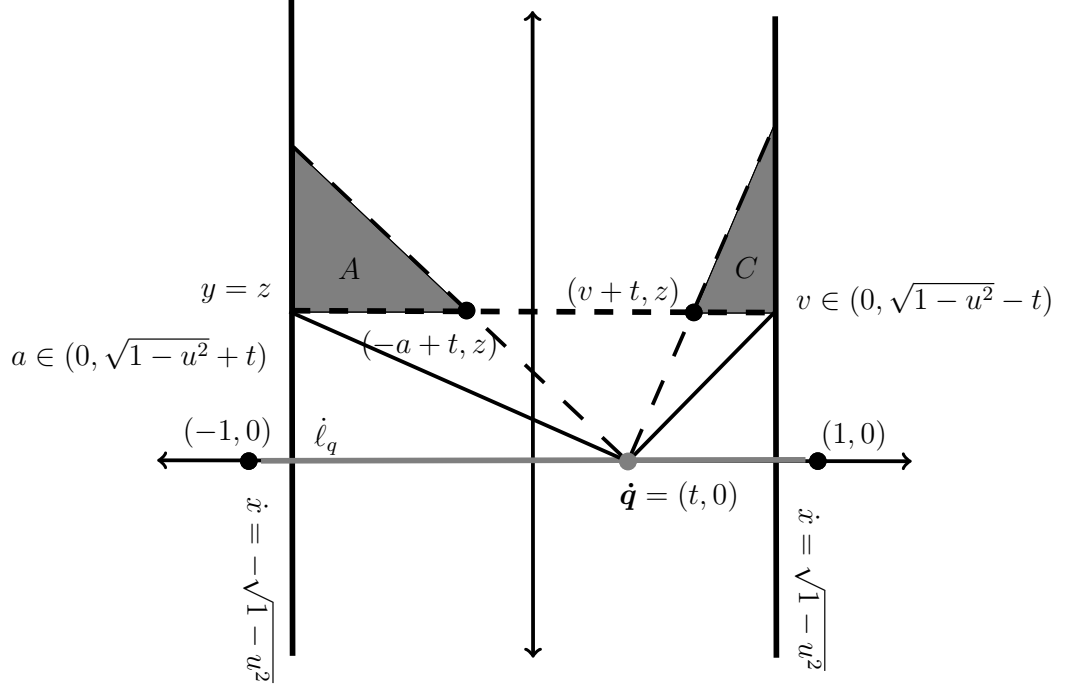
Figure 2.8: Calculations for the mean traffic flow at $\dot{q}$ based on the improper stationary anisotropic line process limit in terms of the triangles A, C and the remaining set of separating lines B.

The above contributions in terms of the intensity measure given by the (y_-, y_+) coordinate system are measured as follows:

In the contribution A the values for y_- can oscillate between $(z\,,\,\frac{z(\sqrt{1-u^2}+t)}{a})$. Thus, for each fixed value y_- on the aforementioned interval, the y_+ coordinate must belong to the interval $(-\frac{\sqrt{1-u^2}-t}{\sqrt{1-u^2}+t}y_-\,,\,y_- - 2\frac{(y_--z)\sqrt{1-u^2}}{\sqrt{1-u^2}+t-a})$ in order for the parametrized line ℓ to separate the point $\dot{q} = (t,0)$ from both points $(-a+t,z)$ and $(v+t,z)$ simultaneously. Therefore

$$
\begin{aligned}
\Lambda(A) &= \frac{1}{4\sqrt{1-u^2}} \int_z^{\frac{z(\sqrt{1-u^2}+t)}{a}} \int_{-\frac{\sqrt{1-u^2}-t}{\sqrt{1-u^2}+t}y_-}^{y_- - 2\frac{(y_--z)(\sqrt{1-u^2})}{\sqrt{1-u^2}+t-a}} \mathrm{d}y_+ \, \mathrm{d}y_- = \\
&\frac{1}{4\sqrt{1-u^2}} \int_z^{\frac{z(\sqrt{1-u^2}+t)}{a}} \sqrt{1-u^2}\left(2\frac{y_-}{\sqrt{1-u^2}+t} - 2\frac{y_--z}{\sqrt{1-u^2}+t-a}\right) \mathrm{d}y_- \\
&= \frac{z^2}{4}\left(\frac{\sqrt{1-u^2}+t}{a^2} - \frac{\sqrt{1-u^2}+t-a}{a^2} - \frac{1}{\sqrt{1-u^2}+t}\right) \\
&= \frac{z^2}{4}\left(\frac{1}{a} - \frac{1}{\sqrt{1-u^2}+t}\right).
\end{aligned}
$$

Similarly, in the contribution C the values for y_+ must belong to the interval $(z\,,\,\frac{z(\sqrt{1-u^2}-t)}{v})$. Then, for each fixed value y_+ on that interval, the y_- coordinate can range between $(-\frac{\sqrt{1-u^2}+t}{\sqrt{1-u^2}-t}y_+\,,\,y_+ - 2\frac{(y_+-z)\sqrt{1-u^2}}{\sqrt{1-u^2}-t-v})$ so the corresponding line ℓ separates $\dot{q}$ from both

42

points $(-a + t, z)$ and $(v + t, z)$ simultaneously. That leads to

$$\Lambda(C) \quad = \quad \frac{1}{4\sqrt{1-u^2}} \int_z^{\frac{z(\sqrt{1-u^2}-t)}{v}} \int_{-\frac{\sqrt{1-u^2}+t}{\sqrt{1-u^2}-t}y_+}^{y_+ - 2\frac{(y_+-z)\sqrt{1-u^2}}{\sqrt{1-u^2}-t-v}} \mathrm{d}y_- \, \mathrm{d}y_+ =$$

$$\frac{1}{4\sqrt{1-u^2}} \int_z^{\frac{z(\sqrt{1-u^2}-t)}{v}} \sqrt{1-u^2}\left(2\frac{y_+}{\sqrt{1-u^2}-t} - 2\frac{y_+ - z}{\sqrt{1-u^2}-t-v}\right) \mathrm{d}y_+$$

$$= \quad \frac{z^2}{4}\left(\frac{\sqrt{1-u^2}-t}{v^2} - \frac{\sqrt{1-u^2}-t-v}{v^2} - \frac{1}{\sqrt{1-u^2}-t}\right)$$

$$= \quad \frac{z^2}{4}\left(\frac{1}{v} - \frac{1}{\sqrt{1-u^2}-t}\right).$$

On the other hand, the lines contained on B correspond to those that have not been covered on A or C. Thus, the y_- coordinate has to range over the interval $(-\frac{\sqrt{1-u^2}+t}{\sqrt{1-u^2}-t}z, z)$. Then, for each fixed value y_- on the above set, the possibilities for y_+ are given by the interval $(-\frac{\sqrt{1-u^2}-t}{\sqrt{1-u^2}+t}y_-, z)$. Then

$$\Lambda(B) \quad = \quad \frac{1}{4\sqrt{1-u^2}} \int_{-\frac{\sqrt{1-u^2}+t}{\sqrt{1-u^2}-t}z}^{z} \int_{-\frac{\sqrt{1-u^2}-t}{\sqrt{1-u^2}+t}y_-}^{z} \mathrm{d}y_+ \, \mathrm{d}y_-$$

$$= \quad \frac{1}{4\sqrt{1-u^2}} \int_{-\frac{\sqrt{1-u^2}+t}{\sqrt{1-u^2}-t}z}^{z}\left(z + \frac{\sqrt{1-u^2}-t}{\sqrt{1-u^2}+t}y_-\right) \mathrm{d}y_-$$

$$= \quad \frac{z^2}{4\sqrt{1-u^2}}\left(1 + \frac{\sqrt{1-u^2}-t}{2(\sqrt{1-u^2}+t)} + \frac{\sqrt{1-u^2}+t}{2(\sqrt{1-u^2}-t)}\right)$$

$$= \quad \frac{z^2\sqrt{1-u^2}}{2(1-u^2-t^2)}.$$

In consequence,

$$\Lambda(A \cup B \cup C) \quad = \quad \Lambda(A) + \Lambda(B) + \Lambda(C) \quad =$$

$$\frac{z^2}{4}\left(\frac{1}{a} - \frac{1}{\sqrt{1-u^2}+t}\right) + \frac{z^2\sqrt{1-u^2}}{2(1-u^2-t^2)} + \frac{z^2}{4}\left(\frac{1}{v} - \frac{1}{\sqrt{1-u^2}-t}\right)$$

$$= \quad \frac{z^2}{4}\left(\frac{1}{a} + \frac{1}{v}\right).$$

Since $\dot{\Pi}$ is a Poisson process, the probability of there being no lines in $\dot{\Pi}$ separating the line segment from $(-a + t, z)$ to $(v + t, z)$ from $\dot{q}$ is

$$\exp\left(-\Lambda(A \cup B \cup C)\right) \quad = \quad \exp\left(-\frac{z^2}{4}\left(\frac{1}{a} + \frac{1}{v}\right)\right). \tag{2.24}$$

Finally, consider the special affine shear symmetries which leaves the vertical line $\dot{x} = t$ fixed. Due to this symmetry group, it follows that the probability of the line segment from $(-a + t, b)$ to $(v + t, w)$ not being separated from $\dot{q}$ will agree with

(2.24) when this line segment passes through the point (t, z). This happens when $z = \frac{bv+aw}{a+v}$. Moreover, if one also sets $p = b - w$ then

$$\left| \frac{\partial(p, z)}{\partial(b, w)} \right| = \left| \begin{pmatrix} 1 & -1 \\ \frac{v}{a+v} & \frac{a}{a+v} \end{pmatrix} \right| = 1 \, .$$

Notice that the mean 4-volume of the region representing the flow through $\dot{q}$ should be separated in its upper region $z \in (0, \infty)$ and its lower region $z \in (-\infty, 0)$, that is

$$\frac{1}{2} \int_0^{\sqrt{1-u^2}+t} \int_0^{\sqrt{1-u^2}-t} \int_0^{\infty} \int_{-\frac{a+v}{a}z}^{\frac{a+v}{v}z} \exp\left(-\frac{z^2}{4}\left(\frac{1}{a} + \frac{1}{v} \right) \right) dp\, dz\, dv\, da +$$

$$\frac{1}{2} \int_0^{\sqrt{1-u^2}+t} \int_0^{\sqrt{1-u^2}-t} \int_{-\infty}^0 \int_{-\frac{a+v}{a}z}^{\frac{a+v}{v}z} \exp\left(-\frac{z^2}{4}\left(\frac{1}{a} + \frac{1}{v} \right) \right) dp\, dz\, dv\, da \, .$$

However, those integrals are symmetric on the z variable. So, the second integral can be transformed into the first one by considering the substitution $\hat{z} = -z$. Therefore, the mean 4-volume of the region representing the flow through $\dot{q}$ is given by

$$\int_0^{\sqrt{1-u^2}+t} \int_0^{\sqrt{1-u^2}-t} \int_0^{\infty} \int_{-\frac{a+v}{a}z}^{\frac{a+v}{v}z} \exp\left(-\frac{z^2}{4}\left(\frac{1}{a} + \frac{1}{v} \right) \right) dp\, dz\, dv\, da$$

$$= \int_0^{\sqrt{1-u^2}+t} \int_0^{\sqrt{1-u^2}-t} \int_0^{\infty} (a+v)\left(\frac{1}{a} + \frac{1}{v} \right) \exp\left(-\frac{z^2}{4}\left(\frac{1}{a} + \frac{1}{v} \right) \right) z\, dz\, dv\, da$$

$$= 2 \int_0^{\sqrt{1-u^2}+t} \int_0^{\sqrt{1-u^2}-t} (a+v)\, dv\, da = 2\sqrt{1-u^2}(1 - u^2 - t^2) \, .$$

$\square$

The following result can be considered as a generalization of [25, Theorem 7], were the previous Lemma 2.3 plays an important role.

THEOREM 2.2. *The scaled quantity T_n^q/n^3 has a limiting distribution given by the analogous flow at the point $\dot{q}$ for the limiting improper stationary anisotropic Poisson line process.*

Proof. Fixed $q = (tn, un) \in \mathcal{B}_n(o)$ and conditioned on the event that the horizontal line $\ell_q : y = un$ belongs to Π. Set the affine shear transformation $\mathcal{T}_n^q(\tilde{x}, \tilde{y}) : [-(\sqrt{1-u^2}+t), \sqrt{1-u^2}-t] \times (0, \infty) \to [-(\sqrt{1-u^2}+t), \sqrt{1-u^2}-t] \times (0, \infty)$ given by $\mathcal{T}_n^q(\tilde{x}, \tilde{y}) = (n\tilde{x}, \sqrt{n}(\tilde{y} + u\sqrt{n}))$. Define for each $n \in \mathbb{N}$ coupled random functions by setting

$$I_n^q : ([-(\sqrt{1-u^2}+t), 0] \times (0, \infty)) \times ([0, \sqrt{1-u^2}-t] \times (0, \infty)) \to \{0, 1\} \, ,$$

$$I_n^q(\tilde{r}, \tilde{s}) = \mathbb{1}_{\{\mathcal{T}_n^q(\tilde{r}) \in \mathcal{B}_n(o)\}} \mathbb{1}_{\{\mathcal{T}_n^q(\tilde{s}) \in \mathcal{B}_n(o)\}} \mathbb{1}_{\{q \in \partial\mathcal{C}(\mathcal{T}_n^q(\tilde{r}), \mathcal{T}_n^q(\tilde{s}))\}} \, .$$

Therefore, I_n^q depends implicitly on the underlying Poisson line process $\tilde{\Pi}_n$. Notice

that if we consider $\mathcal{D}_n^q$ as in (2.1) then by construction

$$I_n^q(\tilde{\boldsymbol{r}}, \tilde{\boldsymbol{s}}) \quad = \quad \mathbb{1}_{\{(\mathcal{T}_n^q(\tilde{\boldsymbol{r}}), \mathcal{T}_n^q(\tilde{\boldsymbol{s}})) \in \mathcal{D}_n^q\}} \,. \tag{2.25}$$

Now remember that we can relate scaled finite-n instances (taking place over the ellipses with horizontal semi-minor axis of length 1 and vertical semi-major axis of length $\sqrt{n}$, see right hand side of figure 2.6) to the limiting case by a coupling argument involving the addition of further lines in such a way that

$$\Lambda_n(\,\mathrm{d}(\tilde{p}, \tilde{\theta})\,) = \frac{1}{2} \frac{\tan\tilde{\theta}\sec^2\tilde{\theta}}{\left(1 + \frac{1}{n}\tan^2\tilde{\theta}\right)^{3/2}}\, \mathrm{d}\tilde{p}\,\mathrm{d}\tilde{\theta} \nearrow \frac{1}{2}\tan\dot{\theta}\sec^2\dot{\theta}\,\mathrm{d}\dot{p}\,\mathrm{d}\dot{\theta} = \Lambda(\,\mathrm{d}(\dot{p}, \dot{\theta})\,)\,.$$

Equivalently, we can start with the limiting improper stationary anisotropic Poisson line process $\dot{\Pi}$ with intensity $\frac{1}{2}\tan\dot{\theta}\sec^2\dot{\theta}\,\mathrm{d}\dot{p}\,\mathrm{d}\dot{\theta}$ and obtain a proper stationary isotropic Poisson line process for each scale $n \in \mathbb{N}$ by randomly thinning the lines in $\dot{\Pi}$ (the thinning process will be different for every n, the bigger the n the less lines we need to thin from the line process $\dot{\Pi}$ to get $\tilde{\Pi}_n$) with retention probability depending monotonically on the line slope [25, page 31]. That is for every $m, n \in \mathbb{N}$ we can couple different Poisson line process $\tilde{\Pi}_m$ and $\tilde{\Pi}_n$, i.e. $I_m^q(\tilde{\boldsymbol{r}}, \tilde{\boldsymbol{s}})(\omega) = 1$ if and only if (almost $\mathbb{P}$-surely) $I_n^q(\tilde{\boldsymbol{r}}, \tilde{\boldsymbol{s}})(\omega) = 1$ (here $(\Omega, \mathcal{F}, \mathbb{P})$ is our underlying probability space where the different Poisson line process $\{\tilde{\Pi}_n : n \in \mathbb{N}\}$ takes place).

Therefore, due to this thinning process we arrange that $I_n^q(\tilde{\boldsymbol{r}}, \tilde{\boldsymbol{s}}) \to I^q(\dot{\boldsymbol{r}}, \dot{\boldsymbol{s}})$ almost surely for Lebesgue almost all $\tilde{\boldsymbol{r}}, \tilde{\boldsymbol{s}}$. Where $I^q(\dot{\boldsymbol{r}}, \dot{\boldsymbol{s}})$ is given by the analogous construction for I_n^q based on the limiting improper stationary anisotropic Poisson line process $\dot{\Pi}$ instead of using the transformation $\mathcal{T}_n^q$. In other words $I^q(\tilde{\boldsymbol{r}}, \tilde{\boldsymbol{s}})$ is the indicator function that traffic from $\dot{\boldsymbol{r}}$ to $\dot{\boldsymbol{s}}$ will pass through the point $\dot{\boldsymbol{q}} = (t, 0)$ when using the semi-perimeter routing rule.

Furthermore, one can realize T_n^q, as in (2.2), using (2.25), that is

$$\frac{T_n^q}{n^3} \quad = \quad \frac{1}{2}\iint I_n^q(\tilde{\boldsymbol{r}}, \tilde{\boldsymbol{s}})\,\mathrm{d}\tilde{\boldsymbol{r}}\,\mathrm{d}\tilde{\boldsymbol{s}}\,.$$

From Theorem 2.1 and Lemma 2.3, it follows that

$$\mathbb{E}\left[\frac{1}{2}\iint I_n^q(\tilde{\boldsymbol{r}}, \tilde{\boldsymbol{s}})\,\mathrm{d}\tilde{\boldsymbol{r}}\,\mathrm{d}\tilde{\boldsymbol{s}}\right] \nearrow \mathbb{E}\left[\frac{1}{2}\iint I^q(\dot{\boldsymbol{r}}, \dot{\boldsymbol{s}})\,\mathrm{d}\dot{\boldsymbol{r}}\,\mathrm{d}\dot{\boldsymbol{s}}\right] = 2\sqrt{1 - u^2}(1 - u^2 - t^2)\,.$$

Moreover, we also have $\mathfrak{L}_1$-convergence of I_n^q to I^q. To deduce that, first restrict our attention to the finite measure space $\Omega \times ([-2, 0] \times (0, K)) \times ([0, 2] \times (0, K))$, for any $K > 0$, and then use the dominated convergence theorem (valid since the indicator function I_n^q are bounded). Recall, $(\Omega, \mathcal{F}, \mathbb{P})$ is the underlying probability space.

Finally, to deduce convergence in distribution, apply Fatou's lemma to the nonnegative functions I_n^q and I^q to deliver $\mathfrak{L}_1$-convergence on all of $\Omega \times ([-2, 0] \times (0, \infty)) \times ([0, 2] \times (0, \infty])$. Therefore

$$\frac{T_n^q}{n^3} \quad = \quad \frac{1}{2} \iint I_n^q(\tilde{\boldsymbol{r}}, \tilde{\boldsymbol{s}}) \, \mathrm{d}\tilde{\boldsymbol{r}} \, \mathrm{d}\tilde{\boldsymbol{s}} \quad \overset{D}{\longrightarrow} \quad \frac{1}{2} \iint I^q(\tilde{\boldsymbol{r}}, \tilde{\boldsymbol{s}}) \, \mathrm{d}\tilde{\boldsymbol{r}} \, \mathrm{d}\tilde{\boldsymbol{s}},$$

as a functions of $\omega \in \Omega$, i.e. as random variables. $\qquad\qquad\square$

In conclusion, Theorem 2.1 and Theorem 2.2 agrees on the asymptotic mean traffic at point $\boldsymbol{q} = (tn, un)$ inside the Poissonian city as $n \to \infty$, conditioning on the presence of an horizontal line $\ell_q : y = un$ in the Poisson line process Π. However, both results are considering that the traffic flow is being generated by any pair of points $\boldsymbol{p}^-$ and $\boldsymbol{p}^+$ inside the disk of radius n: $\mathcal{B}_n(\boldsymbol{o})$. Almost surely $\boldsymbol{p}^-$ and $\boldsymbol{p}^+$ will not belong to the transportation network, i.e. the Poisson line process Π. In the following chapter, we will analyse the asymptotic mean traffic at $\boldsymbol{q} = (tn, un)$, conditioning on $\ell_q \in \Pi$, under the assumption that the traffic flow is being generated by a pair of points $\boldsymbol{x}$ and $\boldsymbol{y}$ that also belongs to the transportation network, in other words $\boldsymbol{x} \in \Pi$ and $\boldsymbol{y} \in \Pi$.

Chapter 3

Palm Theory

Consider a point process viewed as a random pattern $\Phi : (\Omega, \mathcal{F}, \mathbb{P}) \to (\mathbb{S}, \mathcal{S})$. Hence for each $\omega \in \Omega$, $\varphi = \Phi(\omega)$ denotes a specific locally finite set of points in $\mathbb{R}^d$, i.e. a realization of Φ. The Palm distribution $\mathbb{P}^{\boldsymbol{x}}$ at location $\boldsymbol{x}$ for a point process Φ is closely related to the intuitive notion of conditional probability. Here, the conditioning event is that a typical point from the point process Φ is located at $\boldsymbol{x}$, hence $\boldsymbol{x} \in \Phi$. We require for events $E \in \mathcal{S}$:

$$\mathbb{P}^{\boldsymbol{x}}(E) \quad = \quad \mathbb{P}[\Phi \in E \,||\, \boldsymbol{x} \in \Phi] \,. \tag{3.1}$$

Remark: The notation for Palm distribution $\mathbb{P}[\,\cdot\,||\,\boldsymbol{x}]$, must not be confused with the usual notation for conditional probability $\mathbb{P}[\,\cdot\,|\,B]$, that denotes the probability conditioned on the set B.

However, they both share a similar motivation. One version of the theorem that guarantees the existence of conditional probability states the following:

Theorem 3.1 (Conditional Probability). *[5, Theorem 5.3.1]*
Let $X : (\Omega, \mathcal{F}) \to (\mathbb{R}, \mathcal{B})$ be a random variable ($\mathcal{B}$ stands for the Borel σ-algebra in $\mathbb{R}$), and let B be a fixed Borel set. Let $\mathbb{P}_X$ be the probability induced by X, i.e. $\mathbb{P}_X(E) = \mathbb{P}[\{\omega \in \Omega : X(\omega) \in E\}]$, for any $E \in \mathcal{B}$. Then from the Radon-Nikodym Theorem it follows that there exists a real-valued Borel measurable function g on $(\mathbb{R}, \mathcal{B})$ such that for each $E \in \mathcal{B}$,

$$\mathbb{P}[\{X \in E\} \cap B] \quad = \quad \int_E g(x)\mathbb{P}_X(\,\mathrm{d}x\,) \,. \tag{3.2}$$

Furthermore, if h is another such function then $g = h$ $\mathbb{P}_X$-almost surely. We define $\mathbb{P}[B \mid X = x]$ as $g(x)$; which is essentially unique for a given B.

On the other hand, let $\Phi : (\Omega, \mathcal{F}, \mathbb{P}) \to (\mathbb{S}, \mathcal{S})$ be a Poisson point process with intensity λ. The idea for the Palm distribution is to find a function that satisfies an equation similar to (3.2). Consider an arbitrary nonnegative measurable function h

on $\mathbb{R}^d \times \mathbb{S}$, then the Palm distribution $\mathbb{P}^{\boldsymbol{x}}(E)$ is such that

$$\mathbb{E}\left[\sum_{\boldsymbol{x}\in\Phi} h(\boldsymbol{x},\Phi)\right] = \lambda \int_{\mathbb{R}^d} \mathbb{E}\Big[h(\boldsymbol{x},\Phi)\,||\,\boldsymbol{x}\Big]\,\mathrm{d}\boldsymbol{x} = \lambda \int_{\mathbb{R}^d}\int_{\mathbb{S}} h(\boldsymbol{x},\varphi)\mathbb{P}^{\boldsymbol{x}}(\,\mathrm{d}\varphi\,)\,\mathrm{d}\boldsymbol{x}\,. \quad (3.3)$$

The above remark shows that in order for this conditional probability to make sense in general one must consider the measure theoretic framework for Radon-Nikodym densities. We will review this ideas in order to discuss how to give meaning to the relation (3.1) through (3.3).

3.1 Conditional Probability and Radon-Nikodym densities

The elementary definition for conditional probability for a set E with respect to another set B is defined as

$$\mathbb{P}[E\,|\,B] \quad = \quad \frac{\mathbb{P}[E\cap B]}{\mathbb{P}[B]}\,, \quad\quad\quad (3.4)$$

as long as $\mathbb{P}[B] > 0$. Nevertheless, there are examples for which the conditional set B will have null probability, but the intuitive idea behind a conditional probability still make sense and can not be included in the above definition.

EXAMPLE 3.1 (Absolutely continuous random variables). *[5, Section 5.3]*
Let X and Y be random variables with joint density $f : \mathbb{R}^2 \to \mathbb{R}_+$. Namely $\Omega = \mathbb{R}^2$, $\mathcal{F} = \mathcal{B}(\mathbb{R}^2)$, $X(x,y) = x$ and $Y(x,y) = y$, with probability given by

$$\mathbb{P}[E] = \iint_E f(x,y)\,\mathrm{d}x\,\mathrm{d}y\,, \quad\quad \textit{for any } E \in \mathcal{F}\,.$$

Here the event $\{Y = y\}$ is a $\mathbb{P}$-null set for any $y \in \mathbb{R}$. However, there is a reasonable approach to the conditional probability $\mathbb{P}[X \in E\,|\,Y = y]$ related with the limiting case for the conditional probability of the event $\{Y \in (y - \varepsilon, y + \varepsilon)\}$ as $\varepsilon \to 0^+$. Notice that the event $\{Y \in (y - \varepsilon, y + \varepsilon)\}$ has a non-zero probability, therefore its conditional probability can be defined as:

$$\mathbb{P}[X \in E\,|\,y - \varepsilon < Y < y + \varepsilon] = \frac{\mathbb{P}[X \in E, y - \varepsilon < Y < y + \varepsilon]}{\mathbb{P}[X \in \mathbb{R}, y - \varepsilon < Y < y + \varepsilon]}$$

$$= \frac{\int_E \int_{y-\varepsilon}^{y+\varepsilon} f(x,t)\,\mathrm{d}t\,\mathrm{d}x}{\int_{y-\varepsilon}^{y+\varepsilon} \int_{-\infty}^{\infty} f(x,t)\,\mathrm{d}x\,\mathrm{d}t}\,.$$

Denote by $f_1(t) = \int_{-\infty}^{\infty} f(x,t)\,\mathrm{d}x$, which is the density of Y. Then, taking limits as

$\varepsilon \to 0^+$ *one should expect that*

$$\mathbb{P}[X \in E \mid Y = y] = \lim_{\varepsilon \to 0^+} \mathbb{P}[X \in E \mid y - \varepsilon < Y < y + \varepsilon]$$

$$= \lim_{\varepsilon \to 0^+} \frac{2\varepsilon \int_E f(x, y)\, \mathrm{d}x}{2\varepsilon f_1(y)} = \int_E \frac{f(x, y)}{f_1(y)}\, \mathrm{d}x \ . \quad (3.5)$$

This motivates the definition for a conditional density, namely

$$h(x \mid y) \quad = \quad \frac{f(x, y)}{f_1(y)} \ ,$$

that is defined as long as $f_1(y) > 0$. Notice, that is in fact the case up to a $\mathbb{P}$-null set, namely $S = \{(x, y) : f_1(y) = 0\}$. Since

$$\mathbb{P}[(X, Y) \in S] \quad = \quad \int_{\{f_1(y) = 0\}} \int_{-\infty}^{\infty} f(x, t)\, \mathrm{d}x\, \mathrm{d}t = \int_{\{f_1(y) = 0\}} f_1(t)\, \mathrm{d}t \quad = \quad 0 \ .$$

Therefore, the conditional probability $\mathbb{P}[X \in E \mid Y = y]$ can be defined by the relation:

$$\mathbb{P}[X \in E \mid Y = y] \quad = \quad \int_E h(x \mid y)\, \mathrm{d}x \ . \quad (3.6)$$

As mentioned in Theorem 3.1, in general the existence of such a function $h(x \mid y)$, named the conditional density function for $X \mid Y = y$, is a corollary of the Radon-Nikodym Theorem. To be explicit, under the conditions from Theorem 3.1, let $\nu(E) = \mathbb{P}(\{X \in E\} \cap B)$ for any $E \in \mathcal{B}$, then ν is a finite measure on $\mathcal{B}$ and is absolutely continuous with respect to $\mathbb{P}_X$, as clearly $\mathbb{P}_X(E) = 0$ implies that $\nu(E) = \mathbb{P}(\{X \in E\} \cap B) \le \mathbb{P}_X(E) = 0$, thus the existence of the conditional probability follows from Radon-Nikodym theorem.

Similarly in (3.1), the conditioning event $\{\boldsymbol{x} \in \Phi\}$ will be a $\mathbb{P}$ null-set, so the elementary definition of conditional probability cannot be applied. Therefore the Palm probability must be considered as a Radon-Nikodym density. Nevertheless, the later situation is not exactly the same as the one regarding $\mathbb{P}[X \in B \mid Y = y]$, since now the conditional event $\{\boldsymbol{x} \in \Phi\}$ depends not only on the measurable space $(\mathbb{S}, \mathcal{B})$ in question, but also in the location of $\boldsymbol{x} \in \mathbb{R}^d$. This important difference, which has already been presented at (3.3), leads us to the notion of *Campbell measure*.

3.2 Campbell measures

The construction of Palm distribution sketched here follows the ideas described in Baddeley [8, Section 9.3] and Chiu et al. [13, Section 4.4]. Let $(\Omega, \mathcal{F}, \mathbb{P})$ be the underlying probability space and $(\mathbb{S}, \mathcal{S})$ be the corresponding measurable space for point processes in $\mathbb{R}^d$. We write $\Phi(B) = \#[\Phi \cap B]$ for the random number of points from Φ lying in B, as $B \subseteq \mathbb{R}^d$ belongs to the family of Borel subsets of $\mathbb{R}^d$.

Definition 3.1 (Campbell measure). *[13, Section 4.3.4]*
Suppose that the intensity measure $\Lambda(K) = \mathbb{E}[\Phi(K)]$ exists and is finite for all compact sets $K \subset \mathbb{R}^d$. The Campbell measure is a measure on the minimal σ-field of subsets in $\mathbb{R}^d \times \mathbb{S}$ that contains all the sets of the form $B \times E$, for $B \in \mathcal{B}^d$ and $E \in \mathcal{S}$, which will be denoted by $\sigma(\mathcal{B}^d \times \mathcal{S})$, and is defined by

$$\mathscr{C}(B \times E) \quad = \quad \mathbb{E}[\Phi(B)\mathbb{1}_E(\Phi)] \quad = \quad \int_{\mathbb{S}} \varphi(B)\mathbb{1}_E(\varphi)\mathbb{P}(\,\mathrm{d}\varphi\,)\,,$$

for all Borel sets $B \subseteq \mathbb{R}^d$ and all events $E \in \mathcal{S}$, i.e. E is a subset of the family of sequences of points φ in $\mathbb{R}^d$ that are locally finite and simple. Here we use the convention that $\varphi = \Phi(\omega)$ and $\mathbb{P}(\,\mathrm{d}\varphi\,)$ is the induced distribution from Φ over the measurable space $(\Omega, \mathcal{F}, \mathbb{P})$, which could also be denote by $\mathbb{P}_\Phi(\,\mathrm{d}\omega\,)$.

Moreover, the usual measure theoretic approach to integrals of non-negative functions leads to [13, Equation (4.48)]

$$\int_{\mathbb{S}} \sum_{\boldsymbol{x} \in \varphi} h(x, \varphi)\mathbb{P}(\,\mathrm{d}\varphi\,) \quad = \quad \int_{\mathbb{S}} h(x, \varphi)\mathscr{C}(\,\mathrm{d}(x, \varphi)),$$

where h is any non-negative measurable function on $\mathbb{R}^d \times \mathbb{S}$. This brings us closer to the relation (3.3). Actually, a simplified version of (3.3) is given by:

Theorem 3.2 (Campbell Theorem). *[13, Theorem 4.1]*
Let $\Phi : (\Omega, \mathcal{F}, \mathbb{P}) \to (\mathbb{S}, \mathcal{S})$ be a point process with intensity function Λ, that is $\Lambda(B) = \mathbb{E}[\Phi(B)] = \int_{\mathbb{S}} \varphi(\,\mathrm{d}x\,)\mathbb{P}(\,\mathrm{d}\varphi\,)$. Then for any nonnegative measurable function $f : \mathbb{R}^d \to \mathbb{R}_+$:

$$\mathbb{E}\left[\sum_{\boldsymbol{x} \in \Phi} f(\boldsymbol{x})\right] = \int_{\mathbb{S}} \sum_{\boldsymbol{x} \in \varphi} f(\boldsymbol{x})\mathbb{P}(\,\mathrm{d}\varphi\,) = \int_{\mathbb{S}} \int_{\mathbb{R}^d} f(\boldsymbol{x})\varphi(\,\mathrm{d}\boldsymbol{x}\,)\mathbb{P}(\,\mathrm{d}\varphi\,)$$

$$= \int_{\mathbb{R}^d} f(\boldsymbol{x})\Lambda(\,\mathrm{d}\boldsymbol{x}\,)\,. \quad (3.7)$$

3.3 Palm Distribution

The construction of the Palm distribution is closely related to the Campbell measure $\mathscr{C}(\cdot \times \cdot)$. Consider a σ-finite measure μ_E on $\mathbb{R}^d$ defined for each fixed event $E \in \mathcal{S}$ by

$$\mu_E(B) \quad = \quad \mathscr{C}(B \times E)\,,$$

for all bounded Borel sets $B \subset \mathbb{R}^d$. By definition

$$\mu_E(B) \quad = \quad \mathscr{C}(B \times E) = \mathbb{E}[\Phi(B)\mathbb{1}_E(\Phi)] \leq \mathbb{E}[\Phi(B)] \quad = \quad \Lambda(B)\,.$$

So μ_E is absolutely continuous with respect to Λ. Thus by the *Radon-Nikodym*

Theorem there exists a density function $f_E : \mathbb{R}^d \to \mathbb{R}_+$ such that

$$\mu_E(B) \quad = \quad \int_B f_E(\boldsymbol{x})\Lambda(\,\mathrm{d}\boldsymbol{x}\,)\,,$$

for all measurable $B \subset \mathbb{R}^d$. This defines $f_E(\boldsymbol{x})$ up to a Λ-null set N_E in $\boldsymbol{x}$. However *a priori* this null-set will depend on the choice of $E \in \mathcal{S}$. We write $\mathbb{P}^{\boldsymbol{x}}(E) = f_E(\boldsymbol{x})$ so that

$$\mu_E(B) \quad = \quad \mathscr{C}(B \times E) \quad = \quad \mathbb{E}[\Phi(B)\mathbb{1}_E(\Phi)] \quad = \quad \int_B \mathbb{P}^{\boldsymbol{x}}(E)\Lambda(\,\mathrm{d}\boldsymbol{x}\,)\,, \quad (3.8)$$

where

$$\mathbb{P}^{\boldsymbol{x}}(E) \quad = \quad \frac{\mathbb{E}[\Phi(\,\mathrm{d}\boldsymbol{x}\,)\mathbb{1}_E(\Phi)]}{\Lambda(\,\mathrm{d}\boldsymbol{x}\,)} \qquad \Lambda \quad \text{a. s. in } \boldsymbol{x}\,.$$

However, under the right conditions $\{P^{\boldsymbol{x}}(E) : \boldsymbol{x} \in \mathbb{R}\}$ are considered to be a family of probability measures on $\mathcal{S}$. These conditions are discussed in the measure theory framework, as part of the subject of *regular conditional probabilities* (see Kallenberg [22, Chapter 5] and Billingsley [11, Section 33], for example). Basically one requires that the space $\mathbb{S}$ with Borel σ-algebra $\mathcal{S}$ has to be a *complete separable metric space*.

In this case $\mathbb{S}$ is the family of all sequences φ of points over $\mathbb{R}^d$ that are locally finite and simple. So the conditions for the existence of regular conditional probabilities are satisfied. In consequence one can think of $f_E(\boldsymbol{x})$ as the probability for the event E under the Palm distribution at $\boldsymbol{x}$, i.e. $\mathbb{P}^{\boldsymbol{x}}(E)$. Therefore we may assure that the mapping $(\boldsymbol{x}, E) \to \mathbb{P}^{\boldsymbol{x}}(E)$ must be a *regular conditional probability kernel*, that is

- For all $E \in \mathcal{S}$ the function $\boldsymbol{x} \to \mathbb{P}^{\boldsymbol{x}}(E)$ is measurable.

- $\mathbb{P}^{\boldsymbol{x}}(\cdot)$ is a probability measure on Ω for Λ-almost all $\boldsymbol{x} \in \mathbb{R}^d$.

This leads to the following definition

DEFINITION 3.2 (Palm distribution). *[13, Section 4.4.3]*
Set $\Phi : (\Omega, \mathcal{F}, \mathbb{P}) \to (\mathbb{S}, \mathcal{S})$ to be a point process, where $(\mathbb{S}, \mathcal{S})$ is a complete separable metric space. Suppose that the intensity measure $\Lambda(\cdot) = \mathbb{E}[\Phi(\cdot)]$ exists and is σ-finite. This implies that the Campbell measure $\mathscr{C}$ is also σ-finite. Even more, for any configuration set $E \in \mathcal{S}$, the measure $\mathscr{C}(\cdot \times E)$ is absolutely continuous with respect to Λ. Thus, there exists a density function, which depends on E, such that:

$$\mathscr{C}(B \times E) \quad = \quad \int_B \mathbb{P}^{\boldsymbol{x}}(E)\Lambda(\,\mathrm{d}x\,)\,. \quad (3.9)$$

Furthermore, for a fixed $\boldsymbol{x} \in \mathbb{R}$, $\mathbb{P}^{\boldsymbol{x}}(\cdot)$ can be taken as a distribution on $(\mathbb{S}, \mathcal{S})$, that is the Palm distribution of $\mathbb{P}$ with respect to $\boldsymbol{x}$.

An important consequence of this definition for the case of homogeneous Poisson point processes is related with the Campbell Theorem 3.2 and the relation (3.3).

51

Theorem 3.3 (Campbell-Mecke Theorem). *[13, Theorem 4.2]*
Let $\Phi : (\Omega, \mathcal{F}, \mathbb{P}) \to (\mathbb{S}, \mathcal{S})$ be a Poisson point process with intensity λ. Then for any nonnegative measurable function h on $\mathbb{R}^d \times \mathbb{S}$:

$$\mathbb{E}\left[\sum_{\boldsymbol{x} \in \Phi} h(\boldsymbol{x}, \Phi)\right] = \int_{\mathbb{S}} \sum_{\boldsymbol{x} \in \varphi} h(\boldsymbol{x}, \varphi)\mathbb{P}(\mathrm{d}\varphi) = \lambda \int_{\mathbb{R}^d} \int_{\mathbb{S}} h(\boldsymbol{x}, \varphi)\mathbb{P}^{\boldsymbol{x}}(\mathrm{d}\varphi)\,\mathrm{d}\boldsymbol{x}\,.$$

(3.10)

Remark: Substituting $h(\boldsymbol{x}, \varphi) = f(\boldsymbol{x})$ in (3.10) gives (3.7), the simple Campbell Theorem 3.2

There is an important Theorem, namely *Slivnyak - Mecke Theorem* [8, Example 26], which states that the Palm distribution $\mathbb{P}^{\boldsymbol{x}}$ for Poisson point process, Φ, is equivalent to the original distribution of the process modified by adding a fixed point $\boldsymbol{x}$, i.e.

$$\mathbb{P}^{\boldsymbol{x}}(E) = \mathbb{P}[\Phi \in E \mid\mid \boldsymbol{x} \in \Phi] = \mathbb{P}[(\Phi \cup \{\boldsymbol{x}\}) \in E]\,.$$

This is one of the most important results that we will be applying in section 3.5, so we will explain it in more details on the following section.

3.4 Examples

Palm theory arises as a tool for Queueing Theory, more information on this topic can be found at Baccelli and Bremaud [6]. The main interpretation for Palm distribution under the context of queueing theory is as an insight about how the stochastic process is observed by a *typical customer*. Here the stochastic process is the queue itself (which can be seeing as a point process Φ) and a typical customer represents an specific point being part of this process, i.e. $\boldsymbol{x} \in \Phi$. Palm probabilities are relevant to queueing theory, in particular the so called Palm calculus based on Matthes' definition and Mecke formula [28]. The main application for Palm calculus comes as a natural framework for the study of relations between time averages and event averages, such as

1. Little's Theorem $L = \lambda W$ [6, Section 3.1], [30],

2. Brumelle's $H = \lambda G$ formula [6, Section 3.2],

3. Kleinrock's conservation law [6, Section 3.2.4] and

4. PASTA (Poisson Arrivals See Time Averages) property [6, Section 3.3.1].

However, for the purpose of this work we will focus our attention in the application of the Palm theory to the specific cases of Poisson point processes and Poisson line processes.

EXAMPLE 3.2 (Palm distribution for a Poisson point process, Φ). *[13, Example 4.3]*

One of the most common examples arises by the following problem: Given an homogeneous Poisson process Φ of intensity λ, what can be said about the probability of any event $E \in \mathcal{S}$ if one conditions on the presence of a point $\boldsymbol{x}$ as part of Φ. Short answer: the Palm distribution with respect to $\boldsymbol{x}$ is simply the distribution of the original Poisson process plus the added point $\boldsymbol{x}$. This is stated in the Slivnyak - Mecke theorem. *In mathematical language, using the notation from the previous section this can be expressed as follows:*

$$\mathbb{P}^{\boldsymbol{x}}(E) \quad = \quad \mathbb{P}[\Phi \in E \, || \, \boldsymbol{x} \in \Phi] \quad = \quad \mathbb{P}[\Phi \cup \{\boldsymbol{x}\} \in E] \qquad \text{for any } E \in \mathcal{S},$$

or

$$\int_{\mathbb{S}} f(\varphi) \, \mathbb{P}^{\boldsymbol{x}}(\mathrm{d}\varphi) \quad = \quad \int_{\mathbb{S}} f(\varphi \cup \{\boldsymbol{x}\}) \, \mathbb{P}(\mathrm{d}\varphi)$$

for all measurable non-negative functions f on $(\mathbb{S}, \mathcal{S})$.

Proof. This sketch of proof will focus on the plane, that is we are thinking in $\mathbb{R}^2$. For this case the point processes $\Phi : (\Omega, \mathcal{F}) \to (\mathbb{S}, \mathcal{S})$ will be characterized by the configurations sets given by

$$Y_K \quad = \quad \{\varphi \in \mathbb{S} : \varphi(K) = 0\} \subset \mathbb{S}, \tag{3.11}$$

where K is a semi-closed rectangle, that is $K = [a, b) \times [c, d)$ for some real numbers a, b, c, d. Even more, the family of such kind of configurations, say

$$\mathcal{Q} \quad = \quad \{Y_K : K \text{ is a finite union of semi-closed rectangles}\},$$

is a Π-system, since the patterns that do not intersect K_1 and the patterns that do not intersect K_2 are the same patterns that do not intersect $K_1 \cup K_2$, i.e. $Y_{K_1} \cap Y_{K_2} = Y_{K_1 \cup K_2}$.

In consequence, knowledge of $\mathbb{P}[Y_K]$ for all K (finite unions of semi-closed rectangles) will specify $\mathbb{P}$ on $\mathcal{S}$.

To prove the above statement, notice that we can approximate $\varphi(B)$ for any Borel set $B \subset \mathbb{R}^2$ by using the σ-field generated by $\mathcal{Q}$. The idea will be to tessellate B by semi-rectangles that forms a tiling $\mathcal{T}_n = \bigcup_{i \in \mathbb{N}} K_i$, where the diameter of each tile K_i is smaller than $1/n$. We can make the tiles as small as we required by taking $n \to \infty$. Moreover, for n large enough we will have that:

$$\varphi(B) \quad = \quad \sum_{K_i \in \mathcal{T}_n} \varphi(K_i).$$

To show the above equality, first notice that for every $n \in \mathbb{N}$

$$\sum_{K_i \in \mathcal{T}_n} \mathbb{1}_{\{\varphi(K_i) \geq 1\}} \quad \leq \quad \varphi(B) \,, \tag{3.12}$$

since if we count the number of tiles K_i with points from φ, these will always be less than the number of points in B as $K_i \subseteq B$ for all $i \in \mathbb{N}$, and it could be the case that one tile has more than one point from φ. Also the sum in (3.12) is non decreasing in n. Thus, we need to show that

$$\varphi(B) \quad = \quad \lim_{n \to \infty} \sum_{K_i \in \mathcal{T}_n} \varphi(K_i) \,.$$

Suppose the inequality in (3.12) is strict in the limit. That would imply that there is a location $\boldsymbol{x} \in B$ such that the corresponding tiles K_{i_n} (for different tilings $\mathcal{T}_n$ as n increases) always catches more than one point from φ, i.e. $\varphi(K_{i_n}) \geq 2$ for all n, but in the limit this will contradict the simple property, as $\varphi(K_{i_n}) \geq 2$ for all $n \in \mathbb{N}$ (where $\boldsymbol{x} \in K_{i_n}$ for all $n \in \mathbb{N}$) will imply that there are two points from φ in the exact location $\boldsymbol{x}$. Thus the equality must hold in the limit. In consequence the σ-field $\mathcal{S}$ is the same than the minimal σ-field of subsets in $\mathbb{S}$ that contains the family $\mathcal{Q}$.

Therefore, if Φ is a Poisson point process in $\mathbb{R}^2$ with intensity λ and we want to condition on the event $\{\boldsymbol{x} \in \Phi\}$, then we can analyse the Campbell measure for a particular kind of set, say $B \times Y_K$, with Y_K as in (3.11), that is

$$\mathscr{C}(B \times Y_K) = \mathbb{E}\Big[\Phi(B)\mathbb{1}_{Y_K}(\Phi)\Big] = \mathbb{E}\Big[\sum_{\boldsymbol{x} \in \Phi} \mathbb{1}_{\{\boldsymbol{x} \in B\}}\mathbb{1}_{Y_K}(\Phi)\Big]$$

$$= \mathbb{E}\Big[\sum_{\boldsymbol{x} \in \Phi \cap B} \mathbb{1}_{\{\Phi \cap K = \emptyset\}}\Big] = \mathbb{E}\Big[\sum_{\boldsymbol{x} \in \Phi \cap B \setminus K} \mathbb{1}_{\{\Phi \cap K = \emptyset\}}\Big] \,.$$

Recall that by definition $\Phi \in Y_K$ means that there are no points from Φ in the set K. Therefore if we subtract the points from Φ that are in the set K we are actually subtracting nothing, as $\Phi \in Y_K$. Now, recall that $\Phi \cap K$ and $\Phi \cap K^c = \Phi \setminus K$ are independent for a Poisson point process, therefore

$$\mathscr{C}(B \times Y_K) = \mathbb{E}\Big[\sum_{\boldsymbol{x} \in \Phi \cap B \setminus K} 1\mathbb{1}_{\{\Phi \cap K = \emptyset\}}\Big] = \mathbb{E}\Big[\mathbb{1}_{\{\Phi \cap K = \emptyset\}}\Big]\mathbb{E}\Big[\sum_{\boldsymbol{x} \in \Phi \cap B \setminus K} 1\Big]$$

$$= \mathbb{P}\Big[\Phi \cap K = \emptyset\Big]\mathbb{E}\Big[\sum_{\boldsymbol{x} \in \Phi} \mathbb{1}_{\{\boldsymbol{x} \in B \setminus K\}}\Big] = \exp\left(-\lambda \operatorname{Leb}_2(K)\right)\Lambda(B \setminus K)$$

$$= \int_B \mathbb{P}^{\boldsymbol{x}}[Y_K]\Lambda(\,\mathrm{d}x\,) \,.$$

Since

$$\Lambda(B) \;=\; \Lambda(B \cap K) + \Lambda(B \setminus K) \;=\; \Lambda(B \setminus K)\,,$$

because, by definition, under the event Y_K we have that Φ do not have any points on K, i.e. $0 \le \Lambda(B \cap K) \le \Lambda(K) = 0$ for every $B \subset \mathbb{R}^2$.

Now recall that, from definition of the Palm distribution

$$\mathscr{C}(B \times Y_K) \;\;=\;\; \int_B \mathbb{P}^{\boldsymbol{x}}[Y_K]\Lambda(\,\mathrm{d}x\,)\,.$$

Therefore for this case, we will have that:

$$\mathbb{P}^{\boldsymbol{x}}[Y_K] = \begin{cases} 0 & \text{if } \boldsymbol{x} \in K\,, \\ \exp\left(-\lambda\,\mathrm{Leb}_2(K)\right) & \text{if } \boldsymbol{x} \notin K \end{cases}$$

which are the same void probabilities as the one corresponding to a Poisson point process with intensity λ with an extra fixed point at $\boldsymbol{x}$, i.e. $\Phi \cup \{\boldsymbol{x}\}$. From Rényi's Theorem [29] it is known that the family of avoidance probabilities characterizes the Poisson point process. Therefore we have completed the proof, since $\mathcal{Q}$ is a Π-system such that $\sigma(\mathcal{Q}) = \mathcal{S}$ and we have already identified their corresponding void probabilities to be the same as the Poisson point process given by $\Phi \cup \{\boldsymbol{x}\}$. $\qquad\square$

EXAMPLE 3.3 (Palm distribution for a Poisson line process, Π). *[13, Example 4.3] As it has been explained before (see Section 1.3), a line process Π can be identified with a point process over the surface of a half-cylinder in $\mathbb{R}^3$, say*

$$\boldsymbol{C} = \left\{(\cos\theta, \sin\theta, r) \in \mathbb{R}^3 : r \in \mathbb{R}, \theta \in (0, \pi]\right\}\,.$$

Thus, each line $\ell \in \Pi$ is uniquely defined by the pair of parameters (r, θ) where r represents the signed perpendicular distance from ℓ to the origin $\boldsymbol{o}$, and θ is the angle between the line ℓ and the x-axis. Therefore, from the above argument we can conclude that the Palm distribution for a Poisson line process Π with respect to ℓ is given by

$$\mathbb{P}[\Pi \in E \parallel \ell \in \Pi] \;\;=\;\; \mathbb{P}[\Pi \cup \{\ell\} \in E] \qquad \textit{for any } E \in \mathcal{S}\,. \qquad (3.13)$$

3.5 Palm Distribution on the Poissonian city

In this section we are interested in the behaviour for the mean amount of traffic flow across the Poissonian city. It will be informative to compare the traffic distribution throughout the Poissonian city with a specific data set, namely the one presented in the Beeching report [12, Figure 1, Appendix 1] regarding the British Railway system. To establish some notation:

- Π is a Poisson line process of unit intensity.

- $\mathcal{B}_{an}(\boldsymbol{o})$ is a disk of radius an, for some $a \in [0, 1]$, centred at the origin $\boldsymbol{o}$.

- $\mathcal{H}_1^\Pi$ is the Hausdorff 1-dimensional measure [16, 39] over the line process Π, defined for any Borel subset $B \subseteq \mathbb{R}^2$ by $\mathcal{H}_1^\Pi(B) = \mathcal{H}_1(B \cap \Pi)$. Moreover, since Π is a locally finite line process, for any compact set K in $\mathbb{R}^2$ it is the case that $\mathcal{H}_1^\Pi(K) = \mathcal{H}_1(K \cap \Pi) = \sum_{i=1}^{n_K} \mathcal{H}_1(K \cap \ell_i) = \sum_{i=1}^{n_K} \mathcal{H}_1^{\ell_i}(K)$, where $\ell_1, \ell_2, \ldots, \ell_{n_K}$ are the (finite number of) lines from Π that hits the compact set K and $\mathcal{H}_1^{\ell_i}(K) = \mathcal{H}_1(K \cap \ell_i)$. A similar relation holds for any Borel subset $B \subseteq \mathbb{R}^2$, but the sum might be over a countable amount of lines $\ell \in \Pi$ if B is non-compact.

- Φ_1 and Φ_2 are conditionally independent Cox point processes [13, Section 5.2] governed by the random measure $\mathcal{H}_1^\Pi$. That is, conditioning on a particular realization of the line process Π, Φ_1 and Φ_2 are independent Poisson point processes over $\mathcal{B}_n(\boldsymbol{o})$ using $\mathcal{H}_1^\Pi(\cdot)$ as their shared governing measure. Without loss of generality we will consider the points $\boldsymbol{x} \in \Phi_1$ to be sources nodes and the points $\boldsymbol{y} \in \Phi_2$ to be destination nodes.

The idea is to analyze the mean amount of traffic taking place over the subregion $\mathcal{B}_{an}(\boldsymbol{o})$ as a ranges over $[0, 1]$. Traffic runs from Φ_1 to Φ_2, using the semi-perimeter routes arising from the line process Π. So the mean traffic on the subregion $\mathcal{B}_{an}(\boldsymbol{o})$ is given by the following expression:

$$\mathbb{E}\left[\sum_{\boldsymbol{x} \in \Phi_1} \sum_{\boldsymbol{y} \in \Phi_2} \int_{\mathcal{B}_{an}(\boldsymbol{o})} f(\boldsymbol{x}, \boldsymbol{y}, \boldsymbol{q}; \Pi) \mathcal{H}_1^\Pi(\mathrm{d}\boldsymbol{q})\right]. \tag{3.14}$$

Here

- $f(\boldsymbol{x}, \boldsymbol{y}, \boldsymbol{q}; \Pi) = \mathbb{1}_{\{\boldsymbol{q} \in \partial\mathcal{C}(\boldsymbol{x}, \boldsymbol{y})\}} : \mathbb{R}^2 \times \mathbb{R}^2 \times \mathbb{R}^2 \to \{0, 1\}$ is an indicator function. It has value 1 when $\boldsymbol{q} \in \partial\mathcal{C}(\boldsymbol{x}, \boldsymbol{y}) = \gamma_-(\boldsymbol{x}, \boldsymbol{y}) \cup \gamma_+(\boldsymbol{x}, \boldsymbol{y}) \subseteq \Pi$ (the two routes generated by the semi-perimeter routing rule when going from $\boldsymbol{x}$ to $\boldsymbol{y}$) and it is 0 otherwise.

- The expectation is taken with respect to both Cox point processes Φ_1 and Φ_2 and also the line process Π.

In consequence, the formula in (3.14) represents the mean amount of traffic flow over the sub-disk of radius an, concentric with $\mathcal{B}_n(\boldsymbol{o})$. The above idea, regarding the measurement for mean traffic flow for a specific subregion is illustrated in figure 3.2.

The purpose of this section is to find an equivalent expression for (3.14) in terms of the known quantity $\mathbb{E}[T_n^q]$, which has been analyzed in chapter 2. Notice that the Hausdorff 1-dimensional measure $\mathcal{H}_1^\Pi$ over the Poisson line process Π can be decomposed as the countable sum of the Hausdorff 1-dimensional measures $\mathcal{H}_1^\ell$ over
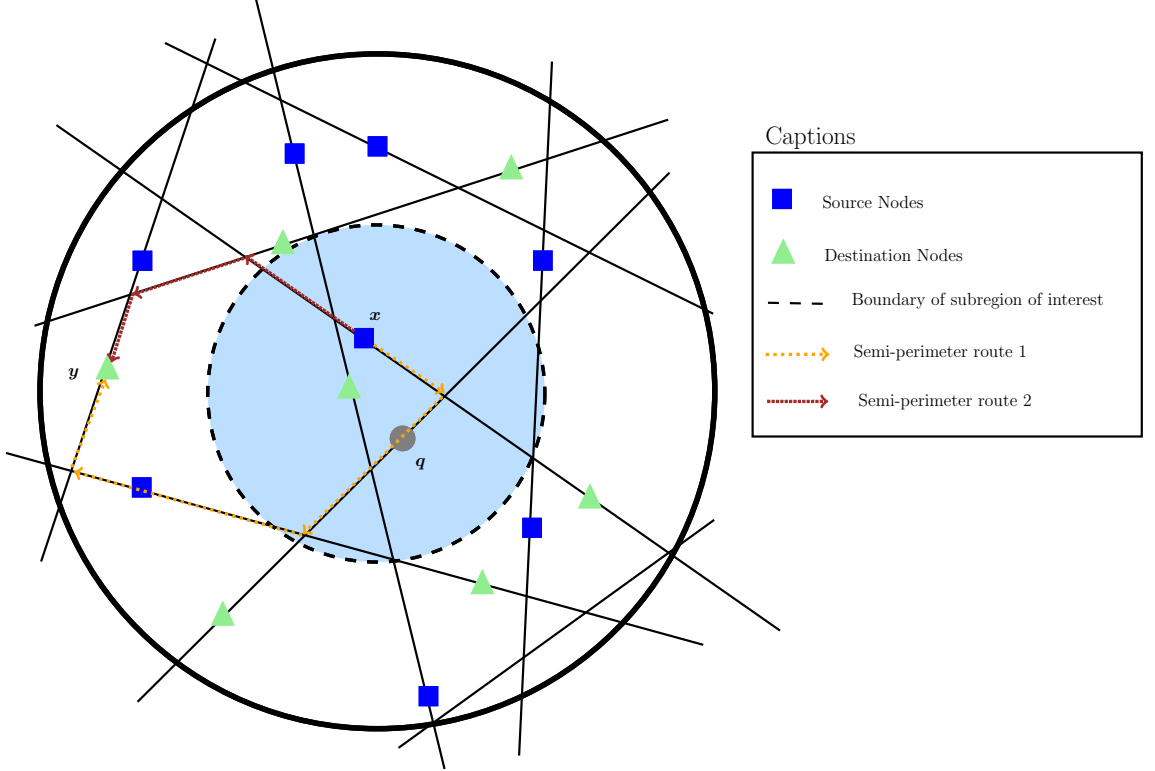
Figure 3.1: An example regarding the measurement for the mean asymptotic traffic in a specific subregion (light blue background). Here we illustrate how an specific pair of source $\boldsymbol{x}$ (squares) and destination $\boldsymbol{y}$ (triangles) nodes, from Φ_1 and Φ_2 respectively, can contribute to the mean traffic for a fixed point $\boldsymbol{q}$ inside the subregion to be considered. In this example, by using the semi-perimeter routing rule, only the first route will pass through $\boldsymbol{q}$. Notice that the source and destination nodes are not necessarily contained in the subregion of interest.

each line $\ell \in \Pi$, i.e. $\mathcal{H}_1^{\Pi}(\cdot) = \sum_{\ell \in \Pi} \mathcal{H}_1^{\ell}(\cdot)$. Thus (3.14) can be rewritten as follows

$$\mathbb{E}\left[\sum_{\boldsymbol{x} \in \Phi_1} \sum_{\boldsymbol{y} \in \Phi_2} \int_{\mathcal{B}_{an}(\boldsymbol{o})} f(\boldsymbol{x}, \boldsymbol{y}, \boldsymbol{q}; \Pi) \mathcal{H}_1^{\Pi}(\,\mathrm{d}\boldsymbol{q}\,)\right] =$$

$$\mathbb{E}\left[\sum_{\boldsymbol{x} \in \Phi_1} \sum_{\boldsymbol{y} \in \Phi_2} \left(\sum_{\ell \in \Pi} \int_{\mathcal{B}_{an}(\boldsymbol{o})} f(\boldsymbol{x}, \boldsymbol{y}, \boldsymbol{q}; \Pi) \mathcal{H}_1^{\ell}(\,\mathrm{d}\boldsymbol{q}\,)\right)\right]. \quad (3.15)$$

Now, conditioning on a specific realization of the line process Π, the point processes for the source and destination nodes, Φ_1 and Φ_2 respectively, can be viewed as two independent Poisson point processes over $\mathcal{B}_n(\boldsymbol{o})$ with common intensity measure given by $\mathcal{H}_1^{\Pi}(\cdot)$. So we can apply the tower property for expectation to re-express (3.15). Moreover, the Campbell-Mecke Theorem [14] can be applied to both point processes Φ_1 and Φ_2. Using the explicit expression for the Palm distribution of

Poisson process the above amount can be expressed as

$$\mathbb{E}\left[\sum_{\boldsymbol{x}\in\Phi_1}\sum_{\boldsymbol{y}\in\Phi_2}\left(\sum_{\ell\in\Pi}\int_{\mathcal{B}_{an}(\boldsymbol{o})}f(\boldsymbol{x},\boldsymbol{y},\boldsymbol{q};\Pi)\mathcal{H}_1^{\ell}(\,\mathrm{d}\boldsymbol{q})\right)\right]$$

$$=\quad\mathbb{E}\left[\mathbb{E}\left[\sum_{\boldsymbol{x}\in\Phi_1}\sum_{\boldsymbol{y}\in\Phi_2}\left(\sum_{\ell\in\Pi}\int_{\mathcal{B}_{an}(\boldsymbol{o})}f(\boldsymbol{x},\boldsymbol{y},\boldsymbol{q};\Pi)\mathcal{H}_1^{\ell}(\,\mathrm{d}\boldsymbol{q})\right)\,\Bigg|\,\Pi\right]\right]\quad=$$

$$\mathbb{E}\left[\int_{\mathcal{B}_n(\boldsymbol{o})}\int_{\mathcal{B}_n(\boldsymbol{o})}\left(\sum_{\ell\in\Pi}\int_{\mathcal{B}_{an}(\boldsymbol{o})}f(\boldsymbol{x},\boldsymbol{y},\boldsymbol{q};\Pi)\mathcal{H}_1^{\ell}(\,\mathrm{d}\boldsymbol{q})\right)\mathcal{H}_1^{\Pi}(\,\mathrm{d}\boldsymbol{y})\mathcal{H}_1^{\Pi}(\,\mathrm{d}\boldsymbol{x})\right].$$

Again, decompose the Hausdorff 1-dimensional measure $\mathcal{H}_1^{\Pi}$ over the Poisson line process Π as the countable sum of the Hausdorff 1-dimensional measures $\mathcal{H}_1^{\ell}$ over all lines $\ell\in\Pi$, that is $\mathcal{H}_1^{\Pi}(\,\mathrm{d}\boldsymbol{x})=\sum_{\ell_1\in\Pi}\mathcal{H}_1^{\ell_1}(\,\mathrm{d}\boldsymbol{x})$. Similarly write $\mathcal{H}_1^{\Pi}(\,\mathrm{d}\boldsymbol{y})=\sum_{\ell_2\in\Pi}\mathcal{H}_1^{\ell_2}(\,\mathrm{d}\boldsymbol{y})$. This leads to the following equality

$$\mathbb{E}\left[\int_{\mathcal{B}_n(\boldsymbol{o})}\int_{\mathcal{B}_n(\boldsymbol{o})}\left(\sum_{\ell\in\Pi}\int_{\mathcal{B}_{an}(\boldsymbol{o})}f(\boldsymbol{x},\boldsymbol{y},\boldsymbol{q};\Pi)\mathcal{H}_1^{\ell}(\,\mathrm{d}\boldsymbol{q})\right)\mathcal{H}_1^{\Pi}(\,\mathrm{d}\boldsymbol{y})\mathcal{H}_1^{\Pi}(\,\mathrm{d}\boldsymbol{x})\right]\quad=$$

$$\mathbb{E}\left[\sum_{\ell_1\in\Pi}\int_{\mathcal{B}_n(\boldsymbol{o})}\left(\sum_{\ell_2\in\Pi}\int_{\mathcal{B}_n(\boldsymbol{o})}\left(\sum_{\ell\in\Pi}\int_{\mathcal{B}_{an}(\boldsymbol{o})}f(\boldsymbol{x},\boldsymbol{y},\boldsymbol{q};\Pi)\mathcal{H}_1^{\ell}(\,\mathrm{d}\boldsymbol{q})\right)\mathcal{H}_1^{\ell_2}(\,\mathrm{d}\boldsymbol{y})\right)\mathcal{H}_1^{\ell_1}(\,\mathrm{d}\boldsymbol{x})\right].$$

$$(3.16)$$

Applying Palm theory to the line process Π, the relation

$$\mathbb{E}\left[\sum_{\ell\in\Pi}h(\ell;\Pi)\right]\quad=\quad\int_{\mathcal{C}}\mathbb{E}[\,h(\ell;\Pi)\,||\,\ell\in\Pi]\,\Lambda(\,\mathrm{d}\ell)\qquad(3.17)$$

holds for any nonnegative and measurable function h on $\mathbb{R}^d\times\mathcal{C}$. Even more, if Π is a Poisson line process we know that the right hand side in the above expression is the same as

$$\int_{\mathcal{C}}\mathbb{E}[\,h(\ell;\Pi)\,||\,\ell\in\Pi]\,\Lambda(\,\mathrm{d}\ell)\quad=\quad\int_{\mathcal{C}}\mathbb{E}[h(\ell;\Pi\cup\{\ell\})]\,\Lambda(\,\mathrm{d}\ell).\qquad(3.18)$$

Thus, we can rearrange the last expression in (3.16). Since the summands are nonnegative and all the sums are countable, Tonelli's Theorem [11] can be used to exchange integrals and sums. Then the above Palm result (3.18), using ℓ in (3.16) as our

conditioning line, leads to

$$
\mathbb{E}\left[\sum_{\ell\in\Pi}\int_{\mathcal{B}_{an}(\boldsymbol{o})}\left(\sum_{\ell_1\in\Pi}\int_{\mathcal{B}_n(\boldsymbol{o})}\left(\sum_{\ell_2\in\Pi}\int_{\mathcal{B}_n(\boldsymbol{o})}f(\boldsymbol{x},\boldsymbol{y},\boldsymbol{q};\Pi)\mathcal{H}_1^{\ell_2}(\,\mathrm{d}\boldsymbol{y}\,)\right)\mathcal{H}_1^{\ell_1}(\,\mathrm{d}\boldsymbol{x}\,)\right)\mathcal{H}_1^{\ell}(\,\mathrm{d}\boldsymbol{q}\,)\right]
$$
$$
=\quad\int_{\mathcal{C}}\mathbb{E}\left[\int_{\mathcal{B}_{an}(\boldsymbol{o})}\left(\sum_{\ell_1\in\Pi\cup\{\ell\}}\int_{\mathcal{B}_n(\boldsymbol{o})}\left(\sum_{\ell_2\in\Pi\cup\{\ell\}}\int_{\mathcal{B}_n(\boldsymbol{o})}f(\boldsymbol{x},\boldsymbol{y},\boldsymbol{q};\Pi\cup\{\ell\})\,\mathcal{H}_1^{\ell_2}(\,\mathrm{d}\boldsymbol{y}\,)\right)\right.\right.
$$
$$
\left.\left.\mathcal{H}_1^{\ell_1}(\,\mathrm{d}\boldsymbol{x}\,)\right)\mathcal{H}_1^{\ell}(\,\mathrm{d}\boldsymbol{q}\,)\right]\Lambda(\,\mathrm{d}\ell\,)\,.
$$

$$(3.19)$$

Using Tonelli's Theorem again, exchange the integration regarding $\boldsymbol{q}$ with the expectation, since $\boldsymbol{q}$ lies on the line ℓ now integrated by $\Lambda(\,\mathrm{d}\ell\,)$ from the Palm argument. This leaves a similar expression to the one in (3.18) inside the expectation. Now regard $\Pi\cup\{\ell\}$ as the underlying line process and ℓ_1 as the conditioning line. Therefore (3.18) yields

$$
\int_{\mathcal{C}}\int_{\mathcal{B}_{an}(\boldsymbol{o})}\mathbb{E}\left[\sum_{\ell_1\in\Pi\cup\{\ell\}}\int_{\mathcal{B}_n(\boldsymbol{o})}\left(\sum_{\ell_2\in\Pi\cup\{\ell\}}\int_{\mathcal{B}_n(\boldsymbol{o})}f(\boldsymbol{x},\boldsymbol{y},\boldsymbol{q};\Pi\cup\{\ell\})\,\mathcal{H}_1^{\ell_2}(\,\mathrm{d}\boldsymbol{y}\,)\right)\right.
$$
$$
\left.\mathcal{H}_1^{\ell_1}(\,\mathrm{d}\boldsymbol{x}\,)\right]\mathcal{H}_1^{\ell}(\,\mathrm{d}\boldsymbol{q}\,)\Lambda(\,\mathrm{d}\ell\,)
$$
$$
=\quad\int_{\mathcal{C}}\int_{\mathcal{B}_{an}(\boldsymbol{o})}\left(\int_{\mathcal{C}}\mathbb{E}\left[\int_{\mathcal{B}_n(\boldsymbol{o})}\left(\sum_{\ell_2\in\Pi\cup\{\ell\}\cup\{\ell_1\}}\int_{\mathcal{B}_n(\boldsymbol{o})}f(\boldsymbol{x},\boldsymbol{y},\boldsymbol{q};\Pi\cup\{\ell\}\cup\{\ell_1\})\,\mathcal{H}_1^{\ell_2}(\,\mathrm{d}\boldsymbol{y}\,)\right)\right.\right.
$$
$$
\left.\left.\mathcal{H}_1^{\ell_1}(\,\mathrm{d}\boldsymbol{x}\,)\right]\Lambda(\,\mathrm{d}\ell_1\,)\right)\mathcal{H}_1^{\ell}(\,\mathrm{d}\boldsymbol{q}\,)\Lambda(\,\mathrm{d}\ell\,)\,.
$$

$$(3.20)$$

Notice that strictly speaking the intensity $\Lambda(\,\mathrm{d}\ell_1\,)$ will include an atom at the line ℓ. Nevertheless, this becomes negligible in the asymptotic behaviour, since the contribution from $\ell_1=\ell$ will be of order n (as $\boldsymbol{x}\in\ell$), while the main contribution for $\boldsymbol{x}\in\ell_1\in\Pi$ is of order $n^{3/2}$.

Finally, repeat the above argument, that is, exchange the integration regarding $\boldsymbol{x}$ and the expectation, since $\boldsymbol{x}$ belongs to the line ℓ_1 which is now being integrated by $\Lambda(\,\mathrm{d}\ell_1\,)$ from the above Palm argument. That yields to a similar expression to the one in (3.18) inside the expectation, now regarding $\Pi\cup\{\ell\}\cup\{\ell_1\}$ as the underlying line process and ℓ_2 as our conditioning line. Therefore applying Palm theory (3.18)

one more time yields

$$
\int_{\mathcal{C}}\int_{\mathcal{B}_{an}(\boldsymbol{o})}\left(\int_{\mathcal{C}}\int_{\mathcal{B}_n(\boldsymbol{o})}\left(\mathbb{E}\left[\sum_{\ell_2\in\Pi\cup\{\ell\}\cup\{\ell_1\}}\int_{\mathcal{B}_n(\boldsymbol{o})}f\left(\boldsymbol{x},\boldsymbol{y},\boldsymbol{q};\Pi\cup\{\ell\}\cup\{\ell_1\}\right)\mathcal{H}_1^{\ell_2}(\,\mathrm{d}\boldsymbol{y}\,)\right]\right)\right.
$$
$$
\left.\mathcal{H}_1^{\ell_1}(\,\mathrm{d}\boldsymbol{x}\,)\,\Lambda(\,\mathrm{d}\ell_1\,)\right)\mathcal{H}_1^{\ell}(\,\mathrm{d}\boldsymbol{q}\,)\,\Lambda(\,\mathrm{d}\ell\,)
$$
$$
=\quad\int_{\mathcal{C}}\int_{\mathcal{B}_{an}(\boldsymbol{o})}\left(\int_{\mathcal{C}}\int_{\mathcal{B}_n(\boldsymbol{o})}\left(\int_{\mathcal{C}}\int_{\mathcal{B}_n(\boldsymbol{o})}\mathbb{E}\left[f\left(\boldsymbol{x},\boldsymbol{y},\boldsymbol{q};\Pi\cup\{\ell\}\cup\{\ell_1\}\cup\{\ell_2\}\right)\right]\mathcal{H}_1^{\ell_2}(\,\mathrm{d}\boldsymbol{y}\,)\,\Lambda(\,\mathrm{d}\ell_2\,)\right)\right.
$$
$$
\left.\mathcal{H}_1^{\ell_1}(\,\mathrm{d}\boldsymbol{x}\,)\,\Lambda(\,\mathrm{d}\ell_1\,)\right)\mathcal{H}_1^{\ell}(\,\mathrm{d}\boldsymbol{q}\,)\,\Lambda(\,\mathrm{d}\ell\,)\,.
$$
$$(3.21)$$

Again, strictly speaking the intensity $\Lambda(\,\mathrm{d}\ell_2\,)$ should include two atoms: one at the line ℓ and another at the line ℓ_1. However, each one of these becomes negligible in the asymptotic behaviour, since the contribution from $\ell_2=\ell$ and $\ell_2=\ell_1$ will be of order n each one, while the main contribution for $\boldsymbol{y}\in\ell_2\in\Pi$ is of order $n^{3/2}$.

The ultimate aim is to find an expression for (3.14) in terms of

$$
\mathbb{E}[T_n^q]\;=\;\frac{1}{2}\iint_{\mathcal{B}_n(\boldsymbol{o})^2}\mathbb{E}[\mathbb{1}_{\{(\boldsymbol{p}^-,\boldsymbol{p}^+)\in\mathcal{D}_n^q\}}]\,\mathrm{d}\boldsymbol{p}^-\;\mathrm{d}\boldsymbol{p}^+\;=\;\frac{1}{2}\iint_{\mathcal{B}_n(\boldsymbol{o})^2}\mathbb{E}[f(\boldsymbol{x},\boldsymbol{y},\boldsymbol{q};\Pi\cup\{\ell\})]\,\mathrm{d}\boldsymbol{x}\;\mathrm{d}\boldsymbol{y}\;,
$$

where the last equality follows by re-labeling the source and destination nodes as $\boldsymbol{x}$, $\boldsymbol{y}$ instead of $\boldsymbol{p}^-$ and $\boldsymbol{p}^+$, respectively. Recall that ℓ, ℓ_1 and ℓ_2 belong to a Poisson line process of unit intensity, and the intensity measure of the Poisson line process is given by $\Lambda(\,\mathrm{d}\ell\,)=\frac{1}{2}\,\mathrm{d}r\,\mathrm{d}\psi$, for $r\in[0,n]$ and $\psi\in[0,\pi]$. Thus, substituting $\Lambda(\,\mathrm{d}\ell\,)=\frac{1}{2}\,\mathrm{d}r\,\mathrm{d}\psi$, $\Lambda(\,\mathrm{d}\ell_1\,)=\frac{1}{2}\,\mathrm{d}r_1\,\mathrm{d}\psi_1$ and $\Lambda(\,\mathrm{d}\ell_2\,)=\frac{1}{2}\,\mathrm{d}r_2\,\mathrm{d}\psi_2$ leads to

$$
\mathbb{E}\left[\sum_{\boldsymbol{x}\in\Phi_1}\sum_{\boldsymbol{y}\in\Phi_2}\int_{\mathcal{B}_{an}(\boldsymbol{o})}f(\boldsymbol{x},\boldsymbol{y},\boldsymbol{q};\Pi)\mathcal{H}_1^{\Pi}(\,\mathrm{d}\boldsymbol{q}\,)\right]\quad=
$$
$$
\int_{\mathcal{C}}\int_{\mathcal{B}_{an}(\boldsymbol{o})}\left(\int_{\mathcal{C}}\int_{\mathcal{B}_n(\boldsymbol{o})}\left(\int_{\mathcal{C}}\int_{\mathcal{B}_n(\boldsymbol{o})}\mathbb{E}\left[f\left(\boldsymbol{x},\boldsymbol{y},\boldsymbol{q};\Pi\cup\{\ell\}\cup\{\ell_1\}\cup\{\ell_2\}\right)\right]\mathcal{H}_1^{\ell_2}(\,\mathrm{d}\boldsymbol{y}\,)\,\Lambda(\,\mathrm{d}\ell_2\,)\right)\right.
$$
$$
\left.\mathcal{H}_1^{\ell_1}(\,\mathrm{d}\boldsymbol{x}\,)\,\Lambda(\,\mathrm{d}\ell_1\,)\right)\mathcal{H}_1^{\ell}(\,\mathrm{d}\boldsymbol{q}\,)\,\Lambda(\,\mathrm{d}\ell\,)\quad=
$$
$$
\frac{1}{8}\int_0^\pi\int_0^{an}\int_{\mathcal{B}_{an}(\boldsymbol{o})}\left(\int_0^\pi\int_0^n\int_{\mathcal{B}_n(\boldsymbol{o})}\left(\int_0^\pi\int_0^n\int_{\mathcal{B}_n(\boldsymbol{o})}\mathbb{E}\left[f\left(\boldsymbol{x},\boldsymbol{y},\boldsymbol{q};\Pi\cup\{\ell\}\cup\{\ell_1\}\cup\{\ell_2\}\right)\right]\right.\right.
$$
$$
\left.\left.\mathcal{H}_1^{\ell_2}(\,\mathrm{d}\boldsymbol{y}\,)\,\mathrm{d}r_2\,\mathrm{d}\psi_2\right)\mathcal{H}_1^{\ell_1}(\,\mathrm{d}\boldsymbol{x}\,)\,\mathrm{d}r_1\,\mathrm{d}\psi_1\right)\mathcal{H}_1^{\ell}(\,\mathrm{d}\boldsymbol{q}\,)\,\mathrm{d}r\,\mathrm{d}\psi\,.
$$
$$(3.22)$$

We now make a change of variables in the last expression of (3.22). At the time we have three variables to represent each point that is lying in the corresponding line pattern. For example, $\boldsymbol{q}$ lying in the line ℓ is represented by the parameters $\tilde{q}$, $\tilde{r}$ and $\tilde{\psi}$, where $\tilde{q}$ represents the signed distance from the point $\boldsymbol{q}$ to the closest

point from the line ℓ to the origin, and $(\tilde{r}, \tilde{\psi})$ are the parameters for the line ℓ, which are the signed distance from ℓ to the origin and the angle it makes with the x-axis, respectively (similarly with $\boldsymbol{x}$ lying in the line ℓ_1 and $\boldsymbol{y}$ lying in the line ℓ_2). Intuitively, one first draws the random line ℓ and then picks a random point over this line. However, this process can be done in the opposite order, that is, first pick a random point $\boldsymbol{q}$ with coordinates (q_1, q_2) inside the disk of radius n and then draw random line ℓ that passes through this point. In this case, as the line must go through $\boldsymbol{q} = (q_1, q_2)$, the parameter $\tilde{r}$ will be completely determined by the angle $\tilde{\psi}$ and the location of $\boldsymbol{q}$. This idea is illustrated by the following change of variables:

$$\tilde{\psi} = \psi; \qquad \tilde{r} = |q_2 \cos(\psi) - q_1 \sin(\psi)|; \qquad \tilde{q} = q_1 \cos(\psi) + q_2 \sin(\psi) \ .$$
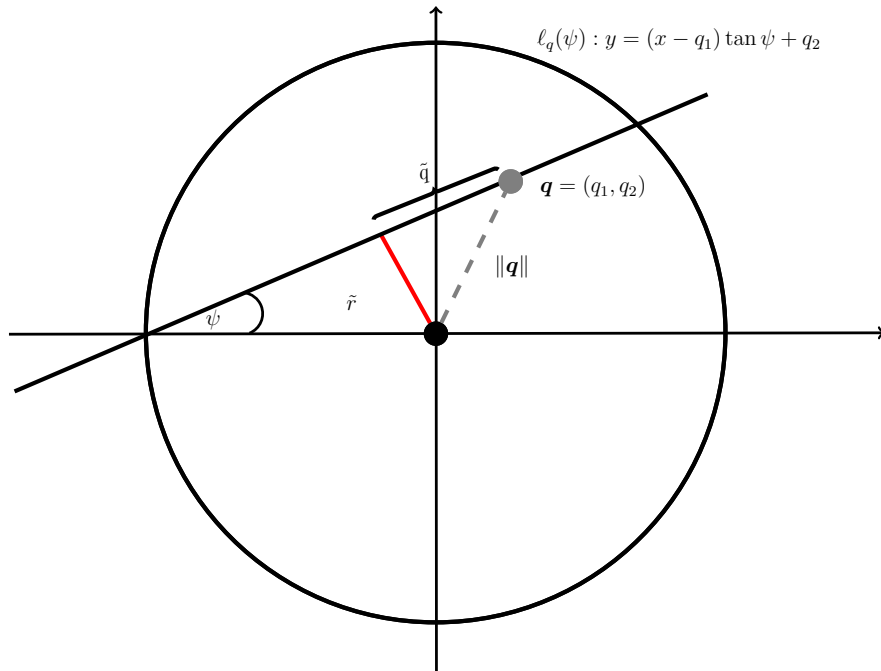
Figure 3.2: Change of variables. Where we have used the formula for a distance from a line to a point and the Pythagorean Theorem to get the values for $\tilde{r}$ and $\tilde{q}$.

To derive the above change of variables. Recall, that $\tilde{r}$ is the distance from $\ell_q(\psi)$ to the origin. Thus, to find its value in terms of $\boldsymbol{q} = (q_1, q_2)$ and $\ell_q(\psi) : y = (x - q_1) \tan \psi + q_2$ we can use the formula for a distance from a line $ax + by + c = 0$ to a point (x_1, y_1), that is given by

$$\frac{|ax_1 + by_1 + c|}{\sqrt{a^2 + b^2}} \quad \text{therefore} \quad \tilde{r} = \frac{|a(0) + b(0) + c|}{\sqrt{a^2 + b^2}} \ ,$$

where, in our case the point we are concerned is the origin $\boldsymbol{o} = (0, 0)$ and the coefficients are given by $a = \sin \psi$, $b = -\cos \psi$ and $c = q_2 \cos \psi - q_1 \sin \psi$. Since we can multiply the expression for $\ell_q(\psi)$ by $\cos \psi$ to obtain the equivalent expression $\ell_q(\psi) : (\sin \psi)x - (\cos \psi)y + (q_2 \cos \psi - q_1 \sin \psi) = 0$. Therefore $\tilde{r} = |q_2 \cos \psi - q_1 \sin \psi|$.

Moreover, as the triangle with sides lengths given by $\tilde{r}$, $\tilde{q}$ and $\|\boldsymbol{q}\|$ is a right triangle with hypotenuse given by $\|\boldsymbol{q}\|$, then it is clear that the signed distance $\tilde{q}$ can be found by the Pythagorean Theorem, that is $\tilde{q} = \pm\sqrt{\|\boldsymbol{q}\|^2 - \tilde{r}^2} = q_1 \cos\psi + q_2 \sin\psi$.

The Jacobian for the above change of coordinates (from ψ, q_1, q_2 to $\tilde{\psi}, \tilde{r}, \tilde{q}$) is 1. Consequently $\mathrm{d}\psi\,\mathrm{d}q_1\,\mathrm{d}q_2 = \mathrm{d}\tilde{q}\,\mathrm{d}\tilde{r}\,\mathrm{d}\tilde{\psi}$. Considering $\mathcal{H}_1^\ell(\mathrm{d}\boldsymbol{q}) = \mathrm{d}\tilde{q}$ and $\mathrm{d}q_1\,\mathrm{d}q_2 = \mathrm{d}\boldsymbol{q}$ (similarly for $\boldsymbol{x}$ and $\boldsymbol{y}$), then (3.22) can be re rewritten as

$$
\frac{1}{8} \int_0^\pi \int_0^{an} \int_{\mathcal{B}_{an}(\boldsymbol{o})} \left(\int_0^\pi \int_0^n \int_{\mathcal{B}_n(\boldsymbol{o})} \left(\int_0^\pi \int_0^n \int_{\mathcal{B}_n(\boldsymbol{o})} \mathbb{E}\left[f(\boldsymbol{x}, \boldsymbol{y}, \boldsymbol{q}; \Pi \cup \{\ell\} \cup \{\ell_1\} \cup \{\ell_2\}) \right] \right.\right.
$$
$$
\left.\left. \mathcal{H}_1^{\ell_2}(\mathrm{d}\boldsymbol{y})\,\mathrm{d}r_2\,\mathrm{d}\psi_2 \right) \mathcal{H}_1^{\ell_1}(\mathrm{d}\boldsymbol{x})\,\mathrm{d}r_1\,\mathrm{d}\psi_1 \right) \mathcal{H}_1^\ell(\mathrm{d}\boldsymbol{q})\,\mathrm{d}r\,\mathrm{d}\psi
$$
$$
= \frac{1}{8} \int_{\mathcal{B}_{an}(\boldsymbol{o})} \int_0^\pi \int_{\mathcal{B}_n(\boldsymbol{o})} \int_0^\pi \int_{\mathcal{B}_n(\boldsymbol{o})} \int_0^\pi \mathbb{E}\left[f(\boldsymbol{x}, \boldsymbol{y}, \boldsymbol{q}; \Pi \cup \{\ell\} \cup \{\ell_1\} \cup \{\ell_2\}) \right]
$$
$$
\mathrm{d}\psi_2\,\mathrm{d}\boldsymbol{y}\,\mathrm{d}\psi_1\,\mathrm{d}\boldsymbol{x}\,\mathrm{d}\psi\,\mathrm{d}\boldsymbol{q} .
$$
$$(3.23)$$

The function to be integrated is similar to the one arising in section 2.1. The difference is that the line process in question here is augmented by the lines ℓ_1 and ℓ_2, containing the source $\boldsymbol{x}$ and destination $\boldsymbol{y}$, respectively. Furthermore, as the function to be integrated is positive, since it is the expectation of an indicator function (i.e. the probability of a measurable event), the order of integration can be exchanged due to Tonelli's Theorem. Therefore the last expression in (3.23) can be rewritten as follows:

$$
\frac{1}{8} \int_{\mathcal{B}_{an}(\boldsymbol{o})} \int_0^\pi \int_{\mathcal{B}_n(\boldsymbol{o})} \int_0^\pi \int_{\mathcal{B}_n(\boldsymbol{o})} \int_0^\pi \mathbb{E}\left[f(\boldsymbol{x}, \boldsymbol{y}, \boldsymbol{q}; \Pi \cup \{\ell\} \cup \{\ell_1\} \cup \{\ell_2\}) \right] \mathrm{d}\psi_2\,\mathrm{d}\boldsymbol{y}\,\mathrm{d}\psi_1\,\mathrm{d}\boldsymbol{x}\,\mathrm{d}\psi\,\mathrm{d}\boldsymbol{q}
$$
$$
= \frac{1}{8} \int_{\mathcal{B}_{an}(\boldsymbol{o})} \int_0^\pi \int_{\mathcal{B}_n(\boldsymbol{o})} \int_{\mathcal{B}_n(\boldsymbol{o})} \int_0^\pi \int_0^\pi \mathbb{E}\left[f(\boldsymbol{x}, \boldsymbol{y}, \boldsymbol{q}; \Pi \cup \{\ell\} \cup \{\ell_1\} \cup \{\ell_2\}) \right]
$$
$$
\mathrm{d}\psi_2\,\mathrm{d}\psi_1\,\mathrm{d}\boldsymbol{y}\,\mathrm{d}\boldsymbol{x}\,\mathrm{d}\psi\,\mathrm{d}\boldsymbol{q} .
$$
$$(3.24)$$

Now, for a fixed pair of $\ell \in \Pi$ and $\boldsymbol{q} \in \mathbb{R}^2$ we focus our attention on the amount given by

$$
\frac{1}{2} \int_{\mathcal{B}_n(\boldsymbol{o})} \int_{\mathcal{B}_n(\boldsymbol{o})} \int_0^\pi \int_0^\pi \mathbb{E}\left[f(\boldsymbol{x}, \boldsymbol{y}, \boldsymbol{q}; \Pi \cup \{\ell\} \cup \{\ell_1\} \cup \{\ell_2\}) \right] \mathrm{d}\psi_2\,\mathrm{d}\psi_1\,\mathrm{d}\boldsymbol{y}\,\mathrm{d}\boldsymbol{x} , \quad (3.25)
$$

which is to be compared with the expression on Theorem 2.1, say

$$
\mathbb{E}[T_n^q(\ell)] = \frac{1}{2} \iint_{\mathcal{B}_n(\boldsymbol{o})^2} \mathbb{E}[f(\boldsymbol{x}, \boldsymbol{y}, \boldsymbol{q}; \Pi \cup \{\ell\})]\,\mathrm{d}\boldsymbol{y}\,\mathrm{d}\boldsymbol{x} . \quad (3.26)
$$

It turns out that as $n \to \infty$ both quantities (3.25) and (3.26) are asymptotically proportional to each other. That is the content of the following Theorem.

THEOREM 3.4. *Consider the traffic generated from the source nodes $\boldsymbol{x} \in \Phi_1$ to the destination nodes $\boldsymbol{y} \in \Phi_2$, where Φ_1 and Φ_2 are two conditionally independent Cox*

point processes governed by the random measure $\mathcal{H}_1^{\Pi}$; here Π is a Poisson line process that will define our transportation network (a Poissonian city). Define the function $f(\boldsymbol{x}, \boldsymbol{y}, \boldsymbol{q}; \Pi) = \mathbb{1}_{\{\boldsymbol{q} \in \partial \mathcal{C}(\boldsymbol{x}, \boldsymbol{y})\}}$, that is f indicates if the point $\boldsymbol{q} = (q_1 n, q_2 n)$ belongs to one of the two routes that connects $\boldsymbol{x}$ to $\boldsymbol{y}$ through the semi-perimeter routing rule, conditioning on the existence of a line $\ell \in \Pi$ that passes through $\boldsymbol{q}$ and makes an angle ψ with the x-axis. Then the mean amount of traffic flow on the subregion $\mathcal{B}_{an}(\boldsymbol{o})$ as a ranges over [0, 1] is given by expression (3.14), i.e.

$$\mathbb{E}\left[\sum_{\boldsymbol{x} \in \Phi_1} \sum_{\boldsymbol{y} \in \Phi_2} \int_{\mathcal{B}_{an}(\boldsymbol{o})} f(\boldsymbol{x}, \boldsymbol{y}, \boldsymbol{q}; \Pi) \mathcal{H}_1^{\Pi}(\mathrm{d}\boldsymbol{q})\right] .$$

Moreover, we can find an expression for the asymptotic behaviour for the mean traffic flow at a fixed $\boldsymbol{q} = (q_1 n, q_2 n)$ conditioning on $\ell \in \Pi$ (ℓ passes through $\boldsymbol{q}$), $\ell_1 \in \Pi$, a line that passes through the source node $\boldsymbol{x}$ making an angle ψ_1 uniformly distributed over $(0, \pi]$; and $\ell_2 \in \Pi$, a line that goes through the destination node $\boldsymbol{y}$ making an angle ψ_2 with the x-axis, where ψ_2 is uniformly distributed over $(0, \pi]$. The expression for the aforementioned asymptotic traffic flow is given by

$$\frac{1}{2} \int_{\mathcal{B}_n(\boldsymbol{o})} \int_{\mathcal{B}_n(\boldsymbol{o})} \int_0^{\pi} \int_0^{\pi} \mathbb{E}\left[f(\boldsymbol{x}, \boldsymbol{y}, \boldsymbol{q}; \Pi \cup \{\ell\} \cup \{\ell_1\} \cup \{\ell_2\})\right] \mathrm{d}\psi_2 \, \mathrm{d}\psi_1 \, \mathrm{d}\boldsymbol{y} \, \mathrm{d}\boldsymbol{x}$$

$$\sim \quad 2\pi^2 \sqrt{1 - u^2}(1 - u^2 - t^2)n^3 , \quad (3.27)$$

with $u = -q_1 \sin\psi + q_2 \cos\psi$ and $t = q_1 \cos\psi + q_2 \sin\psi$.

Proof. The expression (3.14) represents the traffic over the subregion $\mathcal{B}_{an}(\boldsymbol{o})$ as it has been explained throughout this section. Moreover, from the above exposition it is clear that the traffic generated by the points $\boldsymbol{x} \in \ell_1$ and $\boldsymbol{y} \in \ell_2$ for fixed $\boldsymbol{q} \in \ell$ is given by the expression (3.25). Moreover, the indicator function $f(\boldsymbol{x}, \boldsymbol{y}, \boldsymbol{q}; \Pi \cup \{\ell\} \cup \{\ell_1\} \cup \{\ell_2\})$ can be rewritten as a product of $f(\boldsymbol{x}, \boldsymbol{y}, \boldsymbol{q}; \Pi \cup \{\ell\})$ and two other factors that express the probabilities that neither ℓ_1 nor ℓ_2 separate both points $\boldsymbol{x}$ and $\boldsymbol{y}$ simultaneously from $\boldsymbol{q}$. For fixed $\boldsymbol{x}$ and $\boldsymbol{y}$, if ℓ_2 is such that it does not separate $\boldsymbol{x}$ and $\boldsymbol{y}$ simultaneously from $\boldsymbol{q}$ then

$$f(\boldsymbol{x}, \boldsymbol{y}, \boldsymbol{q}; \Pi \cup \{\ell\} \cup \{\ell_1\} \cup \{\ell_2\}) = f(\boldsymbol{x}, \boldsymbol{y}, \boldsymbol{q}; \Pi \cup \{\ell\} \cup \{\ell_1\}) ,$$

and that is achieved as long as ψ_2 belongs to an specific range of angles, say $E_2(\boldsymbol{x}, \boldsymbol{y}, \boldsymbol{q}) \subseteq [0, \pi]$. This happens with probability

$$P_2(\boldsymbol{x}, \boldsymbol{y}, \boldsymbol{q}) = \int_{E_2(\boldsymbol{x}, \boldsymbol{y}, \boldsymbol{q})} \frac{1}{\pi} \, \mathrm{d}\psi_2 .$$

Moreover $f(\boldsymbol{x}, \boldsymbol{y}, \boldsymbol{q}; \Pi \cup \{\ell\} \cup \{\ell_1\} \cup \{\ell_2\}) = 0$ when the angle ψ_2 of the line ℓ_2 does not belong to $E_2(\boldsymbol{x}, \boldsymbol{y}, \boldsymbol{q})$. Furthermore, from the aforementioned Palm theory it turns out that the angles ψ_1 and ψ_2 are independent of each other. Therefore a similar

argument can be applied to ℓ_1. So, if ℓ_1 is such that it does not separate $\boldsymbol{x}$ and $\boldsymbol{y}$ simultaneously from $\boldsymbol{q}$ then

$$f(\boldsymbol{x}, \boldsymbol{y}, \boldsymbol{q}; \Pi \cup \{\ell\} \cup \{\ell_1\}) = f(\boldsymbol{x}, \boldsymbol{y}, \boldsymbol{q}; \Pi \cup \{\ell\}) \,,$$

and this holds for any $\psi_1 \in E_1(\boldsymbol{x}, \boldsymbol{y}, \boldsymbol{q}) \subseteq [0, \pi]$, with probability

$$P_1(\boldsymbol{x}, \boldsymbol{y}, \boldsymbol{q}) = \int_{E_1(\boldsymbol{x}, \boldsymbol{y}, \boldsymbol{q})} \frac{1}{\pi} \, \mathrm{d}\psi_1 \,.$$

Therefore, by independence of ψ_1 and ψ_2 it follows that

$$\int_{\mathcal{B}_n(\boldsymbol{o})} \int_{\mathcal{B}_n(\boldsymbol{o})} \int_0^\pi \int_0^\pi \mathbb{E}\left[f\left(\boldsymbol{x}, \boldsymbol{y}, \boldsymbol{q}; \Pi \cup \{\ell\} \cup \{\ell_1\} \cup \{\ell_2\}\right)\right] \mathrm{d}\psi_2 \, \mathrm{d}\psi_1 \, \mathrm{d}\boldsymbol{y} \, \mathrm{d}\boldsymbol{x} \quad =$$

$$\pi^2 \int_{\mathcal{B}_n(\boldsymbol{o})} \int_{\mathcal{B}_n(\boldsymbol{o})} P_1(\boldsymbol{x}, \boldsymbol{y}, \boldsymbol{q}) P_2(\boldsymbol{x}, \boldsymbol{y}, \boldsymbol{q}) \mathbb{E}\left[f\left(\boldsymbol{x}, \boldsymbol{y}, \boldsymbol{q}; \Pi \cup \{\ell\}\right)\right] \mathrm{d}\boldsymbol{y} \, \mathrm{d}\boldsymbol{x} \,. \quad (3.28)$$

The right hand side can be related to (3.26) by rotating all the points inside the Poissonian city clockwise by an angle ψ, so the line ℓ becomes an horizontal line after this rotation. Thus the cartesian coordinates $\boldsymbol{q} = (q_1 n, q_2 n)$ will correspond, after this rotation, to $\tilde{\boldsymbol{q}} = (tn, un)$ with $t = q_1 \cos\psi + q_2 \sin\psi$ and $u = -q_1 \sin\psi + q_2 \cos\psi$, see figure 3.3. Thus the asymptotic behaviour of the second expression in (3.26) can be analyzed following the same ideas used on Theorem 2.1. First, from Theorem 2.1 it follows that

$$\pi^2 \int_{\mathcal{B}_n(\boldsymbol{o})} \int_{\mathcal{B}_n(\boldsymbol{o})} \mathbb{E}\left[f\left(\tilde{\boldsymbol{x}}, \tilde{\boldsymbol{y}}, \tilde{\boldsymbol{q}}; \Pi \cup \{\tilde{\ell}\}\right)\right] \mathrm{d}\tilde{\boldsymbol{y}} \, \mathrm{d}\tilde{\boldsymbol{x}}$$

$$= \quad \pi^2 \mathbb{E}[T_n^{\tilde{q}}(\tilde{\ell})] \quad \sim \quad \pi^2 2\sqrt{1 - u^2}(1 - u^2 - t^2) n^3 \,.$$
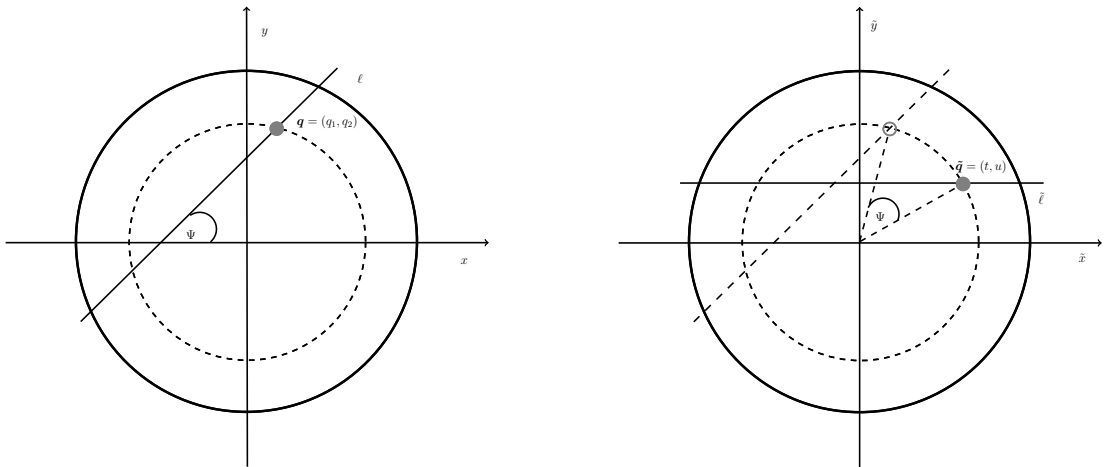

Figure 3.3: Illustration for the change of variables due to a rotation of an angle Ψ clockwise.

So we only need to describe the effects of the factors $P_1(\tilde{\boldsymbol{x}}, \tilde{\boldsymbol{y}}, \tilde{\boldsymbol{q}})$ and $P_2(\tilde{\boldsymbol{x}}, \tilde{\boldsymbol{y}}, \tilde{\boldsymbol{q}})$ on the

asymptotics. Following the treatment of $\mathbb{E}[T_n^{\tilde{q}}(\tilde{\ell})]$ in Theorem 2.1, we express $\tilde{\boldsymbol{x}}$ and $\tilde{\boldsymbol{y}}$ in polar coordinates, translating the origin to $\tilde{\boldsymbol{q}}$, as (r, α_1) and (s, α_2) respectively. Then, consider the auxiliary variables $\theta = \alpha_1 + \alpha_2$ and $\gamma = \alpha_1 - \alpha_2$ to obtain

$$
\pi^2 \int_{\mathcal{B}_n(\boldsymbol{o})} \int_{\mathcal{B}_n(\boldsymbol{o})} P_1(\tilde{\boldsymbol{x}}, \tilde{\boldsymbol{y}}, \tilde{\boldsymbol{q}}) P_2(\tilde{\boldsymbol{x}}, \tilde{\boldsymbol{y}}, \tilde{\boldsymbol{q}}) \mathbb{E}\left[f\left(\tilde{\boldsymbol{x}}, \tilde{\boldsymbol{y}}, \tilde{\boldsymbol{q}}; \Pi \cup \{\ell\}\right)\right] \mathrm{d}\tilde{\boldsymbol{y}}\, \mathrm{d}\tilde{\boldsymbol{x}} \quad =
$$

$$
\pi^2 \left(\frac{1}{2} \iiint_{\mathcal{D}_{n,-}^{\tilde{q}}} P_1(r, s, \theta, \tilde{\boldsymbol{q}}) P_2(r, s, \theta, \tilde{\boldsymbol{q}}) g(r, s, \theta) r\, \mathrm{d}r\, s\, \mathrm{d}s\, \theta\, \mathrm{d}\theta \right.
$$

$$
\left. + \frac{1}{2} \iiint_{\mathcal{D}_{n,+}^{\tilde{q}}} P_1(r, s, \theta, \tilde{\boldsymbol{q}}) P_2(r, s, \theta, \tilde{\boldsymbol{q}}) g(r, s, \theta) r\, \mathrm{d}r\, s\, \mathrm{d}s\, \theta\, \mathrm{d}\theta \right). \quad (3.29)
$$

Here $g(r, s, \theta) = \exp\left(-\frac{1}{2}(r + s - \sqrt{r^2 + s^2 + 2rs\cos\theta})\right)$ is the probability that there are no lines from the Poisson line process Π separating the points $\tilde{\boldsymbol{x}} = (r, \alpha_1)$ and $\tilde{\boldsymbol{y}} = (s, \alpha_2)$. Further

$$
\mathcal{D}_{n,-}^{\tilde{q}} = \{(r, s, \theta) : 0 \le r \le h_1^{\tilde{q}}(\alpha_1) n,\ 0 \le s \le h_2^{\tilde{q}}(\alpha_2) n,\ -\pi \le \theta \le 0\},
$$
$$
\mathcal{D}_{n,+}^{\tilde{q}} = \{(r, s, \theta) : 0 \le r \le h_1^{\tilde{q}}(\alpha_1) n,\ 0 \le s \le h_2^{\tilde{q}}(\alpha_2) n,\ 0 \le \theta \le \pi\},
$$

where

$$
h_1^{\tilde{q}}(\alpha_1) = \left(\left(\sqrt{\sec^2\alpha_1 - (u + t\tan\alpha_1)^2} - \tan\alpha_1(u + t\tan\alpha_1)\right)\cos^2\alpha_1 + t\right)\sec\alpha_1,
$$
$$
h_2^{\tilde{q}}(\alpha_2) = \left(\left(\sqrt{\sec^2\alpha_2 - (u - t\tan\alpha_2)^2} - \tan\alpha_2(u - t\tan\alpha_2)\right)\cos^2\alpha_2 - t\right)\sec\alpha_2.
$$

Now we may analyze each of the integrals on the right hand side of (3.29) separately. The idea is to split each region of integration $\mathcal{D}_{n,-}^{\tilde{q}}$ and $\mathcal{D}_{n,+}^{\tilde{q}}$ in terms of the angle θ. For example $\mathcal{D}_{n,+}^{\tilde{q}}$ can be break down into

$$
\mathcal{D}_{n,+,1}^{\tilde{q}} = \{(r, s, \theta) : 0 \le r \le h_1^{\tilde{q}}(\alpha_1),\ 0 \le s \le h_2^{\tilde{q}}(\alpha_2),\ 0 \le \theta = \alpha_1 + \alpha_2 \le w_n\},
$$
$$
\mathcal{D}_{n,+,2}^{\tilde{q}} = \{(r, s, \theta) : 0 \le r \le h_1^{\tilde{q}}(\alpha_1),\ 0 \le s \le h_2^{\tilde{q}}(\alpha_2),\ w_n \le \theta = \alpha_1 + \alpha_2 \le \pi\}.
$$

Then from Lemma 2.1, the behaviour of the integrals on the right hand side of (3.29) is known for regions with constant bounds for r and s and small θ, say

$$
\mathcal{A}_{n,+,+}^{\tilde{q}} = \{(r, s, \theta) : 0 \le r \le (\sqrt{1 - u^2} + t)n,\ 0 \le s \le (\sqrt{1 - u^2} - t)n,\ 0 \le \theta \le w_n\},
$$
$$
\mathcal{A}_{n,+,-}^{\tilde{q}} = \{(r, s, \theta) : 0 \le r \le h_1^{\tilde{q}}(w_n)n,\ 0 \le s \le h_2^{\tilde{q}}(w_n)n,\ 0 \le \theta \le w_n\}.
$$

Notice that $\mathcal{A}_{n,+,-}^{\tilde{q}} \subseteq \mathcal{D}_{n,+,1}^{\tilde{q}} \subseteq \mathcal{A}_{n,+,+}^{\tilde{q}}$. Even more, suppose $\theta \in [0, w_n]$, where $w_n \to 0^+$ as $n \to \infty$, say $w_n = 1/n^\beta$ for some $\beta > 0$. Thus for any $(\tilde{\boldsymbol{x}}, \tilde{\boldsymbol{y}}) \in D_{n,+,1}^{\tilde{q}}$

the following inequalities holds:

$$1 - \frac{w_n}{\pi} \leq P_1(r, s, \theta, \tilde{\boldsymbol{q}}) \leq 1,$$
$$1 - \frac{w_n}{\pi} \leq P_2(r, s, \theta, \tilde{\boldsymbol{q}}) \leq 1.$$

Therefore, from Lemma 2.1 we can conclude that as $n \to \infty$

$$\left(1 - \frac{w_n}{\pi}\right)^2 (h_1^{\tilde{q}}(w_n) + h_2^{\tilde{q}}(w_n)) h_1^{\tilde{q}}(w_n) h_2^{\tilde{q}}(w_n) n^3 \sim \left(1 - \frac{w_n}{\pi}\right)^2 \iiint\limits_{\mathcal{A}_{n,+,-}^{\tilde{q}}} g(r, s, \theta) r \, dr \, s \, ds \, \theta \, d\theta$$

$$\leq \iiint\limits_{\mathcal{D}_{n,+,1}^{\tilde{q}}} P_1(r, s, \theta, \tilde{\boldsymbol{q}}) P_2(r, s, \theta, \tilde{\boldsymbol{q}}) g(r, s, \theta) r \, dr \, s \, ds \, \theta \, d\theta \leq$$

$$\iiint\limits_{\mathcal{A}_{n,+,+}^{\tilde{q}}} g(r, s, \theta) r \, dr \, s \, ds \, \theta \, d\theta \sim 2\sqrt{1 - u^2}(1 - u^2 - t^2) n^3.$$

Additionally, if $\theta \in [w_n, \pi]$, then by Lemma 2.2, it is known that the integral over the region $\mathcal{E}_n^{\tilde{q}} = \{(r, s, \theta) : 0 \leq r \leq R_3 n, \, 0 \leq s \leq R_3 n, \, w_n \leq \theta \leq \pi\}$ is of order $\mathcal{O}(n^{2+4\beta})$, that is

$$\iiint\limits_{\mathcal{E}_n^{\tilde{q}}} g(r, s, \theta) r \, dr \, s \, ds \, \theta \, d\theta \leq 8 \frac{(\pi^2 - w_n^2) R_3^2}{(1 - \cos w_n)^2} n^2 = \mathcal{O}(n^{2+4\beta}),$$

with $R_3 = 1 + \sqrt{t^2 + u^2}$. Now, since $P_1(r, s, \theta, \tilde{\boldsymbol{q}}) \in [0, 1]$ and $P_2(r, s, \theta, \tilde{\boldsymbol{q}}) \in [0, 1]$, and $\mathcal{D}_{n,+,2}^{\tilde{q}} \subseteq \mathcal{E}_n^{\tilde{q}}$ then one obtains

$$\iiint\limits_{\mathcal{D}_{n,+,2}^{\tilde{q}}} P_1(r, s, \theta, \tilde{\boldsymbol{q}}) P_2(r, s, \theta, \tilde{\boldsymbol{q}}) g(r, s, \theta) r \, dr \, s \, ds \, \theta \, d\theta$$

$$\leq \iiint\limits_{\mathcal{E}_n^{\tilde{q}}} g(r, s, \theta) r \, dr \, s \, ds \, \theta \, d\theta \leq 8 \frac{(\pi^2 - w_n^2) R_3^2}{(1 - \cos w_n)^2} n^2 = \mathcal{O}(n^{2+4\beta}),$$

with the same value for R_3 as above. Therefore

$$\iiint\limits_{\mathcal{D}_{n,+}^{\tilde{q}}} P_1(r, s, \theta, \tilde{\boldsymbol{q}}) P_2(r, s, \theta, \tilde{\boldsymbol{q}}) g(r, s, \theta) r \, dr \, s \, ds \, \theta \, d\theta =$$

$$\iiint\limits_{\mathcal{D}_{n,+,1}^{\tilde{q}}} P_1(r, s, \theta, \tilde{\boldsymbol{q}}) P_2(r, s, \theta, \tilde{\boldsymbol{q}}) g(r, s, \theta) r \, dr \, s \, ds \, \theta \, d\theta$$

$$+ \iiint\limits_{\mathcal{D}_{n,+,2}^{\tilde{q}}} P_1(r, s, \theta, \tilde{\boldsymbol{q}}) P_2(r, s, \theta, \tilde{\boldsymbol{q}}) g(r, s, \theta) r \, dr \, s \, ds \, \theta \, d\theta \sim 2\sqrt{1 - u^2}(1 - u^2 - t^2) n^3.$$

Following exactly the same ideas for the region $\mathcal{D}_{n,-}^{\tilde{q}}$, we obtain

$$\iiint_{\mathcal{D}_{n,-}^{\tilde{q}}} P_1(r,s,\theta,\tilde{\boldsymbol{q}})P_2(r,s,\theta,\tilde{\boldsymbol{q}})g(r,s,\theta)r\,\mathrm{d}r\,s\,\mathrm{d}s\,\theta\,\mathrm{d}\theta \quad =$$

$$\iiint_{\mathcal{D}_{n,-,1}^{\tilde{q}}} P_1(r,s,\theta,\tilde{\boldsymbol{q}})P_2(r,s,\theta,\tilde{\boldsymbol{q}})g(r,s,\theta)r\,\mathrm{d}r\,s\,\mathrm{d}s\,\theta\,\mathrm{d}\theta$$

$$+ \iiint_{\mathcal{D}_{n,-,2}^{\tilde{q}}} P_1(r,s,\theta,\tilde{\boldsymbol{q}})P_2(r,s,\theta,\tilde{\boldsymbol{q}})g(r,s,\theta)r\,\mathrm{d}r\,s\,\mathrm{d}s\,\theta\,\mathrm{d}\theta \quad \sim \quad 2\sqrt{1-u^2}(1-u^2-t^2)n^3\,.$$

In conclusion

$$\int_{\mathcal{B}_n(\boldsymbol{o})}\int_{\mathcal{B}_n(\boldsymbol{o})}\int_0^\pi\int_0^\pi \mathbb{E}\left[f\left(\boldsymbol{x},\boldsymbol{y},\boldsymbol{q};\Pi\cup\{\ell\}\cup\{\ell_1\}\cup\{\ell_2\}\right)\right]\,\mathrm{d}\psi_2\,\mathrm{d}\psi_1\,\mathrm{d}\boldsymbol{y}\,\mathrm{d}\boldsymbol{x}$$

$$= \quad \pi^2\int_{\mathcal{B}_n(\boldsymbol{o})}\int_{\mathcal{B}_n(\boldsymbol{o})} P_1(\boldsymbol{x},\boldsymbol{y},\boldsymbol{q})P_2(\boldsymbol{x},\boldsymbol{y},\boldsymbol{q})\mathbb{E}\left[f\left(\boldsymbol{x},\boldsymbol{y},\boldsymbol{q};\Pi\cup\{\ell\}\right)\right]\,\mathrm{d}\boldsymbol{y}\,\mathrm{d}\boldsymbol{x}$$

$$\sim \quad 2\pi^2\sqrt{1-u^2}(1-u^2-t^2)n^3\,,$$

with $u = -q_1\sin\psi + q_2\cos\psi$ and $t = q_1\cos\psi + q_2\sin\psi$. $\qquad\square$

Theorem 3.4 will be applied in the next chapter to compare the traffic density inside the Poissonian city with the traffic density in the British railway system as presented by Beeching in [12].

Besides, Theorem 3.4 fixes an issue presented in the semi-perimeter routing rule, in which one is forced to add two little line segments that do not belong to the Poisson line process Π, namely the edge that connects $\boldsymbol{p}^-$ with $\tilde{\boldsymbol{p}}^-$ and the one that joins $\tilde{\boldsymbol{p}}^+$ with $\boldsymbol{p}^+$, as shown in figure 2.1. Therefore, with this new construction the actual mean length for the near-geodesics (provided by the semi-perimeter routing rule) is in fact given by:

$$\frac{1}{2}\mathbb{E}\left[\mathcal{H}_1\left(\partial\mathcal{C}(\boldsymbol{p}^-,\boldsymbol{p}^+)\right)\right]\,.$$

Here $\mathcal{H}_1$ stands, as before, for the Hausdorff 1-dimensional measure. The above amount has been widely analysed in [3, 25]; either on its own or through stochastic geometry arguments in order to determined the mean excess length between this near-geodesic and the corresponding Euclidean distance, see [3, Theorem 3] and [25, Theorem 4].

Chapter 4

Comparison with a real data set: The British railway system

From the results developed along chapters 2 and 3 we are now able to compare the asymptotic mean traffic distribution on the Poissonian city with the traffic flow distribution presented by Beeching on [12]. The data presented by Beeching, specifically Figure 1 in its Appendix 1, relates the proportion of the network required in order to get a proportion $T \in [0, 1]$ for the total mean traffic flow on the whole network.

From Theorem 2.1 we know an expression for the asymptotic mean flow at any specific point $\boldsymbol{q}$ conditioned on the presence of an horizontal line ℓ_q that pass through $\boldsymbol{q}$. This idea can be easily generalized to any line $\ell_q(\theta)$ passing through the point $\boldsymbol{q}$ making an angle θ with the x-axis. To show this, it is enough to notice that the disk and the line process Π are rotational invariance; thus after rotating all the points in the Poissonian city by θ clockwise we will end up with the same situation described on Theorem 2.1. That is, from (2.9) it follows that for any specific point $\boldsymbol{q}$, the mean traffic at this point conditioned on any kind of line passing through $\boldsymbol{q}$ is asymptotically, as $n \to \infty$, given by the following expression:

$$\int_0^\pi \mathbb{E}[T_n^q(\theta)]\frac{1}{\pi}\,\mathrm{d}\theta \quad \sim \quad \int_0^\pi (d^-(\theta) + d^+(\theta))d^-(\theta)d^+(\theta)\frac{1}{\pi}\,\mathrm{d}\theta \; . \qquad (4.1)$$

Here $d^-(\theta)$ and $d^+(\theta)$ are the distances from $\boldsymbol{q}$ to the endpoints of $\ell_q(\theta)$ (i.e. the two intersection points between the line $\ell_q(\theta)$ and the circle $x^2 + y^2 = n^2$, marked as $\boldsymbol{x}_*$ and $\boldsymbol{x}^*$ in the figure 4.1). In consequence $d^-(\theta) + d^+(\theta)$ stands for the total length of intersection between the line $\ell_q(\theta)$ and the disk $\mathcal{B}_n(\boldsymbol{o}) = \{(x, y) \in \mathbb{R}^2 \,:\, x^2 + y^2 \leq n^2\}$, see figure 4.1.
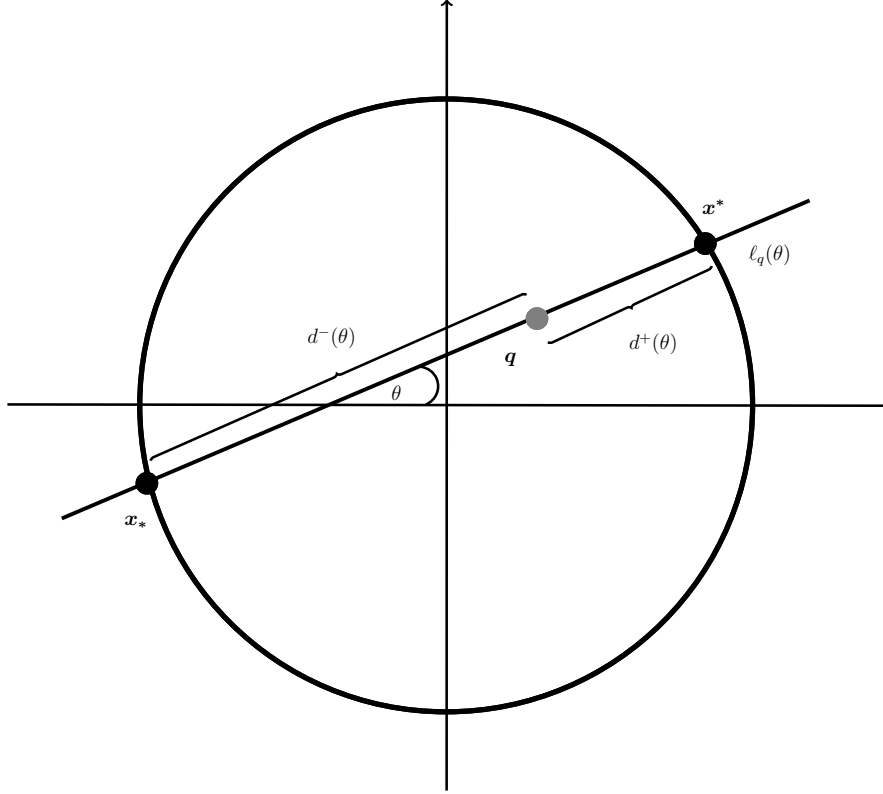
Figure 4.1: Geometric interpretation for the asymptotic mean traffic flow proved on Theorem 2.1

4.1 Numerical approach

To compare the asymptotic mean traffic behaviour around the Poissonian city with the traffic flow in the British railway system we required an analytic expression for the values $d^-(\theta)$ and $d^+(\theta)$ for each specific point $\boldsymbol{q} = (tn, un)$ inside the Poissonian city (the disk of radius n centre at the origin, i.e. $\mathcal{B}_n(\boldsymbol{o})$). This analytic formulae can easily be found once we obtain the coordinates for the two intersection points between the line $\ell_q(\theta)$ that passes through the point $\boldsymbol{q}$ making an angle θ respect to the x-axis and the circle given by $x^2 + y^2 = n$. Lets denote these points by $\boldsymbol{x}_* = (x_1, y_1)$ and $\boldsymbol{x}^* = (x_2, y_2)$. In consequence:

$$
\begin{aligned}
d^-(\theta) &= \|\boldsymbol{q} - \boldsymbol{x}_*\|_2 \,, \\
d^+(\theta) &= \|\boldsymbol{x}^* - \boldsymbol{q}\|_2 \,, \\
d^-(\theta) + d^+(\theta) &= \|\boldsymbol{x}^* - \boldsymbol{x}_*\|_2 \,.
\end{aligned}
$$

Finally, one has to express the coordinates for $\boldsymbol{x}_*$ and $\boldsymbol{x}^*$ in terms of $\boldsymbol{q} = (tn, un)$ and the angle θ. This can be done by intersecting the line $\ell_q(\theta) : y = (x - tn)\tan\theta + un$ and the circle $x^2 + y^2 = n^2$. Thus we have to solve the quadratic equation given by:

$$
x^2 + ((x - tn)\tan\theta + un)^2 = n^2 \,. \tag{4.2}
$$

69

The roots from the above equation (4.2) will correspond to x_1 and x_2; while y_1 and y_2 can be found using the line equation for $\ell_q(\theta)$, i.e. $y_i = (x_i - tn)\tan\theta + un$ for $i = 1, 2$.

Finding the roots of (4.2) is a trivial task, which can be done by using the formula for roots of a quadratic. To this purpose rewrite (4.2) as:

$$(1 + \tan^2\theta)x^2 + 2n(u - t\tan\theta)\tan\theta x + n^2((u - t\tan\theta)^2 - 1) = 0. \qquad (4.3)$$

Moreover, if we denote by $D = u - t\tan\theta$, then the above expression can be simplified further to:

$$(1 + \tan^2\theta)x^2 + 2nD\tan\theta x + n^2(D^2 - 1) = 0, \qquad (4.4)$$

whose roots are given by

$$x_1 = \frac{-B - \sqrt{B^2 - 4AC}}{2A} \quad \text{and} \quad x_2 = \frac{-B + \sqrt{B^2 - 4AC}}{2A}. \qquad (4.5)$$

Where

$$A = 1 + \tan^2\theta, \qquad (4.6)$$
$$B = 2nD\tan\theta, \qquad (4.7)$$
$$C = n^2(D^2 - 1). \qquad (4.8)$$

Finally, after some simple algebra, the roots from (4.4) can be expressed as:

$$x_1 = \left(-\frac{D}{A}\tan\theta - \frac{1}{A}\sqrt{A - D^2}\right)n \quad \text{and} \qquad (4.9)$$

$$x_2 = \left(-\frac{D}{A}\tan\theta + \frac{1}{A}\sqrt{A - D^2}\right)n. \qquad (4.10)$$

Notice that x_1 and x_2 are directly proportional to n; the same will happen to y_1 and y_2; since $y_i = (x_i - tn)\tan\theta + un$ for $i = 1, 2$. So, an equivalent approach to the above problem is to rescale all the above quantities by n. That is, we will work in the disk of radius 1. Therefore we will be considering $\boldsymbol{q} = (t, u)$ instead of $\boldsymbol{q} = (tn, un)$, where $u \in (-1, 1)$ and $t \in (-\sqrt{1 - u^2}, \sqrt{1 - u^2})$. Similarly, we will be intersecting the line $\ell_q(\theta)$ given by the equation $y = (x - t)\tan\theta + u$ with the unit circle $x^2 + y^2 = 1$. From the aforementioned exposition it is clear that the two intersection points for this problem are given by $\boldsymbol{x}_* = (x_1, y_1)$ and $\boldsymbol{x}^* = (x_2, y_2)$, here:

$$x_1 = -\frac{D}{A}\tan\theta - \frac{1}{A}\sqrt{A - D^2},$$
$$y_1 = (x_1 - t)\tan\theta + u,$$
$$x_2 = -\frac{D}{A}\tan\theta + \frac{1}{A}\sqrt{A - D^2},$$
$$y_2 = (x_2 - t)\tan\theta + u.$$

Where A and D are as in (4.6) and (4.4). In consequence, the asymptotic mean traffic flow, as $n \to \infty$, through $\boldsymbol{q}$ conditioned on $\ell_q(\theta) \in \Pi$ behaves as follows

$$\frac{\mathbb{E}[T_n^q(\theta)]}{n^3} \quad \sim \quad \|\boldsymbol{x}^* - \boldsymbol{x}_*\|_2 \|\boldsymbol{q} - \boldsymbol{x}_*\|_2 \|\boldsymbol{x}^* - \boldsymbol{q}\|_2 \ . \tag{4.11}$$

The above function can be programmed using R; see the first code segment presented in the Appendix 1, function *Traffic*. The idea is that given any specific location $\boldsymbol{q} = (t, u)$ (parameter), this code creates a function in terms of the variable θ, the angle that the line $\ell_q(\theta)$ makes with the x-axis. The function represents the asymptotic mean traffic flow through $\boldsymbol{q}$ conditioned on $\ell_q(\theta) \in \Pi$.

Even more, we can integrate this function (*Traffic*) numerically in terms of θ, from 0 to π. Additionally, since the angle $\theta \in (0, \pi]$ has a uniform distribution, we can multiply the aforementioned integral by $1/\pi$ in order to obtain the average (asymptotic mean) traffic at $\boldsymbol{q}$. This integration can be done with the second code from Appendix 1, function I, which returns the value of this integral as a function of the point $\boldsymbol{q}$, as long as the point belongs to the unit disk, otherwise it just returns the value 0 (notice that in the border, i.e. $t^2 + u^2 = 1$, one of the quantities $d^-(\theta)$ or $d^+(\theta)$ will be 0, therefore the asymptotic mean traffic is also 0).

Thus, with the above functions we can create a grid to obtain an approximation for the asymptotic mean traffic distribution across the Poissonian city. This can be done with the third code on the Appendix 1. In figure 4.2 we have a $3D$ plot regarding the (asymptotic mean) traffic across the Poissonian city. Also, the command *persp3d* in R generates an interactive 3D plot that provides a better visualization for the data.
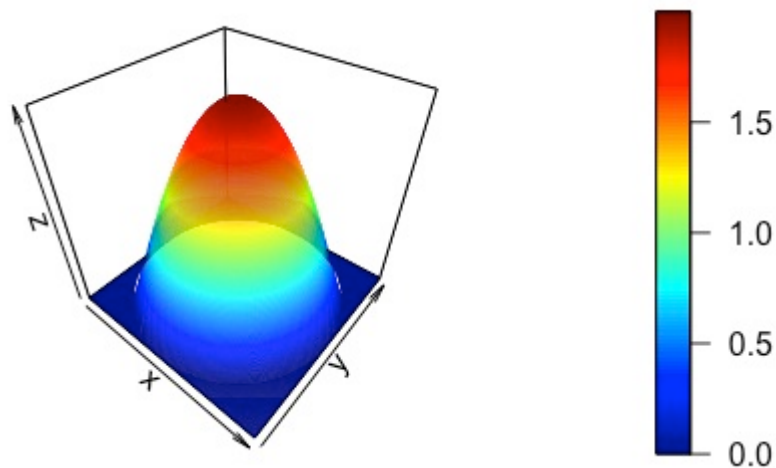

Figure 4.2: Numerical approximation for the asymptotic mean traffic across the Poissonian city. Plot obtained with the *persp3D* command in R. Here the coordinates x and y stand for the cartesian coordinates over the Poissonian city, i.e. $\boldsymbol{q} = (xn, yn)$, while z stands for the asymptotic amount of traffic flow at $\boldsymbol{q}$.

Further, as we will be comparing proportions, we can rescale the total amount of traffic at any particular point in such a way that the maximum value will be given by 1. A simple way to achieve this is by dividing all the (asymptotic mean) traffic values by the maximum value achieved, which happens to be at the centre of the disk, as expected. Then, our aim is to generate a similar plot to the Beeching plot (see figure 1.4 taken from Figure 1 of the Appendix 1 in [12]) for the mean asymptotic traffic distribution on the Poissonian city. Thus, we compute the proportion of the network with traffic per mile less than a level L. This can be approximated by the amount of points from the grid with (asymptotic mean) traffic less or equal than $L \in [0, 1]$. These proportions corresponds to the labels for the x-axis in the Beeching plot. Then, for each level L, we need to obtain the proportion of (asymptotic mean) traffic T corresponding to the specified region by L. This value will be given by the integration of the function I over the specified region, divided by the same integral over the whole disk. One way to approximate this numerically is by adding up all the values (for the mean asymptotic traffic) assigned to the points over the specified region and then divide this by the sum of the (asymptotic mean) traffic over all the points inside the disk.

In summary, given an specific level of traffic L, we first obtained the region where the level of traffic is less or equal than L (denoted by PA/TA in the fourth R code segment from Appendix 1). Then for that same level L we compute the proportion of total traffic T that this region represents (PT/TF using the fourth R code segment from Appendix 1). All this is done in the fourth R code segment from Appendix 1, where the final plot, see figure 4.3 is the one to be compared with the Beeching plot.
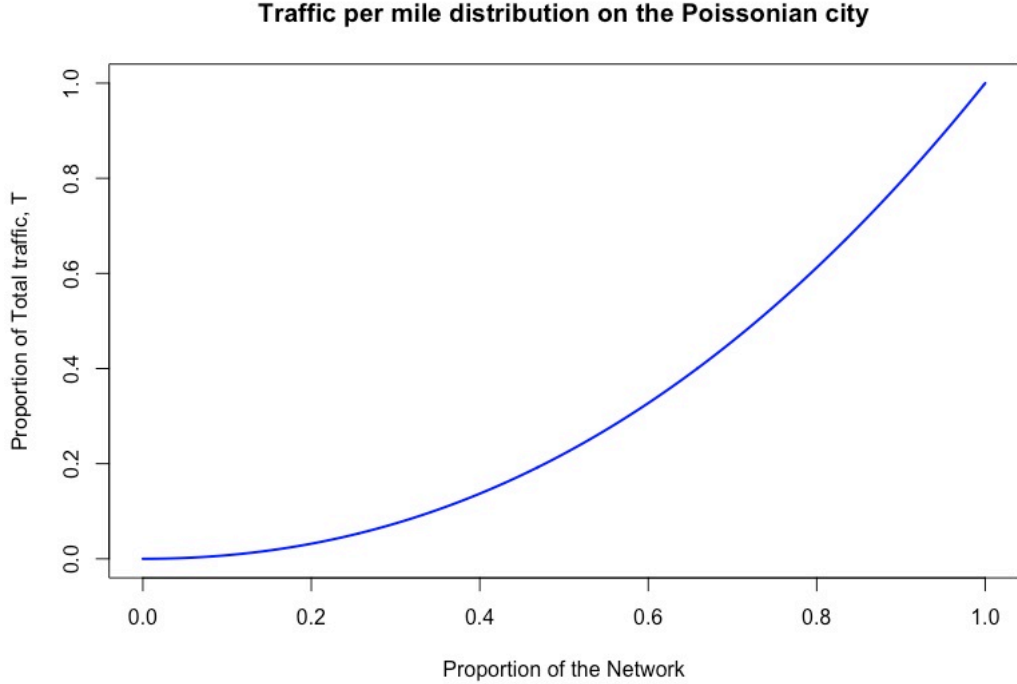
Figure 4.3: Theoretical distribution for the total mean asymptotic traffic per mile on the Poissonian city.

4.2 Analytic Approach: Elliptic Integrals

Another approach to compute the curve plotted in figure 4.3 is by an explicit calculation of the aforementioned integrals. To simplify the formulae first notice that from construction the level sets must have circular symmetry. This can be verified with the 3D plot, where the level sets from the asymptotic mean traffic have a circle shape. Even more, the shape of some level sets can be plotted using the fifth code segment from Appendix 1 (notice that this code uses some objects that are defined on the fourth code segment from Appendix 1), see figure 4.4.

Therefore, as the asymptotic mean traffic at $\boldsymbol{q}$ only depends in the distance from $\boldsymbol{q}$ to the origin $\boldsymbol{o}$ we can obtained an analytic expression for the information plotted in 4.2 in terms of $rn = \|\boldsymbol{q}\|$. For example, we can focus, without loss of generality, on the points $\boldsymbol{q}$ along the positive x-axis, i.e. $\boldsymbol{q} = (rn, 0)$, $r \in [0, 1]$. For this case, we know that $\boldsymbol{x}_* = (x_1 n, y_1 n)$ and $\boldsymbol{x}^* = (x_2 n, y_2 n)$ are given by:

$$
\begin{aligned}
x_1 &= r \sin^2 \theta - \cos \theta \sqrt{1 - r^2 \sin^2 \theta} \,, \\
y_1 &= (x_1 - r) \tan \theta \,, \\
x_2 &= r \sin^2 \theta + \cos \theta \sqrt{1 - r^2 \sin^2 \theta} \,, \\
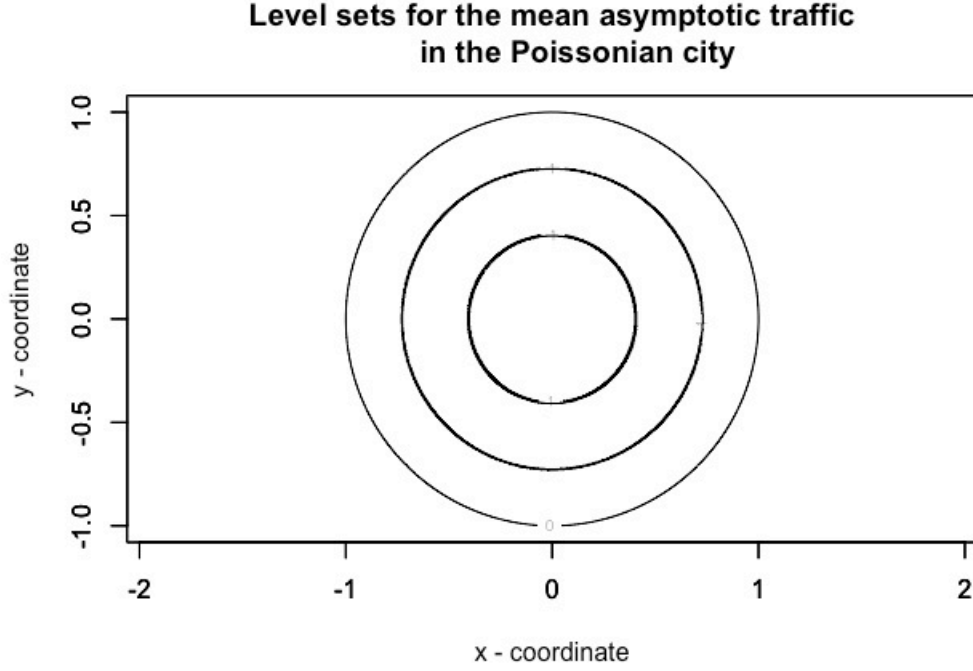y_2 &= (x_2 - r) \tan \theta \,.
\end{aligned}
$$

Figure 4.4: An illustration of the level sets for the asymptotic mean traffic across the Poissonian city. Outer circle corresponds to the unit disk, the middle circle is the level sets for mean asymptotic traffic around 40% of the traffic flow at the centre and the inner circle corresponds to level sets for mean asymptotic traffic around 80% the traffic flow at the centre of the city.

In consequence,

$$
\begin{aligned}
\frac{\|\boldsymbol{q} - \boldsymbol{x}_*\|_2}{n} &= \left| \cos\theta \sqrt{1 - r^2 \sin^2\theta} + r\cos^2\theta \right| |\sec\theta| \,, \\
\frac{\|\boldsymbol{x}^* - \boldsymbol{q}\|_2}{n} &= \left| \cos\theta \sqrt{1 - r^2 \sin^2\theta} - r\cos^2\theta \right| |\sec\theta| \,, \\
\frac{\|\boldsymbol{x}^* - \boldsymbol{x}_*\|_2}{n} &= 2\sqrt{1 - r^2 \sin^2\theta} \,.
\end{aligned}
$$

Accordingly,

$$
\frac{\mathbb{E}[T_n^q(\theta)]}{n^3} \sim \|\boldsymbol{q} - \boldsymbol{x}_*\|_2 \|\boldsymbol{x}^* - \boldsymbol{q}\|_2 \|\boldsymbol{x}^* - \boldsymbol{x}_*\|_2 = 2(1 - r^2)\sqrt{1 - r^2 \sin^2\theta} \,. \quad (4.12)
$$

Even more, to obtain the total flow on the whole Poissonian city we will need to compute the following triple integral:

$$
\begin{aligned}
\int_0^1 \int_0^{2\pi} \int_0^\pi \mathbb{E}[T_n^q(\theta)] \frac{1}{\pi} \, \mathrm{d}\theta \, \mathrm{d}\alpha \, \mathrm{d}r \quad &\sim \\
n^3 \int_0^1 \int_0^{2\pi} \int_0^\pi 2(1 - r^2)&\sqrt{1 - r^2 \sin^2\theta} \frac{1}{\pi} \, \mathrm{d}\theta \, \mathrm{d}\alpha \, \mathrm{d}r \\
&= 4n^4 \int_0^1 (1 - r^2) r \left(\int_0^\pi \sqrt{1 - r^2 \sin^2\theta} \, \mathrm{d}\theta \right) \mathrm{d}r \,. \quad (4.13)
\end{aligned}
$$

Here, $\boldsymbol{q}$ is expressed in polar coordinates as (rn, α) with $r \in [0, 1]$ and $\alpha \in [0, 2\pi]$; while $\theta \in [0, \pi]$ represents the angle between the line $\ell_q(\theta)$ and the x-axis. The last equality follows since the integral regarding α is given by $2\pi n r$, as the integrated function does not depend on α at all.

Remark: The integral $\int \sqrt{1 - r^2 \sin^2 \theta} \, d\theta$ from the right hand side of (4.13) is the well known second kind of Elliptic Integrals [1], this topic will be studied in more depth in chapter 5.

Elliptic integrals in general are not reducible to elementary functions. However, we can compare the Beeching plot with the theoretical curve for the proportions of (asymptotic mean) traffic across the Poissonian city leaving all the analytic formulas in terms of this Elliptic integral.

The 3D plot from figure 4.2 provides us with a helpful insight on how to use the integral (4.13) in order to get an analytic expression for the curve plotted in figure 4.3. From figure 4.2 it is clear the traffic increases as one get closer to the centre. Therefore, we are interested on the development of the integral (4.13) over the annulus region comprehended between the circle of radius n and the circle of radius an for $a \in [0, 1]$. That is given by:

$$4n^4 \int_a^1 (1 - r^2) r \left(\int_0^\pi \sqrt{1 - r^2 \sin^2 \theta} \, d\theta \right) dr \; .$$

On the other hand, for each fixed value of a we will have covered an area given by $A = \pi(1 - a^2)n^2$. Since, we are working with a unit intensity stationary isotropic Poisson line process Π, we know that in average the length intersection of Π with any measurable subset B of $\mathbb{R}^2$ is given by $\text{Leb}_2(B)$, thus the mean proportion of the network length covered by a subset $B \subseteq \mathcal{B}_n(\boldsymbol{o})$ is the same as the proportion represented by the area of B regarding the area of the whole disk. In consequence, we can express the proportions of length network and the proportions of traffic, PA/TA and PT/TF in terms of the fourth R code segment from Appendix 1, respectively, as follows:

$$\frac{PA}{TA} \;=\; \frac{\pi(1 - a^2)n^2}{\pi n^2} \;=\; (1 - a^2) \,, \tag{4.14}$$

$$\frac{PT}{TF} \;=\; \frac{\int_a^1 (1 - r^2) r \left(\int_0^\pi \sqrt{1 - r^2 \sin^2 \theta} \, d\theta \right) dr}{\int_0^1 (1 - r^2) r \left(\int_0^\pi \sqrt{1 - r^2 \sin^2 \theta} \, d\theta \right) dr} \;. \tag{4.15}$$

Finally, since our aim is to plot PT/TF in terms of PA/TA we can get rid of the auxiliary variable a through the relation (4.14). Thus PT/TF in terms of PA/TA,

which is denoted by A in the following formula, is given by:

$$\frac{PT}{TF} = 1 - \frac{\int_0^{\sqrt{1-A}} (1-r^2)r \left(\int_0^\pi \sqrt{1 - r^2 \sin^2\theta}\, \mathrm{d}\theta\right) \mathrm{d}r}{\int_0^1 (1-r^2)r \left(\int_0^\pi \sqrt{1 - r^2 \sin^2\theta}\, \mathrm{d}\theta\right) \mathrm{d}r} \,. \tag{4.16}$$

The sixth R code segment from Appendix 1 provides an alternative way to plot the curve shown on figure 4.3 using the relation (4.16). We now explained the ideas behind how this R code segment works. First, the function $F1$ creates the function $g_1(\theta) = \sqrt{1 - r^2 \sin^2\theta}$ in terms of θ, where r works as a fixed parameter. Then $I1$ integrates the function g_1 from 0 to π, in terms of θ, $int1vec$ is used to apply $I1$ to a vector of different values for r (used as a fixed parameter in $I1$). Now, $F2$ creates the function

$$f_1(r) = 4(1-r^2)r \left(\int_0^\pi \sqrt{1 - r^2 \sin^2\theta}\, \mathrm{d}\theta\right) ,$$

by using the already defined function $I1$. Then, similarly to $I1$, $I2$ integrates the function f_1 from 0 to a, in terms of r, where a is used as a fixed parameter. Next, $int2vec$ applies $I2$ to a vector of different values for a. To conclude the function g uses $int2vec$ to creates the relation (4.16) for a vector of different values of the parameter a. Thus the final line plots the desired traffic curve using the function g and the fact that the parameter a can be rewritten as $\sqrt{1-A}$, where A stands for the proportion of the length network (denoted by PA/TA in previous R code segments).

4.3   Final comments on the comparison

To conclude this chapter we compare the theoretical curve for proportions of total (mean asymptotic) traffic in terms of the length proportions of the network for the Poissonian city with the Beeching plot. A simple way to achieve this is by superimposing the plots, as in figure 4.5.

From figure 4.5 it is clear that the curves are not the same. Nevertheless, they share the same kind of shape. This could be explained by the construction of this curve in the Poissonian city. That is, for any point along the curve as we move to the right we are adding up new route miles that increase the proportion of traffic flow with a higher value than any of the proportions (of traffic flow) considered until this point. In other words, the differential of traffic proportion regarding the network proportion is always increasing faster (as we are always adding up miles with higher traffic flow) which explains the convex shape of the curve. However, in the British railway system this differential of traffic density keeps increasing in a faster way that the one presented in the Poissonian city.

On the other hand their difference could be explained by different factors. For ex-
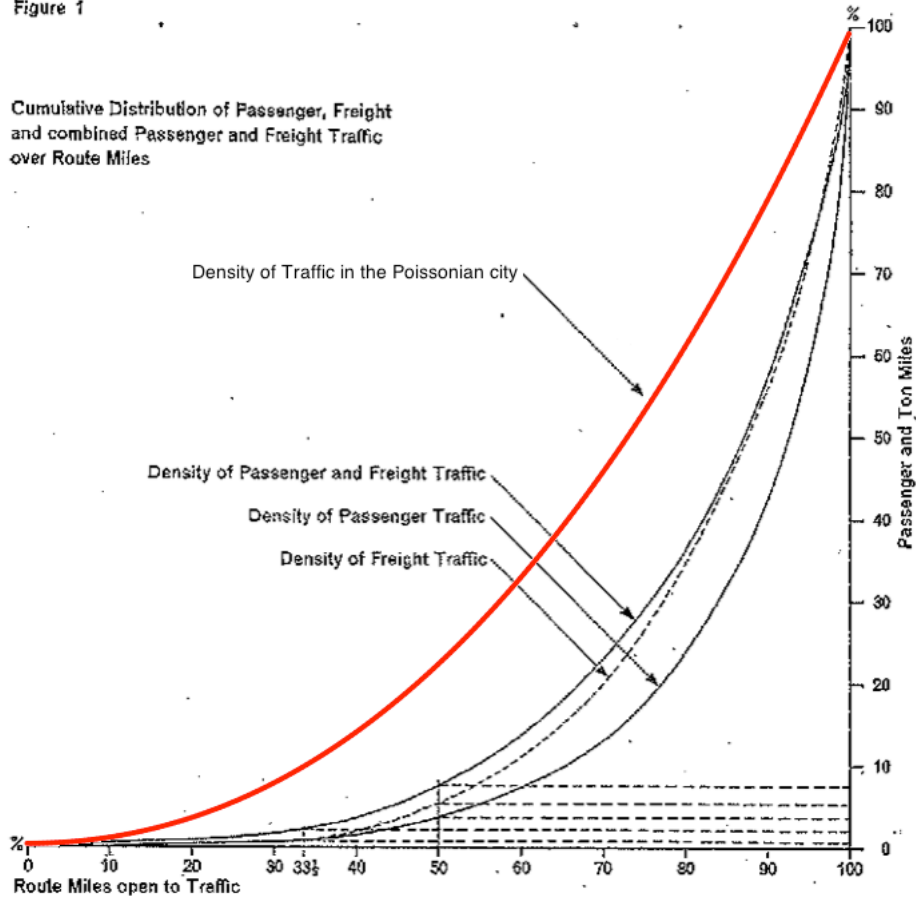
Figure 4.5: Comparison between traffic distribution on the Poissonian city and the British railway system as provided in Figure 1 from Appendix 1 in British Railways Board [12].

ample: the shape of Great Britain is not isotropic (opposite to the design of the Poissonian city on the disk), source and destination nodes on the British railway system are not uniformly distributed over the whole network (one of the assumptions in the Poissonian city model). Also the railways have a bounded length, not indefinite (or infinite length as in our asymptotic considerations) as the lines used in the Poissonian city. Also, the railways are not perfectly straight lines, they could be better approximated by fibres with small curvature. In the following chapter we will adapt the Poissonian city model to an ellipse shape to see if that improves the fit between the theoretical curve for traffic distribution in the Poissonian city and the Beeching plot.

Chapter 5

The Elliptic case

The purpose of this chapter is to generalize previous results from the original Poissonian city over a disk to a modified Poissonian city over an ellipse. So, instead of considering the line process Π being intersected with a disk of radius n, here we consider the line process taking place over a variety of ellipses by adding an extra parameter $c \in (0,1]$. The parameter c is related to the *eccentricity* of the ellipse in question. The eccentricity of an ellipse provides a measure regarding how out of round an ellipse is and it is given by the ratio between the distance from the centre of the ellipse to one of its foci and the distance between that foci to a vertex. In some literature, the distance between the centre of the ellipse and either of its foci is referred as the *linear eccentricity*, denoted by f. Therefore, the *eccentricity* of an ellipse with semi-major axis a and semi-minor axis b can be defined as the ratio between its *linear eccentricity* ($f = \sqrt{a^2 - b^2}$) and its semi-major axis a, i.e. $e = \sqrt{1 - \frac{b^2}{a^2}}$.

This motivates us to focus on the ratio between the semi-minor axis b and the semi-major axis a. Thus if we define $a = 1/c$ and $b = c$ for any $c \in (0,1]$ then $b/a = c^2$. Even more, it is clear that $e = \sqrt{1 - c^4}$. Therefore the results developed along chapters 2, 3 and 4 will be analysed considering that the Poisson line process Π is intersected with the interior of the ellipse given by

$$\boldsymbol{E}_c = \left\{ (x,y) \in \mathbb{R}^2 : (cx)^2 + \left(\frac{y}{c}\right)^2 \leq n^2 \right\}, \qquad \text{for some } c \in (0,1] \,.$$

Notice that the original Poissonian city, over a disk of radius n, is recovered when $c = 1$. Along this chapter the traffic behaviour will be analysed asymptotically as $n \to \infty$. The motivation is to study the way in which mean traffic depends on the geometry of the region in question. Also, we are interested in the effects this could have in the theoretical curve for the traffic density in the Poissonian city; we wish to see if this improves the fit with the Beeching plot regarding the traffic density on the British railway system.

5.1 Poissonian city over an ellipse

Consider the mean traffic at a particular point $q \in E_c$ on the Poissonian city over an ellipse E_c conditional on $\ell_q(\theta_0) \in \Pi$, meaning that there is a line passing through the point q which makes an angle $\theta_0 \in (0, \pi]$ with the x-axis. From here on, this will be denoted by $T_n^q(\theta_0)$. It turns out that the geometrical interpretation of Theorem 2.1 still applies to this case. Thus conditioning on the line process Π having an specific line $\ell_q(\theta_0)$ that goes through the point q, then the mean traffic at this point is asymptotically given by the product of three quantities: $d_c^-(\theta_0)$, $d_c^+(\theta_0)$ and $(d_c^-(\theta_0) + d_c^+(\theta_0))$, see figure 5.1.

As in chapter 4:

- $d_c^-(\theta_0)$ and $d_c^+(\theta_0)$ are the distances from q to the endpoints of $\ell_q(\theta_0)$.

- Therefore $(d_c^-(\theta_0) + d_c^+(\theta_0))$ is the total length of intersection between the line $\ell_q(\theta_0)$ and the interior of the ellipse E_c.
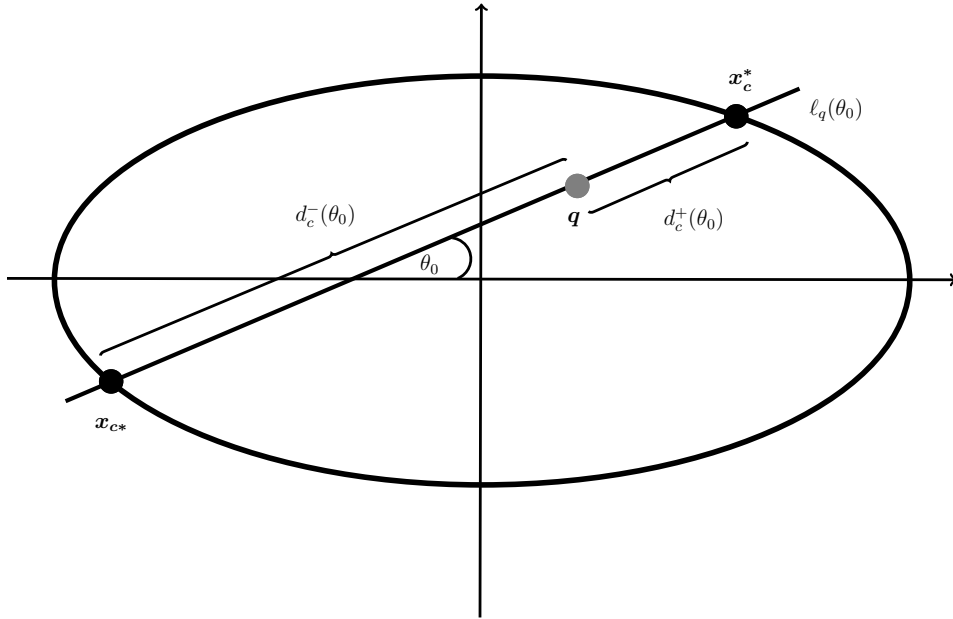
Figure 5.1: Geometrical interpretation of Theorem 2.1 applied to an elliptic Poissonian city.

The proof of Theorem 2.1 only has to be modified to take into account that the functions $h_1^q(\alpha_1)$ and $h_2^q(\alpha_2)$ now represent the boundary of the ellipse E_c instead of the disk of radius n. However, as long as these functions are continuous and differentiable, a Taylor series argument can still be applied to accomplish the same result. That is the essence of the next corollary

COROLLARY 5.1 (Mean flow through any point $q \in E_c$). *The mean traffic flow through $q \in E_c$ conditioned on $\ell_q(\theta_0) \in \Pi$ is asymptotically given by the following*

expression:

$$\mathbb{E}[T_n^q(\theta_0)] \quad \sim \quad (d_c^-(\theta_0) + d_c^+(\theta_0))d_c^-(\theta_0)d_c^+(\theta_0), \quad \text{as } n \to \infty, \qquad (5.1)$$

where $d_c^-(\theta_0)$ and $d_c^+(\theta_0)$ are as in figure 5.1.

Proof. From Theorem 2.1 we know that the expected value of traffic through the point $\boldsymbol{q} \in \boldsymbol{E}_c$ is given by the following integrals

$$\mathbb{E}[T_n^q(\theta_0)] \quad = \quad \frac{1}{2} \iiint_{\mathcal{D}_{n,-}^q} g(r,s,\theta)r \, dr \, s \, ds \, \theta \, d\theta \quad + \quad \frac{1}{2} \iiint_{\mathcal{D}_{n,+}^q} g(r,s,\theta)r \, dr \, s \, ds \, \theta \, d\theta.$$

$$(5.2)$$

Here $g(r,s,\theta) = \exp\left(-\frac{1}{2}(r + s - \sqrt{r^2 + s^2 + 2rs\cos\theta})\right)$ is the probability that there are no lines from the Poisson line process Π separating the points $\boldsymbol{p}^- = (r, \alpha_1)$ and $\boldsymbol{p}^+ = (s, \alpha_2)$ (expressed in polar coordinates with $\boldsymbol{q}$ as the reference point and $\ell_q(\theta_0)$ as the reference line for the angles) simultaneously from $\boldsymbol{q}$, where $\theta = \alpha_1 + \alpha_2$. While $\mathcal{D}_{n,\pm}^q$ are the appropriate regions of integration for (r,s,θ) which depends on the location of the point $\boldsymbol{q}$. Thus

$$\mathcal{D}_{n,-}^q \quad = \quad \{(r,s,\theta) : 0 \le r \le h_1^q(\alpha_1)n, \, 0 \le s \le h_2^q(\alpha_2)n, \, -\pi \le \theta \le 0\}, \qquad (5.3)$$
$$\mathcal{D}_{n,+}^q \quad = \quad \{(r,s,\theta) : 0 \le r \le h_1^q(\alpha_1)n, \, 0 \le s \le h_2^q(\alpha_2)n, \, 0 \le \theta \le \pi\}. \qquad (5.4)$$

Here $h_1^q(\alpha_1)$ (respectively $h_2^q(\alpha_2)$) is a continuous function that expresses how the maximum allowed distance from the point $\boldsymbol{p}^-$ (respectively $\boldsymbol{p}^+$) to $\boldsymbol{q}$ changes depending on the angle α_1 (respectively α_2). Therefore

$$h_1^q(\alpha_1) \quad = \quad (x_1 + t)\sec\alpha_1 \qquad \text{and} \qquad h_2^q(\alpha_2) \quad = \quad (x_2 - t)\sec\alpha_2,$$

here x_1 (respectively x_2) is the absolute value of the x-coordinate from the intersection point between the line $y = -(x-t)\tan\alpha_1 + u$ (respectively $y = (x-t)\tan\alpha_2 + u$) and the ellipse $(cx)^2 + (y/c)^2 = 1$. Notice that the implicit function theorem [10, Section 41] guarantees that the functions $h_1^q(\alpha_1)$ and $h_2^q(\alpha_2)$ will be smooth, in such a way that the proof from Theorem 2.1 still holds with the appropriate modifications on these functions.

$\square$

The above corollary provide us a way to compute the asymptotic mean traffic at any particular point $\boldsymbol{q} \in \boldsymbol{E}_c$ given that $\ell_q(\theta_0) \in \Pi$.

In section 5.3 we will develop some numerical computations for the integrated mean traffic across the Poissonian city over ellipses with different values for the parameter c (therefore different values of eccentricity) to analyse if the eccentricity of the region plays a role on the asymptotic traffic flow.
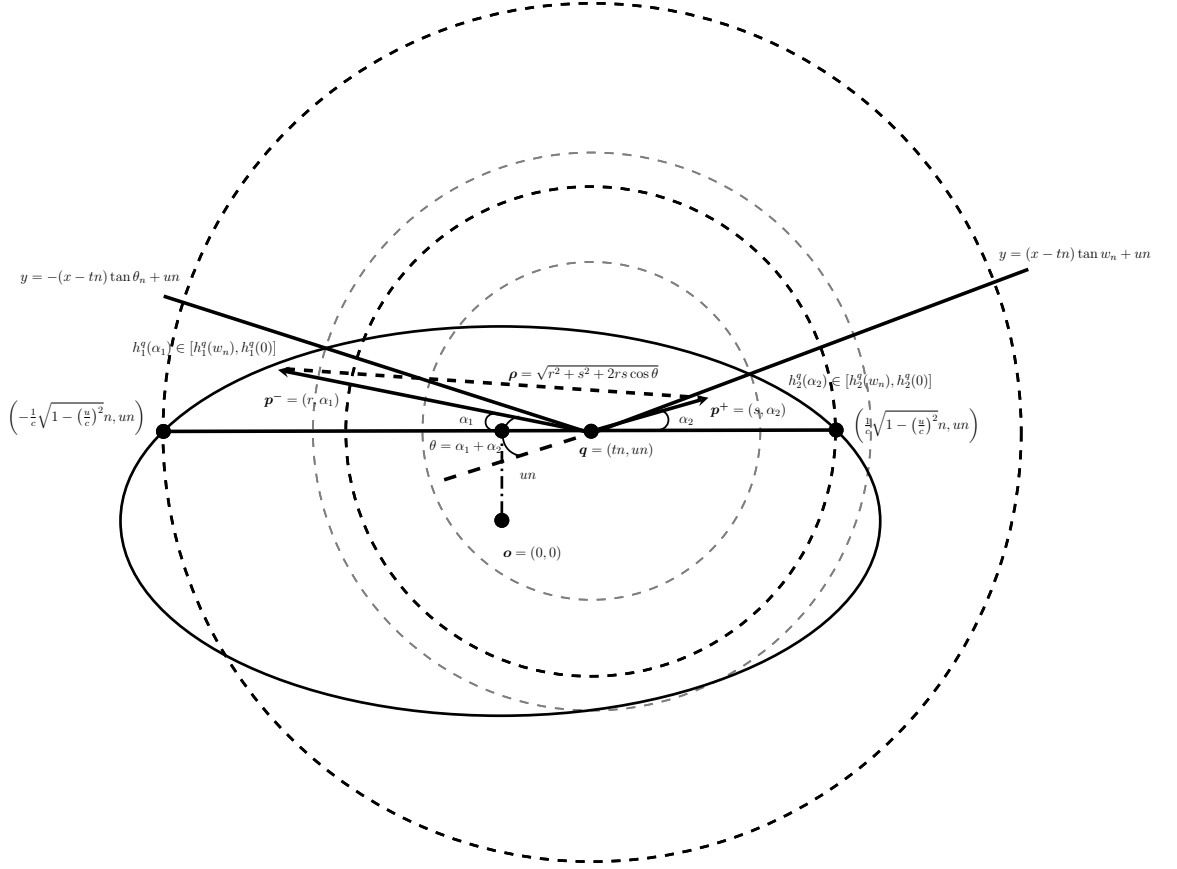
Figure 5.2: Illustration from the concepts explained along the proof for Corollary 5.1. Here we follow the same notation as in Theorem 2.1.

5.2 Anisotropic Poisson line process, Elliptic case

The contents of this section are closely related to the work done in Kendall [25, Section 3.3]. As in the case for the Poissonian city over a disk of radius n, there is another approach to verify the computations regarding the asymptotic mean traffic at a particular point $q \in E_c$ conditioning on the presence of a line $\ell_q(\theta_0)$. An anisotropic Poisson line process provides a shorter and more conceptual exposition. Nevertheless, the results developed in this section will not provide any information regarding the error of the asymptotic approximations. This error is given by the second leading term on the asymptotics behaviour for the mean traffic at the point q.

The main difference between this section and the ideas developed on section 2.2 is the fact that an ellipse does not have rotational invariance. Therefore, it is not enough to consider the case where the conditioning line $\ell_q(\theta_0) \in \Pi$ is an horizontal line (as we did for the whole chapter 2). However there is a way to develop results which are similar to those in section 2.2.

The scaling limit for the distribution of traffic flow through any point, q, in the

Poissonian city over an ellipse can be represented by using an improper stationary anisotropic Poisson line process, $\dot{\Pi}$. In this case one has to condition on the existence of a line $\ell_q(\theta_0) \in \Pi$ that passes through $\boldsymbol{q} = (tn, un)$ and makes an angle $\theta_0 \in (0, \pi]$ with the x-axis.

The first step to approach this problem is to rotate our coordinate system, given by the cartesian coordinates (x, y), in order to make the line $\ell_q(\theta_0)$ an horizontal one. This can be done either by a clockwise rotation by θ_0 or by an anti-clockwise rotation by $(\pi - \theta_0)$. Without lost of generality we chose to make an anti-clockwise rotation, see figure 5.3. Call the rotated coordinate system $(\hat{x}, \hat{y})$. Also, to abbreviate some notation we will refer to $\ell_q(\hat{\theta}_0)$ by ℓ_q from here on.
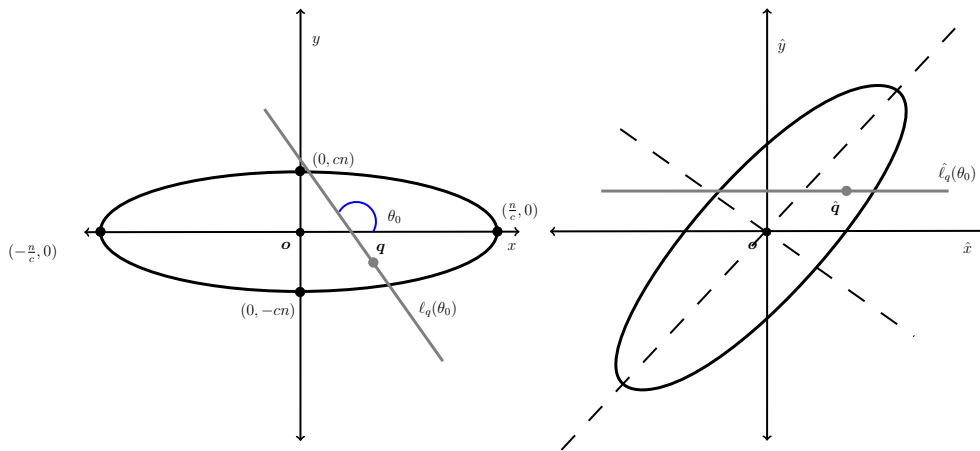

Figure 5.3: Rotation by $(\pi - \theta_0)$ anti-clockwise.

Recall that a line process can be parametrized in different ways. So, instead of using the standard coordinates (r, θ), where r represents the distance of the line ℓ to the origin and θ the angle it makes regarding an horizontal line (x-axis). We will use $(p, \hat{\theta})$, with p being the signed distance from $\hat{\boldsymbol{q}}$ to the intersection between the given horizontal line ℓ_q and the line ℓ that is being parametrised, and $\hat{\theta}$ represents the angle between these two lines (ℓ_q and ℓ), see figure 5.4.

In the latter case, the intersection points with the line ℓ_q will form a stationary Poisson point process and the angle density is given by $\frac{1}{2} \sin \hat{\theta}$ for $\hat{\theta} \in [0, \pi]$. However, there is a setback with the parametrization $(p, \hat{\theta})$ as all parallel lines to ℓ_q will not be represented, since they do not intersect with ℓ_q. Nonetheless, this kind of lines are contained on a null set, say the set of lines such that $\theta = 0$, using the first coordinate system (r, θ).

Guided by the results developed in section 2.2 we rescale the cartesian coordinates $(\hat{x}, \hat{y})$ in the following way: shrink the x-axis by a factor of $1/n$ and contract the y-axis by $1/\sqrt{n}$. Therefore, the new set of coordinates is given by $(\tilde{x}, \tilde{y}) = (\hat{x}/n, \hat{y}/\sqrt{n})$, see
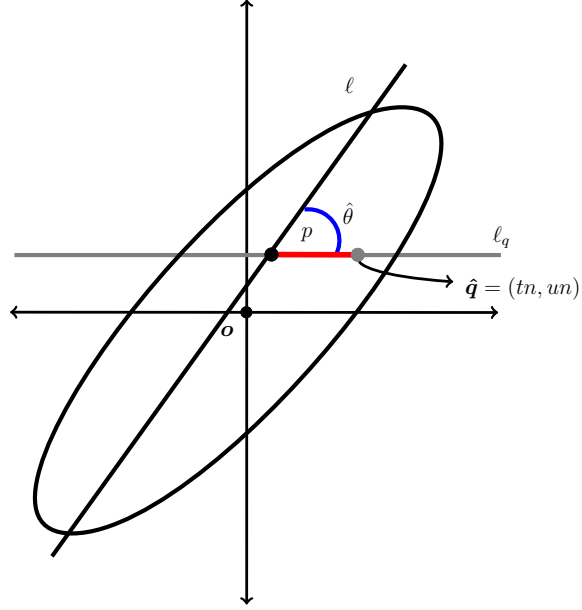
Figure 5.4: Illustration for the alternative coordinates $(p, \hat{\theta})$ used to parametrise a line process Π. For this particular case, p will be a negative number.

figure 5.5. Accordingly, the new parameters for the line process $(\tilde{p}, \tilde{\theta})$ can be related with $(p, \hat{\theta})$ by the relations:

$$\tilde{p} = p/n \qquad \text{and} \qquad \tan \tilde{\theta} = \sqrt{n} \tan \hat{\theta} \, .$$
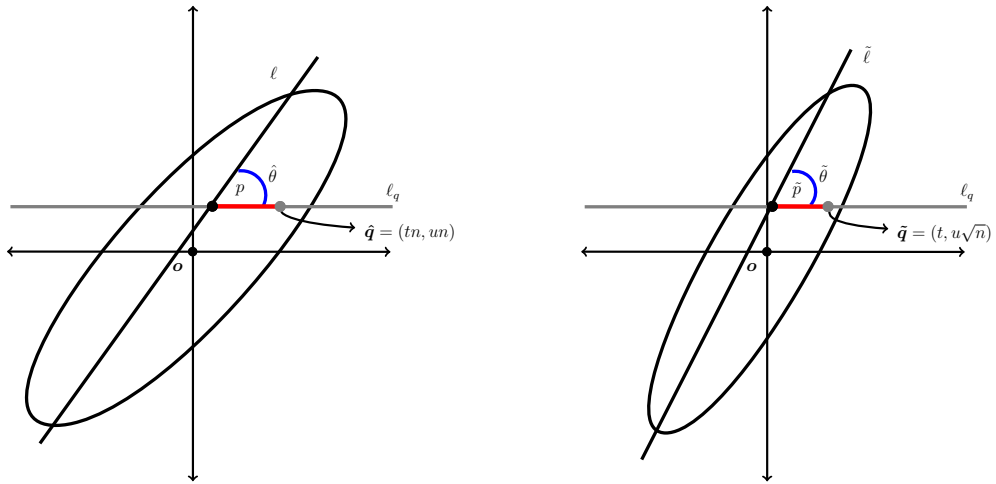
Figure 5.5: Change of coordinates from $(p, \hat{\theta})$ to $(\tilde{p}, \tilde{\theta})$.

So, the line process Π is being transformed into another line process $\tilde{\Pi}$. The intensity of $\tilde{\Pi}$ can be expressed in terms of $(\tilde{p}, \tilde{\theta})$. The Jacobian for the above change of coordinates, i.e. $p = n\tilde{p}$ and $\hat{\theta} = \arctan\left(\frac{1}{\sqrt{n}} \tan \tilde{\theta}\right)$, is given by

$$\left| \frac{\partial(p, \hat{\theta})}{\partial(\tilde{p}, \tilde{\theta})} \right| = \left| \begin{pmatrix} n & 0 \\ 0 & \frac{\sec^2 \tilde{\theta}}{1 + \frac{1}{n} \tan^2 \tilde{\theta}} \frac{1}{\sqrt{n}} \end{pmatrix} \right| = \sqrt{n} \frac{\sec^2 \tilde{\theta}}{1 + \frac{1}{n} \tan^2 \tilde{\theta}} \, .$$

83

Also, observe that

$$\sin\hat{\theta} \quad = \quad \sin\left(\arctan\left(\frac{1}{\sqrt{n}}\tan\tilde{\theta}\right)\right) \quad = \quad \frac{\tan\tilde{\theta}}{\left(n\left(1+\frac{1}{n}\tan^2\tilde{\theta}\right)\right)^{1/2}}.$$

Therefore, the line process $\tilde{\Pi}$ can be parametrized as a Poisson point process on the $(\tilde{p},\tilde{\theta})$ space with intensity

$$\Lambda(\,\mathrm{d}(\tilde{p},\tilde{\theta})\,) \quad = \quad \frac{1}{2}\frac{\tan\tilde{\theta}\sec^2\tilde{\theta}}{\left(1+\frac{1}{n}\tan^2\tilde{\theta}\right)^{3/2}}\,\mathrm{d}\tilde{p}\,\mathrm{d}\tilde{\theta}\,.$$

The $\tilde{x}$-axis can be translated to the horizontal line ℓ_q. Denote the new coordinates after this translation by $(\dot{x},\dot{y})$, notice that intensity of the line process $\dot{\Pi}$ is the same as the intensity of $\tilde{\Pi}$. Taking the limit as $n\to\infty$ one obtains an improper station-ary anisotropic Poisson line process with intensity $\Lambda(\,\mathrm{d}(\dot{p},\dot{\theta})) = \frac{1}{2}\tan\dot{\theta}\sec^2\dot{\theta}\,\mathrm{d}\dot{p}\,\mathrm{d}\dot{\theta}$. Based on this line process one can achieve a proper stationary isotropic Poisson line process at scale n by randomly thinning the lines with a retention probability that depends monotonically on the line slope, details on this ideas can be found at Kendall [25, page 31].

Notice that once the $\dot{x}$-axis is fixed to coincide with the horizontal line ℓ_q, then eventually, as $n\to\infty$, the only points that will be inside the tilted ellipse will be delimited by the vertical strip comprehended between the vertical lines $\dot{x} = -x_1$ and $\dot{x} = x_2$. Here the values $|x_1|+t$ and $|x_2|-t$ corresponds to the distances from $\boldsymbol{q}$ to the intersections points of the ellipse and the line $\ell_q(\theta)$, which implicitly depends on the value for the eccentricity (related with the variable c), see figure 5.6.

Remark: In the case treated in section 2.2 the values for $|x_1|+t$ and $|x_2|-t$ were given by $\sqrt{1-u^2}+t$ and $\sqrt{1-u^2}-t$, respectively. These values are relevant when representing the asymptotic mean traffic flow at $\boldsymbol{q}$ as a 4-volume region as done in Lemma 2.3.

Even more, the improper anisotropic Poisson line process may be represented in a simple way by a different set of coordinates. Represent each line in the line process by its intercepts y_- and y_+ on the vertical axis $\dot{x} = -x_1$ and $\dot{x} = x_2$, respectively, see figure 5.6. Therefore for a line represented by $(\dot{p},\dot{\theta})$ one have the following relations:

$$y_- \quad = \quad -\tan\dot{\theta}(|x_1|+\dot{p}) \qquad \text{and} \qquad y_+ \quad = \quad \tan\dot{\theta}(|x_2|-\dot{p}).$$
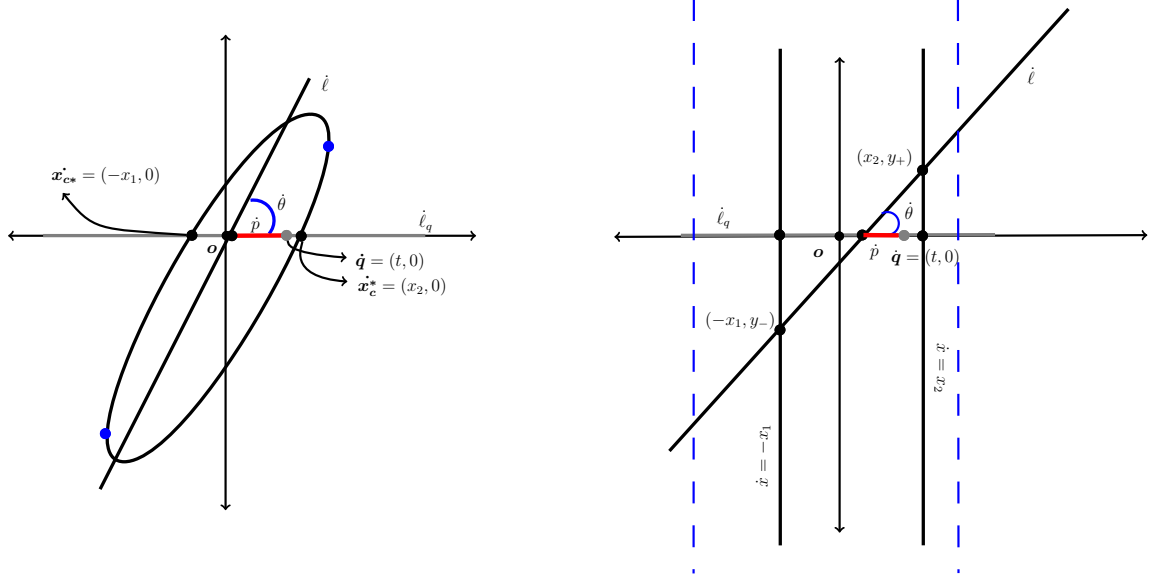
Figure 5.6: Change of coordinates from $(\dot{p}, \dot{\theta})$ to (y_-, y_+).

The Jacobian for this change of coordinates is given by

$$
\left| \frac{\partial(\dot{p}, \dot{\theta})}{\partial(y_-, y_+)} \right| = \left| \frac{\partial(y_-, y_+)}{\partial(\dot{p}, \dot{\theta})} \right|^{-1}
$$

$$
= \left| \begin{pmatrix} -\tan\dot{\theta} & -(|x_1|+\dot{p})\sec^2\dot{\theta} \\ -\tan\dot{\theta} & (|x_2|-\dot{p})\sec^2\dot{\theta} \end{pmatrix} \right|^{-1} = \frac{1}{(|x_1|+|x_2|)\tan\dot{\theta}\sec^2\dot{\theta}} .
$$

Thus the intensity becomes

$$
\Lambda(\,\mathrm{d}(y_-, y_+)\,) = \frac{1}{2}\tan\dot{\theta}\sec^2\dot{\theta}\frac{1}{(|x_1|+|x_2|)\tan\dot{\theta}\sec^2\dot{\theta}}\,\mathrm{d}y_-\,\mathrm{d}y_+
$$

$$
= \frac{1}{2(|x_1|+|x_2|)}\,\mathrm{d}y_-\,\mathrm{d}y_+ .
$$

The above construction enable us to identify the limiting behaviour for the asymptotic mean traffic flow through the point $\boldsymbol{q} \in \boldsymbol{E}_c$ conditioned on the event that $\ell_q(\theta) \in \Pi$ passing through $\boldsymbol{q}$. This could be done by applying Lemma 2.3 with the required modifications. Notice, that main required change is to adapt the 4-volume for the region that represents the flow through $\boldsymbol{q}$, see figure 2.8. Therefore, in the elliptic case the mean 4-volume of the region will be given by:

$$
\int_0^{|x_1|+t}\int_0^{|x_2|-t}\int_0^\infty\int_{-\frac{a+v}{a}z}^{\frac{a+v}{v}z}\exp\left(-\frac{z^2}{4}\left(\frac{1}{a}+\frac{1}{v}\right)\right)\mathrm{d}p\,\mathrm{d}z\,\mathrm{d}v\,\mathrm{d}a
$$

$$
= \int_0^{|x_1|+t}\int_0^{|x_2|-}\int_0^\infty (a+v)\left(\frac{1}{a}+\frac{1}{v}\right)\exp\left(-\frac{z^2}{4}\left(\frac{1}{a}+\frac{1}{v}\right)\right)z\,\mathrm{d}z\,\mathrm{d}v\,\mathrm{d}a
$$

$$
= 2\int_0^{|x_1|+t}\int_0^{|x_2|-t}(a+v)\,\mathrm{d}v\,\mathrm{d}a = (|x_1|+|x_2|)(|x_1|+t)(|x_2|-t) .
$$

Notice that the amount $(|x_1|+|x_2|)(|x_1|+t)(|x_2|-t)$ agrees with the geometrical interpretation of Theorem 2.1, as explained in figure 5.1. Similarly, Theorem 2.2 can be applied to the elliptic case, with its required modifications, to determine the limiting distribution for T_n^q/n^3.

5.3 Numerical computations for the traffic density in an elliptic Poissonian city

From the contents of sections 4.1 and 4.2 together with the ideas regarding Palm theory developed in chapter 3 we can compare the asymptotic mean traffic across the Poissonian city over an elliptic region in a similar manner as the one used in chapter 4. Again, our final aim for this section is to compute the traffic density curve corresponding to the elliptic Poissonian city, that is we will relate the proportion $T \in [0, 1]$ for the total traffic flow from the transportation network in terms of the proportion of the length network open to traffic.

Due to corollary 5.1 we know an expression for the asymptotic mean flow at any specific point $\boldsymbol{q} \in \boldsymbol{E}_c$ conditioned on the presence of an specific line $\ell_q(\theta)$ that passes through $\boldsymbol{q}$, i.e. $\ell_q(\theta) \in \Pi$. Even more, the angle $\theta \in [0, \pi]$ is distributed uniformly, therefore the average traffic flow at $\boldsymbol{q}$ conditioned on any kind of line passing through $\boldsymbol{q}$ is asymptotically given by the expression:

$$\int_0^\pi \mathbb{E}[T_n^q(\theta)]\frac{1}{\pi}\,\mathrm{d}\theta \quad \sim \quad \int_0^\pi (d_c^-(\theta) + d_c^+(\theta))d_c^-(\theta)d_c^+(\theta)\frac{1}{\pi}\,\mathrm{d}\theta\,, \qquad (5.5)$$

with $d_c^-(\theta)$ and $d_c^+(\theta)$ as illustrated in figure 5.1. Now, to find an analytic expression for $d_c^-(\theta)$ and $d_c^+(\theta)$ we follow a similar approach to the one used in section 4.1. So, we can express:

$$\begin{aligned} d_c^-(\theta) &= \|\boldsymbol{q} - \boldsymbol{x_{c*}}\|_2\,, \\ d_c^+(\theta) &= \|\boldsymbol{x_c^*} - \boldsymbol{q}\|_2\,, \\ d_c^-(\theta) + d^+(\theta) &= \|\boldsymbol{x_c^*} - \boldsymbol{x_{c*}}\|_2\,. \end{aligned}$$

Here $\boldsymbol{x_{c*}} = (x_1, y_1)$ and $\boldsymbol{x_c^*} = (x_2, y_2)$ stands for the two intersection points between the line $\ell_q(\theta) : y = (x - tn)\tan\theta + un$ and the ellipse $(cx)^2 + (y/c)^2 = n^2$. Thus, we have to express the coordinates (x_1, y_1) and (x_2, y_2) in terms of c, θ and $\boldsymbol{q} = (tn, un)$, where $u \in (-c, c)$ and $t \in (-1/c\sqrt{1 - (u/c)^2}, 1/c\sqrt{1 - (u/c)^2})$. To achieve this, we simply intersect the line $y = (x - tn)\tan\theta + un$ with the ellipse $(cx)^2 + (y/c)^2 = n^2$. So, we will have to solve the following quadratic equation:

$$c^2x^2 + \frac{((x - tn)\tan\theta + un)^2}{c^2} = n^2\,, \qquad (5.6)$$

to obtain the values for x_1 and x_2. Then substitute these values in the line $\ell_q(\theta)$ to

obtain the y-coordinates, that is $y_i = (x_i - tn)\tan\theta + un$ for $i = 1, 2$.

To solve for the roots of (5.6), the equation can be rewritten as:

$$(c^4 + \tan^2\theta)x^2 + 2n(u - t\tan\theta)\tan\theta x + n^2((u - t\tan\theta)^2 - c^2) = 0 . \qquad (5.7)$$

Remark: When $c = 1$ we recover the disk case presented in equation (4.3).

Moreover, if we denote by $D = u - t\tan\theta$, then (5.7) can be simplified further to:

$$(c^4 + \tan^2\theta)x^2 + 2nD\tan\theta x + n^2(D^2 - c^2) = 0 , \qquad (5.8)$$

whose roots are given by the quadratic formula

$$x_1 = \frac{-B - \sqrt{B^2 - 4AC}}{2A} \quad \text{and} \quad x_2 = \frac{-B + \sqrt{B^2 - 4AC}}{2A} . \qquad (5.9)$$

Where

$$A = c^4 + \tan^2\theta , \qquad (5.10)$$
$$B = 2nD\tan\theta , \qquad (5.11)$$
$$C = n^2(D^2 - c^2) . \qquad (5.12)$$

Finally, after some simple algebra, the roots from (5.8) can be expressed as:

$$x_1 = \left(-\frac{D}{A}\tan\theta - \frac{c}{A}\sqrt{A - c^2 D^2}\right) n \quad \text{and} \qquad (5.13)$$
$$x_2 = \left(-\frac{D}{A}\tan\theta + \frac{c}{A}\sqrt{A - c^2 D^2}\right) n . \qquad (5.14)$$

Notice that the values for x_1 and x_2 are directly proportional to n; the same will happen to y_1 and y_2, since $y_i = (x_i - tn)\tan\theta + un$ for $i = 1, 2$. So, an equivalent approach to the above problem will be given by rescaling all the aforementioned quantities by n. That is, we will be working inside the ellipse $\hat{\boldsymbol{E}}_c = (cx)^2 + (y/c)^2 \leq 1$. So, we will be considering $\boldsymbol{q} = (t, u) \in \hat{\boldsymbol{E}}_c$ instead of $\boldsymbol{q} = (tn, un) \in \boldsymbol{E}_c$. Thus, in this rescale version we will be intersecting $\ell_q(\theta) : y = (x - t)\tan\theta + u$ with the ellipse $(cx)^2 + (y/c)^2 = 1$. From the previous exposition it is clear that the two intersection points for this problem are given by $\boldsymbol{x}_{c*} = (x_1, y_1)$ and $\boldsymbol{x}_c^* = (x_2, y_2)$, here:

$$x_1 = -\frac{D}{A}\tan\theta - \frac{c}{A}\sqrt{A - c^2 D^2} ,$$
$$y_1 = (x_1 - t)\tan\theta + u ,$$
$$x_2 = -\frac{D}{A}\tan\theta + \frac{c}{A}\sqrt{A - c^2 D^2} ,$$
$$y_2 = (x_2 - t)\tan\theta + u .$$

Where A and D are as in (5.10) and (5.8). In consequence, the asymptotic mean traffic flow through $\boldsymbol{q}$ conditioned on $\ell_q(\theta) \in \Pi$ behaves as follows

$$\frac{\mathbb{E}[T_n^q(\theta)]}{n^3} \quad \sim \quad \|\boldsymbol{x}_c^* - \boldsymbol{x}_{c*}\|_2 \|\boldsymbol{q} - \boldsymbol{x}_{c*}\|_2 \|\boldsymbol{x}_c^* - \boldsymbol{q}\|_2 \, . \qquad (5.15)$$

To program this function using R we can modify the code presented in Appendix 1, specifically the functions *Traffic* and I written in the first and second R code segments, respectively. The required changes are presented in the Appendix 2, in which we added the new parameter to be considered: c. In this code we used the value $c = 0.75$ as an specific example. However, the code can be run for any value of $c \in (0, 1]$. Notice, that the value $c = 1$ is equivalent to the original code presented in Appendix 1.

As before the function *Traffic* (from Appendix 2, first R code) represents the asymptotic mean traffic flow through $\boldsymbol{q}$ conditioned on $\ell_q(\theta) \in \Pi$. Furthermore, we can integrate the function (*Traffic*) numerically in terms of θ, from 0 to π. Additionally, since the angle $\theta \in (0, \pi]$ has a uniform distribution, we can multiply the aforementioned integral by $1/\pi$ in order to obtain the average (asymptotic mean) traffic at $\boldsymbol{q}$. This integration can be done with the second code from Appendix 2, function I, which returns the value of this integral as a function of the point $\boldsymbol{q}$, as long as the point belongs to the ellipse with eccentricity given by $\sqrt{1 - c^4}$, otherwise it just returns the value 0 (notice that in the border, i.e. $c^2 t^2 + u^2/c^2 = 1$, one of the quantities $d_c^-(\theta)$ or $d_c^+(\theta)$ will be 0, therefore the asymptotic mean traffic is also 0 for any angle θ, so its average is also 0).

Thus, with the above functions we can create a grid to obtain an approximation for the asymptotic mean traffic distribution across the Poissonian city over an ellipse $\boldsymbol{E}_c$. This can be done with the third code segment from the Appendix 2, which is basically the same as the third R code from Appendix 1, with a slight change to take into account the elliptic shape. Figure 5.7 presents a $3D$ plot regarding the (asymptotic mean) traffic across the Poissonian city. Also, the command *persp3d* in R generates an interactive 3D plot that provides a better visualization for the data.

Remark: Notice that the values for the total (asymptotic mean) traffic flow can be higher than in the disk case. Nevertheless, we are interested in the traffic density, so we need to work with proportions of traffic across the network.

Similarly to the analysis developed on section 4.1, since we want to compare proportions, we can rescale the total amount of traffic at any particular point in such a way that the maximum value will be given by 1. A simple way to achieve this is by dividing all the (asymptotic mean) traffic values by the maximum value achieved, which happens to be at the centre of the ellipse, the same way as it happened with
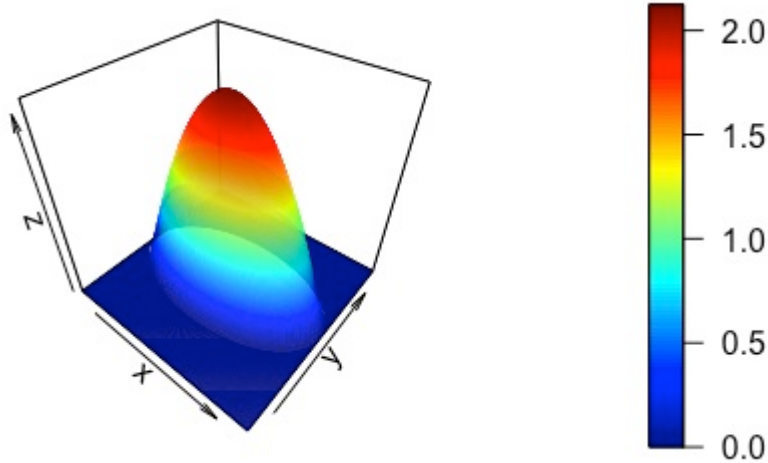
Figure 5.7: Numerical approximation for the asymptotic mean traffic across the Poissonian city in the ellipse $\boldsymbol{E}_{0.75}$. Plot obtained with the *persp3D* command in R. Here the coordinates x and y stand for the cartesian coordinates over the elliptic Poissonian city, i.e. $\boldsymbol{q} = (xn, yn)$, while z stands for the asymptotic amount of traffic flow at $\boldsymbol{q}$.

the disk, even though with a higher value. Our aim is to generate a similar plot to the Beeching plot (see figure 1.4 taken from Figure 1 of the Appendix 1 in British Railways Board [12]) for the asymptotic mean traffic density on an elliptic Poissonian city. One approach to achieve this is by computting the proportion of the network with (asymptotic mean) traffic less than a specific value L; this can be approximated by the amount of points from the grid with (asymptotic mean) traffic less or equal than $L \in [0, 1]$. Then, we need to obtain the proportions of (asymptotic mean) traffic T corresponding to these regions. This value will be given by the integration of the function I over the specified region, divided by the same integral over the whole ellipse. One way to approximate this numerically is by adding up all the values assigned to the points over this region and then divide this by the sum of the (asymptotic mean) traffic over all the points inside the ellipse.

In summary, given an specific level of traffic L, first we compute the region where the level of traffic (per mile) is less or equal than L (denoted by PA/TA in the fourth R code segment from Appendix 1). Then for that same level L we compute the proportion of total traffic T that this region represents (PT/TF using the fourth R code segment from Appendix 1). All this can be done with the fourth R code segment from Appendix 1. The final plot is shown in figure 5.8, this curve is the one to be compared with the Beeching plot.

Remark: Surprisingly, the curve shown in figure 5.8 is numerically identical to the original curve, based on the disk of radius n, see figure 4.3. The same analysis can be done in R for different values for the parameter c and we still get the same results. The next section provides an initial analytic approach to this phenomenon, although
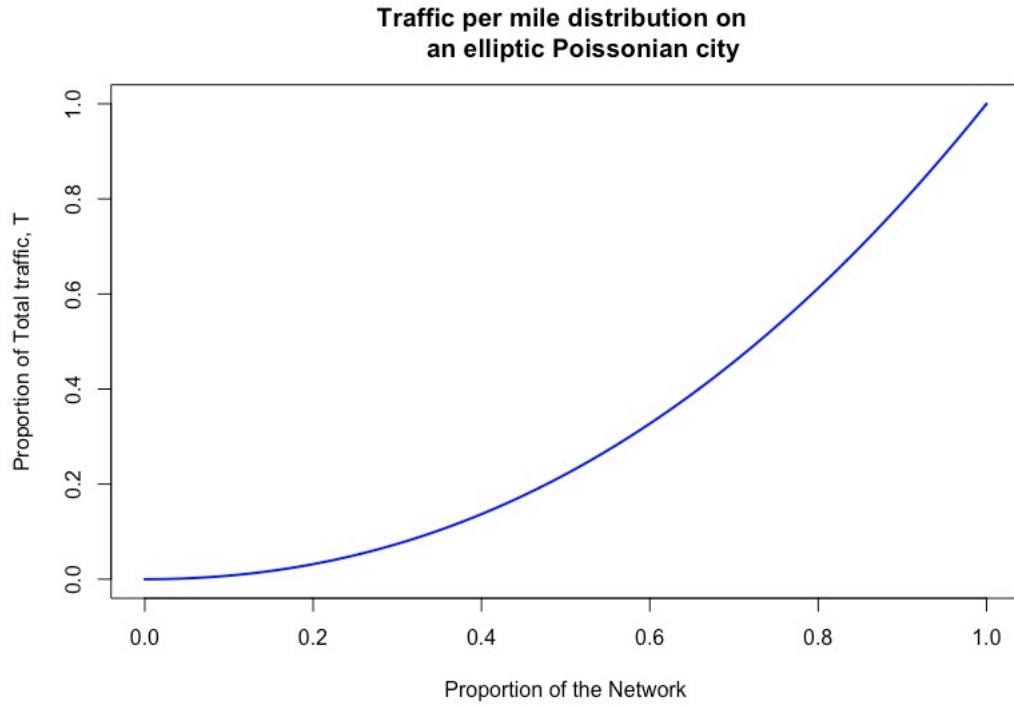
Figure 5.8: Theoretical distribution for the total asymptotic mean traffic per mile on an elliptic Poissonian city, for this plot we take $c = 0.75$.

a full explanation awaits further work.

5.4 Invariance Conjecture

From the numerics presented in the previous section it seems that the traffic density curve in the Poissonian city is invariant under changes in the eccentricity of the ellipse $\boldsymbol{E}_c$. To verify this conjecture we will provide an analytic approach for the traffic density curve sketched in the previous section. To obtain the traffic density curve sketched in figure 5.8 we will need to compute triple integrals of the following form:

$$\int_a^1 \int_0^{2\pi} \int_0^\pi \mathbb{E}[T_n^q(\theta)] \frac{1}{\pi} \, d\theta \, d\alpha \, dr \quad \rightarrow$$

$$\int_a^1 \int_0^{2\pi} \int_0^\pi \frac{\|\boldsymbol{x}_c^* - \boldsymbol{x}_{c*}\|_2 \|\boldsymbol{q} - \boldsymbol{x}_{c*}\|_2 \|\boldsymbol{x}_c^* - \boldsymbol{q}\|_2}{\pi} \, d\theta \, d\alpha \, dr \, , \quad (5.16)$$

here $a \in [0, 1]$ controls the subregion of integration (we are considering ellipse shaped rings of width $1 - a$, thus as a goes to 0 the bigger the subregion of integration becomes) for points $\boldsymbol{q} = (r(\alpha)an, \alpha) \in \boldsymbol{E}_c$ in polar coordinates. In consequence

$$r(\alpha) \;=\; \frac{c}{\sqrt{c^4 \cos^2 \alpha + \sin^2 \alpha}} \, n \, ,$$

to take into account that the elliptic shape. Recall $\boldsymbol{x}_c^*$ and $\boldsymbol{x}_{c*}$ stands for the intersection points between the ellipse $c^2 x^2 + (y^2/c^2) = n^2$ and the line $\ell_q(\theta) : y = (x - tn) \tan \theta + un$ as illustrated in figure 5.1, for the corresponding $\boldsymbol{q} = (tn, un)$ in cartesian coordinates.

From the previous section it is natural to conjecture that the mean traffic flow across the Poissonian city in an ellipse $\boldsymbol{E}_c$ behaves in such a way that its level sets (contours) are ellipses preserving the same eccentricity of $\boldsymbol{E}_c$. Notice that the rotational symmetry that existed in chapter 4 does not hold anymore, thus there is no analytic certainty regarding the level sets shape in this case. One way to analyzed the level sets numerically is by changing the fifth R code segment in Appendix 1 to take into account the elliptic shape. That is done in the fourth R code segment from Appendix 2 and the final plot is presented in figure 5.9. Recall that similar to the exposition done in chapter 4, all the R segment codes works inside the scaled ellipse given by

$$\hat{\boldsymbol{E}}_c = \left\{ (x, y) \in \mathbb{R}^2 : (cx)^2 + \left(\frac{y}{c}\right)^2 \leq 1 \right\}, \qquad \text{for some } c \in (0, 1] \, ,$$

which provides the analogous object to the unit disk used in chapter 4 (this case corresponds to the value $c = 1$).

Subject to this conjecture, to analyse how the integrated traffic changes in different subregions of the Poissonian city it is enough to concentrate on the semi-major axis, as any point inside the ellipse will have the same mean traffic flow as one of these
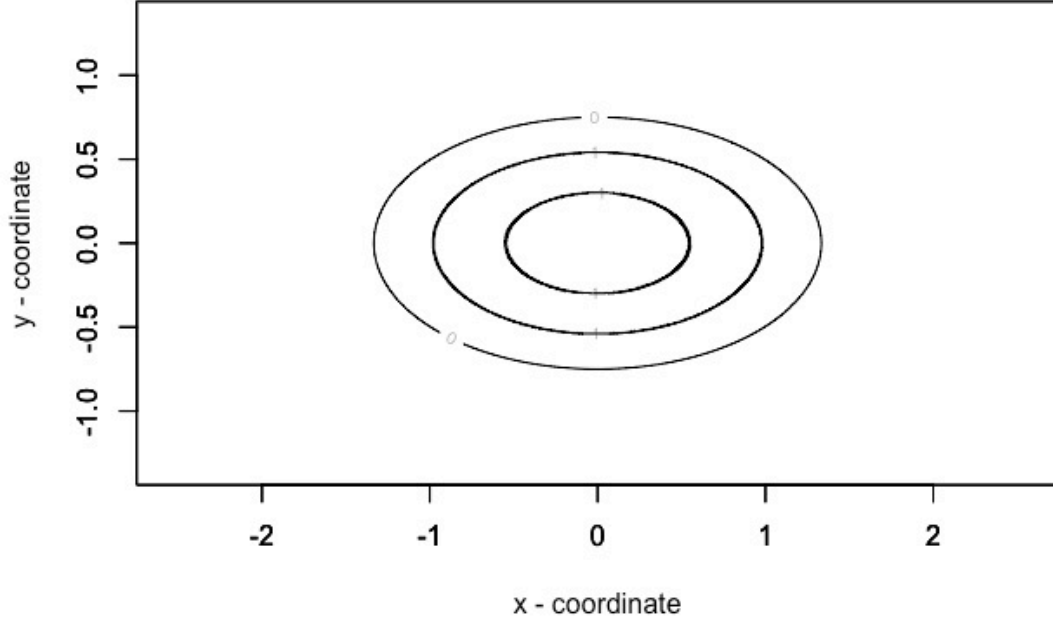
Figure 5.9: An illustration of the level sets for the asymptotic mean traffic across an elliptic Poissonian city, $c = 0.75$. Outer ellipse corresponds to $\hat{E}_c$, the middle ellipse is the level sets for mean asymptotic traffic around 40% of the traffic flow at the centre and the inner ellipse corresponds to level sets for mean asymptotic traffic around 80% the traffic flow at the centre of the elliptic city.

points on the semi-major axis. Since any point on the ellipse will correspond to a specific level set, and this level set has a unique point belonging to the semi-major axis. In other words, without loss of generality, we are selecting the points on the semi-major axis as the representatives for their corresponding level sets.

Thus suppose that $\boldsymbol{q} \in \boldsymbol{E}_c$ belongs to the semi-major axis, then $\boldsymbol{q} = (rn, 0)$ for some $r \in (0, 1/c)$. Moreover, if there is a line $\ell_q(\theta)$ passing through $\boldsymbol{q}$ and making an angle $\theta \in (0, \pi]$ with the x-axis, then the analytic expressions for $d_c^-(\theta)$ and $d_c^+(\theta)$ can be simplified. Set

$$K_c^2(\theta) \quad = \quad c^2 \cos^2 \theta + \frac{\sin^2 \theta}{c^2} \ . \tag{5.17}$$

In order to obtain the following expressions

$$\frac{d_c^-(\theta)}{n} \quad = \quad \frac{\sqrt{K_c^2(\theta) - r^2 \sin^2 \theta} - c^2 r \cos \theta}{K_c^2(\theta)} \ ,$$

$$\frac{d_c^+(\theta)}{n} \quad = \quad \frac{\sqrt{K_c^2(\theta) - r^2 \sin^2 \theta} + c^2 r \cos \theta}{K_c^2(\theta)} \ .$$

Therefore, by corollary 5.1, the average amount of traffic through $\boldsymbol{q}$ conditioning on

$\ell_q(\theta)$ will behave asymptotically, as $n \to \infty$, as follows:

$$\frac{\mathbb{E}_c[T_n^q(\ell_q(\theta))]}{n^3} \quad \sim \quad 2(1 - r^2 c^2)\frac{\sqrt{K_c^2(\theta) - r^2 \sin^2 \theta}}{(K_c^2(\theta))^2} \; .$$

here $r \in (0, 1/c)$. Even more, for a fixed point $\boldsymbol{q} = (rn, 0)$ (meaning $r \in (0, 1/c)$ is fixed) the above quantity can be averaged in terms of θ. As it has been explained on chapter 3, the distribution for the angle θ that the line $\ell_q(\theta)$ makes with the x-axis follows an uniform distribution between 0 and π. Thus as $n \to \infty$

$$\int_0^\pi \frac{\mathbb{E}_c[T_n^q(\ell_q(\theta))]}{n^3}\frac{1}{\pi}\,\mathrm{d}\theta \quad \sim \quad \frac{2(1 - r^2 c^2)}{\pi}\int_0^\pi \frac{\sqrt{K_c^2(\theta) - r^2 \sin^2 \theta}}{(K_c^2(\theta))^2}\,\mathrm{d}\theta \; . \qquad (5.18)$$

Now, we have to weight each point on the semi-major axis according to the level set it represents. In section 4.2 was clear that this weight is given by the perimeter of the corresponding circle ($2\pi nr$, $r \in [0, 1]$). Analogously, in this case the corresponding weight for the point $\boldsymbol{q} = (rn, 0)$ will be given by the perimeter of the ellipse with semi-major axis rn and semi-minor axis $c^2 rn$. Unfortunately, the circumference of an ellipse does not have a simple closed formulae. Even more, this simple task provides an insight for the second kind of elliptic integrals which we already mentioned briefly in section 4.2. For this case our ellipse is given by $c^2 x^2 + y^2/c^2 = r^2 n^2$. In parametric form, the ellipse is $x = \frac{rn}{c}\cos\alpha$, $y = rnc\sin\alpha$, and the circumference $P_c(r)$ will be given by

$$\begin{aligned}
P_c(r) &= \int_0^{2\pi} \sqrt{\frac{r^2 n^2}{c^2}\cos^2\alpha + r^2 n^2 c^2 \sin^2\alpha}\,\mathrm{d}\alpha \\
&= 4rn\int_0^{\frac{\pi}{2}} \sqrt{\frac{1}{c^2}(1 - \sin^2\alpha) + \frac{c^4}{c^2}\sin^2\alpha}\,\mathrm{d}\alpha \\
&= 4\frac{rn}{c}\int_0^{\frac{\pi}{2}} \sqrt{1 - (1 - c^4)\sin^2\alpha}\,\mathrm{d}\alpha \\
&= 4\frac{rn}{c}\int_0^{\frac{\pi}{2}} \sqrt{1 - e^2 \sin^2\alpha}\,\mathrm{d}\alpha \; , \qquad (5.19)
\end{aligned}$$

where $e = \sqrt{1 - c^4} \in [0, 1)$ is the eccentricity of the ellipse being considered.

Consequently a simplified formulae for the right hand side of (5.16) is given by:

$$H_c(a) = \int_a^{\frac{1}{c}} P_c(r)\frac{2(1 - r^2 c^2)}{\pi}\int_0^\pi \frac{\sqrt{K_c^2(\theta) - r^2 \sin^2 \theta}}{(K_c^2(\theta))^2}\,\mathrm{d}\theta\,\mathrm{d}r \; , \qquad (5.20)$$

with $a \in [0, 1/c]$. Therefore, the sketched curve in figure 5.8, that corresponds to the proportions of traffic (PT/TF_c) in terms of the proportions of the network considered

(PA/TA_c) will be given by $\varphi(\frac{PA}{TA}_c(a), \frac{PT}{TF}_c(a))$ for $a \in [0, 1/c]$, where:

$$\frac{PT}{TF}_c(a) = \frac{H_c(a)}{H_c(0)}, \tag{5.21}$$

$$\frac{PA}{TA}_c(a) = \frac{(1 - a^2c^2)n^2\pi}{n^2\pi} = 1 - a^2c^2. \tag{5.22}$$

Even more, the integral regarding θ in (5.20) is an elliptic integral [1, 45]. Thus, one way to verify the invariance conjecture, under the assumption of elliptic level sets (with the same eccentricity as the original ellipse $\boldsymbol{E}_c$), is given by considering the function $\frac{PT}{TF}_c(a)$ and analyse its partial derivative regarding c. To achieve this we first simplify the expression for $H_c(a)$, which will be the purpose of the following subsection.

5.4.1 Elliptic Integrals

First, as explained above, the expression for (5.19) corresponds to the second canonical form of an elliptic integral. Now, (5.18) can be expressed as a linear combination of the three canonical forms of elliptic integrals. But, first we can decomposed (5.18) in terms of the range for θ as follows

$$\int_0^\pi \frac{\sqrt{K_c^2(\theta) - r^2\sin^2\theta}}{(K_c^2(\theta))^2} \, d\theta =$$
$$\int_0^{\pi/2} \frac{\sqrt{K_c^2(\theta) - r^2\sin^2\theta}}{(K_c^2(\theta))^2} \, d\theta + \int_{\pi/2}^\pi \frac{\sqrt{K_c^2(\theta) - r^2\sin^2\theta}}{(K_c^2(\theta))^2} \, d\theta.$$

Then, consider the substitution $\psi = \pi - \theta$ on the integral were θ range from $\pi/2$ to π to obtain

$$\int_{\pi/2}^\pi \frac{\sqrt{K_c^2(\theta) - r^2\sin^2\theta}}{(K_c^2(\theta))^2} \, d\theta = \int_0^{\pi/2} \frac{\sqrt{K_c^2(\psi) - r^2\sin^2\psi}}{(K_c^2(\psi))^2} \, d\psi,$$

since $\cos(\pi - \psi) = -\cos(\psi)$ and $\sin(\pi - \psi) = \sin(\psi)$. Thus

$$\int_0^\pi \frac{\sqrt{K_c^2(\theta) - r^2\sin^2\theta}}{(K_c^2(\theta))^2} \, d\theta = 2\int_0^{\pi/2} \frac{\sqrt{K_c^2(\theta) - r^2\sin^2\theta}}{(K_c^2(\theta))^2} \, d\theta. \tag{5.23}$$

Now, the right hand side integral in (5.23) can be rewritten as a general elliptic integral. By this we are saying that the function to be integrated can be expressed as a rational algebraic function $R(x, \sqrt{Q(x)})$ where $Q(x)$ is a cubic or quartic polynomial in x with no repeated factors. Therefore, our purpose is to express

$$\int \frac{\sqrt{K_c^2(\theta) - r^2\sin^2\theta}}{(K_c^2(\theta))^2} \, d\theta \quad \text{as} \quad \int R(x, \sqrt{Q(x)}) \, dx,$$

for some rational algebraic function $R(x, \sqrt{Q(x)})$ with the aforementioned characteristics. Then the theory of elliptic integrals can be applied to the function

$R(x, \sqrt{Q(x)})$ in order to express the integral as a linear combination of the three canonical forms of elliptic integrals [20]:

$$\text{The first kind} \quad \int [(A_1 t^2 + B_1)(A_2 t^2 + B_2)]^{-1/2} \, dt , \tag{5.24}$$

$$\text{The second kind} \quad \int t^2 [(A_1 t^2 + B_1)(A_2 t^2 + B_2)]^{-1/2} \, dt , \tag{5.25}$$

$$\text{The third kind} \quad \int (1 + N t^2)^{-1}[(A_1 t^2 + B_1)(A_2 t^2 + B_2)]^{-1/2} \, dt . \tag{5.26}$$

To achieve this goal consider the change of variable given by $x = \tan(\theta/2)$ (notice this implies that $\cos(\theta/2) = 1/\sqrt{1+x^2}$ and $\sin(\theta/2) = x/\sqrt{1+x^2}$), therefore $dx = \sec^2(\theta/2)/2 \, d\theta$, so $d\theta = 2\cos^2(\theta/2) \, dx = 2/(1+x^2) \, dx$. Also recall the trigonometric identities $\sin\theta = 2\sin(\theta/2)\cos(\theta/2) = 2x/(1+x^2)$ and $\cos\theta = \cos^2(\theta/2) - \sin^2(\theta/2) = (1-x^2)/(1+x^2)$. All this and some algebraic simplifications leads to

$$\int_0^{\pi/2} \frac{\sqrt{K_c^2(\theta) - r^2 \sin^2\theta}}{(K_c^2(\theta))^2} \, d\theta \quad =$$

$$2 \int_0^1 \frac{(1 + x^2)^2 \left[c^2(1 - 2x^2 + x^4) + 4x^2 \left(\frac{1}{c^2} - r^2 \right) \right]^{1/2}}{\left(c^2(1 - x^2)^2 + \frac{4x^2}{c^2} \right)^2} \, dx ,$$

Additionally, if we denote $x^4 + 2(\frac{2}{c^4} - \frac{2r^2}{c^2} - 1)x^2 + 1$ by $Q(x)$ and multiply both numerator and denominator of the integrand function by $\sqrt{Q(x)}$ the right hand side expression can be rewritten as,

$$\frac{2}{c^3} \int_0^1 \frac{(1 + x^2)^2 Q(x)}{\left(x^4 + 2\left(\frac{2}{c^4} - 1\right) x^2 + 1 \right)^2 [Q(x)]^{1/2}} \, dx . \tag{5.27}$$

Notice, that this expression can be simplified using some auxiliary variables, say:

$$b = \frac{2}{c^4} - \frac{2r^2}{c^2} - 1 \quad \text{and} \quad \tilde{b} = \frac{2}{c^4} - 1 .$$

Thus, one can rewrites $Q(x)$ as $(x^2 + \hat{y}_-)(x^2 + \hat{y}_+)$, where

$$\hat{y}_- = b - \sqrt{b^2 - 1}, \quad \text{and} \quad \hat{y}_+ = b + \sqrt{b^2 - 1} .$$

Similarly, $x^4 + 2\left(\frac{2}{c^4} - 1\right) x^2 + 1$ can be rewritten as $(x^2 + \hat{z}_-)(x^2 + \hat{z}_+)$, with

$$\hat{z}_- = \tilde{b} - \sqrt{\tilde{b}^2 - 1}, \quad \text{and} \quad \hat{z}_+ = \tilde{b} + \sqrt{\tilde{b}^2 - 1} .$$

Therefore, (5.27) is equivalent to

$$\frac{2}{c^3} \int_0^1 \frac{(1 + x^2)^2 (x^2 + \hat{y}_-)(x^2 + \hat{y}_+)}{(x^2 + \hat{z}_-)^2 (x^2 + \hat{z}_+)^2 [(x^2 + \hat{y}_-)(x^2 + \hat{y}_+)]^{1/2}} \, dx . \tag{5.28}$$

Notice that ultimately we should be writing $\hat{y}_-(r, c), \hat{y}_+(r, c), \hat{z}_-(c), \hat{z}_+(c)$ to empha-size the dependance on the values of r and c. However to simplify the notation we simply write $\hat{y}_-, \hat{y}_+, \hat{z}_-, \hat{z}_+$, respectively.

The rest of this section analyses the integral in (5.28) by using the elliptic integral reduction procedure as explained in Whittaker and Watson [45]. The first step is to apply partial fractions to the ratio of polynomials that we get on (5.28), yielding

$$
\int_0^1 \frac{(1 + x^2)^2(x^2 + \hat{y}_-)(x^2 + \hat{y}_+)}{(x^2 + \hat{z}_-)^2(x^2 + \hat{z}_+)^2[(x^2 + \hat{y}_-)(x^2 + \hat{y}_+)]^{1/2}}\, dx \quad =
$$
$$
D_0 \int_0^1 \frac{1}{[(x^2 + \hat{y}_-)(x^2 + \hat{y}_+)]^{1/2}}\, dx + D_1 \int_0^1 \frac{1}{(x^2 + \hat{z}_-)[(x^2 + \hat{y}_-)(x^2 + \hat{y}_+)]^{1/2}}
$$
$$
+ D_2 \int_0^1 \frac{1}{(x^2 + \hat{z}_+)[(x^2 + \hat{y}_-)(x^2 + \hat{y}_+)]^{1/2}}
$$
$$
+ D_3 \int_0^1 \frac{1}{(x^2 + \hat{z}_-)^2[(x^2 + \hat{y}_-)(x^2 + \hat{y}_+)]^{1/2}}
$$
$$
+ D_4 \int_0^1 \frac{1}{(x^2 + \hat{z}_+)^2[(x^2 + \hat{y}_-)(x^2 + \hat{y}_+)]^{1/2}} \, . \quad (5.29)
$$

Here, the constant coefficients (regarding the integration variable x) $D_0, \ldots, D_4$ can be expressed in terms of $\hat{y}_-, \hat{y}_+, \hat{z}_-, \hat{z}_+$, which ultimately depend on the values of r and c as mentioned before. The values for $D_0, \ldots, D_4$ can be determined with the use of mathematical/symbolic software like Mathematica or Maple. Notice that in (5.29) the integrals corresponding to the coefficients D_0, D_1 and D_2 are already in a canonical form. D_0 corresponds to an elliptic integral of the first kind, while D_1 and D_2 corresponds to elliptic integrals of the third kind. Thus we only require an expression for the last two integrals in (5.29), i.e. the integrals with coefficients D_3 and D_4.

Due to the symmetry on these two integrals regarding the variables $\hat{z}_-$ and $\hat{z}_+$ it is enough to only analyse one of them as the other will have an equivalent expression just substituting $\hat{z}_-$ with $\hat{z}_+$ accordingly. Thus from here on we will focus our attention on the integral

$$
\int_0^1 \frac{1}{(x^2 + \hat{z}_-)^2[(x^2 + \hat{y}_-)(x^2 + \hat{y}_+)]^{1/2}} \, . \quad (5.30)
$$

As before, denote $(x^2 + \hat{y}_-)(x^2 + \hat{y}_+)$ by $Q(x)$, and consider the function

$$
g_-(x) = \frac{x\sqrt{Q(x)}}{(x^2 + \hat{z}_-)} \, ,
$$

Differentiating $g_-(x)$ one obtains the following relation

$$
g_-'(x) = \frac{\sqrt{Q(x)}}{(x^2 + \hat{z}_-)} - \frac{2x^2\sqrt{Q(x)}}{(x^2 + \hat{z}_-)} + \frac{1}{2}\frac{xQ'(x)}{(x^2 + \hat{z}_-)\sqrt{Q(x)}} \, . \quad (5.31)
$$

96

Moreover (5.31) can be rewritten in such a way that the denominator of every term contains $\sqrt{Q(x)}$, i.e.

$$g_{-}^{'}(x) = \frac{Q(x)}{(x^2 + \hat{z}_{-})\sqrt{Q(x)}} - \frac{2x^2 Q(x)}{(x^2 + \hat{z}_{-})\sqrt{Q(x)}} + \frac{1}{2} \frac{xQ^{'}(x)}{(x^2 + \hat{z}_{-})\sqrt{Q(x)}} \ . \qquad (5.32)$$

Finally, divide $x^2 Q(x)$ by $(x^2 + \hat{z}_{-})^2$ as the first one has order 6 and the latter one has order 4. The division leads to

$$\frac{x^2 Q(x)}{(x^2 + \hat{z}_{-})} = x^2 + (\hat{y}_{-} + \hat{y}_{+} - 2\hat{z}_{-}) + \frac{(\hat{y}_{-}\hat{y} - 2\hat{y}_{-}\hat{z}_{-} - 2\hat{y}_{+}\hat{z}_{-} + 3\hat{z}_{-}^2)}{(x^2 + \hat{z}_{-})}$$
$$+ \frac{(-\hat{y}_{-}\hat{y}\hat{z}_{-} + \hat{y}_{-}\hat{z}_{-}^2 + \hat{y}_{+}\hat{z}_{-}^2 - \hat{z}_{-}^3)}{(x^2 + \hat{z}_{-})^2} \ . \qquad (5.33)$$

Again, we can simplify the notation with the following conventions:

$$K_1(\hat{z}_{-}) = K_1(\hat{y}_{-}, \hat{y}_{+}, \hat{z}_{-}) = \hat{y}_{-} + \hat{y}_{+} - 2\hat{z}_{-} \ , \qquad (5.34)$$
$$K_2(\hat{z}_{-}) = K_2(\hat{y}_{-}, \hat{y}_{+}, \hat{z}_{-}) = \hat{y}_{-}\hat{y}_{+} - 2\hat{y}_{-}\hat{z}_{-} - 2\hat{y}_{+}\hat{z}_{-} + 3\hat{z}_{-}^2 \ , \qquad (5.35)$$
$$K_3(\hat{z}_{-}) = K_3(\hat{y}_{-}, \hat{y}_{+}, \hat{z}_{-}) = -\hat{y}_{-}\hat{y}_{+}\hat{z}_{-} + \hat{y}_{-}\hat{z}_{-}^2 + \hat{y}_{+}\hat{z}_{-}^2 - \hat{z}_{-}^3 \ . \qquad (5.36)$$

In conclusion, after integrating (5.32) from 0 to 1 and substituting (5.33) accordingly we get the following identity

$$\frac{\sqrt{Q(1)}}{1 + \hat{z}_{-}} = \int_0^1 \frac{Q(x)}{(x^2 + \hat{z}_{-})\sqrt{Q(x)}} \, \mathrm{d}x + \frac{1}{2} \int_0^1 \frac{xQ^{'}(x)}{(x^2 + \hat{z}_{-})\sqrt{Q(x)}} \, \mathrm{d}x$$
$$- 2 \left(\int_0^1 \frac{x^2}{\sqrt{Q(x)}} \, \mathrm{d}x + K_1(\hat{z}_{-}) \int_0^1 \frac{1}{\sqrt{Q(x)}} \, \mathrm{d}x + K_2(\hat{z}_{-}) \int_0^1 \frac{1}{(x^2 + \hat{z}_{-})\sqrt{Q(x)}} \, \mathrm{d}x \right.$$
$$\left. + K_3(\hat{z}_{-}) \int_0^1 \frac{1}{(x^2 + \hat{z}_{-})^2 \sqrt{Q(x)}} \, \mathrm{d}x \right) \ . \qquad (5.37)$$

From here, we can solve for the desired integral (5.30). Recall that $Q(x) = (x^2 + \hat{y}_{-})(x^2 + \hat{y}_{+}) = x^4 + (\hat{y}_{-} + \hat{y}_{+})x^2 + \hat{y}_{-}\hat{y}_{+}$, consequently $xQ^{'}(x) = 4x^4 + 2(\hat{y}_{-} + \hat{y}_{+})x^2$. Thus, we obtain the following expression for (5.30):

$$\int_0^1 \frac{1}{(x^2 + \hat{z}_{-})^2 [(x^2 + \hat{y}_{-})(x^2 + \hat{y}_{+})]^{1/2}} = \frac{1}{K_3(\hat{z}_{-})} \left(-\frac{1}{2} \left(\frac{Q(1)}{1 + \hat{z}_{-}} \right. \right.$$
$$- 3 \int_0^1 \frac{x^4}{(x^2 + \hat{z}_{-})\sqrt{Q(x)}} \, \mathrm{d}x - 2(\hat{y}_{-} + \hat{y}_{+}) \int_0^1 \frac{x^2}{(x^2 + \hat{z}_{-})\sqrt{Q(x)}} \, \mathrm{d}x$$
$$\left. - (\hat{y}_{-}\hat{y}_{+} - 2K_2(\hat{z}_{-})) \int_0^1 \frac{1}{(x^2 + \hat{z}_{-})\sqrt{Q(x)}} \, \mathrm{d}x \right)$$
$$\left. - K_1(\hat{z}_{-}) \int_0^1 \frac{1}{\sqrt{Q(x)}} \, \mathrm{d}x - \int_0^1 \frac{x^2}{\sqrt{Q(x)}} \, \mathrm{d}x \right) \ . \qquad (5.38)$$

Therefore, all the integrals from the right hand side of (5.38) can be related with an integral of the following form

$$\int_0^1 \frac{x^{2m}}{(x^2 + \hat{z}_-)^n \sqrt{Q(x)}} \, dx \qquad \text{for} \quad m = 0, 1, 2 \quad \text{and} \quad n = 0, 1 \, . \qquad (5.39)$$

So, as long as we can obtain expressions for all the combinations of m and n in (5.39) in terms of the canonical elliptic integrals we will be done.

First, notice the trivial cases for (5.39):

- $m = 0$ and $n = 0$ in (5.39) represents an elliptic integral of the first kind.

- $m = 0$ and $n = 1$ in (5.39) represents an elliptic integral of the third kind.

- $m = 1$ and $n = 0$ in (5.39) represents an elliptic integral of the second kind.

Remark: Some literature provides a different expression for an elliptic integral of the second kind, say something of the form

$$\int_0^1 \frac{(x^2 + \hat{y}_-)^{1/2}}{(x^2 + \hat{y}_+)^{1/2}} \, dx \, . \qquad (5.40)$$

However, one should notices that:

$$\int_0^1 \frac{x^2}{\sqrt{Q(x)}} \, dx = \int_0^1 \frac{x^2}{\sqrt{(x^2 + \hat{y}_-)(x^2 + \hat{y}_+)}} \, dx$$

$$= \int_0^1 \frac{x^2 + \hat{y}_-}{\sqrt{(x^2 + \hat{y}_-)(x^2 + \hat{y}_+)}} \, dx - \int_0^1 \frac{\hat{y}_-}{\sqrt{(x^2 + \hat{y}_-)(x^2 + \hat{y}_+)}} \, dx \, , \quad (5.41)$$

where, clearly

$$\int_0^1 \frac{x^2 + \hat{y}_-}{\sqrt{(x^2 + \hat{y}_-)(x^2 + \hat{y}_+)}} \, dx = \int_0^1 \frac{(x^2 + \hat{y}_-)^{1/2}}{(x^2 + \hat{y}_+)^{1/2}} \, dx \, ,$$

and the last term in (5.41) is just a multiple of an elliptic integral of the first kind.

For the last two cases in (5.39), observe the following:

- $m = 1$ and $n = 1$.

$$\int_0^1 \frac{x^2}{(x^2 + \hat{z}_-)\sqrt{Q(x)}} \, dx = \int_0^1 \frac{x^2 + \hat{z}_-}{(x^2 + \hat{z}_-)\sqrt{Q(x)}} \, dx - \hat{z}_- \int_0^1 \frac{1}{(x^2 + \hat{z}_-)\sqrt{Q(x)}} \, dx$$

$$= \int_0^1 \frac{1}{\sqrt{Q(x)}} \, dx - \hat{z}_- \int_0^1 \frac{1}{(x^2 + \hat{z}_-)\sqrt{Q(x)}} \, dx \, ,$$

that is a linear combination of an elliptic integral of the first kind and an elliptic integral of the third kind, respectively.

- $m = 2$ and $n = 1$.

$$\int_0^1 \frac{x^4}{(x^2+\hat{z}_-)\sqrt{Q(x)}}\,\mathrm{d}x = \int_0^1 \frac{x^4-\hat{z}_-^2}{(x^2+\hat{z}_-)\sqrt{Q(x)}}\,\mathrm{d}x + \hat{z}_-^2\int_0^1 \frac{1}{(x^2+\hat{z}_-)\sqrt{Q(x)}}\,\mathrm{d}x$$

$$= \int_0^1 \frac{(x^2-\hat{z}_-)(x^2+\hat{z}_-)}{(x^2+\hat{z}_-)\sqrt{Q(x)}}\,\mathrm{d}x + \hat{z}_-^2\int_0^1 \frac{1}{(x^2+\hat{z}_-)\sqrt{Q(x)}}\,\mathrm{d}x$$

$$= \int_0^1 \frac{x^2}{\sqrt{Q(x)}}\,\mathrm{d}x - \hat{z}_-\int_0^1 \frac{1}{\sqrt{Q(x)}}\,\mathrm{d}x + \hat{z}_-^2\int_0^1 \frac{1}{(x^2+\hat{z}_-)\sqrt{Q(x)}}\,\mathrm{d}x\,,$$

that is a linear combination of an elliptic integral of the second kind, an elliptic integral of the first kind and an elliptic integral of the third kind, respectively.

Thus, making the appropriate substitutions in (5.38) we find out a way to express the integral (5.30) as a linear combination from the three canonical elliptic integrals. To achieve this we have to recall the symmetry in the last two integrals in (5.29), so the integral corresponding to the coefficient D_4 will have a similar expression to (5.38) substituting $\hat{z}_-$ by $\hat{z}_+$. Recall that the coefficients in (5.38) are given by (5.34), (5.35) and (5.36) which depends on the value of $\hat{z}_-$. In consequence, a similar definitions will hold for $K_1(\hat{z_+})$, $K_2(\hat{z_+})$ and $K_3(\hat{z_+})$, say

$$K_1(\hat{z}_+) = K_1(\hat{y}_-,\hat{y}_+,\hat{z}_+) = \hat{y}_- + \hat{y}_+ - 2\hat{z}_+\,, \tag{5.42}$$

$$K_2(\hat{z}_+) = K_2(\hat{y}_-,\hat{y}_+,\hat{z}_+) = \hat{y}_-\hat{y}_+ - 2\hat{y}_-\hat{z}_+ - 2\hat{y}_+\hat{z}_+ + 3\hat{z}_+^2\,, \tag{5.43}$$

$$K_3(\hat{z}_+) = K_3(\hat{y}_-,\hat{y}_+,\hat{z}_+) = -\hat{y}_-\hat{y}_+\hat{z}_+ + \hat{y}_-\hat{z}_+^2 + \hat{y}_+\hat{z}_+^2 - \hat{z}_+^3\,. \tag{5.44}$$

Therefore, replacing in (5.29) the two integrals that are in the from of (5.30) we find out an expression for (5.28) as a linear combination of the three canonical elliptic integrals. This can be done with a simplified notations as follows

$$\frac{2}{c^3}\int_0^1 \frac{(1+x^2)^2(x^2+\hat{y}_-)(x^2+\hat{y}_+)}{(x^2+\hat{z}_-)^2(x^2+\hat{z}_+)^2[(x^2+\hat{y}_-)(x^2+\hat{y}_+)]^{1/2}}\,\mathrm{d}x =$$
$$M_0 + \frac{2}{c^3}\Big(M_1 I_1 + M_2 I_2 + M_3 I_3(\hat{z}_-) + M_4 I_3(\hat{z}_+)\Big)\,, \tag{5.45}$$

where the elliptic integrals are denoted as folllows:

- I_1 stands for the first kind of elliptic integral, say

$$I_1 = \int_0^1 \frac{1}{\sqrt{Q(x)}}\,\mathrm{d}x\,.$$

- I_2 stands for the second kind of elliptic integral, say

$$I_2 = \int_0^1 \frac{(x^2+\hat{y}_-)^{1/2}}{(x^2+\hat{y}_+)^{1/2}}\,\mathrm{d}x\,.$$

- $I_3(\hat{z}_-)$ stands for the third kind of elliptic integral, say

$$I_3(\hat{z}_-) = \int_0^1 \frac{1}{(x^2 + \hat{z}_-)\sqrt{Q(x)}}\, \mathrm{d}x .$$

- $I_3(\hat{z}_+)$ stands for the third kind of elliptic integral, say

$$I_3(\hat{z}_+) = \int_0^1 \frac{1}{(x^2 + \hat{z}_+)\sqrt{Q(x)}}\, \mathrm{d}x .$$

On the other hand, the corresponding coefficients $M_0, \ldots, M_4$ can be expressed in terms of $\hat{y}_-, \hat{y}_+, \hat{z}_-, \hat{z}_+$ as follows:

$$
\begin{aligned}
M_0 &= -\frac{2}{c^3}\left(\frac{D_3}{K_3(\hat{z}_-)}\frac{\sqrt{Q(1)}}{2(\hat{z}_- + 1)} + \frac{D_4}{K_3(\hat{z}_+)}\frac{\sqrt{Q(1)}}{2(\hat{z}_+ + 1)} \right) , \\
M_1 &= 1 + \frac{D_3}{K_3(\hat{z}_-)}\left(\hat{y}_+ + \frac{1}{2}\hat{y}_- - \frac{3}{2}\hat{z}_- - K_1(\hat{z}_-) \right) \\
&\quad + \frac{D_4}{K_3(\hat{z}_+)}\left(\hat{y}_+ + \frac{1}{2}\hat{y}_- - \frac{3}{2}\hat{z}_+ - K_1(\hat{z}_+) \right) , \\
M_2 &= \frac{D_3}{2K_3(\hat{z}_-)} + \frac{D_4}{2K_3(\hat{z}_+)} , \\
M_3 &= D_1 + \frac{D_3}{K_3(\hat{z}_-)}\left(\frac{3}{2}\hat{z}_-^2 - (\hat{y}_- + \hat{y}_+)\hat{z}_- - (\hat{y}_-\hat{y}_+ - 2K_2(\hat{z}_-)) \right) , \\
M_4 &= D_2 + \frac{D_4}{K_3(\hat{z}_+)}\left(\frac{3}{2}\hat{z}_+^2 - (\hat{y}_- + \hat{y}_+)\hat{z}_+ - (\hat{y}_-\hat{y}_+ - 2K_2(\hat{z}_+)) \right) .
\end{aligned}
$$

A final step to prove the invariance conjecture for the traffic density curve will be to obtain the values for $D_0, \ldots, D_4$ in terms of $\hat{y}_-, \hat{y}_+, \hat{z}_-, \hat{z}_+$. Then substitute these in $M_0, \ldots, M_4$ and finally recall the formulae for $\hat{y}_-, \hat{y}_+, \hat{z}_-, \hat{z}_+$ in terms of r and c as given before (5.28). Finally (5.45) needs to be replace in the expression for $H_c(a)$ as given by (5.20). This will be left for a future research, as it is still an extensive algebraic work.

Chapter 6

Final Remarks and other possible generalizations

In this chapter we briefly explain alternative approaches to generalize the Poissonian city model (different from the one where we have considered the Poisson line process taking place over an ellipse, changing the eccentricity of the ellipse $\boldsymbol{E}_c$ in question).

This chapter mainly focusses on the properties of Poisson segment processes. Thus, the first section addresses how to define these and get an equivalent expression for the length intensity of Poisson line processes. However, this new framework brings new open problems, mainly the percolation of paths and the absence of a convex hull to generate a lower bound for the excess length resulting from considering the semi-perimeter routing rule instead of the corresponding Euclidean distance. These problems are introduced and explained in the second section. Here we briefly discuss related work and literature that can provide an insight to solve them. For example, Baccelli et al. [7] studies the behaviour for a path of segments on the Delaunay graph [43], in particular they show that the path in question is Markovian and gave an asymptotic result regarding the excess distance of this path against the corresponding Euclidean distance. Finally, the third section provides some final remarks, briefly explains another possible directions for the Poissonian city and areas for future research.

6.1   Segment line process

Consider a stationary Poisson segment line process with fixed length h. Here we address the following problem: what intensity, ν_λ^h (for the marked point process of intensity λ defining the segments) leads to a length intensity equivalent to the unit intensity for a Poisson line process?

We denote by Ξ_h the segment line process with fixed length h and intensity λ with rose of directions given by ρ (we measure the angles from the horizontal axis in the

anti-clockwise direction). We seek an expression for its *length intensity*, given by

$$\nu_\lambda^h \;\;=\;\; \frac{\mathbb{E}[L(\Xi_h \cap K)]}{A(K)} \;\;=\;\; \frac{\mathbb{E}[\text{Leb}_1([K])]}{\text{Leb}_2(K)}\;, \tag{6.1}$$

for any compact convex set $K \subseteq \mathbb{R}^2$. Here $[K]$ stands for the hitting set, which is defined as the set of segments of Ξ that hit K, i.e. $[K] = \{\xi \in \Xi_h : \xi \Uparrow K\}$, where we denoted by $\xi \Uparrow K$ the event "ξ hits K", meaning $\xi \cap K \neq \emptyset$.

We can identify the segment process Ξ_h with a marked point process Φ^* in $\mathbb{R}^2 \times (0, \pi]$. Here each point $\boldsymbol{x}$ of the process represents the lower-end point of the segment ξ (in case of horizontal segments we chose the left-end point). Thus $\boldsymbol{x} = (x^*, y^*)$ where:

$$y^* \;\;=\;\; \inf\{y : (x, y) \in \xi \text{ for some } x\},$$
$$x^* \;\;=\;\; \inf\{x : (x, y^*) \in \xi\}.$$

We can construct the Poisson segment process by requiring that the points (x^*, y^*) form a Poisson point process of intensity λ. Also the angular marks θ should be independent of the positions $\boldsymbol{x}$ and independent of each other with identical distribution given by $\rho(\,\mathrm{d}\theta\,)$. Viewed as a point process in (x^*, y^*, θ) space, the intensity mean of this point process is given by $\lambda(\text{Leb}_2 \otimes \rho)$.

To address this question we focus in the case where the angular mark distribution for θ is nonrandom. This can be done by considering the following rotation

$$R(\xi) = R_\theta(x, y) = (x \cos\theta + y \sin\theta, -x \sin\theta + y \cos\theta, 0) = (\tilde{x}, \tilde{y}, 0)\,,$$

for each segment $\xi = (x, y, \theta)$. The rotated segments will all be horizontal. The rotation $R_\theta(x, y)$ moves the segment ξ in such a way that its reference point, $\boldsymbol{x}$, is still at the same distance, $\|\boldsymbol{x}\|$, from the origin but it has been rotated θ radians in clockwise direction so that the segment is now horizontal, see figure 6.1. This converts Ξ_h into a new segment process $R(\Xi_h)$ for which all segments are horizontal, but such that the length of intersection with any disk centered at the origin is unchanged.

In particular the new point process is still Poisson.

THEOREM 6.1. *If Φ^* is a marked Poisson point process in $\mathbb{R}^2 \times (0, \pi]$, with intensity λ and rose of directions ρ then $\tilde{\Phi} = \{(\tilde{x}, \tilde{y}) : (\tilde{x}, \tilde{y}, 0) = R_\theta(x, y) \text{ with } (x, y, \theta) \in \Phi^*\}$ is a Poisson point process of intensity λ.*

Proof. From Renyi's Theorem [29] we know that the family of avoidance probabilities determines the distribution of a point process. So it is enough to show that:

$$\mathbb{P}[\tilde{\Phi} \cap \tilde{E} = 0] \;\;=\;\; \exp\left(-\lambda \,\text{Leb}_2(\tilde{E})\right),$$
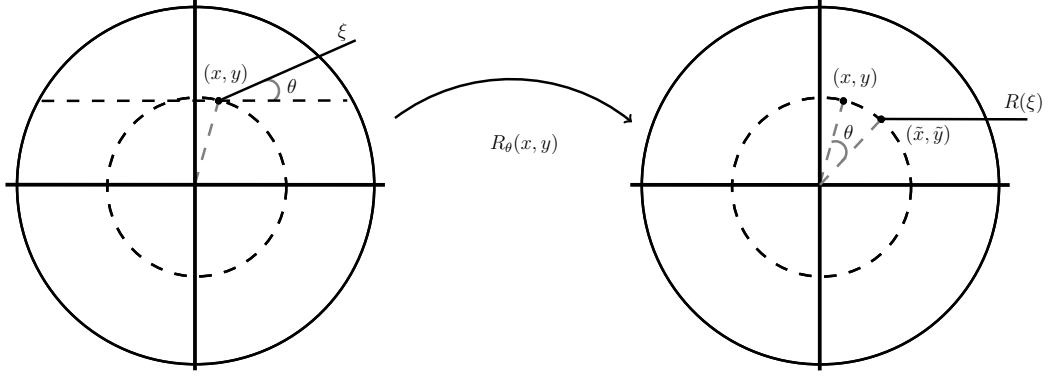
Figure 6.1: Illustration of the rotation $R_\theta(x, y)$.

for all measurable $\tilde{E} \subseteq \mathbb{R}^2$.

For $\tilde{E}$ any measurable subset in $\mathbb{R}^2$, we define $E \subseteq \mathbb{R}^2 \times (0, \pi]$ as follows:

$$E \quad = \quad \left\{ (x, y, \theta) : (x \cos\theta + y \sin\theta, -x \sin\theta + y \cos\theta) \in \tilde{E} \right\} .$$

Therefore $\{\tilde{\Phi} \cap \tilde{E} = 0\} = \{\Phi^* \cap E = 0\}$. By the rotation invariance of the Leb_2 measure and the fact that ρ is a probability measure we can compute the intensity measure for $\tilde{\Phi}$:

$$\lambda (\mathrm{Leb}_2 \otimes \rho)(E) \;=\; \lambda \int_0^\pi \left(\iint_{\mathbb{R}^2} \mathbb{1}_E(x, y, \theta) \, \mathrm{Leb}_2(\, \mathrm{d}x \, \mathrm{d}y\,) \right) \rho(\, \mathrm{d}\theta\,)$$

$$=\; \lambda \int_0^\pi \left(\iint_{\mathbb{R}^2} \mathbb{1}_{\tilde{E}}(R_\theta(x, y)) \, \mathrm{Leb}_2(\, \mathrm{d}x \, \mathrm{d}y\,) \right) \rho(\, \mathrm{d}\theta\,)$$

$$=\; \lambda \int_0^\pi \left(\iint_{\mathbb{R}^2} \mathbb{1}_{\tilde{E}}(\tilde{x}, \tilde{y}) \, \mathrm{Leb}_2(\, \mathrm{d}\tilde{x} \, \mathrm{d}\tilde{y}\,) \right) \rho(\, \mathrm{d}\theta\,) \;=\; \lambda \iint_{\mathbb{R}^2} \mathbb{1}_{\tilde{E}}(\tilde{x}, \tilde{y}) \, \mathrm{Leb}_2(\, \mathrm{d}\tilde{x} \, \mathrm{d}\tilde{y}\,)$$

$$=\quad \lambda \, \mathrm{Leb}_2(\tilde{E}) .$$

Hence,

$$\mathbb{P}[\tilde{\Phi} \cap \tilde{E} = 0] = \mathbb{P}[\Phi^* \cap E = 0] = \exp\left(-\lambda (\mathrm{Leb}_2 \otimes \rho)(E)\right) = \exp\left(-\lambda \, \mathrm{Leb}_2(\tilde{E})\right)$$

as required. $\qquad\square$

Now we relate the length intensity at (6.1) to the lengths of the segments h. Due to Theorem 6.1 we only need to consider the case where all segments are horizontal, because if K is a disk centered at the origin we know that $\mathbb{E}[L(\Xi_h \cap K)] = \mathbb{E}[L(R(\Xi_h) \cap K)]$. Hence, as $R(\Xi_h)$ can be represented by $\Phi \oplus [0, h]$, where Φ is a planar Poisson point process of intensity λ. In consequence (6.1) becomes

$$\nu_\lambda^h \quad = \quad \frac{\mathbb{E}[\mathrm{Leb}_1([K])]}{\mathrm{Leb}_2(K)} \quad = \quad \frac{\mathbb{E}[\mathrm{Leb}_1\left((\Phi \oplus [0, h]) \cap K\right)]}{\mathrm{Leb}_2(K)} .$$

However, if $h_1 \in (0, h)$, it is clear that we can express $\Phi \oplus [0, h]$ as the following disjoint union $(\Phi \oplus [0, h_1]) \cup (\Phi \oplus [h_1, h])$. So ν_λ^h is linear in h

$$
\begin{aligned}
\nu_\lambda^h &= \frac{\mathbb{E}[\mathrm{Leb}_1\left((\Phi \oplus [0, h]) \cap K\right)]}{\mathrm{Leb}_2(K)} \\
&= \frac{\mathbb{E}[\mathrm{Leb}_1\left((\Phi \oplus [0, h_1]) \cap K\right)]}{\mathrm{Leb}_2(K)} + \frac{\mathbb{E}[\mathrm{Leb}_1\left((\Phi \oplus [h_1, h]) \cap K\right)]}{\mathrm{Leb}_2(K)} \\
&= \nu_\lambda^{h_1}(K) + \frac{\mathbb{E}[\mathrm{Leb}_1\left((\{\Phi + h_1\} \oplus [0, h - h_1]) \cap K\right)]}{\mathrm{Leb}_2(K)} = \nu_\lambda^{h_1} + \nu_\lambda^{h - h_1} \; .
\end{aligned}
$$

Here $\Phi + h_1$ has the same distribution as Φ, since Φ is a stationary Poisson point process. As a consequence we may deduce $\nu_\lambda^h = h\nu_\lambda^1$.

But ν_λ^h is also linear in λ: apply the superposition theorem to decompose the original Poisson point process Φ of intensity λ into two independent Poisson point process Φ_1 and Φ_2 with respective intensities λ_1 and λ_2, such that $\lambda = \lambda_1 + \lambda_2$. Therefore

$$
\nu_\lambda^h = \nu_{\lambda_1}^h + \nu_{\lambda_2}^h \; .
$$

In sum, we conclude that ν_λ^h should be of the form $k\lambda h$. We determine the value for $k = \nu_1^1$ by considering the case when K is the unit square $[0, 1]^2$. If we denote by $\Phi(K)$ the amount of points from Φ (a Poisson point process with intensity λ) that falls in K we get (recall $\Phi(K) \sim Po(\lambda \, \mathrm{Leb}_2(K))$)

$$
\begin{aligned}
\nu_\lambda^h &= h\nu_\lambda^1 = h\frac{\mathbb{E}\left[\mathrm{Leb}_1\left((\Phi \oplus [0, 1]) \cap [0, 1]^2\right)\right]}{\mathrm{Leb}_2([0, 1]^2)} \\
&= h\mathbb{E}\left[\sum_{\xi \Uparrow [0,1]^2} \mathrm{Leb}_1(\xi \cap [0, 1]^2)\right] = h\mathbb{E}\left[\sum_{k=1}^{\Phi([0,1]^2)} U(0, 1) + \sum_{k=1}^{\Phi([-1,0]\times[0,1])} U(0, 1)\right] \\
&\qquad\qquad = 2h\mathbb{E}[\Phi([0, 1]^2)] \times \mathbb{E}[U(0, 1)] = h\lambda \; .
\end{aligned}
$$

Here we are using the fact that if $\xi \Uparrow [0, 1]^2$, then its marker point $\boldsymbol{x}$ falls either in $[0, 1]^2$ or in $[-1, 0] \times [0, 1]$, see figure 6.2. Either way, $\mathrm{Leb}_1(\xi \cap [0, 1]^2)$ is distributed according to a $U[0, 1]$ random variable (recall the construction of the Poisson point process where we draw $\Phi([0, 1]^2)$ points scattered as independent and identically distributed uniformly on $[0, 1]^2$).

Now, recalling that the unit Poisson line process Π (where $\lambda = 1/2$, since we are considering undirected lines) has length intensity equal to $\pi/2$. To obtain this result notice that the length of a chord (a line at a distance r from the origin $\boldsymbol{o}$) in $\mathcal{B}_1(\boldsymbol{o})$ is given by $2\sqrt{1 - r^2}$, see figure 6.3. Therefore the calculations for the length intensity
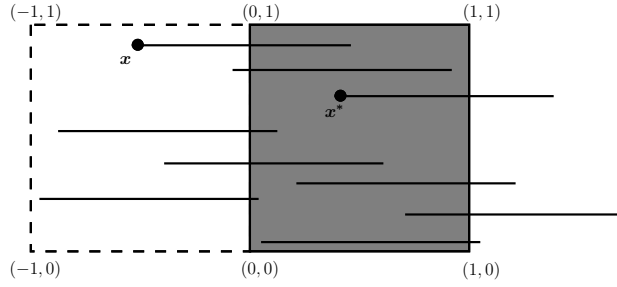
Figure 6.2: Explanation for the fact that $\text{Leb}_1(\xi \cap [0,1]^2)$ has distribution $2U(0,1)$. If there is a left-end point $\boldsymbol{x} = (x_1, y_1)$ in the square $[-1,0] \times [0,1]$ then the length of the intersection of that segment with the square $[0,1]^2$ is given by $1 + x_1$ which is Uniform on $(0,1)$. Similarly, if there is a left-end point $\boldsymbol{x^*} = (x_2, y_2)$ in the square $[0,1]^2$ then the length of that segment with the square $[0,1]^2$ is given by $1 - x_2$ which is again Uniform $(0,1)$.

leads to:

$$\nu_\lambda = \frac{\mathbb{E}[L(\Pi \cap \mathcal{B}_1(\boldsymbol{o}))]}{\text{Leb}_2(\mathcal{B}_1(\boldsymbol{o}))} = \frac{\lambda}{\pi} \int_0^\pi \int_{-1}^1 2\sqrt{1 - r^2} \, \mathrm{d}r \, \mathrm{d}\theta$$

$$= \frac{2\lambda\pi}{\pi} \int_{-1}^1 \sqrt{1 - r^2} \, \mathrm{d}r = \lambda\pi = \frac{\pi}{2} \, .$$
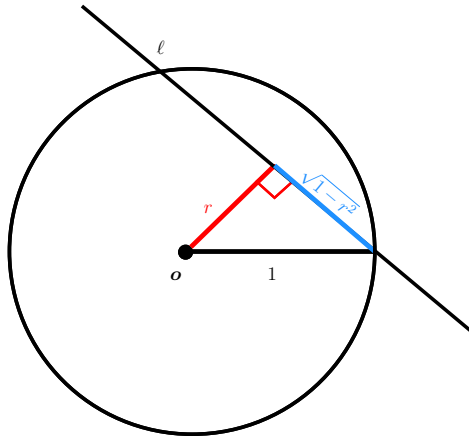

Figure 6.3: Illustration of the length of the chord in $\mathcal{B}_1(\boldsymbol{o})$.

Therefore $k = \pi/2$ gives the similar desired result for segment processes. Our particular interest is with the case where ρ is a uniform distribution. Notice that a Poisson segment process of length h with intensity $\lambda = 1/h$ has the same length intensity as an unit Poisson line process.

6.2 Open problems for the Segment line process framework

There are mainly two new open problems to be consider for future research when working with the Poisson segment processes framework. First, when connections are

being made through a Poisson line segment process there might not exist a continuous path from one point to another. This problem can be related to the Percolation of paths, as the length for the segment process are being fixed for this new model, then there is a phase transition, that is for each fixed length h there will exist a critical value for the intensity, namely λ_c, such that all points in the network will be connected through the Poisson segment process as long as they have intensity higher than λ_c and there will be some disconnected points from the network when the Poisson segment process has intensity lower than λ_c. An important literature review regarding continuum percolation is provided by Meester and Roy [33]. Besides some papers that can provide some insight regarding the interaction between percolation and stochastic geometry are Roy [40], Popov and Vachkovskaia [37] and Roy and Tanemura [41].

Secondly, for the Poisson line process Kendall [25, Theorem 4] provides a lower bound for the mean excess length between the route used to connect any pair of points through the semi-perimeter routing rule and the corresponding Euclidean distance. Along these computations, the presence of a convex hull, as the one given by the cell $\mathcal{C}(\boldsymbol{p}^-, \boldsymbol{p}^+)$ in the semi-perimeter routing rule, play an important role; since the stochastic geometry arguments they used to measure the mean length of these near-geodesics, given by

$$\frac{1}{2}\mathbb{E}\Big[\mathcal{H}_1\Big(\partial\mathcal{C}(\boldsymbol{p}^-, \boldsymbol{p}^+)\Big)\Big] \, ,$$

depends heavily on the convex property of this region. Nevertheless, the convexity from the hull $\mathcal{C}(\boldsymbol{p}^-, \boldsymbol{p}^+)$, in the Poisson line process framework, is a consequence of the Poisson line process; property that is not preserved in the Poisson segment process. Therefore, the computations in [25] can not be generalize to the new framework of Poisson segment processes.

However, Baccelli et al. [7] provides a relevant approach that could be modified accordingly to the Poisson segment process, as it deals with line segments of bounded length and not infinite long lines (as the Poisson line process case). Even though, the paths analysed by Baccelli et al. [7] are not Poisson segment processes, they do have an important interaction with the stochastic geometry field. Mainly with random tessellation models [43], specifically the Voronoi tessellation and its dual Dalaunay graph [35] with respect to the vertex set Φ, given by a planar stationary Poisson point process.

6.3 Final remarks

This thesis explored the mean asymptotic traffic behaviour across the Poissonian city in more depth. The first meaningful result was presented in chapter 2, that is

Theorem 2.1, were we generalize the result Kendall [25, Theorem 5] to any point $q = (tn, un)$ inside the disk of radius n $\mathcal{B}_n(o)$ conditioning on the presence of an horizontal line $\ell_q : y = un$, that is $\ell_q \in \Pi$. Also, along section 2.2 we verified this result using an improper anisotropic Poisson line process, which follows the outline presented in [25, Section 3.3] with the required modifications.

Later on, in chapter 3 we study ideas regarding Palm theory and how it can be applied in the Poissonian city to compute the asymptotic mean traffic density across the Poissonian city. At the same time, we provide a different version for Theorem 2.1, where the source and destination nodes belong to the disk $\mathcal{B}_n(o)$, but not necessarily to the transportation network Π, actually almost surely they will not belong to Π. In contrast, Theorem 3.4 analyse the same mean asymptotic traffic with the source and destination nodes being a Poisson point process over the transportation network given by the Poisson line process Π.

Theorem 3.4 is applied in chapter 4 to make a comparison between the theoretical (mean asymptotic) traffic density in the Poissonian city with the data compiled by British Railways Board [12] for the British railway system. Some numerics are done here to sketch the traffic density curve in the Poissonian city. Also, we developed an analytic expression for the asymptotic mean traffic at any point q conditioned on the presence of a line that goes through q, the integral in question turns out to be an *Elliptic integral*. The comparison shows some evident differences between the model (Poissonian city) and the reality (British railway system). Those differences motivates some changes in the Poissonian city model, in order to make it a more realistic model.

Along chapter 5, we adapted previous results from the original Poissonian city in the disk $\mathcal{B}_n(o)$ to an elliptic Poissonian city over an ellipse with eccentricity given by $e = \sqrt{1 - c^4}$ for different values of $c \in (0, 1]$. Theorem 2.1 still holds true, even more, the proof given in Corollary 5.1 suggests that Theorem 2.1 will still hold true for any convex region with smooth boundaries, however this could be proved in a future work. Again, some numerics are done to sketch the traffic density curve in the Poissonian city, unexpectedly the numerics suggests that the density curve will remain exactly the same regardless of the eccentricity of the region. A first analytic approach was started in section 5.4 to prove this conjecture, but the Elliptic integrals involved in the elliptic Poissonian city still requires more work to prove this conjecture rigorously.

Finally, in chapter 6 we presented another possibility to generalize the original Poissonian city which involves the use of Poisson segment processes Ξ_h, instead of a Poisson line processes Π, as the spatial transportation network to make the connections. Now, with this new framework there are new open problems that were briefly discussed in section 6.2.

Some future work could focus on the study of Poisson segment processes, or new approaches to make the Poissonian city a more realistic model, at least more similar to the British railway system. Some of this approaches could be given by a new density function for the source and destination nodes, an intensity that decreases as one gets far away from the city centre could provide a traffic density more similar to the one observed in British railway system. Another generalization could be done with fibres of small curvature, in this framework it will be interesting to see if the geometric interpretation for Theorem 2.1 has an analogy. A final third approach could involve a more dynamic model, in which the route each passenger takes from the source node to the destination node depends on the traffic flow over each possible route. Nevertheless, analytical approaches could become more complicated in these new cases; however, numerical simulations could be done as a first attempt. Also, the invariance conjecture regarding the traffic density curve in elliptic Poissonian cities is left as an open and interesting problem. Finally, some generalizations to Theorem 2.1 seems to be attainable, as explained before, for convex and smooth regions.

Appendix A

R code segments for the disk

First segment code

```
Traffic <- function(a,b)
{
  K <- function(t)
  {
    A <- 1 + (tan(t))^2
    D <- b - a*tan(t)
    x1 <- -D/A*tan(t) - sqrt(A-D^2)/A
    x2 <- -D/A*tan(t) + sqrt(A-D^2)/A
    y1 <- tan(t)*(x1 - a) + b
    y2 <- tan(t)*(x2 - a) + b
    return(sqrt((x1 - x2)^2 + (y1 - y2)^2) *
          sqrt((a - x2)^2 + (b - y2)^2)* sqrt((x1 - a)^2 + (y1 - b)^2))
  }
  return(K)
}
```

Second segment code

```
I <- function(a,b)
{
  if(a^2 + b^2 >= 1)
  {
    return(0)
  }
  else
  {
    return(1/pi*integrate(Traffic(a,b),lower=0, upper=pi)$value)
  }
}
```

Third segment code

```
n <- 500
x <- seq(-1,1,1/n)
y <- x

T <- matrix(0,2*n+1,2*n+1)
for(i in 1:(2*n+1))
{
  T[,i] <- sapply(x, b=y[i], I)
}


persp3d(x,y,T,col="blue")
persp3D(x,y,T)
```

Fourth segment code

```
T <- T/max(T)
L <- seq(0,1,1/n)
TA <- sum(T > 0) #Amount of points inside the disk
NP <- sum(T==0) #Amount of points outside the disk
PA <- rep(0,n+1)
#To collect the proportion of area that has less or equal
#than certain level of traffic.
for(j in 1:(n+1))
{
    PA[j] <- sum(T <= L[j]) - NP
}


PT <- rep(0,n+1)
TF <- sum(T) #Total traffic flow
#To collect the proportion of traffic flow given by a region
#with traffic less or equal than certain level of traffic.
for(j in 1:(n+1))
{
  PT[j] <- sum((T <= L[j])*T)
}


plot(PA/TA,PT/TF,type="l",lwd=2,col="blue",
        xlab="Proportion of the Network",
        ylab="Proportion of Total traffic, T",
        main="Traffic per mile distribution on the Poissonian city")
```

Fifth segment code

```
Z <- outer(x,y,function(x,y) x^2 + y^2 - 1)
Z1 <- (L[199] <= T & T <= L[203]) #40% Level set
Z2 <- (L[399] <= T & T <= L[403]) #80% Level set
contour(x,y,Z,levels=0, xlab="x - coordinate",
              ylab="y - coordinate", asp=1)
#Plot unit disk
title("Level sets for the mean asymptotic traffic
in the Poissonian city")
par(new=TRUE)#To keep plot on the same window
contour(x,y,Z1,levels=1, asp=1)
#Plot of level sets around 40%
par(new=TRUE)#To keep plot on the same window
contour(x,y,Z2,levels=1, asp=1)
#Plot of level sets around 80%
```

Sixth segment code

```
x <- seq(0,pi,0.0005)
y <- seq(0,1,0.00005)
O <- rep(1, length(y))
o <- rep(0, length(y))


F1 <- function(r)
{
  f1 <- function(x)
  {
    return((1 - (r*sin(x))^2)^(1/2))
  }
  return(f1)
}


I1 <- function(r)
{
  return(integrate(F1(r),lower=0, upper=pi)$value)
}


int1vec <- function(t)
{
  return(sapply(t,I1))
}


F2 <- function(a)
```

```
{
  f2 <- function(r)
  {
    return(4*r*(1 - r^2)*I1(r))
  }
  return(f2)
}


I2 <- function(a)
{
  return(integrate(F2(a),lower=0, upper=a)$value)
}


int2vec <- function(s)
{
  return(sapply(s,I2))
}


g <- function(x)
{
  return(1 - int2vec(x)/int2vec(0))
}


plot(y,g(sqrt(1-y)),type="l",lwd=2,col="blue",
        xlab="Proportion of the Network",
        ylab="Proportion of Total traffic, T",
        main="Traffic per mile distribution on the Poissonian city")
```

Appendix B

R code segments for the ellipse

First segment code

```
Traffic <- function(a,b)
{
  K <- function(t)
  {
    c <- 0.75
    A <- c^4 + (tan(t))^2
    D <- b - a*tan(t)
    x1 <- -D/A*tan(t) - c/A*(A-(c*D)^2)^(1/2)
    x2 <- -D/A*tan(t) + c/A*(A-(c*D)^2)^(1/2)
    y1 <- tan(t)*(x1 - a) + b
    y2 <- tan(t)*(x2 - a) + b
    return(sqrt((x1 - x2)^2 + (y1 - y2)^2) *
           sqrt((a - x2)^2 + (b - y2)^2)* sqrt((x1 - a)^2 + (y1 - b)^2))
  }
  return(K)
}
```

Second segment code

```
I <- function(a,b)
{
  c <- 0.75
  if((c*a)^2 + (b/c)^2 >= 1)
  {
    return(0)
  }
  else
  {
    return(1/pi*integrate(Traffic(a,b),lower=0, upper=pi)$value)
```

```
  }
}
```

Third segment code

```
c <- 0.75
n <- 500
x <- seq(-1,1,1/n)
y <- x/c
x <- x/c

T <- matrix(0,2*n+1,2*n+1)
for(i in 1:(2*n+1))
{
  T[,i] <- sapply(x, b=y[i], I)
}

persp3d(x,y,T,col="blue")
persp3D(x,y,T)
```

Fourth segment code

```
c <- 0.75
Z <- outer(x,y,function(x,y) (c*x)^2 + (y/c)^2 - 1)
Z1 <- (L[199] <= T & T <= L[203]) #40% Level set
Z2 <- (L[399] <= T & T <= L[403]) #80% Level set
contour(x,y,Z,levels=0, xlab="x - coordinate",
               ylab="y - coordinate", asp=1)
#Plot unit disk
title("Level sets for the mean asymptotic traffic
in an elliptic Poissonian city")
par(new=TRUE)#To keep plot on the same window
contour(x,y,Z1,levels=1,asp=1)
#Plot of level sets around 40%
par(new=TRUE)#To keep plot on the same window
contour(x,y,Z2,levels=1, asp=1)
#Plot of level sets around 80%
```

Bibliography

[1] Abramowitz, M. and Stegun, I. (1964). *Handbook of Mathematical Functions: With Formulas, Graphs, and Mathematical Tables*. Applied mathematics series. Dover Publications.

[2] Aldous, D. J., Cheng, Y., Friedman, J., Huoh, Y.-J., Lee, W., and Liu, H. (2007). Route-Length Efficiency in Spatial Transportation Networks. Preprint on webpage at `https://www.stat.berkeley.edu/~aldous/Unpub/sharp_curve.pdf`.

[3] Aldous, D. J. and Kendall, W. S. (2008). Short-length routes in low-cost networks via Poisson line patterns. *Advances in Applied Probability*, 40(1):1–21.

[4] Aldous, D. J. and Shun, J. (2010). Connected Spatial Networks over Random Points and a Route-Length Statistic. *Statistical Science*, 25(3):275–288.

[5] Ash, R. and Doléans-Dade, C. (2000). *Probability and Measure Theory*. Harcourt/Academic Press.

[6] Baccelli, F. and Bremaud, P. (2002). *Elements of Queueing Theory: Palm Martingale Calculus and Stochastic Recurrences*. Stochastic Modelling and Applied Probability. Springer Berlin Heidelberg, Second edition.

[7] Baccelli, F., Tchoumatchenko, K., and Zuyev, S. (2000). Markov paths on the Poisson-Delaunay graph with applications to routing in mobile networks. *Advances in Applied Probability*, 32(1):1–18.

[8] Baddeley, A. (1999). *A crash course in stochastic geometry*, volume 80 of *Monographs on Statistics and Applied Probability*, pages 1–35. Chapman and Hall.

[9] Baddeley, A. and Jensen, E. B. V. (2005). *Stereology for Statisticians*. Chapman & Hall/CRC.

[10] Bartle, R. (1976). *The elements of real analysis*. Wiley international edition. Wiley.

[11] Billingsley, P. (2012). *Probability and Measure*. Wiley Series in Probability and Statistics. Wiley.

[12] British Railways Board (1963). The reshaping of British railways, Part 1: Report. *Her Majesty's Stationery Office*.

[13] Chiu, S., Stoyan, D., Kendall, W., and Mecke, J. (2013). *Stochastic Geometry and Its Applications*. Wiley Series in Probability and Statistics. Wiley.

[14] Daley, D. J. and Vere-Jones, D. (2008). *An introduction to the theory of point processes. Vol. II: General Theory and Structure*. Probability and its Applications. Springer, New York, Second edition.

[15] Dujmović, V., Morin, P., and Smid, M. H. M. (2015). Average Stretch Factor: How Low Does It Go? *Discrete & Computational Geometry*, 53(2):296 – 326.

[16] Falconer, K. (2013). *Fractal Geometry: Mathematical Foundations and Applications*. Wiley.

[17] Gameros Leal, R. M. (2014). Traffic in Poissonian line networks. MSc. Dissertation submitted to The University of Warwick.

[18] Gastner, M. T. and Newman, M. E. J. (2006). Shape and efficiency in spatial distribution networks. *Journal of Statistical Mechanics: Theory and Experiment*, 2006(01):P01015.

[19] Gorroochurn, P. and Levin, B. (2013). On Two Historical Aspects of Buffon's Needle Problem. *Electronic Journal for History of Probability and Statistics*, 9.

[20] Hall, L. M. (1995). Special functions. Lecture notes available at `http://web.mst.edu/~lmhall/SPFNS/spfns.pdf`.

[21] Johnstone, I. M. and Silverman, B. W. (1990). Speed of Estimation in Positron Emission Tomography and Related Inverse Problems. *The Annals of Statistics*, 18(1):251–280.

[22] Kallenberg, O. (2002). *Foundations of Modern Probability*. Probability and Its Applications. Springer New York.

[23] Kendall, W. S. (2000). Stationary countable dense random sets. *Advances in Applied Probability*, 32(1):86–100.

[24] Kendall, W. S. (2008). Networks and Poisson line patterns: fluctuation asymptotics. *Oberwolfach Reports*, 5(4):2670 – 2672.

[25] Kendall, W. S. (2011). Geodesics and flows in a Poissonian city. *The Annals of Applied Probability*, 21(3):801–842.

[26] Kendall, W. S. (2014a). Lines and Networks. *Markov Processes and Related Fields*, 20(1):81–106.

[27] Kendall, W. S. (2014b). Return to the Poissonian city. *Journal of Applied Probability*, 51A:297–309.

[28] Kerstan, J., Matthes, K., and Mecke, J. (1978). *Infinitely divisible point processes*. Wiley series in probability and mathematical statistics. Wiley.

[29] Kingman, J. (1992). *Poisson Processes*. Oxford studies in probability. Clarendon Press.

[30] Little, J. D. C. (1961). A proof of the queueing formula $L = \lambda W$. *Operations Research*, 9:383–387.

[31] Marr, R. B. (1974). On the reconstruction of a function on a circular domain from a sampling of its line integrals. *Journal of Mathematical Analysis and Applications*, 45(2):357 – 374.

[32] Mecke, J. (1981). Stereological formulas for manifold processes. *Probability and Mathematical Statistics*, 2(1):31 – 35.

[33] Meester, R. and Roy, R. (1996). *Continuum Percolation*. Cambridge Tracts in Mathematics. Cambridge University Press.

[34] Molchanov, I. (2006). *Theory of random sets*. Springer.

[35] Okabe, A. (2000). *Spatial tessellations: concepts and applications of Voronoi diagrams*. Wiley series in probability and statistics: Applied probability and statistics. Wiley.

[36] O'Sullivan, F. (1995). A Study of Least Squares and Maximum Likelihood for Image Reconstruction in Positron Emission Tomography. *The Annals of Statistics*, 23(4):1267–1300.

[37] Popov, S. Y. and Vachkovskaia, M. (2002). A note on percolation of poisson sticks. *Brazilian Journal of Probability and Statistics*, 16(1):59–67.

[38] Prömel, H. J. and Steger, A. (2002). *The Steiner Tree Problem : A Tour through Graphs, Algorithms, and Complexity*. Advanced Lectures in Mathematics. Springer, Wiesbaden.

[39] Rogers, C. (1998). *Hausdorff Measures*. Cambridge Mathematical Library. Cambridge University Press.

[40] Roy, R. (1993). Percolation of Poisson Sticks on the Plane. *Theory of Probability and its Applications*, 37(1):167–168. Original Russian article in *Teor. Veroyatnost. i Primenen.*, **37**(1), (1992), pp. 203–204.

[41] Roy, R. and Tanemura, H. (2003). The structure of finite clusters in high intensity Poisson Boolean stick process. *ArXiv Mathematics e-prints: 0312480*.

[42] Schneider, R. and Weil, W. (2008). *Stochastic and Integral Geometry*. Probability and Its Applications. Springer.

[43] van Lieshout, M. (2012). An introduction to planar random tessellation models. *Spatial Statistics*, 1(Supplement C):40 – 49.

[44] Vardi, Y., Shepp, L., and Kaufman, L. (1985). A statistical model for positron emission tomography. *Journal of the American Statistical Association*, 80(389):8–20.

[45] Whittaker, E. and Watson, G. (1996). *A Course of Modern Analysis.* A Course of Modern Analysis: An Introduction to the General Theory of Infinite Processes and of Analytic Functions, with an Account of the Principal Transcendental Functions. Cambridge University Press.

[46] Winston, C. and Mannering, F. (2014). Implementing technology to improve public highway performance: A leapfrog technology from the private sector is going to be necessary. *Economics of Transportation*, 3(2):158 – 165. Special Issue in Honor of Herbert Mohring.